

Università degli Studi dell'Insubria
Dipartimento di Scienza e Alta Tecnologia



**CHIRAL IRON AND TITANIUM COMPLEXES AS CATALYSTS FOR
STERESELECTIVE REDOX REACTIONS**

PhD in Chemical and Environmental Sciences, XXXIV cycle

PhD Dissertation:

Giovanni Maria Fusi

Supervisor: Prof. Dr. Umberto PIARULLI

Co-Supervisor: Prof. Dr. Albrecht BERKESSEL

2020-2021

Acknowledgments

I would like to express my gratitude to my family for the tireless support given during my journey as a PhD student. I would also like to thank all of my friends and all the people involved in the projects described in this thesis:



Prof. Umberto Piarulli, for guiding me through my PhD, for all the help and advice, and for the support to my growth as a chemist.

Dr. Silvia Gazzola

All the members of the research group.



Prof. Albrecht Berkessel, for kindly welcoming me in his research group during my six months abroad and for all the helpful suggestions.

Dr. Fabian Severin

Dr. Jörg Martin Neudörfl for the XRD analyses

Sarwar Aziz

All the members of the AKB group



Prof. Luca Pignataro

Prof. Cesare Gennari

Tommaso Gandini

Prof. Valentina Colombo for the XRD analyses

Prof. Oliver Reiser (Universität Regensburg)

Prof. Vittorio Pace (Università degli Studi di Torino)

Prof. Tiziana Benincori (Università degli Studi dell'Insubria)

for reviewing my thesis and for being part of my examination committee.

Table of Contents

1. Preface	12
1.1. Base Metals in Homogeneous Catalysis	12
2. Part A.	15
2.1. Iron Complexes	15
2.2. Iron Complexes in Asymmetric Catalysis	16
2.2.1. Asymmetric hydrogenation reactions	18
2.2.2. Asymmetric <i>cis</i> -Dihydroxylation Reactions	25
2.2.3. Asymmetric Epoxidation Reactions	27
2.2.4. Asymmetric Sulfoxidation Reactions	30
2.2.5. Enantioselective Reactions Involving the Formation of C-C bonds	31
2.3. (Cyclopentadienone)Iron Tricarbonyl Complexes	36
2.3.1. Reactivity of (Cyclopentadienone)iron Tricarbonyl Complexes	39
2.3.2. Structural Modifications	43
2.3.3. (Cyclopentadienone)iron Complexes in Asymmetric Catalysis	46
2.4. Aim of the Thesis	51
2.5. Complex deriving from a chiral 3-substituted cyclooctyne	54
2.6. Sonogashira Cross-Coupling and Synthesis of α,ω-Diyne Pre-Ligands	60
2.6.1. Synthesis of dialkyne precursors for the carbonylative cyclization through Sonogashira coupling	64
2.6.2. (<i>R,R</i>)-1,8-bis[2'-methoxy-(1,1'-binaphthalen)-2-yl]octa-1,7-diyne (72)	64
2.6.3. Alkynes Connected to a (<i>R</i>)-2,2'-bis(methoxymethoxy)-[1,1'-binaphthalen]-3-yl Moiety	69
2.6.4. Mono-substituted 1,7-octadiynes	71
2.7. Iron Complexes Containing 1,1'-Binaphthyl-based C_2-symmetric Cyclopentadienone Ligands	75
2.7.1. Synthesis of complex 102	76
2.7.2. Synthesis of Complexes 103-106	77
2.7.3. Catalytic tests with complexes 102 and 103-106	80
2.8. Diastereoisomerically Pure Complexes containing 1,1'-Binaphthyl-based C_2-Symmetric Cyclopentadienone Ligands	84

2.8.1. Synthesis and Catalytic Activity of Diastereoisomerically Pure (Cyclopentadienone)iron Tricarbonyl Complexes 109-111	86
2.8.2. Complexes Containing C_2 -Symmetric Cyclopentadienones Functionalized with Different Aromatic Systems	88
2.8.3. Complexes Prepared from 1,1'-Binaphthyl-based Terminal Alkynes	90
2.9. Conclusions and Outlook	94
3. Part B.	98
3.1. Titanium Complexes	98
3.2. Titanium Salalen Complexes	99
3.3. Asymmetric Epoxidation of Allylic Alcohols	106
3.4. Results and Discussion	109
3.4.1. Asymmetric Epoxidation of Enantiopure Terminal Allylic Alcohols	111
3.4.2. Asymmetric Epoxidation of a Chiral Allyl Ether	115
3.4.3. Synthetic Application: Preparation of a Subunit of Montanacin D	117
3.4.4. Synthesis of Titanium Salalen Complex 138	120
3.5. Conclusions and Outlook	121
4. 4. Experimental Section	123
4.1. Materials and Methods	123
4.2. Instrumentations	123
4.3. Synthesis and Carbonylative Cyclization of <i>rac</i>-3-Methoxycyclooctyne	125
4.3.1. <i>rac</i> -3-Bromocyclooctene (65)	125
4.3.2. <i>rac</i> -Cyclooct-2-en-3-ol (66)	125
4.3.3. <i>rac</i> -3-Methoxycyclooctene (67)	126
4.3.4. <i>rac</i> -2-Bromo-3-methoxycyclooctene (68)	127
4.3.5. <i>rac</i> -3-Methoxycyclooctyne (69)	127
4.3.6. Carbonylative Cyclization/Complexation of <i>rac</i> -3-Methoxycyclooctyne (69)	128
4.4. Synthesis of (<i>R</i>)-2-iodo-2'-methoxy-1,1'-binaphthalene (76)	129
4.4.1. (<i>R</i>)-2-Methoxy-[1,1'-binaphthalen]-2-ol (75)	129
4.4.2. (<i>R</i>)-2'-Methoxy-[1,1'-binaphthalen]-2-yl trifluoromethanesulfonate (73)	129
4.4.3. (<i>R</i>)- <i>N</i> -Benzyl-2'-methoxy-[1,1'-binaphthalen]-2-amine (77)	130
4.4.4. (<i>R</i>)-2'-Methoxy-[1,1'-binaphthalen]-2-amine (78)	131
4.4.5. (<i>R</i>)-2-Iodo-2'-methoxy-1,1'-binaphthalene (76)	131

4.5. Sonogashira Cross-Coupling Reactions on Iodide 76	132
4.5.1. (<i>R</i>)-((2'-Methoxy-[1,1'-binaphthalen]-2-yl)ethynyl)trimethylsilane (79)	132
4.5.2. (<i>R</i>)-2-Methoxy-2'-(phenylethynyl)-1,1'-binaphthalene (80)	133
4.6. Synthesis of mono-Substituted 1,7-Octadiynes 91-95	134
4.6.1. Trimethyl(octa-1,7-diyn-1-yl)silane (91)	134
4.6.2. 1-Phenyl-1,7-octadiyne (92)	134
4.6.3. 1-Mesityl-1,7-octadiyne (93)	135
4.6.4. 1,2,3,4,5-Pentafluoro-6-(octa-1,7-diyn-1-yl)benzene (94)	136
4.6.5. 1,3-Dimethoxy-2-(octa-1,7-diyn-1-yl)benzene (95)	137
4.7. Synthesis of 3-iodo-2,2'-bis(methoxymethoxy)-1,1'-binaphthalene (82)	138
4.7.1. (<i>R</i>)-2,2'-Bis(methoxymethoxy)-1,1'-binaphthalene (83)	138
4.7.2. (<i>R</i>)-3-Iodo-2,2'-bis(methoxymethoxy)-1,1'-binaphthalene (82)	138
4.8. Sonogashira Cross-Coupling Reactions on Iodide 82	139
4.4.3. 1,8-Bis((<i>R</i>)-2,2'-bis(methoxymethoxy)-[1,1'-binaphthalen]-3-yl)octa-1,7-diyne (81)	139
4.8.2. General Procedure for the Coupling of Iodide 82 with Alkynes 90-95 (A)	140
4.8.3. (<i>R</i>)-2,2'-Bis(methoxymethoxy)-3-(nona-1,7-diyn-1-yl)-1,1'-binaphthalene (84)	140
4.8.4. (<i>R</i>)-(8-(2,2'-Bis(methoxymethoxy)-[1,1'-binaphthalen]-3-yl)octa-1,7-diyn-1-yl)trimethylsilane (85)	141
4.8.5. (<i>R</i>)-2,2'-Bis(methoxymethoxy)-3-(8-phenylocta-1,7-diyn-1-yl)-1,1'-binaphthalene (86)	142
4.8.6. (<i>R</i>)-3-(8-Mesitylocta-1,7-diyn-1-yl)-2,2'-bis(methoxymethoxy)-1,1'-binaphthalene (87)	143
4.8.7. (<i>R</i>)-2,2'-Bis(methoxymethoxy)-3-(8-(perfluorophenyl)octa-1,7-diyn-1-yl)-1,1'-binaphthalene (88)	144
4.8.8. (<i>R</i>)-3-(8-(2,6-Dimethoxyphenyl)octa-1,7-diyn-1-yl)-2,2'-bis(methoxymethoxy)-1,1'-binaphthalene (89)	145
4.8.1. (<i>R</i>)-3-(2,2'-bis(methoxymethoxy)-[1,1'-binaphthalen]-3-yl)prop-2-yn-1-ol (96)	146
4.9. Synthesis of Iron Complex 102	147
4.9.1. (<i>R</i>)-2-ethynyl-2'-methoxy-1,1'-binaphthalene (107)	147
4.9.2. 1,8-bis((<i>R</i>)-2'-methoxy-[1,1'-binaphthalen]-2-yl)octa-1,7-diyne (72)	147
4.9.3. Complex 102	148
4.10. Synthesis of Complexes 103-106	149

4.10.1. Complex 103	149
4.10.2. Complex 104	151
4.10.3. Complex 105	152
4.10.4. Complex 106	153
4.11. Synthesis of Iron Complexes 109-114	154
4.11.1. General Procedure for the Carbonylative Cyclization of Alkynes 84-89 (B)	154
4.11.2. Complexes 109a-b	154
4.11.3. Complexes 110a-b	155
4.11.4. Complexes 111a-b	156
4.11.5. Complexes 112a-b	158
4.11.6. Complexes 113a-b	159
4.11.7. Complexes 114a-b	161
4.12. Synthesis of Iron Complexes 115a-b	163
4.12.1. (<i>R</i>)-2,2'-bis(methoxymethoxy)-3-(octa-1,7-diyn-1-yl)-1,1'-binaphthalene (101)	163
4.12.2. Complexes 115a-b	164
4.13. Synthesis of Iron Complexes 117a-b	165
4.13.1. (<i>R</i>)-2,2'-bis(methoxymethoxy)-3-(3-(prop-2-yn-1-yloxy)prop-1-yn-1-yl)-1,1'-binaphthalene (116)	165
4.13.2. Complexes 117a-b	166
4.14. AH and ATH tests	167
4.14.1. General Procedure for AH of Acetophenone	167
4.14.2. General Procedure for ATH of Acetophenone	168
4.14.3. Conditions for the Determination of Conversion and <i>ee</i> Values	168
4.14.4. Hydrogenation of <i>N</i> -(4-methoxyphenyl)-1-phenylethan-1-imine	168
4.15. Synthesis of Titanium Complex 138	169
4.15.1. 2',3',4',5',6'-pentafluoro-[1,1'-biphenyl]-2-ol (168)	169
4.15.2. 2',3',4',5',6'-pentafluoro-2-hydroxy-[1,1'-biphenyl]-3-carbaldehyde (169)	170
4.15.3. Ligand 137	170
4.15.4. Complex 138	171
4.16. Synthesis and Resolution of Allylic Alcohols 142, 144 and 151-153	172
4.16.1. Synthesis of Racemic Allylic Alcohols <i>rac</i> -142, <i>rac</i> -144 and <i>rac</i> -151-153	172

4.16.2. General Procedure for the Enzymatic Kinetic Resolution of Allylic Alcohols 142, 144 and 151-153 (C)	172
4.16.3. (<i>R</i>)-Undec-1-en-ol, (<i>R</i>)-142	173
4.16.4. (<i>R</i>)-Pentadec-1-en-3-ol, (<i>R</i>)-144	174
4.16.5. (<i>S</i>)-1-Cyclohexylprop-2-en-1-ol, (<i>S</i>)-151	175
4.16.6. (<i>S</i>)-4,4-Dimethylpent-1-en-3-ol, (<i>S</i>)-152	176
4.16.7. (<i>R</i>)-1-Phenylbut-3-en-2-ol, (<i>R</i>)-153	176
4.17. (<i>S</i>)-(1-Methoxyallyl)cyclohexane, (<i>S</i>)-161	178
4.18. Synthesis of the Racemic Epoxides	179
4.18.1. General Procedure for the Epoxidation with <i>m</i> -CPBA (D)	179
4.18.2. Determination of the Absolute Configurations and of the <i>syn/anti</i> Ratios for Epoxides 143, 145, 158-160, 162	179
4.18.3. 1,2-Epoxyundecan-3-ol (143)	179
4.18.4. 1,2-Epoxy-pentadecan-3-ol (145)	180
4.18.5. 3-Cyclohexyl-1,2-epoxypropan-3-ol (158)	181
4.18.6. 4,4-Dimethyl-1,2-epoxypentan-3-ol (159)	181
4.18.7. 4-Phenyl-1,2-epoxybutan-3-ol (160)	182
4.18.8. 3-Cyclohexyl-3-methoxy-1,2-epoxypropane (162)	183
4.19. Epoxidation Tests	183
4.19.1. General Procedure for the Asymmetric Epoxidation Catalyzed by 138	183
4.19.2. Determination of the <i>ee</i> , of the <i>syn/anti dr</i> , and of the Absolute Configuration of the Epoxidation Products	184
4.19.3. (<i>2R,3R</i>)-1,2-Epoxyundecan-3-ol, (<i>2R,3R</i>)-143	184
4.19.4. (<i>2R,3R</i>)-Pentadecan-3-ol, (<i>2R,3R</i>)-145	185
4.19.5. (<i>2R,3R</i>)-3-Cyclohexyl-1,2-epoxypropan-3-ol, (<i>2R,3R</i>)-158	187
4.19.6. (<i>2R,3R</i>)-4,4-Dimethyl-1,2-epoxypentan-3-ol, (<i>2R,3R</i>)-159	190
4.19.7. (<i>2R,3R</i>)-4-Phenyl-1,2-epoxybutan-3-ol, (<i>2R,3R</i>)-160	191
4.19.8. (<i>2R,3R</i>)-3-Cyclohexyl-3-methoxy-1,2-epoxypropan-3-ol, (<i>2R,3R</i>)-162	192
4.19.9. Synthesis of (<i>2R,3R</i>)-162 through Methylation of (<i>2R,3R</i>)-158	194
4.20. Synthesis of Building Block 167	195
4.20.1. <i>tert</i> -Butyl[<i>((R)</i> -1-[(<i>R</i>)-oxiran-2-yl]tridecyl)oxy]diphenylsilane (164)	195
4.20.2. (<i>5R,6R</i>)-6-[(<i>tert</i> -butyldiphenylsilyl)oxy]octadec-1-en-5-ol (165)	196

4.20.3. (2 <i>R</i> ,5 <i>R</i>)-5-[(<i>R</i>)-1-[(<i>tert</i> -butyldiphenylsilyl)oxy]tridecyl]tetrahydrofuran-2-yl]methanol (167)	197
5. References	198
6. NMR Spectra	209
6.1. Complex 103	209
6.2. Complex 104	210
6.3. Complex 105	211
6.4. Complex 106	212
6.5. Complex 110a	213
6.6. Complex 110b	214
6.7. Complex 112a	215
6.8. Complex 112b	216
6.9. Complex 113a	217
6.10. Complex 113b	219
6.11. Complex 114a	221
6.12. Complex 114b	222
6.13. Complex 117a	223
6.14. Complex 117b	224
6.15. Epoxy Alcohol 159	225
6.16. Epoxide 162	226
6.17 Epoxy Alcohol 145	227
6.18. Compound 164	228
6.19. Compound 165	229
6.20. Compound 167	230
7. List of Abbreviations	231

1. Preface

1.1. Base Metals in Homogeneous Catalysis

Catalysts are, by definition, substances that participate to a chemical reaction increasing its rate without modifying the total Gibbs energy of the process and without being modified or consumed during the process.^[1]

Two main types of catalysis can be outlined: heterogeneous and homogeneous catalysis. Reactions in the former category involve the use of catalytic systems in a different phase from that of the reagents, most commonly in a solid state, while the catalytically active species and the reagents are all contained in the same phase in the case of homogeneous catalysis.

Many organic and inorganic transformations are feasible thanks to the use of catalysis, to the point that nowadays over 90% of the synthetic routes followed to produce compounds commercialized by chemical industries are estimated to rely on catalysis at least in one stage.

Among the diverse catalytic systems that are known, transition metals have been playing a key role during the last century. Success of metal-based catalysts derives from the wide spectrum of different electronic properties that can be found running through the transition group.

When metal complexes are employed as homogeneous catalysts, high selectivity (chemo- regio- and stereoselectivities) can also be achieved by the proper choice and design of the surrounding ligands. Development of new reactivities in academic research was made possible by transition metal complexes, as well as the large-scale preparation of otherwise difficult to achieve substances, often with remarkable effects on economics and society.^[2] Complexes containing noble metals, like ruthenium, rhodium, iridium, palladium, and platinum, in particular have afforded excellent results both in terms of catalytic activity and selectivity.

However, while heterogeneous catalysts are generally very robust and easy to separate from the products of reaction, homogeneous catalysts are usually more selective and allow to run reactions in milder conditions, but they are less robust, leading to lower TONs, and they imply more elaborated separation techniques to isolate pure products. The latter feature represents a particularly relevant issue in the case of catalysts based on noble metals, which are toxic, both for the environment and for human health. Industrial application of noble-metal-based catalysts is often limited by the high purity required for the final products in many of its sectors (ranging from pharmaceutical and cosmetic to food and agrochemical industry): costs related to the necessary purification procedures, summed up to the cost of the metals themselves, pushes towards the research for cheaper alternatives, like complexes containing base metals (Figure 1).

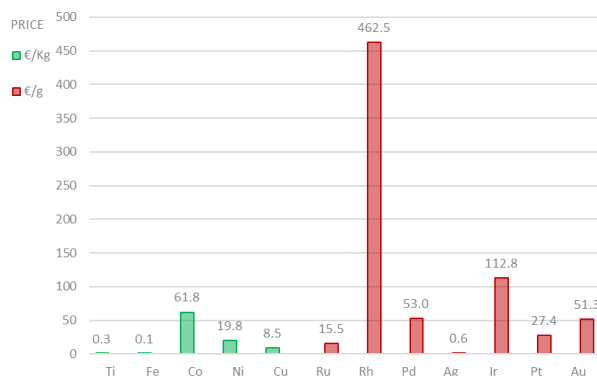


Figure 1. Cost of noble and base metals commonly used in catalysis (updated to January 2022).^[3]

On the other hand, sustainability has become in recent years a foreground topic in many aspects of society and economics, as well as in the field of chemistry. The use of catalysis instead of reactions requiring stoichiometric reagents is one of the twelve principles (principle number 9) of green chemistry,^[4] but avoiding dangerous and toxic chemicals, as well as employing renewable sources are included in the list as well (3rd principle): both environmental issues and low availability of noble metals imply that a greener alternative would be preferable.

A possible solution can be found in first row transition metals, which are more abundant (iron and titanium are the two most abundant transition metals on Earth's crust), less expensive, and in most cases are less harmful for the environment. Thus, the research for new catalytic systems relying on base metals has greatly increased, both in search for methods to substitute noble metals, and to investigate new catalytic processes. As an example of the growing attention towards these elements, a comparison between the documents about catalysis promoted by iron and ruthenium published in the last two decades is reported in Figure 2.^[5]

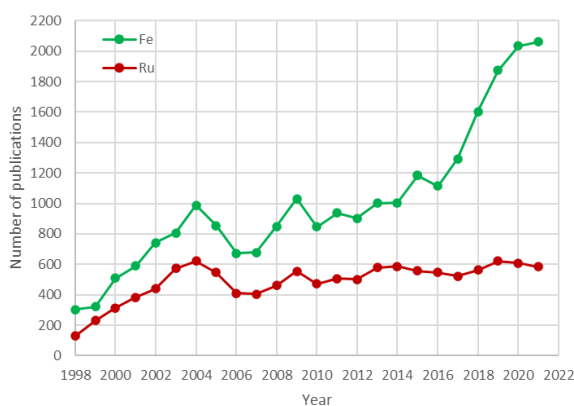


Figure 2. Number of published documents per year related to catalysis involving iron and ruthenium.

Nevertheless, limitations to the practical application of catalysis involving the use of cheap metals are still relevant. Complexes containing base metals often generate less robust and active catalytic systems: in order to compensate for these downsides, the use of elaborate ligands, which may be more costly and valuable than the metal itself, is necessary in many cases.

This is particularly true for stereoselective catalysis, field in which the number of implemented industrial processes is still limited by the issues connected with noble metals and the lack of good alternatives. Non-enantioselective synthesis followed by resolution of the racemic products are often preferred to asymmetric catalysis, even though this would represent a valuable way to directly generate enantiopure products with excellent atom economy.

For all these reasons, the development of new chiral complexes based on inexpensive transition metals, that can act as robust, efficient and selective catalytic systems would be of great importance both from a scientific and industrial point of view.

This thesis is focused on the study of chiral complexes containing first row transition metals and on their application as catalysts in asymmetric redox reactions. The elaborate is divided into two sections.

In **Part A**, the synthesis of several new chiral (cyclopentadienone)iron tricarbonyl complexes and the test of their activity and selectivity in asymmetric hydrogenations of carbonyl compounds are described.

Part B concerns the investigation of an innovative method for the diastereoselective epoxidation of chiral terminal allylic alcohols, achieved through the use of the titanium salalen complex known as *Berkessel-Katsuki epoxidation catalyst*.

2. Part A.

New Chiral (Cyclopentadienone)iron Tricarbonyl Complexes as Catalysts for Enantioselective Reduction of Polar Double Bonds

2.1. Iron Complexes

Iron is an element of the first row of the transition, and it belongs to group VIII, showing the electronic configuration $[\text{Ar}]3d^64s^2$. It is an ubiquitous element in nature, being the second most abundant metal on Earth's crust, where it is mostly found in oxidized forms. The most common oxidation states of iron are +2 and +3, the latter being the most frequently observed under atmospheric conditions (in the presence of air and moisture). However, +6, 0, -1, and -2 oxidation numbers can be found as well in some compounds.

Fe^{II} (d^6) centers are usually hexacoordinated and are contained in complexes with an octahedral geometry, even though pentacoordinate complexes exploiting square planar square based pyramidal geometries are often formed when the metal is confined by polydentate macrocyclic ligands like porphyrines and phthalocyanines.^[6] Fe^{III} (d^5) can assume diverse coordination numbers but is often found in six-coordinated species with octahedral geometries. Fe^0 (d^8) complexes generally show tetrahedral or trigonal bipyramidal geometries, like in the air-stable homoleptic carbonyl $\text{Fe}(\text{CO})_5$.

Reactivity of Fe^{II} and Fe^{III} ions is characterized on their behavior as Lewis acids: in accordance with the *hard soft acids and bases* theory,^[7] iron is a hard acid especially in its oxidation state 3 ($\eta = 13.1$), as can be observed by the reactivity of compounds like FeCl_3 . Fe^0 is softer as Lewis acid ($\eta = 3.9$), while lower oxidation states like Fe^{-2} are reactive mainly as nucleophiles (e.g. species like $\text{Na}_2\text{Fe}(\text{CO})_4$ are known to promote nucleophilic substitutions and additions).^[8]

On the other hand, the reactivity of Fe^{II} and Fe^{III} centers revolves around their redox properties: the transition between these two stable oxidation states involves the transfer of a single electron, which is at the basis of many iron-catalyzed reactions,^[9] including biomimetic and biological processes.^[10] Most of the transformations promoted by classical noble-metal-containing catalytic systems however are based on steps like oxidative addition and reductive elimination, which involve two electrons, for which the $\text{Fe}^{\text{II}}/\text{Fe}^{\text{III}}$ couple is unsuitable.

In contrast, Fe^0 can be oxidized to Fe^{II} through the removal of two electrons, making its complexes interesting alternatives to classical catalysts. However, many Fe^0 complexes suffer from poor stability to air or moisture and undergo easy oxidation or degradation.

Another typical limitation to the application of iron to catalysis is the paramagnetic nature of many of its complexes, which makes their analysis via NMR unfeasible, requiring to rely on methods like X-ray diffractometry, mass spectroscopy or Mössbauer spectroscopy.

Besides the nature of the metal center, ligands play a crucial role in iron-based catalysis. Polydentate chelating ligands are frequently used in order to enhance complex stability, while strong-field ligands can stabilize Fe^{II} and Fe^0 complexes in a low-spin state, which, being diamagnetic, makes characterization via NMR possible. Most interestingly, some ligands allow also two-electron processes to take place on Fe^{II} complexes: this is the case of “non-innocent” ligands.^[11] *Redox non-innocent* ligands can delocalize the electron density of the complex, altering the oxidation state of the metal center during the catalysis and allowing thus multi-electronic processes otherwise unfeasible. When the electron density is significantly delocalized on the ligands, they may become able to undergo reversible chemical transformation during catalysis and directly take part in the redox transformation, and are defined as *Cooperating* ligands^[12] (e.g. cyclopentadienone ligands).

2.2. Iron Complexes in Asymmetric Catalysis

A proper asymmetric environment around the metal center is at the basis of the ability of a chiral metal-based catalyst to direct the stereoselective approach of the substrate to the active site, and thus to control the enantioselectivity of an organic transformation. In the majority of cases, the necessary asymmetric environment derives from the asymmetric hindrance generated by chiral ligands.^[13] If surrounded by properly selected ligands, configurationally stable metal stereocenters can also be the main source of the stereochemical information.^[14] These systems are often referred to as stereogenic- or chiral-at-metal complexes,^[15] and sometimes turned out to be even more selective than catalysts basing their selectivity solely on the effect of chirality at the ligands.^[16] However, only in few cases the metal is the only stereocenter in the structure, and the majority of these chiral catalysts rely also on chiral ligands.

The main obstacle that still limits the application of this strategy is represented by the difficult isolation of enantiopure stereogenic-at-metal complexes when the ligands are not sufficiently kinetically stable: labile ligands can lead to epimerization at the metal stereocenter with generation of numerous possible stereoisomers.^[17] Notwithstanding these potential drawbacks,

examples of stereogenic-only-at-metal complexes of noble metals^[18] have been reported in recent years. Relatively fewer examples are based on complexes of 3d elements like iron, due to the postulated lower configurational stability of complexes of 3d metals.^[19] However, stereogenic-at-metal iron complexes often allow good stereoselection in catalysis, and many of the iron-based catalytic systems currently employed in enantioselective transformations actually contain a stereocenter at metal.

Recent developments in enantioselective iron-catalyzed organic reactions will be presented in the following paragraphs, both based on complexes containing chiral ligands, and on stereogenic-at-metal systems.

Chiral iron complexes (usually containing a Fe(II) ion) with octahedral geometry cover most of the currently available literature about asymmetric catalysis, and in particular polydentate ligands are employed to provide the conformational, and thus configurational, stability necessary for selectivity in catalytic transformations. In the case of complexes with two achiral bidentate ligands, it is possible to identify epimers-at-iron with opposite helicity described by the stereochemical descriptors Λ and Δ (Figure 3).

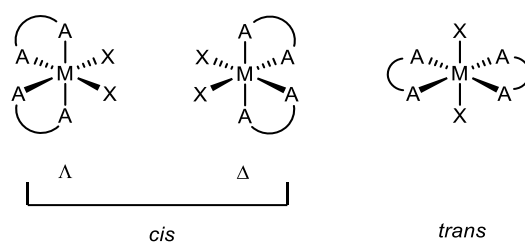


Figure 3. Octahedral complexes containing bidentate ligands with *cis*- and *trans*- geometries and the relative chirality descriptors.

Three coordination geometries can be observed when tetradentate ligands are involved: *cis- α* , *cis- β* and *trans* (Figure 4). Both the *cis- α* and *cis- β* isomers can exist as pairs of epimers with opposite configuration of the metal stereocenter. With both bidentate and tetradentate ligands the *trans* topology is not related to stereogenicity at the metal center when achiral or C_2 -symmetrical ligands, even though the use of chiral ligands still leads to the formation of chiral complexes that can be used in asymmetric catalysis.^[20] Two coordination sites are in all cases occupied by labile ligands that allow the catalytic process to take place on the metal.

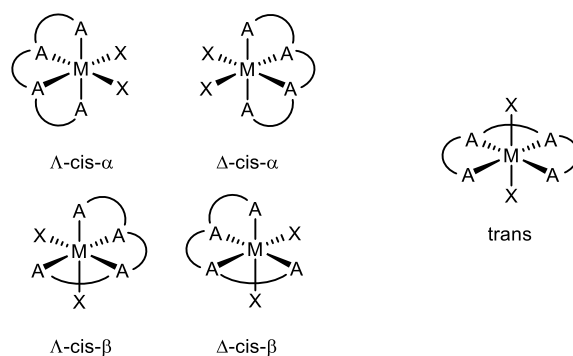
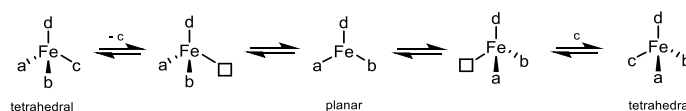


Figure 4. Octahedral complexes containing bidentate ligands with *cis*- and *trans*- geometries and the relative chirality descriptors.

Tetracoordinated iron complexes usually show a tetrahedral geometry, whose absolute configuration usually suffers of a lower integrity. Racemization can easily occur via dissociation of a labile ligand, followed by inversion of the configuration through a planar intermediate, even in mild conditions (Scheme 1).^[21]



Scheme 1. Racemization of a tetrahedral complex through dissociation of a labile ligand.

Isolation of enantiopure tetrahedral iron complexes is made difficult by this issue, and their application to catalysis is thus limited.^[18a] The examples reported in literature are mainly half-sandwich complexes containing a cyclopentadienyl or other arene ligands, which impart a higher conformational stability thanks to the π back-bonding from iron atom to empty orbitals of the ligand,^[22] even though racemization processes are still relevant.^[23]

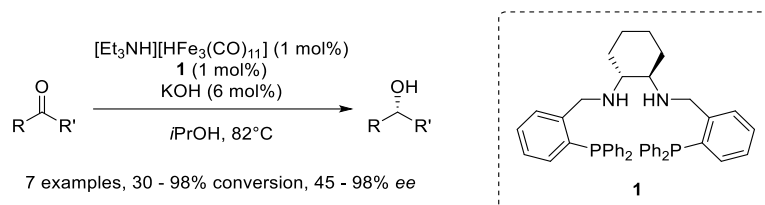
2.2.1. Asymmetric hydrogenation reactions

Octahedral iron complexes have been mainly investigated as catalysts for the enantioselective asymmetric hydrogenation or asymmetric transfer hydrogenation of ketones.^[24] Reduction of carbon-carbon multiple bonds in the presence of iron catalysts has been vastly studied as well, but enantioselective applications are still lacking to the best of our knowledge.^[25]

The first example of non-enantioselective iron-catalyzed hydrogenation of ketones dates back to 1980, when Markó and coworkers reported that the combination of $\text{Fe}(\text{CO})_5$ and triethylamine

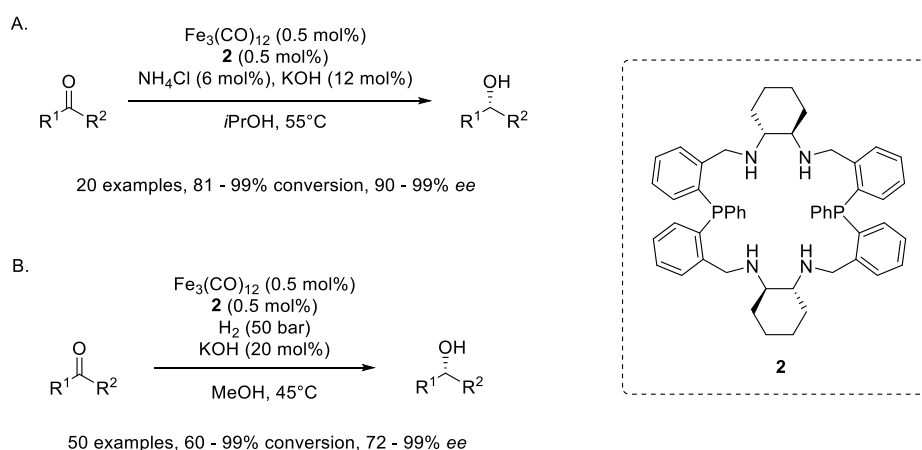
could catalyze the reduction of aldehydes and ketones promoted by hydrogen, even though in harsh conditions (100 bar of pressure and 150 °C for ketones).^[26]

The analogous catalytic system $[\text{Et}_3\text{NH}][\text{HFe}_3(\text{CO})_{11}]$ was employed by Gao and coworkers in combination with a P-N-N-P ligand containing a (*R,R*)-1,2-diaminocyclohexane backbone (**1**, Scheme 2), affording the reduction of ketones in transfer hydrogenation conditions with modest to good *ee*'s.^[27]



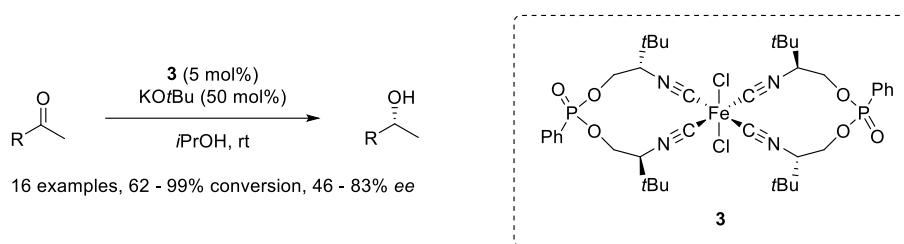
Scheme 2. Asymmetric hydrogenation of ketones promoted by the carbonyl(hydrido)cluster $[\text{Et}_3\text{NH}][\text{HFe}_3(\text{CO})_{11}]$ in the presence of chiral ligand **1.**

Chiral macrocyclic ligand **2** was later synthesized in the same research group and employed in reduction reactions in the presence of $\text{Fe}_3(\text{CO})_{12}$. Asymmetric transfer hydrogenation^[30] and asymmetric hydrogenation^[29] of ketones promoted by this catalytic system are reported in Scheme 3.



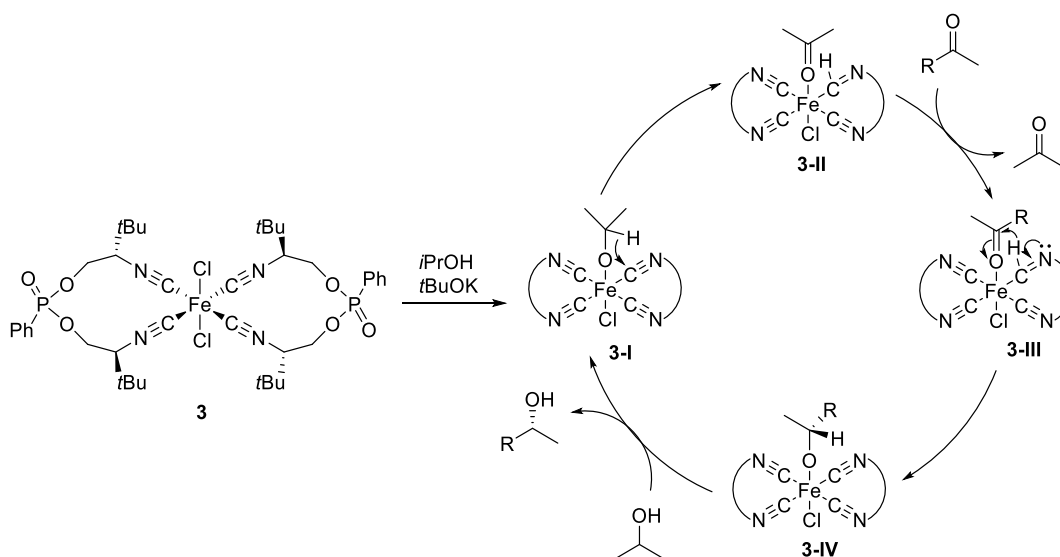
Scheme 3. A. Hydrogenation and B. transfer hydrogenation of ketones promoted by $\text{Fe}_3(\text{CO})_{12}$ in the presence of ligand **2.**

Enantioselective transfer hydrogenation of aromatic ketones catalyzed by bis(isonitrile)iron(II) complex **3** was reported by Reiser in 2010 (Scheme 4). Good conversions were observed in isopropanol at room temperature and in the presence of KOtBu as base, along with moderate *ee*'s.^[30]



Scheme 4. Hydrogenation of aryl and heteroaryl ketones catalyzed by bis(isonitrile)iron(II) complex 3.

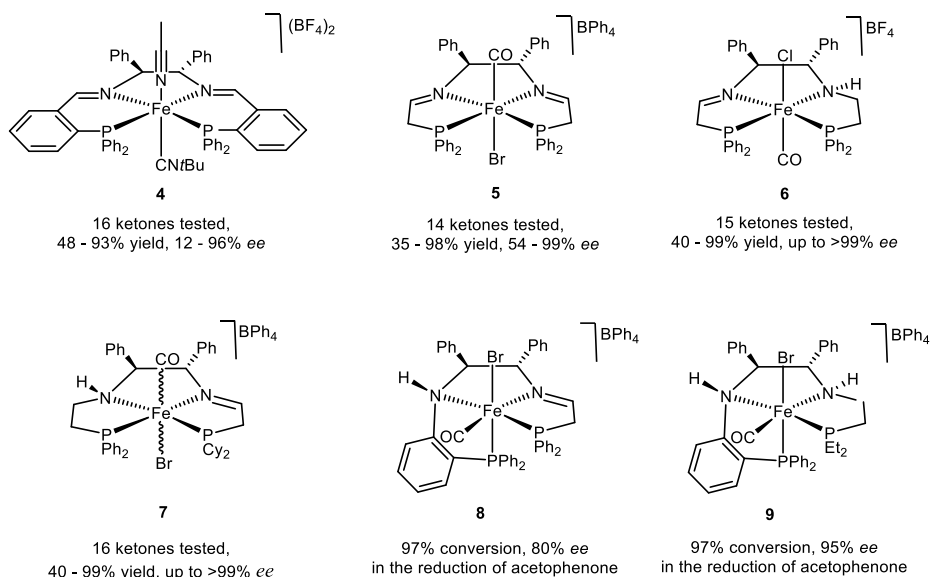
The strategy for asymmetric induction resides in this case in the use of two chiral C_2 -symmetric bidentate ligands, which were found to be directly involved in the catalytic cycle as *cooperating* ligands. A Meerwein-Ponndorf-Verley-type mechanism was proposed for the reaction (Scheme 5): after deprotonation with $KOtBu$, isopropanol coordinates iron, forming the active species **3-I**. One of the isocyanides is then able to abstract one hydrogen from the coordinated isopropoxide. After coordination of the ketone to iron, the generated imine moiety in intermediate **3-III** can thus transfer the hydride to the carbonyl group of the substrate, leading to the reduced product and to the regeneration of the active species **3-I**.



Scheme 5. Proposed mechanism for the hydrogenation of ketones promoted by 3.

An interesting class of complexes in which an iron(II) center is coordinated to tetradentate P-N-N-P ligands showing good activity and selectivity in the reduction of ketones was developed by Morris and co-workers. Selected examples of the catalysts studied by Morris over the last years are reported in Scheme 6: the two nitrogen donors derive both from imines in complexes **4** and **5**,^[31] from an imine and an amine in complexes **6** to **8**^[32] or from two amines in complex **9**.^[32c]

Complexes **4-9** were shown to be active and enantioselective in the transfer hydrogenation of ketones: 98% *ee* and 71% conversion in the Asymmetric Transfer Hydrogenation of acetophenone to (*R*)-1-phenylethanol were reached using complex **7** in the presence of KOtBu in isopropanol, while other ketones were reduced with *ee*'s up to 99%.^[33]



Scheme 6. Structure of selected examples of iron complexes containing tetradentate P-N-N-P ligands developed by Morris' research group.

Mechanistic studies demonstrated that the hydrogenation of catalyzed by complexes **4-9** follows a concerted outer-sphere hydrogen transfer, in which the iron hydride complex (**9-I**, Figure 5) is the catalytically active species, and the cooperating ligand plays a key role acting as proton donor.

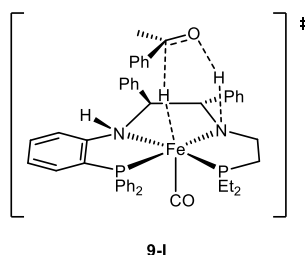
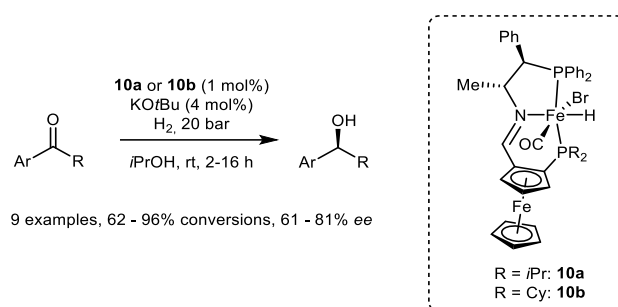


Figure 5. Proposed transition state for the reduction of acetophenone promoted by a 3rd generation Morris' catalyst

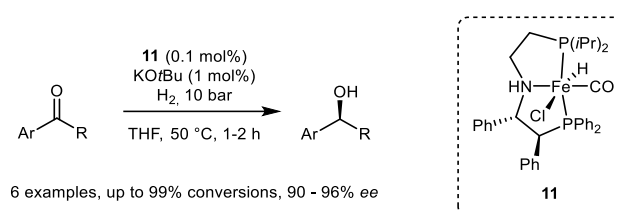
Morris' research group also investigated the use in asymmetric catalysis of complexes containing chiral P-NH-P pincer ligands. Complexes **10a-b**, containing ferrocenyl-phosphine-based ligands,

were tested for the reduction of several alkyl aryl ketones in good yields and moderate to good enantioselectivities (Scheme 7).^[34]



Scheme 7. Hydrogenation of alkyl aryl ketones catalyzed by iron complexes 10a-b.

Complex **11** was employed in the hydrogenation of alkyl aryl ketones under 10 bar of pressure of hydrogen at 50 °C in THF (Scheme), affording in most cases the corresponding alcohols in high conversions and *ee*'s between 90% and 96%.^[35]



Scheme 8. Asymmetric hydrogenation of ketones promoted by 11.

The same P-N-N-P binding sequence present in compounds **4-9** can be found in a series of macrocyclic ligands synthesized and studied by Mezzetti and co-workers. Ligands **12a** and **12b** were firstly prepared in 2014, and contain a chiral diphosphine linked to chiral 1,2-diamines through imine bonds (Figure 6).^[36]

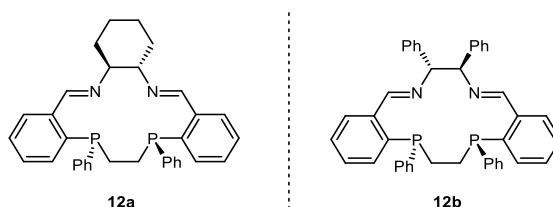


Figure 6. Structure of macrocyclic ligands 12a and 12b.

Iron complexes $[\text{Fe}(\text{MeCN})_2(\mathbf{12a})](\text{BF}_4)_2$ (**13a**) and $[\text{Fe}(\text{MeCN})_2(\mathbf{12b})](\text{BF}_4)_2$ (**13b**) were prepared and characterized: **13a** was isolated as a 3:1 mixture of *trans*- and Λ -*cis*- β stereoisomers, a single isomer with

configuration Λ -*cis*- β was confirmed for **13b** through ^{13}P -NMR analysis (Figure 7). However, both **13a** and **13b** achieved only low conversion when employed in catalytic hydrogenations, probably due to stability issues in the reaction environment.

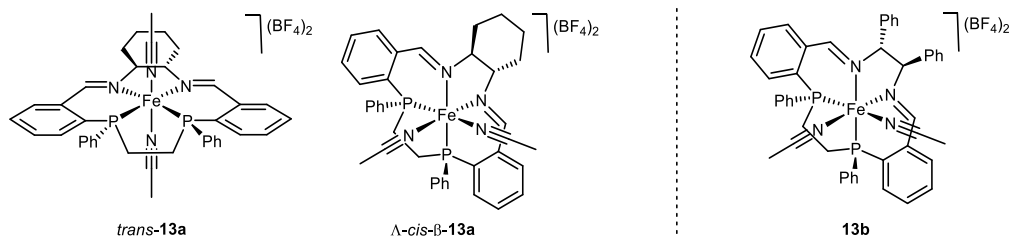
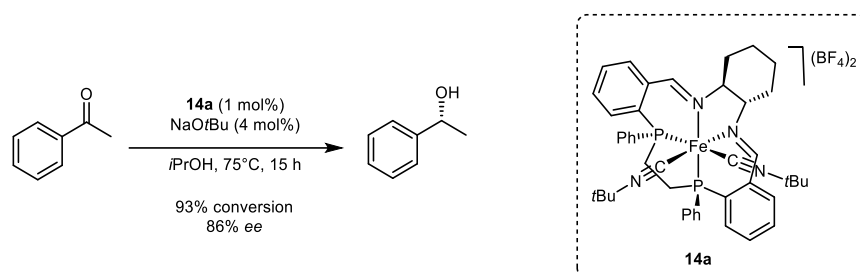


Figure 7. Structure of iron complexes 13a and 13b.

Exchange of the two ancillary acetonitriles with isocyanide ligands led to more stable and active catalytic species. Complex **14a**, containing two *tert*-butyl isocyanide ligands, afforded the reduction of acetophenone to (*R*)-1-phenylethanol in 93% conversion and 86% *ee* (Scheme 9).^[37]



Scheme 9. Asymmetric transfer hydrogenation of acetophenone promoted by pre-catalyst 14a.

Reduction of the two imine moieties in the macrocyclic ligand to amines proved beneficial both in terms of activity and selectivity: complexes **15a** and **15b**, bearing respectively CNCEt_3 and the *N*-isocyanide CNNiPr_2 as ancillary ligands (Figure 8), afforded the reduction of acetophenone in mild transfer hydrogenation conditions with >90% conversion and >96% *ee*.

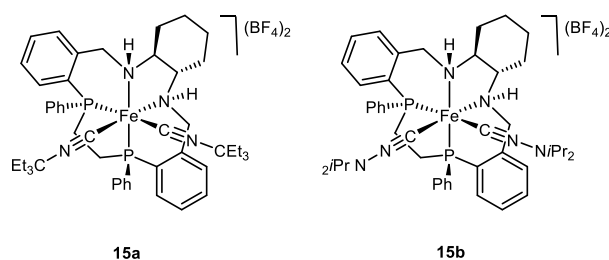
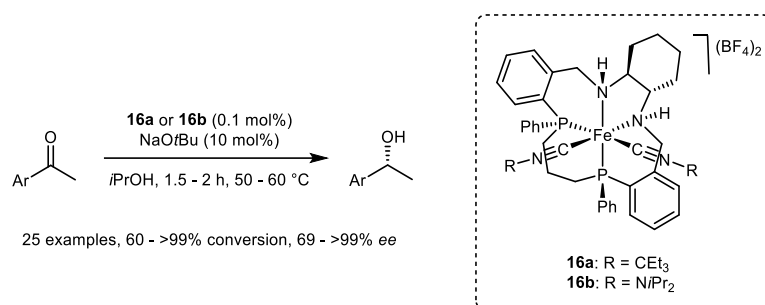


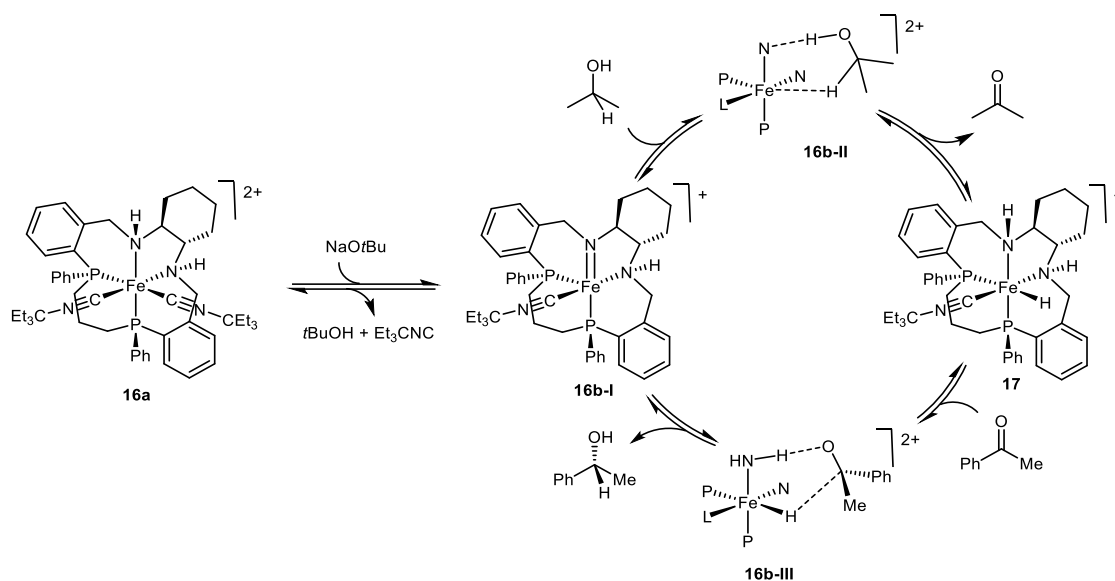
Figure 8. Structure of complexes 15a and 15b.

15-membered macrocycle, showing an extended bridge between the two phosphines, was later prepared, and coordinated to iron. Complexes **16a** and **16b** showed outstanding activity and selectivity as catalysts for transfer hydrogenation, being able to promote the enantioselective reduction of acetophenone and several other alkyl aryl ketones in up to >99% *ee* (Scheme 10).^[38] Improvement in selectivity was imputed to the more conformationally rigid P-Fe-P six-membered chelate ring.



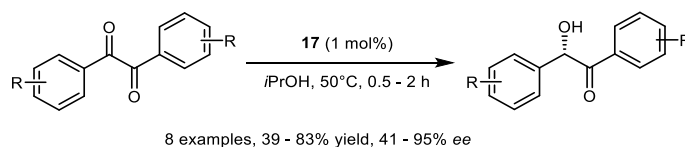
Scheme 10. Asymmetric transfer hydrogenation of aryl ketones promoted by complexes 16a and 16b.

As in the case of Morris' catalysts (Figure 5), the direct involvement of one of the amine donors in the catalytic cycle was proposed: the iron hydride moiety in intermediate **17** can transfer a hydride to the substrate, while the *non-innocent* ligand acts as proton donor (Scheme 11). The rigid conformation of the macrocyclic ligand, the Δ -*cis*- β topology of complexes **16a-b**, which is maintained also in the intermediates directly involved in catalysis, and the use of bulky isonitriles, resulted in an efficient discrimination of the approach of the ketone enantioface to the complex, leading to an iron-based catalytic systems with one of the best selectivities to date.



Scheme 11. Schematic mechanism for the catalytic transfer hydrogenation of acetophenone promoted by 16a.

Iron hydride intermediate **17** (Scheme 11) could also be isolated and employed with success in the asymmetric semi-reduction of aryls to α -hydroxyketones (Scheme 12), which are otherwise difficult to obtain in an enantiopure fashion due to their sensitivity to basic conditions often required by other catalytic systems.^[39]



8 examples, 39 - 83% yield, 41 - 95% ee

Scheme 12. Enantioselective transfer hydrogenation of 1,2-diketones promoted by 17.

Concerning the investigation of tetracoordinated half-sandwich iron species for their application to asymmetric reduction of polar double bonds, increasing attention has been devoted in recent years to (cyclopentadienone)iron complexes, whose use as enantioselective catalyst is described in detail in Section 2.3.3.

2.2.2. Asymmetric *cis*-Dihydroxylation Reactions

Chelating ligands containing four nitrogen donors have been widely employed for the development of iron-based catalytic systems able to promote oxidation processes by miming the activity of enzymes, such as oxidases.^[40] Modular N_4 ligands containing two N -heterocyclic rings

connected by a chiral diamine are commonly used, mostly in epoxidation or *cis*-dihydroxylation reactions.^[41]

Que and coworkers reported in 2001 the first example of iron-catalyzed *cis*-dihydroxylation of alkenes, involving the use of complexes **18a** and **18b** (Figure 9).^[42]

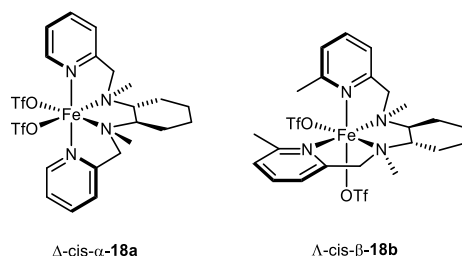
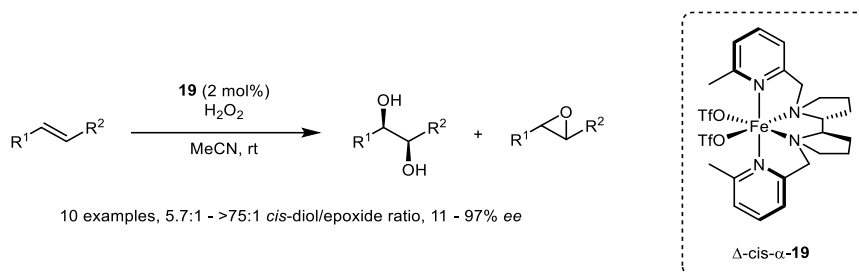


Figure 9. Structure of complexes 18a and 18b.

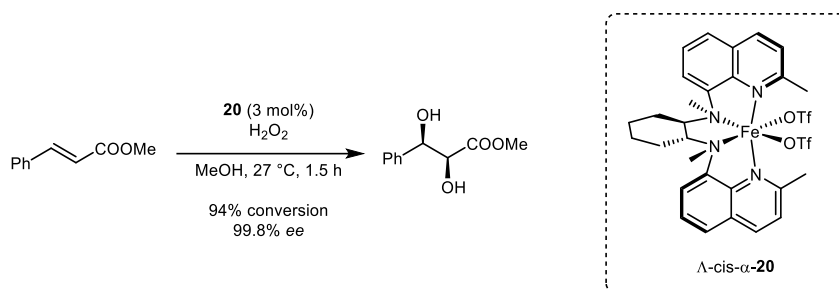
Oxidation of *trans*-2-heptene promoted by H₂O₂ afforded *cis*-2,3-heptanediol and 2-butyl-3-methyloxirane as a mixture of products with both catalysts *cis*-2,3-heptanediol was isolated in 29% *ee* using **18a**, while 79% *ee* was reached with **18b**.

Replacement of the 1,2-diaminocyclohexane linker with a (*R,R*)-2,2'-bipyrrolidine moiety was studied in 2008 by Que.^[43] Complex **19** was tested in the oxidation of electron-rich (*E*)-alkenes with H₂O₂ as oxidating agent (Scheme 13), and led to a generally high diol/epoxide ratios, along with high *ee*'s in some cases (97% for *cis*-2,3-heptanediol, 96% for *cis*-2,3-octanediol).



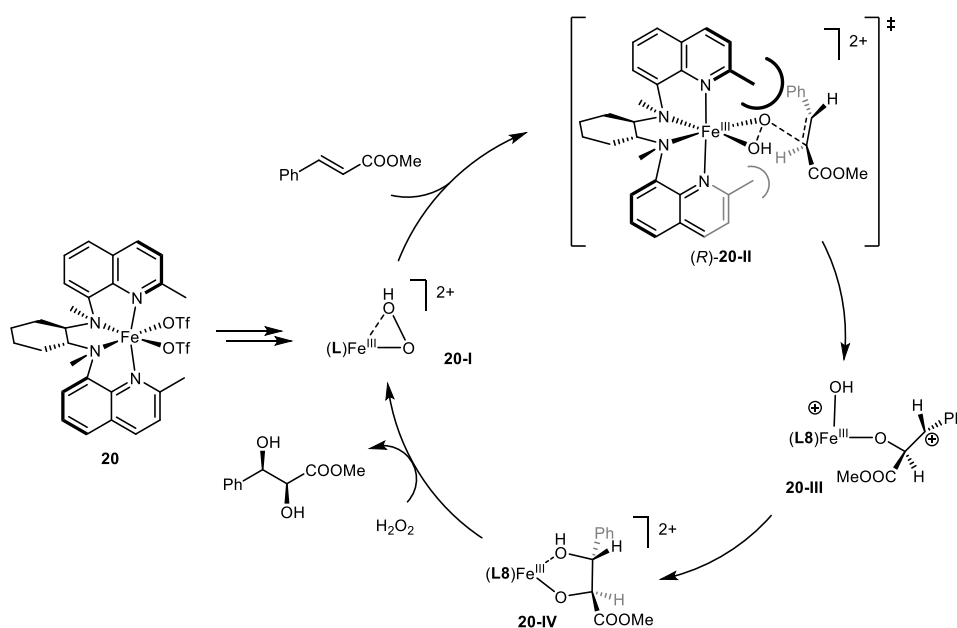
Scheme 13. *cis*-dihydroxylation of alkenes catalyzed by complex 19.

Highly stereoselective H₂O₂-mediated *cis*-dihydroxylation of alkenes was achieved by Che and coworkers in 2016, with the use of complex **20** (Scheme 14).^[44] Both electron-rich and electron-deficient (*E*)-alkenes were selectively oxidized to the corresponding *cis*-diols with >90% *ee*'s. Lower excesses were obtained in the *cis*-dihydroxylation of (*Z*)-alkenes.



Scheme 14. *cis*-dihydroxylation of methyl (*E*)-cinnamate catalyzed by complex **20**.

The proposed catalytic cycle for the reaction of *cis*-dihydroxylation of methyl (*E*)-cinnamate is reported in Scheme 15. Reaction of the pre-catalyst with H_2O_2 leads to the generation of a $\text{Fe}^{\text{III}}-\eta^1\text{-OOH}$ moiety,^[45] which was identified by Che as the species directly responsible for the oxidation of the substrate. The structure of transition state (*R*)-**20-II** is responsible for the enantioselectivity in this reaction: a difference in free energy between the (*R*)- and (*S*)-configured transition states of $-2.6 \text{ kcal mol}^{-1}$ (corresponding to 97.7% *ee*) was calculated through DFT calculations and agrees with the experimental value of 99.8%.^[43]

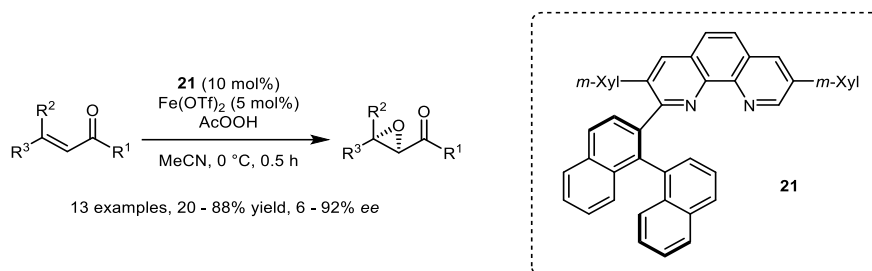


Scheme 15. Proposed mechanism for the *cis*-dihydroxylation of methyl (*E*)-cinnamate promoted by **20**.

2.2.3. Asymmetric Epoxidation Reactions

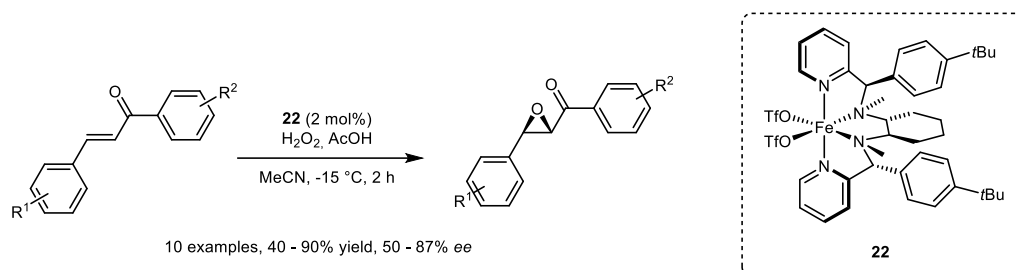
The first example of iron-catalyzed selective epoxidation of alkenes was reported by Yamamoto in 2011 and is based on the use of chiral bidentate *o*-phenanthroline ligand **21** in combination with $\text{Fe}(\text{OTf})_2$ (Scheme 16).^[46] (*E*)-1,3-diphenyl-2-buten-1-one was oxidized in the presence of

peracetic acid to the corresponding epoxide in 80% yield and with 90% *ee*. Other β,β -disubstituted were tested, reaching up to 92% *ee*'s.



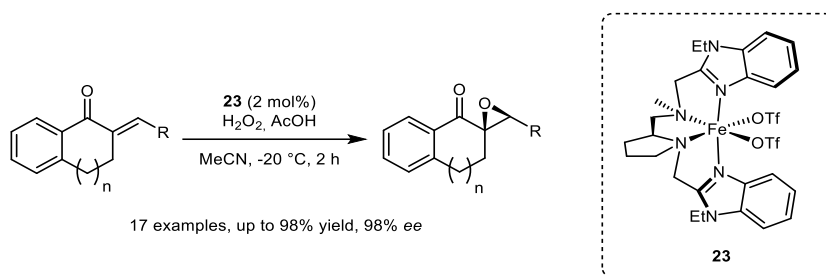
Scheme 16. Epoxidation reaction of β,β -disubstituted alkenes promoted by iron complexes containing ligand 21.

In 2011, Sun and coworkers studied the H_2O_2 -mediated epoxidation of α,β -unsaturated ketones in the presence of iron complex **22** (Scheme 17), and over-stoichiometric amounts of acetic acid, which are essential to avoid the competitive formation of *cis*-dihydroxylation products. Chalcone and derivatives functionalized on the aromatic rings were epoxidized at $-15\text{ }^\circ\text{C}$ with *ee*'s up to 87%.^[47]



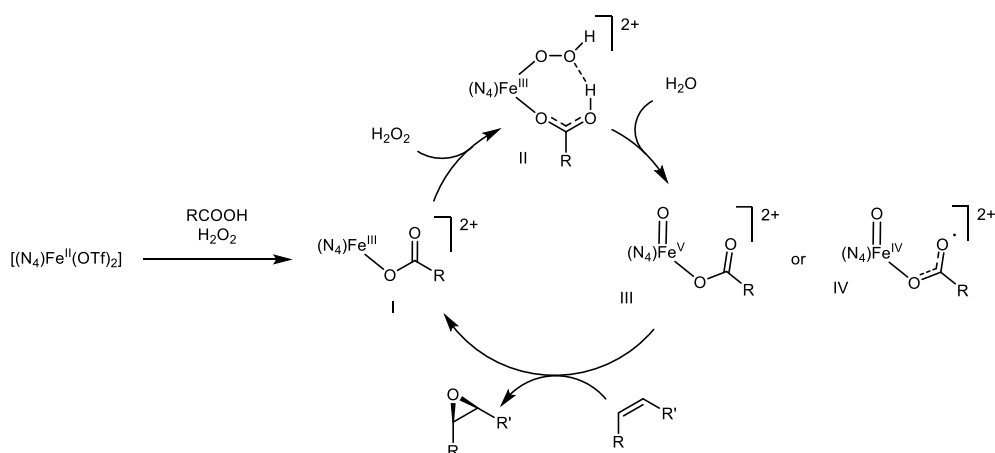
Scheme 17. Epoxidation of chalcones catalyzed by complex 22.

Complex **23**, containing a C_1 -symmetric tetradentate ligand derived from proline and benzimidazole, afforded an increase in both yield and enantioselectivity in the epoxidation of chalcone (90% yield and 92% *ee*).^[48] Epoxides were obtained from the oxidation of several other enones in up to 98% *ee* (Scheme 18).



Scheme 18. Epoxidation of α,β -unsaturated tetralones catalyzed by complex 23.

The mechanism of the reported examples of epoxidation reactions (Scheme 19) was supposed to proceed through the initial oxidation of the Fe^{II} center to Fe^{III} , followed by formation of a $[\text{Fe}^{\text{III}}(\text{OOH})(\text{RCOOH})]^{2+}$ species, that evolves to intermediates containing iron in higher oxidation state (**III**^[49] and **IV**^[50]). **III** and **IV** are regarded as the species responsible for the oxidation process. The presence of the carboxylic moiety in these intermediates explains the effect of the acid additives on activity and enantioselectivity.



Scheme 19. Mechanism for an asymmetric epoxidation reaction catalyzed by iron(II) complexes containing non-heme N_4 ligands.

Enantiomeric excesses and yields could also be improved by the introduction of electron-donating groups on the pyridine rings of the ligand: complexes **24** and **25** (Figure 10), developed respectively by Sun^[50b] and by Costas^[51] both led to epoxidation of several aryl alkenes in up to >99% ee, using either 2-ethylhexanoic, *S*-Ibuprofen or (1*R*,3*S*)-(+)-Camphoric acid.

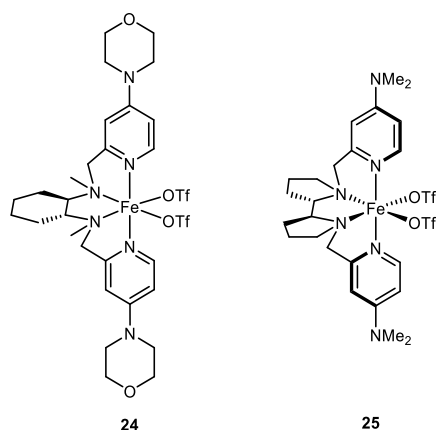
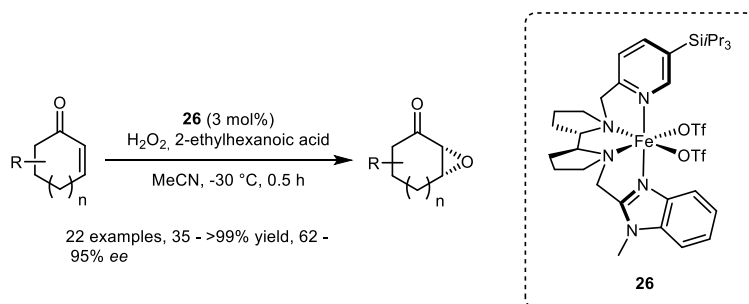


Figure 10. Structure of complexes **24** and **25**.

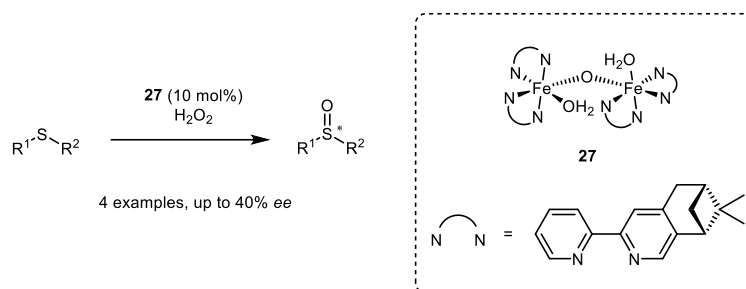
More recently, enantioselective epoxidation of aliphatic cyclic enones was also achieved by the use of complex **26** (Scheme 20): epoxidation of 2-cyclohexenone and 2-cyclopentenone occurred in the presence of 2-ethylhexanoic acid in high yields and in 90% *ee*.^[50b,52] Good results were obtained with several substituted cyclohexenones and cyclohexenyl alkyl ketones as well.



Scheme 20. Asymmetric epoxidation of cyclohexenones catalyzed by complex **26**.

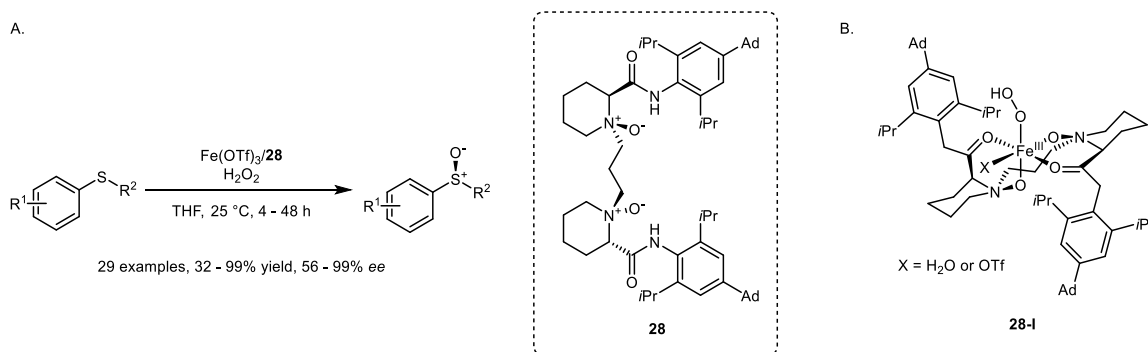
2.2.4. Asymmetric Sulfoxidation Reactions

Examples of oxidation of sulfides to the corresponding sulfoxides mediated by iron-based catalysts are reported in literature.^[42b,53] dinuclear complex **27** (Scheme 21) was developed in 1997 was tested in the asymmetric oxidation of pro-chiral sulfides already in 1997, even though with low to moderate enantioselectivities.^[54]



Scheme 21. Asymmetric sulfoxidation promoted by complex 27.

In 2020 $\text{Fe}(\text{OTf})_3$, combined with ligand **28**, was tested in sulfoxidation reaction (Scheme 22A).^[55] Aryl alkyl sulfides were converted to the corresponding sulfoxides in high yields and up to 99% *ee*. The structure of a $\text{Fe}^{\text{III}}(\text{OOH})$ intermediate (**28-I**) is reported in Scheme 22B. **28-I** was proposed as species responsible for the oxidation process: the chirality of the ligand leads to the generation of a single topological stereoisomer, whose configuration is probably responsible for enantioselection.



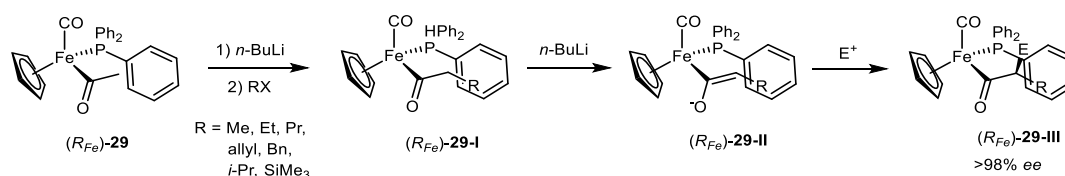
Scheme 22. A. Asymmetric oxidation of aryl alkyl sulfides catalyzed by iron(II) triflate in the presence of ligand 28; B. Structure of intermediate 28-I.

2.2.5. Enantioselective Reactions Involving the Formation of C-C bonds

Among the few tetraordinated iron complexes that have been isolated in an enantiopure form,^[18a] some species were applied as chiral auxiliaries for the generation of carbon stereocenters through the formation of new carbon-carbon bonds.

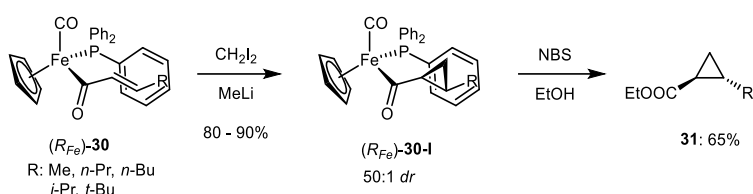
A notable example is the chiral acyl-iron complex **29** (Scheme 23).^[56] After a first functionalization of the position in α to the carbonyl, intermediate **29-I** is formed. Removal of a second proton with *n*-BuLi leads to (*E*)-enolate (R_{Fe})-**29-II**. One of the phenyl rings of the triphenylphosphine ligand is parallel to the plane of the enolate and hinders one of its two faces:^[57] reaction with an electrophile affords thus complex ($R_{\text{Fe}}, S_{\text{C}}$)-**29-III** as a single

diastereoisomer. This intermediate was successfully employed in several asymmetric transformations such as alkylation, aldol condensations, Dienes-Alders reactions, Michael additions and stereoselective synthesis of β -lactams.^[15,58]



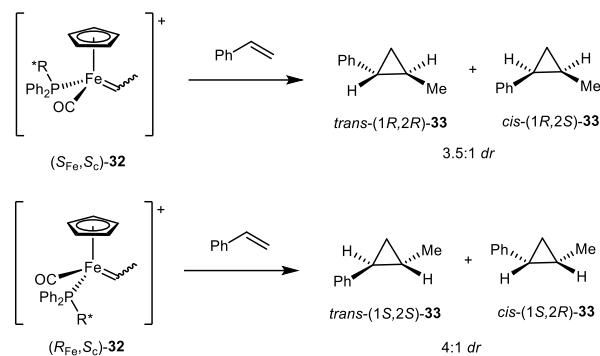
Scheme 23. Enantioselective attack of enolate 29-II on a generic electrophile.

The (*E*)- α,β -unsaturated-acyl iron complex **30** was used as substrate in stereoselective Simmons-Smith cyclopropanation. *trans*-Cyclopropane ethyl ester **31** was isolated in $>50:1$ *dr* after decomposition of the complex (Scheme 24).^[59]



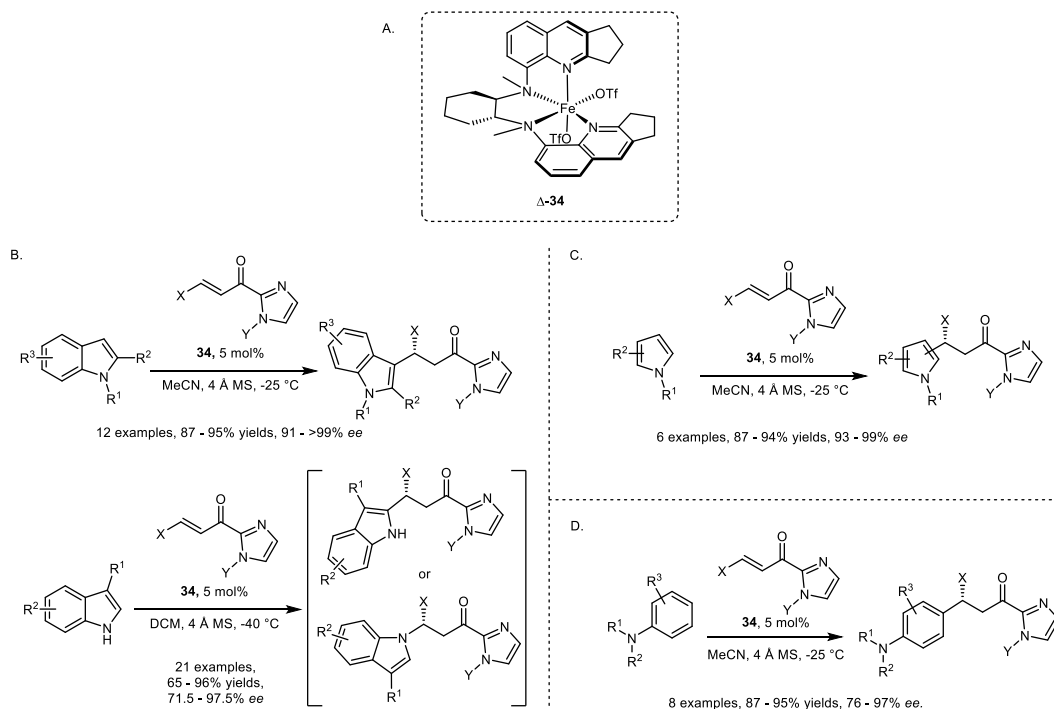
Scheme 24. Enantioselective Simmons-Smith cyclopropanation performed on chiral iron complex 30.

Enantioselective cyclopropanation was investigated by Brookhart and coworkers also using iron carbene complexes (S_{Fe},S_C)-**32** and (R_{Fe},S_C)-**32**, which can transfer a methylene moiety to an olefinic substrate, as chiral auxiliaries (Scheme 25). The two ethylidene complexes were isolated as pure diastereomers thanks to the presence of an enantiopure phosphine ligand and were separately tested in the reaction with styrene. (S_{Fe},S_C)-**32** afforded *trans*-(1*R*,2*R*)-**33** and *cis*-(1*R*,2*S*)-**33** as products, in high *ee*'s (90% *ee* and 84% *ee*) and in 3.5:1 *trans/cis* diastereoisomeric ratio. (R_{Fe},S_C)-**32** led to the opposite enantiomers *trans*-(1*S*,2*S*)-**33** (90% *ee*) and *cis*-(1*S*,2*R*)-**33** (84% *ee*) in a 4:1 *trans/cis* *dr*.^[60]



Scheme 25. Cyclopropanation of styrene performed with complexes (S_{Fe}, S_C)-32 and (R_{Fe}, S_C)-32.

More recently, Che developed a method for the enantioselective alkylation of pyrroles, indoles and *N,N*-disubstituted anilines that involved complex **34** as catalyst (Scheme 26A).^[61] Conjugate addition of α,β -unsaturated 2-acyl imidazoles to variously substituted indoles was achieved, with regioselectivity towards positions 1, 2 or 3 of indole, depending on the substrate, but always with high yields and *ee*'s up to >99% (Scheme 26B). Alkylation of both pyrroles (Scheme 26C) and anilines (Scheme 26D) gave excellent results in terms of enantioselectivity.



Scheme 26. A. Structure of complex 34; B. Alkylation of indole derivatives; C. Alkylation of pyrroles; D. Alkylation of anilines catalyzed by 34.

Mechanistic studies on the functionalization of an imidazole derivative with *N*-methylindole allowed the identification of structure **34-I** (Figure 11) as key intermediate for the

enantioselective outcome. Coordination of the imidazole derivative to iron activates the C=C to nucleophilic attack by the indole, which approaches selectively the *Re* enantioface of the substrate.

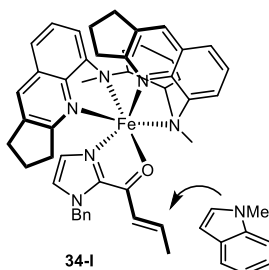
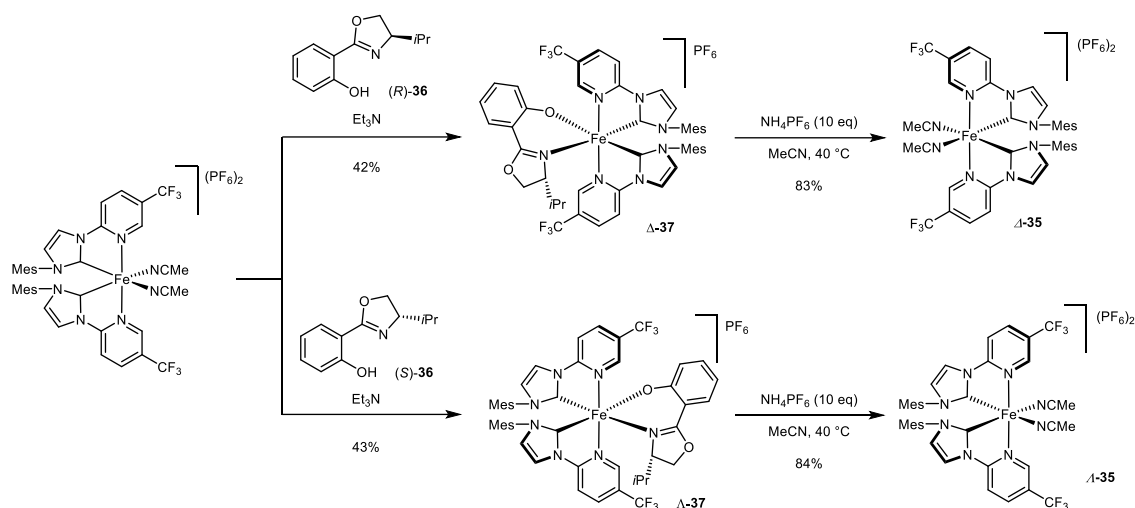


Figure 11. Enantioselective approach of *N*-methylindole to key intermediate 34-I.

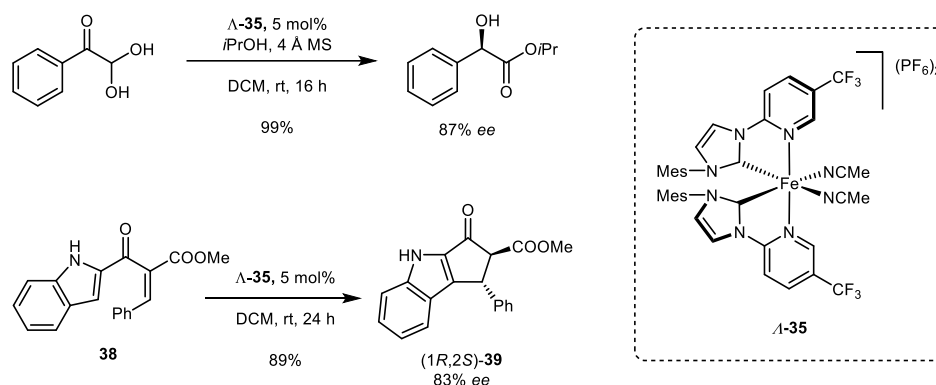
To the best of our knowledge, the only example of a stereogenic-only-at-metal iron complex used in catalysis was reported by Meggers and coworkers in 2019.^[20] Complexes Δ -**35** and Λ -**35** contain only achiral ligands, namely two acetonitrile molecules and two pyridyl-NHC ligands: however, kinetic stability of the coordination of the bidentate ligands allows the isolation of enantiomerically pure complexes. Resolution of the two enantiomers was achieved through coordination of chiral oxazoline ligands (*R*)-**36** and (*S*)-**36** (Scheme 27).

Diastereomers Δ -**37** and Λ -**37** were isolated and treated with NH_4PF_6 , obtaining the pure enantiomers of complex **35**, whose absolute configurations were confirmed via CD spectroscopy. Evidence of the configurational stability of Δ -**35** and Λ -**35** was shown by the authors in subsequent studies:^[62] the configuration is preserved in solution in coordinating solvents or if coordinating solvents are present in solution even in minor amounts, while racemization can occur in non-coordinating solvents if air and moisture are not properly excluded from the reaction environment.



Scheme 27. Route for the resolution of a racemic mixture of complexes Δ -35 and Λ -35.

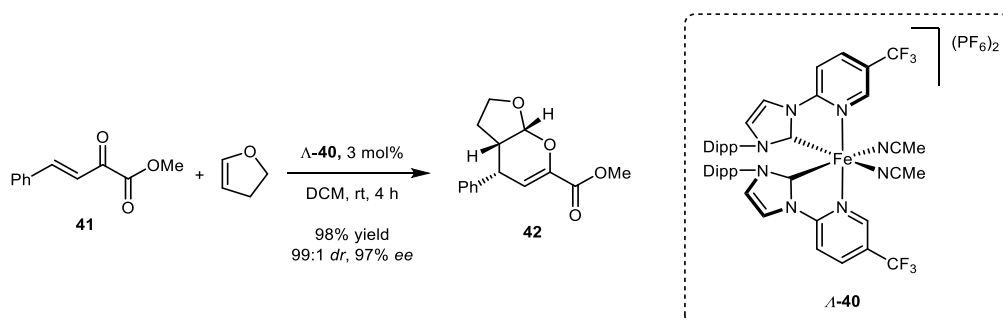
The two enantiopure complexes showed to be active as catalysts for intramolecular Cannizzaro reactions: treatment of phenylglyoxal monohydrate with Δ -35 and Λ -35 afforded isopropyl (*S*)-mandelate and isopropyl (*R*)-mandelate respectively, in both cases with 87% *ee* (Scheme 28A). Λ -35 was also employed as catalyst for the asymmetric Nazarov cyclization performed on substrate **38**, achieving a good enantioselective outcome (Scheme 28B).



Scheme 28. A. Intramolecular Cannizzaro reaction catalyzed by chiral iron complex Δ -35; **B.** Asymmetric Nazarov cyclization catalyzed by Δ -35.

Replacement of the mesityl substituents on the imidazolynylidene ligand with the bulkier 2,6-diisopropylphenyl had a beneficial effect on selectivity, without any detriment to the configurational stability.^[62] Complex Λ -40 (Scheme 29) was isolated in its enantiopure form through the same route described in Scheme 27, and it was tested in the enantioselective hetero-Diels-Alder cycloaddition between β,γ -unsaturated α -ketoester **41** and 2,3-dihydrofuran, which afforded adduct **42** in high yield, 99:1 *dr* and 97% *ee*. The reaction was studied on a small

library of different ketoesters and dienophiles, with excellent diastereoselectivities and enantioselectivities.



Scheme 29. Asymmetric hetero-Diels-Alder reaction catalyzed by complex Λ -40.

The hetero-Diels-Alder reaction proceeds through an *endo* transition state, whose structure was proposed to be as depicted in Figure 12 (Λ -40-I). The steric hindrance generated by the 2,6-diisopropylbenzene groups was hypothesized to shield one enantioface of the β,γ -unsaturated α -ketoester coordinated to iron in Λ -40-I, forcing thus the stereoselective approach of 2,3-dihydrofuran.

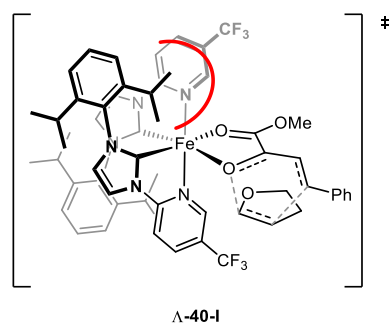


Figure 12. Proposed transition state for the hetero-Diels-Alder cycloaddition.

2.3. (Cyclopentadienone)Iron Tricarbonyl Complexes

Among the several iron-based species known to be active in catalysis, (cyclopentadienone)iron tricarbonyl complexes (Figure 13) have gathered growing interest over the course of the last few years, due to their peculiar stability and their disposition to be involved in two-electron redox processes. These properties made the study of chiral (cyclopentadienone)iron tricarbonyl complexes for their application to asymmetric catalysis an attractive research field.

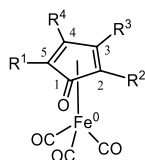
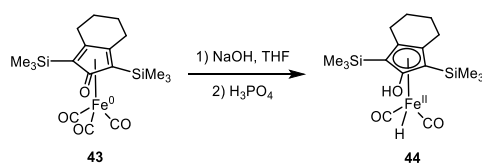


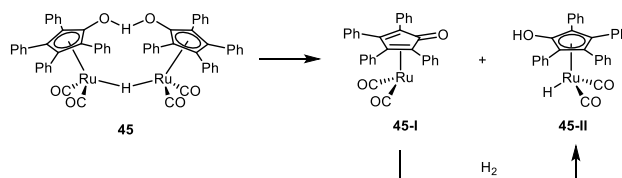
Figure 13. General structure of a (cyclopentadienone)iron tricarbonyl complex.

The first examples of (cyclopentadienone)iron tricarbonyl complexes were reported in 1953 by Reppe and Vetter.^[63] The stability of these coordination compounds to air, moisture and to acidic conditions was immediately acknowledged, and their structure was elucidated by Schrauazer in 1959.^[64] but the key features of their reactivity were observed and investigated only years later, by Knölker^[65] and Pearson.^[66] While screening methods for the isolation of free cyclopentadienones via demetallation of complex **43**, Knölker and coworkers isolated an air- and moisture-sensitive species identified as (hydroxycyclopentadienyl)iron dicarbonyl hydride **44**.^[67] The formation of complex **44** was achieved through a Hieber-base reaction^[68] by treatment of **43** with aqueous NaOH in THF and subsequent addition of an acid. (Scheme 30).



Scheme 30. Generation of (hydroxycyclopentadienyl)iron dicarbonyl hydride complex 44 through Hieber-base reaction.

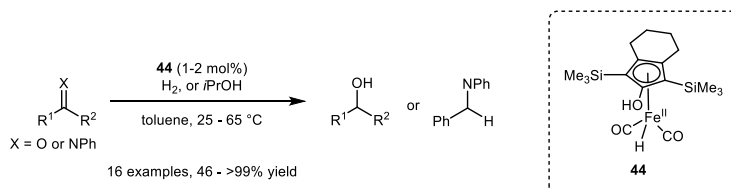
The reactivity of this new Fe^{II} hydride complex was studied more in depth in 2007 by Casey and Guan,^[69] who recognized the structural similarity between **44** and the catalytically active species generated from the dinuclear ruthenium hydride complex known as Shvo catalyst (**45-II**, Scheme 31).^[70]



Scheme 31. Dissociation of dinuclear ruthenium-based complex 45, known as Shvo catalyst.

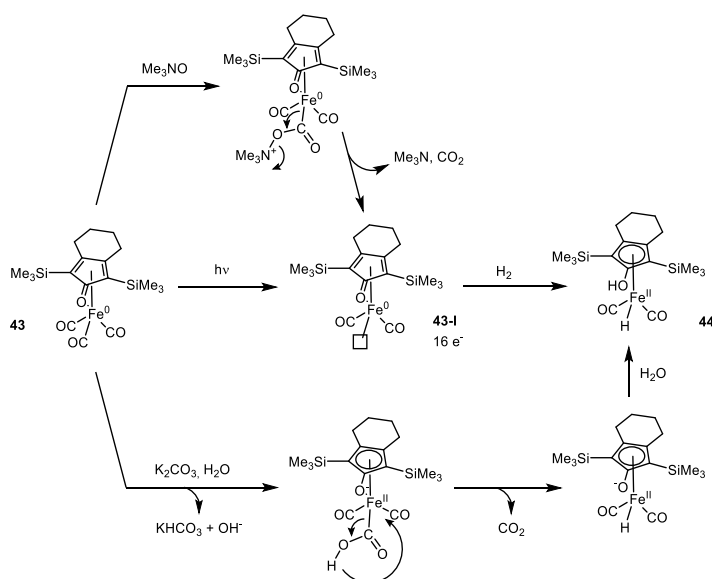
Catalyst **45-II** is formed both by dissociation in solution of **45** and by reaction of the 16-electron complex **45-I** with hydrogen, and is able to promote the hydrogenation of ketones,^[70] imines,^[71] and alkenes.^[72]

Casey and Guan reported that also **44** could catalyze the hydrogenation of ketones and imines, in analogy with **45-II**. Mild conditions were sufficient to achieve good conversions, and reduction through transfer hydrogenation was successfully achieved as well (Scheme 32).^[69,73] Furthermore, the catalytic system showed good chemoselectivity and tolerated diverse functional groups, including carbon-carbon double and triple bonds, halides, epoxides, esters, and nitro groups.



Scheme 32. Hydrogenation/transfer hydrogenation of C=X double bonds catalyzed by complex 44.

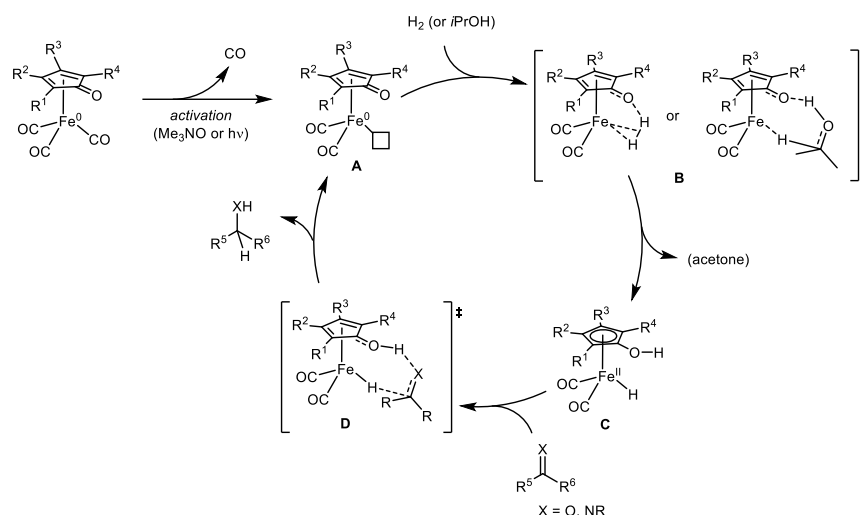
The main drawback related to the use of **44** remained the necessity of preparing and handling it under inert atmosphere. This issue was later solved by generating the active species *in situ* from the parent cyclopentadienone complex. Activation of (cyclopentadienone)iron tricarbonyl complexes can be achieved by treatment with bases, such as K_2CO_3 ,^[74] which leads directly to the Fe^{II} hydride species, or in alternative by decooordination of one CO ligand through oxidative cleavage with trimethylamine *N*-oxide^[75] or photolytic cleavage.^[76] The latter methods lead to the generation of coordinatively unsaturated 16-electron species **43-I**. **44** is then formed by treatment with H_2 or isopropanol (Scheme 33).



Scheme 33. Activation of (cyclopentadienone)iron tricarbonyl complexes through oxidative CO-decoordination, photolytic CO-decoordination and Hieber base reaction.

2.3.1. Reactivity of (Cyclopentadienone)iron Tricarbonyl Complexes

The mechanism through which (cyclopentadienone)iron tricarbonyl pre-catalysts promote the hydrogenation of carbonyl compounds was investigated in depth (Scheme 34).^[77] The catalytic cycle the unusual interconversion between Fe^0 and Fe^{II} , and a key role in this process is played by the cyclopentadienone, which can be regarded to as *redox non-innocent* and *cooperating* ligand. Species **A**, obtained after removal of one CO ligand, acts as a frustrated Lewis pair and promotes the heterolytic cleavage of dihydrogen. In this step the iron center is formally oxidized to a +2 state, and two electrons are transferred from the metal to the cyclopentadienone, which is converted to the aromatic hydroxycyclopentadienyl form shown in structure **C**. The ligand is then directly involved in the reduction: the substrate is activated via hydrogen bonding (**D**), and a proton is transferred from the hydroxycyclopentadienyl moiety to the heteroatom of the $\text{C}=\text{X}$ double bond, while the hydride bound to iron attacks the carbonyl. The reduced product (alcohol or amine) is released, and the 16-electron species **A** is regenerated.



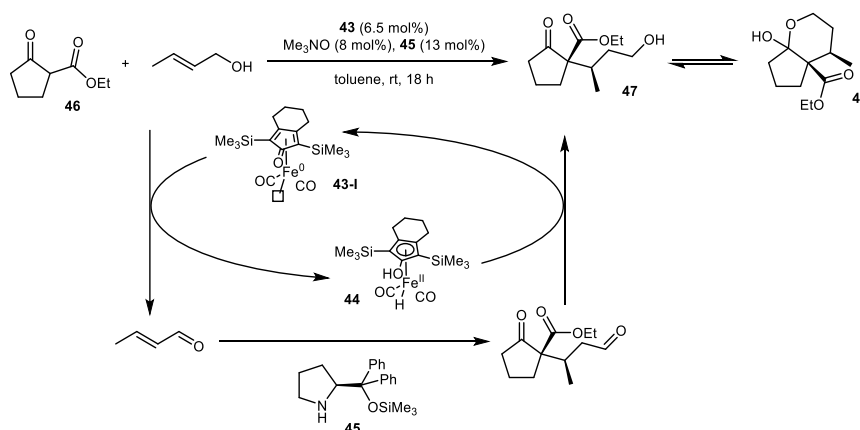
Scheme 34. Schematic representation of the catalytic cycle for hydrogenation of carbonyl compounds promoted by (cyclopentadienone)iron tricarbonyl complexes.

Hydrogenation of acetophenone catalyzed by “Knölker-type” complexes was afforded with TON’s up to 3800 in optimized conditions.^[78] Furthermore, complex **43** was proven an efficient catalyst also in the reduction of sodium bicarbonate to sodium formate,^[79] as well as in the reduction of trifluoroacetates to trifluoroethanol,^[80] and in the photochemical reduction of CO_2 to CO (in combination with an iridium-based photosensitizer).^[81]

The role of **43** in redox processes is not limited to hydrogenation: in the absence of reducing agents, **43** promotes the dehydrogenation of alcohols, affording the corresponding carbonyl compounds in an Oppenauer-type oxidation process.

The ability of **43** to reversibly transfer hydrogen to C=O and C=N double bonds led to the recent investigation of the catalytic activity of (cyclopentadienone)iron tricarbonyl complexes in redox-neutral hydrogen borrowing reactions.^[82]

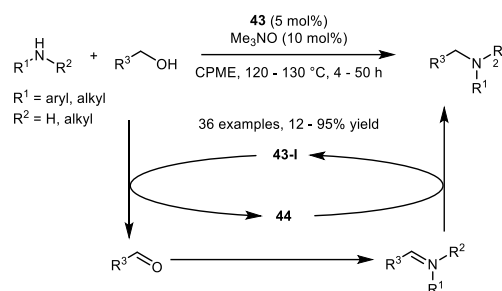
The first example of this reactivity was reported in 2013 by Quintard and Rodriguez, who demonstrated that the dual catalytic system composed by **43** and chiral amine **45** was able to afford a Michael-type condensation between 1,3-diketones and primary allylic alcohols (Scheme 36).^[83] The reaction starts with the dehydrogenation of the alcohol promoted by the 16-electron species **43-I**. Michael addition and subsequent hydrogenation of the aldehyde promoted by **44** afford product **48** in a one-pot procedure.



Scheme 35. α -alkylation of aryl methyl ketones promoted by complex 43.

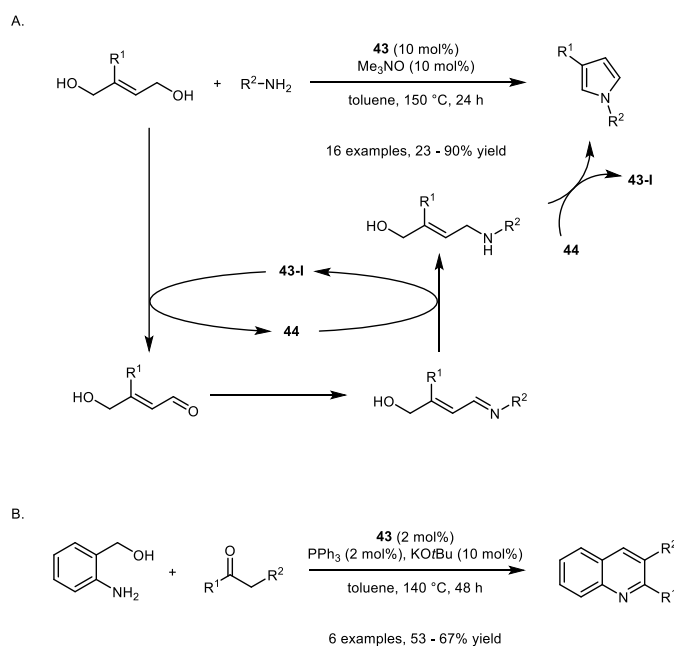
Darcel, Sortais and coworkers reported that **43**, in the presence of Cs₂CO₃ and PPh₃, was able to catalyze the α -alkylation of aryl methyl ketones with primary alcohols in a hydrogen borrowing process.^[84]

N-alkylation of amines with alcohols, which proceeds through initial alcohol dehydrogenation, followed by formation of the imine and its reduction, was firstly reported by Feringa and coworkers in 2014.^[85] The reaction was initially described for several amines in combination with aliphatic alcohols, and later extended to benzylic alcohols in the same research group,^[85] and to secondary alcohols by Zhao and coworkers.^[86]



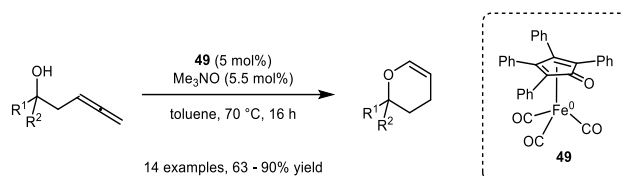
Scheme 36. N-alkylation of amines catalyzed by complex 43.

Oxidative processes involving multiple hydrogen transfer steps have been described as well: Sundararaju and co-workers reported the synthesis of pyrroles starting from primary amines and but-2-ene-1,4-diol derivatives (Scheme 36A).^[87] Sortais, Darcel and co-workers reported a Friedländer-type synthesis of quinolines involving the use of **43** in the presence of PPh₃ and KOtBu and as catalyst (Scheme 37B).^[84] In both these examples, a hydrogen borrowing process takes place, followed by a final oxidation step.



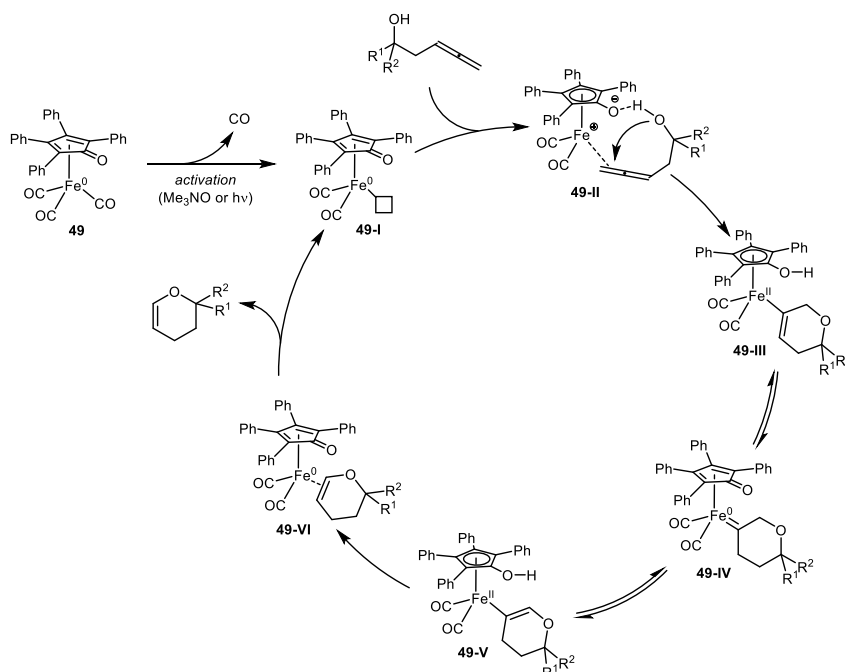
Scheme 37. A. Synthesis of pyrroles promoted by complex 43. B. Synthesis of quinolines catalyzed by complex 43.

The use of **43** and other (cyclopentadienone)iron tricarbonyl complexes was also extended to the iron-catalyzed cyclization of β -allenols by Rueping and coworkers (Scheme 38).^[88]



Scheme 38. Cyclization of β -allenols catalyzed by complex 49.

The reaction mechanism, reported in Scheme 39, involves the coordination of the terminal double bond of the allenic substrate to the iron center of **49-I**, with simultaneous formation of a hydrogen bond between the ligand and the alcohol moiety. The activated substrate undergoes a 6-*endo* cyclization, with concomitant formation of the hydroxycyclopentadienyl form of the ligand. Isomerization between iron vinylidene species **49-III** and **49-V** then occurs through two consecutive proton transfers mediated by the oxygen atom of the cyclopentadienone/hydroxycyclopentadienyl ligand. A protodemetalation step leads to the release of the product and the regeneration of **49-I**.



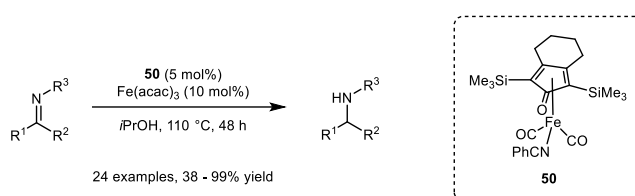
Scheme 39. Proposed catalytic cycle for the carboetherification of β -allenols promoted by complex 49.

The scope of the reaction was then extended to α -allenols and protected α -allenic amines by Rueping and by Bäckvall, with formation of 2,3-dihydrofurans and 2,3-dihydropyrroles.^[89]

2.3.2. Structural Modifications

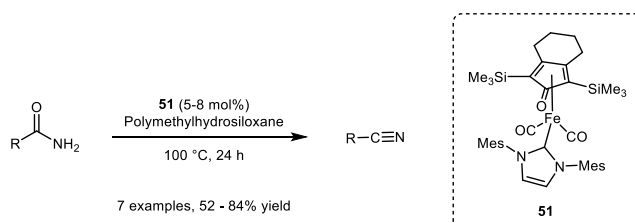
Over the course of the last few years, activity of (cyclopentadienone)iron complexes in redox reactions was further improved through modification of the structure of the cyclopentadienone framework or through exchange of one CO with other ligands, allowing also to experiment new reactivities.^[90]

The exchange of CO has been reported with nitriles,^[69,91] pyridines,^[69] amines,^[66b] phosphines^[66] and N-heterocyclic carbenes (NHCs).^[92] Transfer hydrogenation of ketimines was achieved in good yields using complex **50**, in which one of the CO ligands is substituted with benzonitrile, in the presence of Fe(acac)₃ as Lewis acid co-catalyst (Scheme 40).^[93]



Scheme 40. Transfer hydrogenation of ketimines promoted by complex **50**.

Catalyst **51**, bearing a NHC ligand, was reported to be active in the catalytic dehydration of aromatic or α,β -unsaturated primary amides (Scheme 41).^[92]



Scheme 41. Dehydration of imines catalyzed by complex **51**.

Modification of the cyclopentadienone has been widely investigated by replacing the original six-membered ring fused to positions 3 and 4,^[94] as well as by varying the substitution pattern on positions 2 and 5.^[77,90,95] Noteworthy examples of structures based on this strategy are complexes **52a**, firstly synthesized by Poater and Renaud in 2015,^[96] and **53**, reported in 2017 by Piarulli and coworkers (Figure 14).^[95]

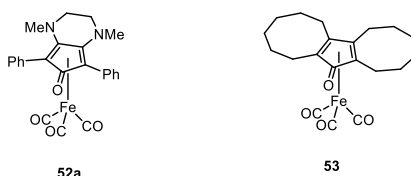
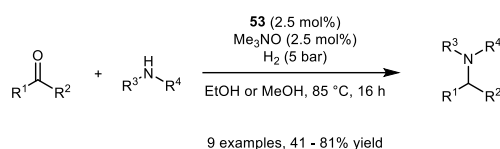


Figure 14. Structure of highly active pre-catalysts 52 and 53.

The two amine moieties attached to the cyclopentadienone ring were reported to increase the electron density of the ligand system, enhancing its Lewis base nature and thus making the activation of C=X double bonds easier. Pre-catalyst **52a** was sufficiently active to be used in the reductive amination of ketones (Scheme 42),^[96] as well as in the conversion of sodium bicarbonate to sodium formate, and in the hydrogenation of CO₂ in the presence of bases.^[97]

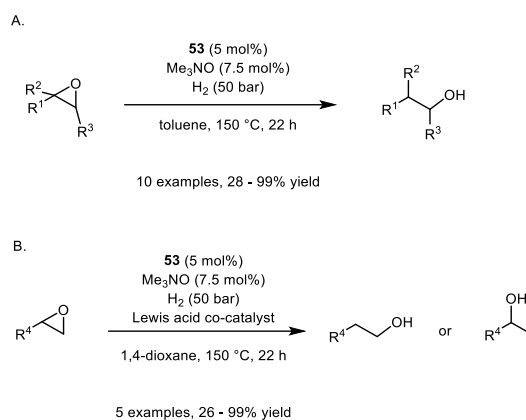


Scheme 42. Reductive amination of aldehydes and ketones catalyzed by complex 53.

The use of **52a** in hydrogen borrowing reactions, such as alkylation of ketones^[98] and of position 3 of indoles and 2-oxindoles,^[99] was also reported.

The concept of increasing the electron density on the ligand was further explored by the same research group, through the preparation of cationic (aminocyclopentadienyl)iron complex **52b**, which afforded reductive amination reactions even at room temperature (Scheme 43A).^[100] Substitution of one CO with PPh₃ was tested as well: complex **52c** was able to promote the 1,4-reduction of α,β -unsaturated ketones with good chemoselectivity (Scheme 43B).^[101]

possible regioisomers of the alcohol product by proper choice of the co-catalysts was remarked (Scheme 45B).



Scheme 45. Hydrogenative opening of epoxides promoted by complex 53.

2.3.3. (Cyclopentadienone)iron Complexes in Asymmetric Catalysis

Considerable efforts have been devoted over the last few years to the preparation of chiral (cyclopentadienone)iron tricarbonyl complexes which could be employed in enantioselective catalysis.^[90,104]

The development of pre-catalysts suitable for the asymmetric hydrogenation of ketones was pioneered by Berkessel and coworkers, who reported in 2011 the exchange of one of the CO in the iron tricarbonyl moiety with chiral phosphoramidite ligands (complexes **54a-e**, Figure 15).^[76]

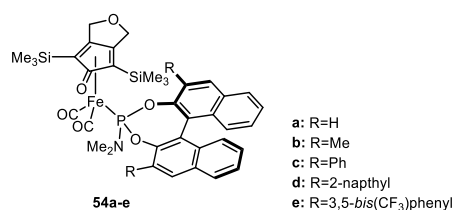
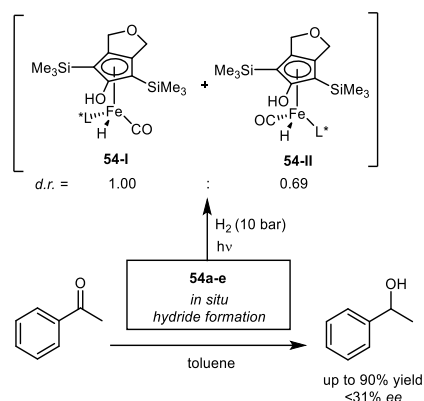


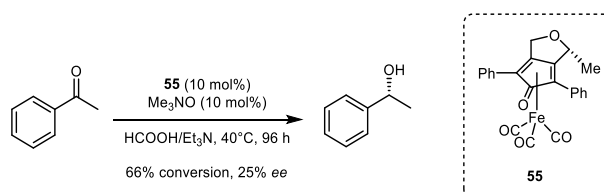
Figure 15. Structure of chiral (cyclopentadienone)iron complexes 54a-e.

Complexes **54a-e** were tested in the hydrogenation of acetophenone, but <31% *ee*'s were observed in the formation of 1-phenylethanol. The low selectivity was ascribed to the generation of a stereocenter at the metal center upon substitution of one of the remaining CO ligands with hydride: ¹H-NMR and ³¹P-NMR experiments showed that activation of the complex with UV light in the presence of hydrogen leads to the formation of both possible stereogenic-at-metal iron hydride diastereomers **54-I** and **54-II** in 1:0.69 ratio (Scheme 46).



Scheme 46. Formation of two possible iron hydride diastereomers during the hydrogenation of acetophenone involving pre-catalyst 54.

Wills and co-workers were the first to experiment the introduction of a stereocenter into the ligand framework: complex **55** was isolated in 2012 and was reported to promote the asymmetric transfer hydrogenation of acetophenone to (*R*)-1-phenylethanol mediated by formic acid and triethylamine in up to 25% ee.^[105]



Scheme 47. Asymmetric transfer hydrogenation of acetophenone catalyzed by chiral complex 55.

In 2015 Piarulli and coworkers described the synthesis of a library of complexes containing chiral cyclopentadienones with a 1,1'-binaphthyl-based backbone (Complexes **56a-j**, Figure 16).^[106]

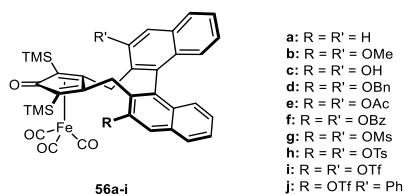
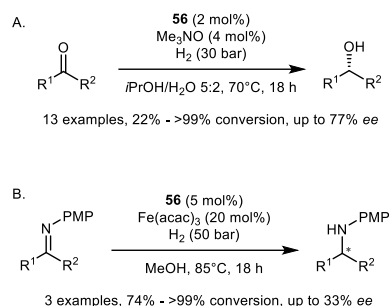


Figure 16. Structure of chiral 1,1'-binaphthyl-based complexes 55a-j.

Complexes **55a-j** were tested in the hydrogenation of acetophenone, and **55b**, containing methoxy substituents on positions 3 and 3' of the binaphthyl system, was identified as the optimal catalyst in terms of activity and selectivity. Full conversion and 54% ee towards (*R*)-1-

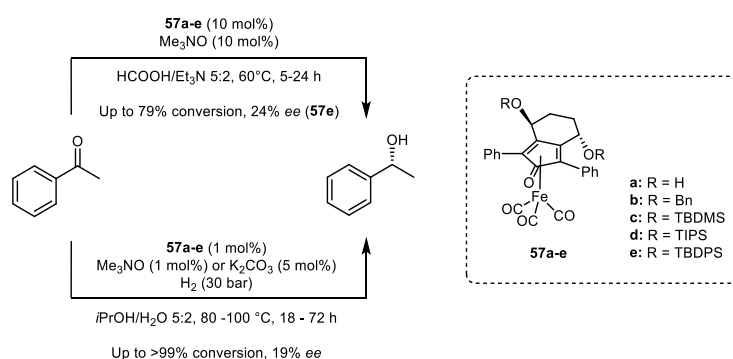
phenylethanol were observed, and the asymmetric reduction of other alkyl aryl ketones and dialkyl ketones was achieved with up to 77% *ee* (Scheme 48A), which remain the highest excesses observed to date with (cyclopentadienone)iron catalysts.



Scheme 48. A. Asymmetric hydrogenation of ketones and B. of imines promoted by complex 56.

The positioning of one of the two methoxy residues near the iron tricarbonyl moiety was proposed as the key feature at the base of enantioselectivity. Hydrogenation of alkyl aryl ketimines in the presence of $\text{Fe}(\text{acac})_3$ as co-catalyst was later reported by the same research group with *ee*'s up to 33% (Scheme 48B).^[102] Replacement of one of the carbonyl ligands of **56** with (*R*)- or (*S*)-MONOPHOS was also investigated, but hydrogenation of acetophenone occurred without major improvements in terms of enantioselectivity (up to 39% *ee*).^[104]

Complexes **57a-e**, containing C_2 -symmetric ligands with two stereocenters in the six membered ring fused to the cyclopentadienone, were synthesized in 2018 by Wills and coworkers, and were reported to catalyze the transfer hydrogenation or the hydrogenation of acetophenone in up to 20% *ee*'s (Scheme 49).^[107]



Scheme 49. Asymmetric hydrogenation and transfer hydrogenation catalyzed by 57a-e.

Introduction of chiral phosphoramidite ligands in place of one CO did not lead also in this case to improvements in selectivity. A second generation of chiral complexes, with modified substituents on the stereocenters and on positions 2 and 5 of the cyclopentadienone ring were

later described in the same research group (complexes **58a-g**, Figure 17):^[108] the highest enantiomeric excess of 36% was observed in the transfer hydrogenation of acetophenone with pre-catalyst **58f**.

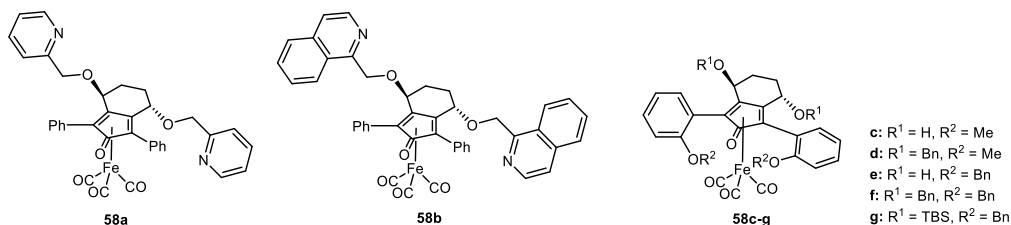
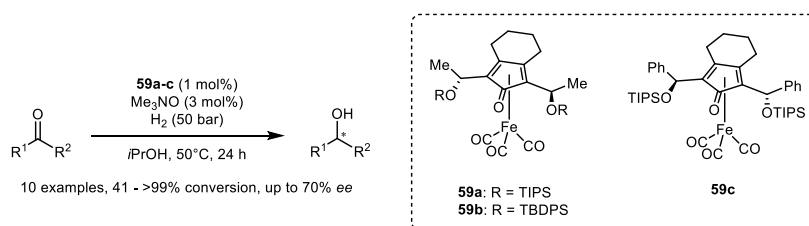


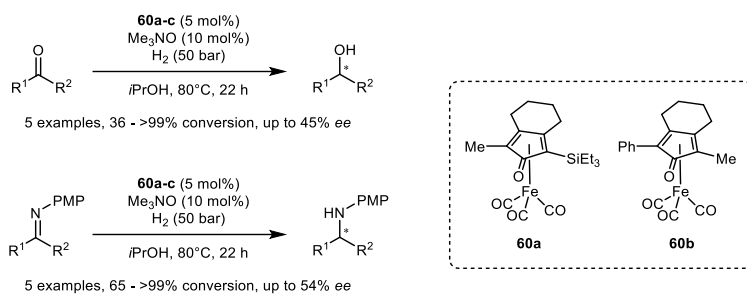
Figure 17. Structure of the second generation of chiral complexes developed by Wills and coworkers.

Higher enantioselectivities were achieved by positioning stereocenters in the front portion of the molecule: De Wildeman and co-workers reported in 2019 the synthesis of complexes **59a-c**, which contain two stereocenters attached to positions 2 and 5 of the ligand (Scheme 50). Complex **59c** afforded the hydrogenation of ketones in up to 70 % *ee*.^[109]



Scheme 50. Hydrogenation of ketones catalyzed by chiral complexes **59a-c**.

Finally, a different approach to the generation of the enantioselective environment around the active site was reported by Gennari and co-workers in 2019. A small library of achiral cyclopentadienones with differently hindered substituents on positions 2 and 5 was prepared: a stereogenic plane is generated upon coordination of the ligand to iron, leading to pairs of enantiomeric complexes. Isolation of enantiopure compounds **60a** and **b** was achieved by resolution through semipreparative HPLC, and the two pre-catalysts were tested in asymmetric hydrogenation. Up to 40% *ee*'s in the hydrogenation of ketones and up to 54% *ee*'s in the hydrogenation of ketimines were observed (Scheme 51).^[110]



Scheme 51. Hydrogenation of ketones and ketimines catalyzed by chiral complexes 60a-b.

Overall, the application of (cyclopentadienone)iron tricarbonyl complexes to enantioselective catalysis is still limited, but the promising results obtained with structures like **56b** and **59c** still draw attention towards this research area.

2.4. Aim of the Thesis

As described in the previous chapter, several approaches to the structural modification of (cyclopentadienone)iron complexes have been investigated during the last decade, in order to optimize their properties and generate more active and selective pre-catalysts. In Figure 18, a summary of the most relevant chiral structures employed so far in asymmetric catalysis is reported.^[90]

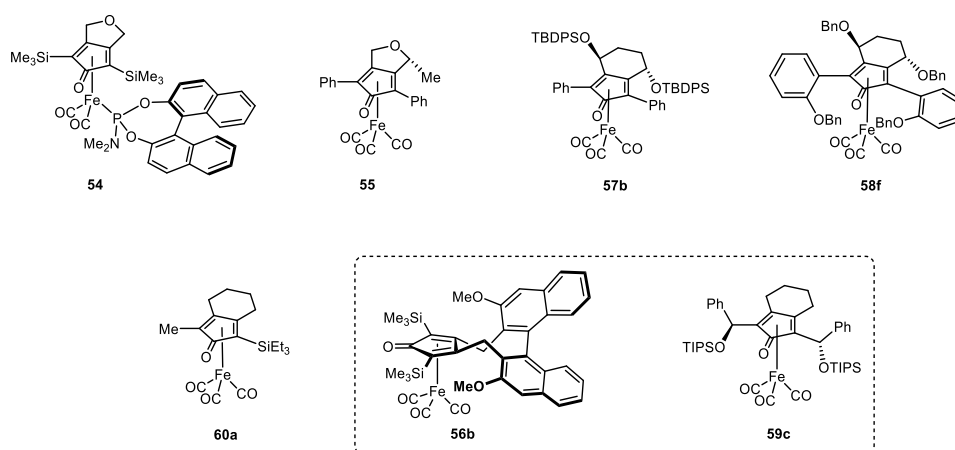


Figure 18. Selected examples of chiral (cyclopentadienone)iron pre-catalysts tested in asymmetric reduction reactions.

The chiral nature of these structures was achieved through different strategies:

- Insertion of one or more stereocenters on the cyclopentadienone ligand (complexes **55**, **57b**, **58b** and **59c**).^[105,107,108,109]
- Use of cyclopentadienone ligands containing an axial-stereogenic binaphthyl moiety (**56b**).^[106]
- Substitution of one CO ligand with a chiral phosphoramidite ligand (complex **54**).^[76]
- Generation of a stereogenic plane through coordination to iron of cyclopentadienones asymmetrically substituted on positions 2 and 5 (complex **60a**).^[110]

However, enantioselectivities observed in the reduction of ketones both in hydrogenation and transfer hydrogenation conditions were generally low. Only complexes **56b** and **59c** afforded 1-phenylethanol in >50% *ee*, and other chiral alcohols in up to >70% *ee*.

On the other hand, the peculiar stability of (cyclopentadienone)iron complexes and their ability to promote hydrogenation reactions in the absence of bases as co-catalysts (which are usually found in asymmetric reductions with other iron-based catalysts) still make the study of new chiral structures an attractive research field.

The aim of the synthetic work reported in this elaborate was the preparation of new iron complexes containing chiral cyclopentadienone ligands, and the evaluation of their activity and selectivity in the asymmetric reduction of carbonyl compounds. Specifically, we focused our efforts on the investigation of methods to generate a proper chiral environment on the front portion of the complexes.

We observed that the best results in terms of selectivity were obtained in those cases in which the steric hindrance of the groups that generated the chiral environment is positioned in proximity of the active site of the catalyst. Complex **56b**, due to the conformationally stable binaphthyl backbone, has a particularly rigid structure (Figure 19), in which one of the methoxy groups bound to the ligand is placed near the iron tricarbonyl moiety, as revealed via X-ray crystallographic analysis. The second methoxy unit hinders the upper face of the cyclopentadienone ring and has no effect on the catalytic process.

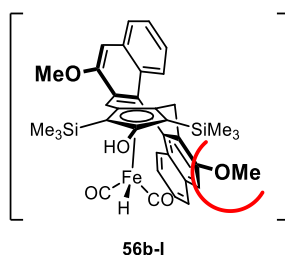
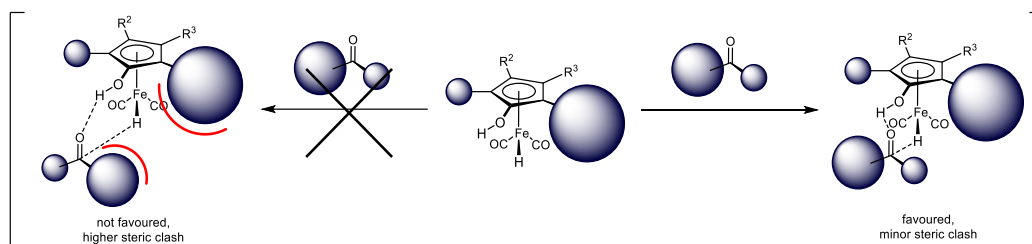


Figure 19. Structure of hydroxycyclopentadienyl iron hydride intermediate 56b-I, obtained from reaction of complex 56b with hydrogen.

In compound **59c** the two stereocenters directly connected to the positions in α to the carbonyl group both bear bulky substituents: thanks to the C_2 -symmetrical nature of the cyclopentadienone, a conformation in which only one of the two triisopropyl silyl groups occupies the space between the iron center and the ligand was proposed.

We aimed thus at preparing (cyclopentadienone)iron tricarbonyl pre-catalysts containing a substitution pattern suitable to generate steric hindrance only on one side of the active site, so that the approach of the ketone to the iron complexes would be forced to happen selectively on the enantioface that causes a minor steric clash (Scheme 52).



Scheme 52. Schematic representation of the enantioselective approach of a ketone to the active site of a (hydroxycyclopentadienyl)iron hydride complex.

Two main strategies for the synthesis of new chiral structures, which will be described in the following chapters, were planned:

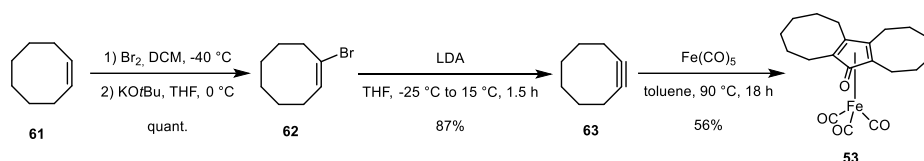
- Preparation of complexes containing C_2 -symmetric cyclopentadienone ligands in which positions 2 and 5 are functionalized with substituents containing stereogenic elements, whose conformation defines the chiral environment around the C=O moiety.
- Preparation of complexes containing C_1 -symmetric cyclopentadienone ligands, bearing substituents with different steric bulk on positions 2 and 5.

The latter strategy is similar to the one already reported for complex **60a**, but a stereogenic element was included in the ligand structure, in order to allow the easier isolation of diastereoisomerically pure complexes.

Since the majority of the novel complexes that have been studied contains aromatic rings connected to the cyclopentadienone ligand, the diyne pre-ligands that were used had to be prepared via Sonogashira cross-coupling reaction between aryl halides and alkynes: a chapter of this thesis will be thus dedicated to the application of this reaction to the synthesis of symmetrically and asymmetrically α,ω -disubstituted α,ω -dienes.

2.5. Complex deriving from a chiral 3-substituted cyclooctyne

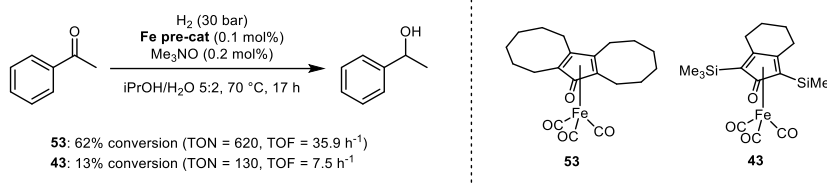
Among the diverse structures based on the (cyclopentadienone)iron tricarbonyl backbone that have been investigated in recent years, [bis(hexamethylene)cyclopentadienone]iron tricarbonyl can be highlighted as one of the most active and versatile pre-catalysts for reduction reactions. This complex can be easily prepared in three synthetic steps from commercially available cyclooctene (Scheme 53).^[95]



Scheme 53. Synthesis of [bis(hexamethylene)cyclopentadienone]iron tricarbonyl **53**.

(Cyclopentadienone)iron tricarbonyl complexes are generally synthesized via one-pot cyclative carbonylation of diynes promoted by a large excess of an iron source (i.e. Fe(CO)_5 or $\text{Fe}_2(\text{CO})_9$), which results also in the complexation of the iron tricarbonyl moiety. Substrates in which the two triple bonds are tethered by a chain of three or four atoms are generally employed, since five- or six-membered rings fused to position 3 and 4 of the cyclopentadienone are generated. Synthesis through intermolecular reaction between two discrete alkynes is far less common, and it was reported to occur in synthetically useful yields only with alkynes bearing specific substituents, such as trialkylsilyl groups,^[111] Cl,^[112] OtBu,^[113] or CF_3 .^[114] Cyclooctyne can easily react with iron pentacarbonyl due to the highly strained geometry of the alkyne moiety and the resulting high reactivity, leading to both cyclative carbonylation/complexation and cyclotrimerization: careful control of the temperature allows to drive the reaction towards the selective formation of **53**.

53 was shown to be remarkably more active in the reduction of acetophenone than other Knölker-Casey-type pre-catalysts like **43** (Scheme 54),^[69b] achieving higher turnover numbers and turnover frequencies.



Scheme 54. Comparison between the activity of complexes **43 and **53** in the hydrogenation of acetophenone.**

Kinetic studies based on the observation of the hydrogen uptake over time demonstrated that the difference in reactivity is related to the fact that the catalytically active species generated from **43** remains active for a shorter interval of time, and the reaction proceeds to completion with a reduced rate. The more robust catalytic system originated from **53** prevents reduction of the reaction rate.

Preparation of a chiral analogue of **53** was thus identified as a potentially valuable strategy for the development of a pre-catalyst showing good activity as well as good selectivity. Thus, the synthesis of a (cyclopentadienone)iron tricarbonyl complex from a cyclooctyne with a stereocenter on position 3 was planned (complex **64**, Figure 20).

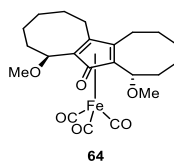


Figure 20. Structure of chiral complex **64.**

The idea of synthesizing a cyclic alkyne substituted at position 3 stems from the observation of the structure of **53**: the two eight-membered rings have a well-defined conformation, in which the two methylene groups directly connected to positions 2 and 5 of the cyclopentadienone bear one hydrogen atom pointing towards the active site of the catalyst, and the other one pointing in the opposite direction. Installation of two stereocenters on these positions leads to a C₂-symmetric cyclopentadienone ligand that ideally, when bound to iron, should generate steric hindrance only on one side of the active portion of the catalyst (Figure 21).

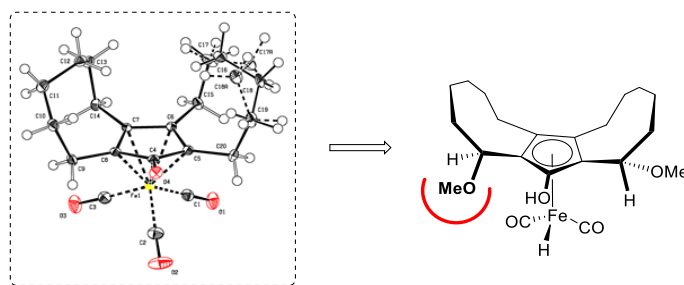
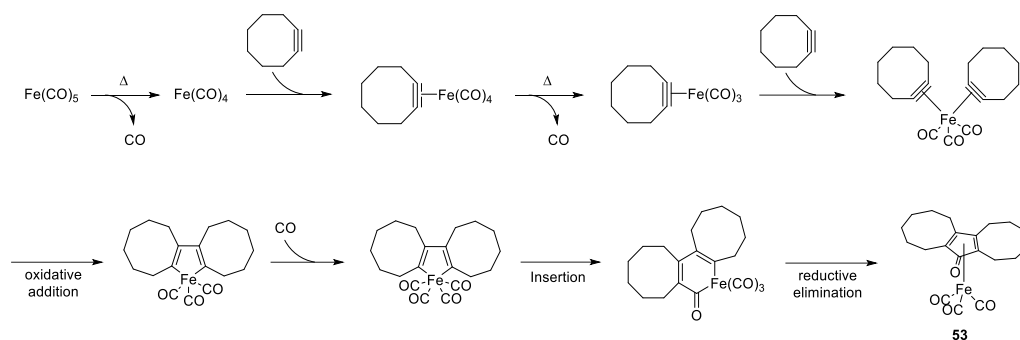


Figure 21. ORTEP diagram (CCDC 1511079) of the molecular structure of **53 compared with a schematic representation of the structure hypothesized for complex **64**.**

Synthesis of (cyclopentadienone)iron tricarbonyl complexes with ligands bearing stereocenters directly connected to their positions 2 and 5 was recently reported by De Wildeman and coworkers: pre-catalysts **59a-c**, described in chapter 2.3.3. (Scheme 50), were tested in the hydrogenation of acetophenone and led to interesting results in terms of enantioselectivities.^[109] Selectivity in these systems is probably imparted by the spatial disposition of the bulky substituents on the two stereocenters, as only one of them is placed on the lower face of the dienone ligand, near the iron center. Nevertheless, rotation around the bond between carbon atoms on positions 2 and 5 of the cyclopentadienone and the stereocenters is in principle still possible to some extent.

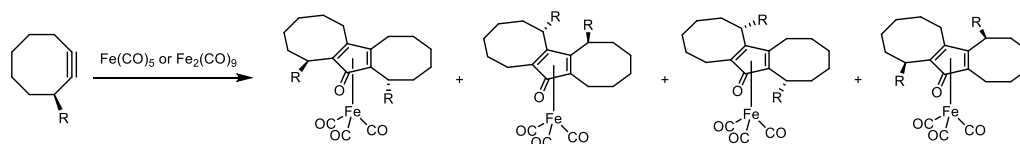
On the other hand, the inclusion of the stereocenters in the cyclic structures fused to the cyclopentadienone ring as represented in Figure 21 prevents rotation and should thus lead to a conformationally locked chiral environment.

A [2+2+1] iron-mediated cycloaddition mechanism has been proposed for the reaction of two equivalents of cyclooctyne with an iron tricarbonyl source to give complex **53** (Scheme 55).^[115] The reaction starts with the sequential substitution of two CO ligands with two alkyne molecules, after which oxidative addition leads then to the formation of a ferrocyclopentadiene intermediate. Upon coordination and insertion of one more carbon monoxide, ferrohexasdienone is generated. The latter metallacycle undergoes reductive elimination, affording iron complex **53**.



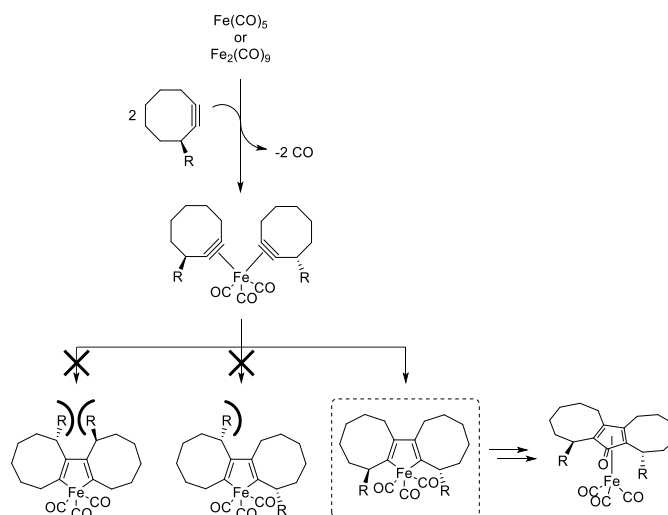
Scheme 55. Mechanism proposed for the formation of complex 53.

The same [2+2+1] pathway can be hypothesized also for the carbonylative cyclization of two molecules of a 3-substituted cyclooctyne: if the reaction is performed on one enantiomer of the substrate, four regio- and stereo-isomers can be generated (Scheme 56), depending on the regiochemistry of the oxidative coupling step.



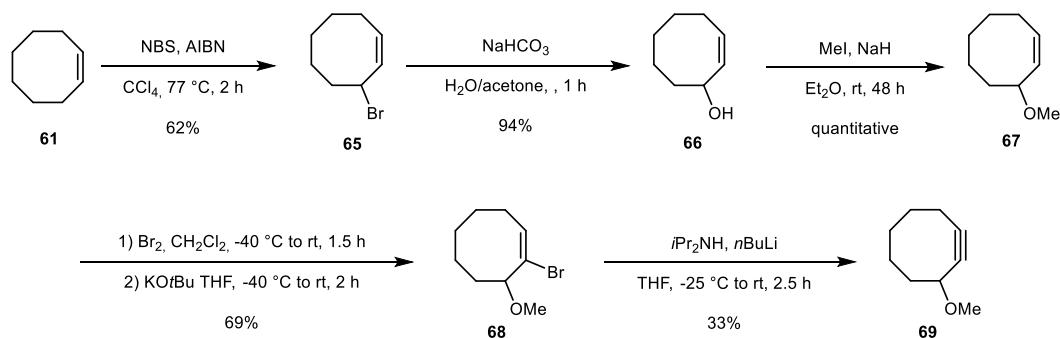
Scheme 56. Possible products deriving from the carbonylative cyclization of an enantiopure 3-substituted cyclooctyne.

Nevertheless, a regioselective outcome was considered possible due to the steric effects of the substituents (Scheme 57), in agreement with the selectivity reported for Pauson-Khand type reactions, where the carbon atoms of the alkyne substrates bearing the bulkier substituents generally binds the carbonyl group.^[116] As an example of this behavior, cyclative carbonylation of ethynyltrimethylsilane with $\text{Fe}(\text{CO})_5$ at 140 °C leads exclusively to the formation of the complex in which the trimethylsilyl residues are bound to positions 2 and 5 of the cyclopentadienone ligand.^[110]



Scheme 57. Regioselective outcome proposed for the carbonylative cyclization of a 3-substituted cyclooctyne.

In order to verify if the supposed regiochemical outcome could be obtained, the complex formation was initially tested on *rac*-3-methoxycyclooctyne. The alkyne was prepared following modified literature procedures starting from *cis*-cyclooctene (Scheme 58).^[117,118]

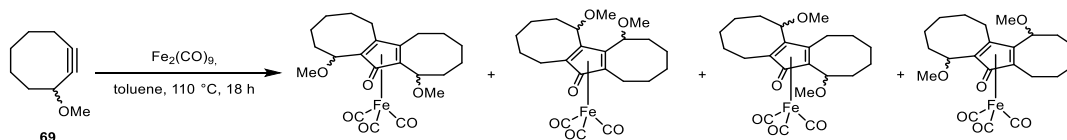


Scheme 58. Synthetic pathway followed for the preparation of *rac*-3-methoxycyclooctyne 69.

Allylic bromination of cyclooctene with NBS followed by hydrolysis of the C-Br bond in basic conditions led to *rac*-3-hydroxycyclooctene **66**, which was quantitatively converted into the corresponding methyl ether **67** using methyl iodide. 1,2-Dibromo-3-methoxycyclooctane was formed through addition of bromine to the double bond of **67** and was treated with KOtBu *in situ* to obtain (*E*)-1-bromo-8-methoxycyclooctene **68** as major isomer. Elimination of the second equivalent of HBr was performed with 0.5 equivalents of lithium diisopropylamide: *rac*-3-methoxycyclooctyne was isolated in 33% yield after purification through distillation and chromatographic column on silica gel.

This synthetic pathway was purposefully chosen because it involves alcohol **66** as intermediate, which could have been later used as starting material for a classical or enzymatic kinetic resolution for the preparation of the enantiopure target alkyne.

At first, carbonylative cyclization was tested in conditions similar to those reported for [bis(hexamethylene)cyclopentadienone]iron tricarbonyl complex **53** (using $\text{Fe}(\text{CO})_5$ as iron source in toluene at 100 °C), but only degradation of the alkyne substrate was observed besides formation of trace amounts of products that could not be identified. Analogous results were obtained working in *m*-xylene at 120 °C. Reaction with $\text{Fe}_2(\text{CO})_9$ (Scheme 59) finally afforded a complex mixture of products, from which four fractions were isolated after separation through chromatographic column in yields ranging from 2% to 4%. All the fractions were analyzed through Mass Spectroscopy and were identified as regio- and stereo-isomers of the target iron complex.

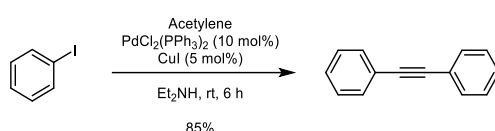


Scheme 59. Carbonylative cyclization of alkyne *rac*-69 with diiron nonacarbonyl.

The presence of multiple isomers, along with the low yields obtained, make the complexation reaction an unattractive way for the synthesis of the desired chiral complex **64**. Thus, synthesis and carbonylative cyclization of enantiopure 3-methoxycyclooctyne were not pursued.

2.6. Sonogashira Cross-Coupling and Synthesis of α,ω -Diyne Pre-Ligands

The alkynylation reaction defined as Sonogashira cross-coupling is one of the most valuable strategies for the formation of a bond between a sp^2 carbon and a sp carbon. The reaction, as it was first published in 1975 by Kenkichi Sonogashira, Tohda and Nobue Hagihara, consists in the coupling between a terminal alkyne and an aryl halide promoted by $PdCl_2(PPh_3)_2$ and copper(I) iodide in diethylamine (Scheme 60).^[119]

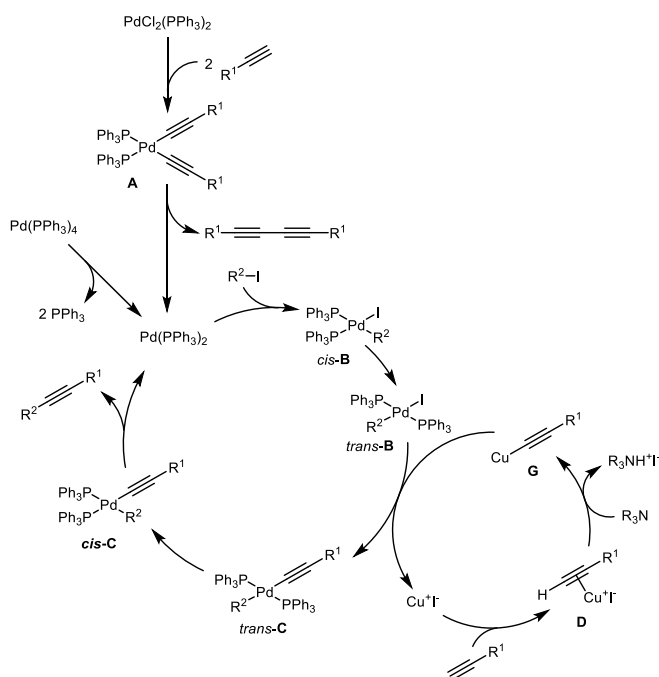


Scheme 60. Synthesis of diphenylacetylene as reported by Sonogashira in 1975.

Copper-mediated synthesis of diarylacetylenes was pioneered by Stephens and Castro, through treatment of aryl iodides with copper(I) acetylides in refluxing pyridine under nitrogen atmosphere.^[120] The reaction represents a straightforward route for the functionalization of terminal triple bonds, although it is limited by the use of copper acetylides, which are not compounds of easy isolation and handling.

In 1975, efficient procedures for the palladium catalyzed alkynylation of vinyl and aryl halides were separately published by Cassar and Heck, but in both cases the conditions were rather harsh. Cassar's method involved the coupling of an aryl halide and an alkyne in the presence of a Pd^0 source and of strong bases ($NaOMe$) to generate the acetylide anion in situ;^[121] in Heck's alkynylation, reaction of aryl or vinyl halides with an alkyne was mediated by a palladium source in an amine as solvent, at 100 °C.^[122]

Sonogashira combined the use of palladium as catalyst, and of copper iodide as co-catalyst, achieving the isolation of diarylacetylenes in good to high yields at room temperature.^[119] The efficacy of this cross-coupling reaction resides in the combination of two separate catalytic cycles involving palladium and copper (Scheme 61).^[123-125]



Scheme 61. Catalytic cycle of the Sonogashira cross-coupling.

The active catalytic species in the Sonogashira coupling is considered to be a low-ligated palladium(0) complex with the structure $[\text{Pd}^0\text{L}_2]$, where L is commonly a phosphine. Starting from complexes like $\text{Pd}(\text{PPh}_3)_4$, the coordinatively unsaturated species $[\text{Pd}^0\text{L}_2]$ is generated by simple de-coordination of two triphenylphosphines. If Pd^{II} compounds, such as the more soluble and stable $\text{PdCl}_2(\text{PPh}_3)_2$, reduction to Pd^0 must take place first: the process is believed to proceed through coordination of two acetylides to the palladium center, and subsequent reductive elimination. $[\text{Pd}^0(\text{PPh}_3)_2]$ is thus formed, along with a small amount of a diacetylene byproduct, whose amount can be larger if oxygen is present in the reaction mixture.

The catalytically active $[\text{Pd}^0\text{L}_2]$ can then coordinate the aryl halide and go through an oxidative addition process that leads first to a *cis*- $[\text{ArPd}^{\text{II}}\text{XL}_2]$ complex, which quickly isomerizes to *trans*- $[\text{ArPd}^{\text{II}}\text{XL}_2]$.

In parallel, the Cu^{I} can form a π -complex with the triple bond of the alkyne substrate. The coordinated terminal alkyne can be deprotonated by the amine, leading to a copper(I) acetylide complex. Through a transmetalation step, the acetylide moiety is transferred from copper to palladium, regenerating the initial Cu^{I} species and intermediate *trans*-C. Conversion from a *trans*- to a *cis*-disposition of the aryl and acetylide ligands allows the final reductive elimination: the functionalized alkyne product is released and the species $[\text{Pd}^0\text{L}_2]$ is regenerated.

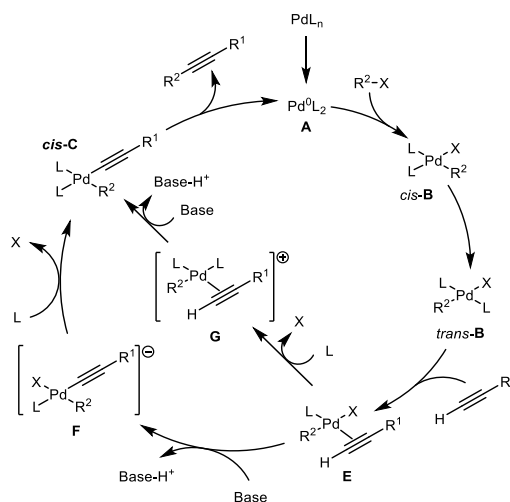
The Sonogashira reaction is thus a well versatile method for the synthesis of substituted alkynes, as it can be performed easily on different alkynes. Aryl, heteroaryl and vinyl iodides can be used as substrates, as well as many bromides. Applications of this reactivity thus are found in the

synthesis of heterocycles and natural products, as well as in the preparation of sensors, dyes, polymers, and many other materials.

Nevertheless, there are limitations related to the operative conditions: since copper(I) species are involved, a strict oxygen-free atmosphere must be maintained to avoid parasite reaction like the copper(II)-mediated homocoupling between two alkynes (Glaser reaction).^[126] Furthermore, the nature of the halide on the sp^2 carbon can influence the yields: chlorides and bromides, especially if the aromatic system is electronrich, undergo oxidative addition more slowly, requiring harsher conditions to react.

Diverse strategies have been developed to make the reaction suitable for less activated halides. The use of microwave heating proved to be beneficial, allowing the isolation of the products of cross-coupling with ethynyltrimethylsilane in excellent yields and short reaction times, with different aryl bromides and triflates, as well as with a chloropyridine.^[127] Modification of the catalytic system has often been an effective strategy: specifically, ways to enhance the ability of palladium to undergo oxidative addition and reductive elimination have been investigated. The use of strong σ -donor and bulky ligands is at the base of this strategy.^[124] Electron-rich phosphine ligands like $P(t\text{-Bu})_3$ or PCy_3 increase the electron density on the metal center favoring the oxidative addition step. Due to the steric hindrance of the substituents on phosphorus the cone angle of such ligands is also large, leading to the stabilization of low-coordinated palladium species like $[Pd^0(\text{phosphine})_2]$ and thus to a higher rate of the reductive elimination. $P(t\text{-Bu})_3$ combined with palladium sources bearing labile ligands $[Pd(OAc)_2, PdCl_2(PhCN)_2, Pd_2(dba)_3]$ allowed the alkylation of aryl bromides at room temperature. Furthermore, rate and yields of the coupling performed in the presence of these trialkylphosphines was not affected when copper was excluded as co-catalyst.^[128]

When copper is not included in the catalytic system, the reaction is often referred to as *copper-free* Sonogashira coupling, and only one catalytic cycle is involved. Also in this case, the aforementioned $[Pd^0L_2]$ is regarded as the starting point of the mechanism (Scheme 62).



Scheme 62. Catalytic cycle for the “copper-free” Sonogashira cross-coupling.

Oxidative addition of the organohalide generates intermediate *cis-B*, which rapidly isomerizes to *trans-B*. The alkyne then replaces one of the neutral ligands, binding palladium through the π -system of the triple bond (intermediate *E*). The commonly accepted mechanism for the formation of the σ -bond between the metal and the sp carbon is believed to require at this point the base-mediated deprotonation of the alkyne. This can happen directly on *E*, generating the anionic species *F*, or after substitution of the halide with a neutral ligand, through a cationic pathway. As in the classical conditions, the product is released after reductive elimination from *cis-C*.

Dialkylbiarylphosphines developed by Buchwald (Figure 14)^[129] have been employed with great success as ligands for the Sonogashira reaction in copper-free conditions with aryl bromides, chlorides and even tosylates.^[130] These species have also the advantage of being more stable and easier to handle than trialkylphosphines. Interestingly, in these cases inhibition of the coupling process was observed when copper(I) salts were added as co-catalysts.

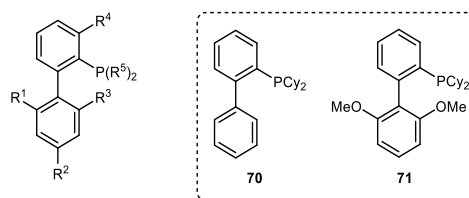


Figure 22. General structure of the dialkylbiarylphosphines developed by Buchwald and of CyJohnPhos (70) and SPhos (71).

Numerous other ligands at phosphorus have been tested, such as ferrocenylphosphines,^[131] multidentate phosphines^[132] or bulkier compounds.^[133] Other examples of sterically hindered

ligands used in Sonogashira cross-coupling are arsines^[134] and NHC ligands.^[135] Finally, also the use of additives like TBAF proved to be beneficial.^[136]

The application of the Sonogashira cross-coupling to the synthesis of α,ω -dialkynes is described in this Section: both classical and copper-free conditions were experimented, and copper-free conditions involving the use of dialkylbiarylphosphines like **70** and **71** (Figure 22) proved beneficial for some of the reactions performed.

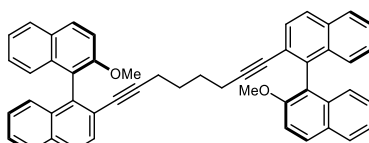
2.6.1. Synthesis of dialkyne precursors for the carbonylative cyclization through Sonogashira coupling

Cyclopentadienone-containing metal complexes can be prepared via direct complexation of a pre-formed cyclopentadienone,^[77,90] but often the most direct way to obtain these compounds involves the *in situ* formation of the dienone moiety via carbonylative cyclization/complexation of a dialkyne precursor in presence of a proper metal source. Many examples of (cyclopentadienone)iron tricarbonyl complexes have been synthesized using this strategy starting from 1,7-octadiyne, 1,6-heptadiyne or other dialkynes.^[77,90] When aliphatic substituents or heteroatoms are attached to the terminal position of the triple bonds, the mono- or di-substituted dialkynes can be prepared through S_N^2 reactions, after deprotonation of the terminal CH: On the other hand, in order to obtain a mono- or di-substitution with aromatic groups from the non-substituted dialkyne, cross-coupling reactions are the most direct way of synthesis.

The focus of the project here described is the synthesis of new chiral (cyclopentadienone)iron tricarbonyl complexes whose ligands contain 1,1'-binaphthyl groups directly connected to the cyclopentadienone ring. Thus, considerable attention has been addressed to the optimization of the synthesis of the dialkyne pre-ligands through cross-coupling reactions.

2.6.2. (*R,R*)-1,8-bis[2'-methoxy-(1,1'-binaphthalen)-2-yl]octa-1,7-diyne (**72**)

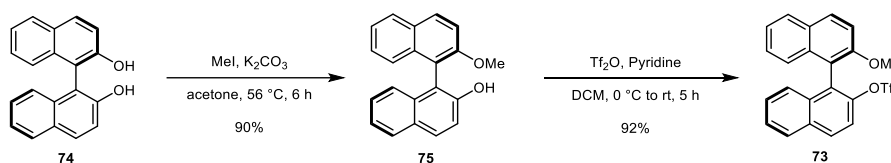
The synthesis of the symmetrically di-substituted 1,7-octadiyne **72** (Figure 23) through Sonogashira coupling was investigated.



72

Figure 23. Structure of 1,8-bis[2'-methoxy-(1,1'-binaphthalen)-2-yl]octa-1,7-diyne (72).

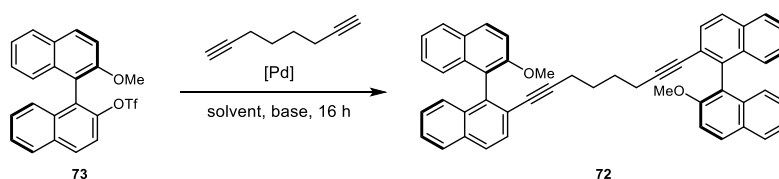
At first, the preparation of **72** was planned through the coupling between commercially available 1,7-octadiyne and aryl triflate **73**, which was isolated starting from (*R*)-BINOL in two synthetic steps (Scheme 63).^[137]



Scheme 63. Synthetic pathway for the preparation of triflate 73.

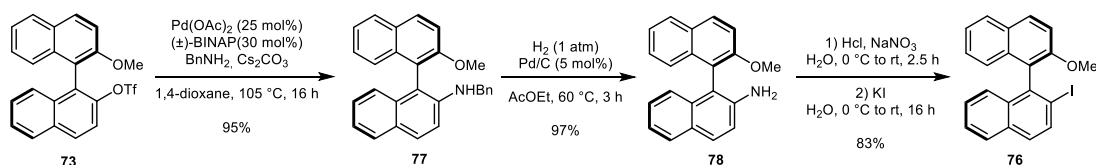
The fact that triflate **73** is not reactive in Sonogashira couplings was already reported in literature for the reaction with ethynyltrimethylsilane.^[137] Nevertheless, coupling with 1,7-octadiyne was tested. Classical Sonogashira conditions were screened, using different Palladium sources both in presence and absence of copper(I), but the starting material was always recovered (Table 1) and formation of product **S1** was not observed.

Table 1. Screening of different condition for the cross-coupling between 73 and 1,7-octadiyne.



Entry	Catalyst	Solvent	Base	Temperature (°C)	Yield in 72 (%)
1	Pd(PPh ₃) ₄ (5 mol%) CuI (10 mol%)	DMF	Et ₃ N	70	<1
2	PdCl ₂ (PPh ₃) ₂ (5 mol%) CuI (10 mol%)	DMF	Et ₃ N	70	<1
3	Pd(PPh ₃) ₄ (5 mol%)	DMF	Et ₃ N	70	<1
4	Pd(PPh ₃) ₄ (5 mol%) CuI (10 mol%)	DMF	Et ₃ N	90	<1

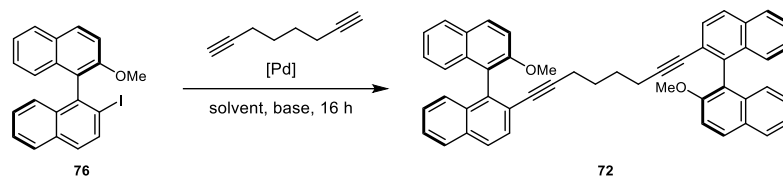
Inadequate activation of the C(sp²)-heteroatom bond (Cl<OSO₂R, Br<I) was identified as a possible reason for the unsatisfactory outcome of the alkylation reaction. 2-iodo-2'-methoxy-1,1'-binaphthyl (**76**) was thus prepared starting from **73** through three more synthetic steps (Scheme 64):^[138] compound **73** was converted to 2-amino-2'-methoxy-1,1'-binaphthyl (**78**) via Buchwald-Hartwig amination with benzylamine, followed by hydrogenolysis of the benzyl group. A diazonium intermediate was formed from amine **78** and treated with KI to give iodide **76**.



Scheme 64. Synthetic pathway followed for the preparation of iodide **76**.

Reaction between 1,7-octadiyne and **76** was investigated: initially, classical Sonogashira coupling conditions were adopted, but no reaction was observed also in this case (Table 2).

Table 2. Screening of conditions for the Sonogashira coupling between **76** and 1,7-octadiyne.

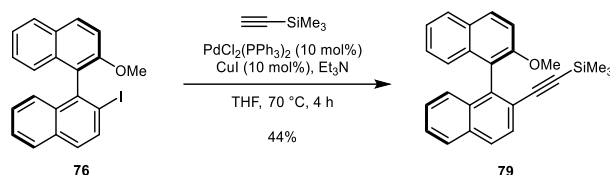


Entry	Catalyst	Solvent	Base	Temperature (°C)	Yield in 72 (%)
1	Pd(PPh ₃) ₄ (5 mol%), CuI (10 mol%)	THF	<i>i</i> Pr ₂ NH	25	<1
2	PdCl ₂ (PPh ₃) ₂ (5 mol%), CuI (10 mol%)	DMF	Et ₃ N	70	<1
3	Pd(PPh ₃) ₄ (10 mol%), CuI (10 mol%)	MeCN/Et ₃ N 1:1	Et ₃ N	80	<1

Even working in harsher conditions, i.e. conducting the reaction at reflux in a 1:1 mixture of acetonitrile and triethylamine, formation of the product was not observed and only minor decomposition of the starting material was detected. In order to verify whether the problem resided in the nature of the aryl iodide or in the alkyne, cross-coupling reactions with different partners were performed on both the starting materials.

Substitution on both the terminal carbon atoms of 1,7-octadiyne through palladium-catalyzed couplings have been already reported in literature: the use of aryl iodides usually allows the

application of standard Sonogashira coupling conditions,^[139] while the reaction with bromoarenes is sometimes feasible as well, even though with different catalytic systems.^[140] On the other hand, a single example is known in literature for the alkynylation of 2-iodo-1,1'-binaphthyl with phenylacetylene,^[141] while Sonogashira couplings involving 2-iodo-2'-methoxy-1,1'-binaphthyl (**76**) or other 2-iodo-1,1'-binaphthyl derivatives have not been published. The reactivity of **76** was investigated more in depth, screening other alkynes as reaction partners: coupling with ethynyltrimethylsilane yielded compound **79** in 44% yield (using THF as solvent, PdCl₂(PPh₃)₄ and CuI as catalysts, and triethylamine at room temperature, Scheme 65).

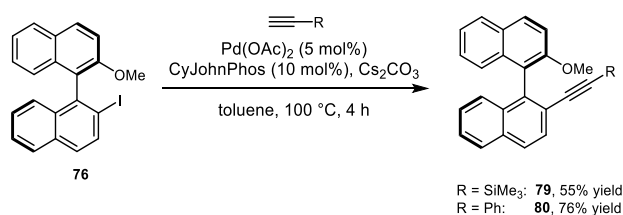


Scheme 65. Synthesis of 79 through cross-coupling between 76 and ethynyltrimethylsilane.

On the other hand, reaction of **76** with prop-2-yn-1-ylbenzene, propargyl ether and trimethyl(octa-1,7-diyn-1-yl)silane resulted again in the recovering of the untouched starting materials.

Isolation of compound **79** confirmed that substrate **76** is not completely inert towards alkynylation reaction, thus the study of this chemistry was extended to the use of more active catalytic systems. More specifically, copper-free conditions were screened: Pd(OAc)₂ was used as palladium source in the presence of electron rich and bulky phosphines.

Conducting the reaction between **76** and ethynyltrimethylsilane in toluene at 100 °C with Pd(OAc)₂ and [1,1'-biphenyl]-2-ylidicyclohexylphosphane (CyJohnPhos, **70**) led to an improvement in the yield on **79**, going from 44% to 55%. The same protocol was successfully applied also to the reaction with phenylacetylene, yielding compound **80** in 76% yield (Scheme 66).

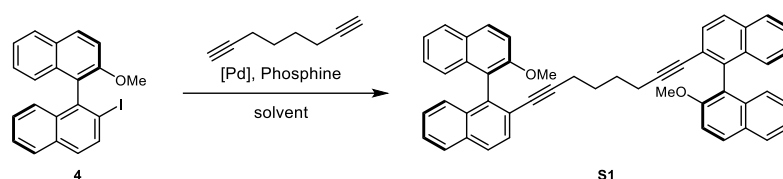


Scheme 66. Conditions for the copper-free Sonogashira coupling performed on 76.

By using Dicyclohexyl(2',6'-dimethoxy-[1,1'-biphenyl]-2-yl)phosphane (SPhos, **71**) along with an excess of ethynyltrimethylsilane (2 equivalents), compound **79** could be isolated in up to 68% yield.

Unfortunately, the same copper-free procedure led to less satisfying results with other alkynes. Coupling between two equivalents of **76** and 1,7-octadiyne in toluene at 100 °C in the presence of Pd(OAc)₂, CyJohnPhos and Cs₂CO₃ led to the formation of compound **72** in 12% yield, but the reaction proved to be scarcely reproducible: **72** could not be isolated again in the same conditions, and variation of the phosphine or of the base did not lead to better results (Table 3).

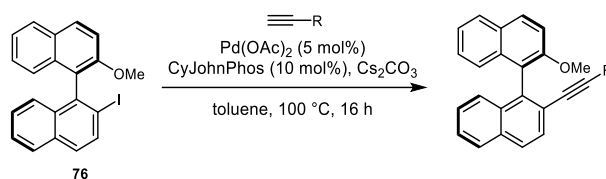
Table 3. Screening of conditions for the copper-free coupling between 76 and 1,7-octadiyne.



Entry	Pd source [%]	Phosphine [%]	Base	Solvent	Temperature (°C)	Time (h)	Yield (%)
1	Pd(OAc) ₂ [7]	CyJohnPhos [10]	Cs ₂ CO ₃	Toluene	100	3	12
2	Pd(OAc) ₂ [7]	CyJohnPhos [10]	Cs ₂ CO ₃	Toluene	100	16	<1
3	Pd(OAc) ₂ [5]	CyJohnPhos [10]	Cs ₂ CO ₃	Toluene	100	6	<1
4	Pd(OAc) ₂ [5]	SPhos [10]	Cs ₂ CO ₃	Toluene	90	16	<1
5	Pd(OAc) ₂ [5]	<i>rac</i> -BINAP [10]	K ₂ CO ₃	Toluene	100	16	<1

The behavior of **76** in the copper-free conditions was then screened more in depth with other alkynes (Table 4). Mono-protected dialkyne trimethyl(octa-1,7-diyn-1-yl)silane was used (entry 4), but no reaction occurred. Propargyl ether was tested as well, but the cross-coupling product was not formed (entry 5). Finally, reaction with prop-2-yn-1-ylbenzene did not lead to the product once again. The presence of propargylic protons in the alkyne moiety, in combination with the low reactivity of **76**, were hypothesized to concur to worsen the outcome of the reaction: the electron-rich alkyne quickly interacts with the palladium catalyst, making the oxidative addition, which is already difficult due to the low reactivity of **76**, even slower. However, products deriving from the degradation of the alkynes were not isolated and characterized.

Table 4. Tests of Sonogashira cross-coupling on 76 with different alkynes.



Entry	Alkyne	Yield (%)
1		55
2		76
3		<1
4		<1
5		<1
6		<1

2.6.3. Alkynes Connected to a (*R*)-2,2'-bis(methoxymethoxy)-[1,1'-binaphthalen]-3-yl Moiety

As previously described for complex **72**, we aimed to prepare C_2 -symmetric dialkyne **81** (Figure 24) through a Sonogashira cross-coupling performed on the two terminal positions of 1,7-octadiyne. In this case, the $C\equiv C$ triple bonds are bound to the aromatic system on position 3 of the binaphthyl derivative.

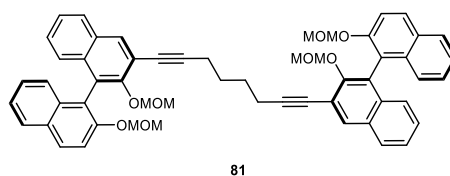
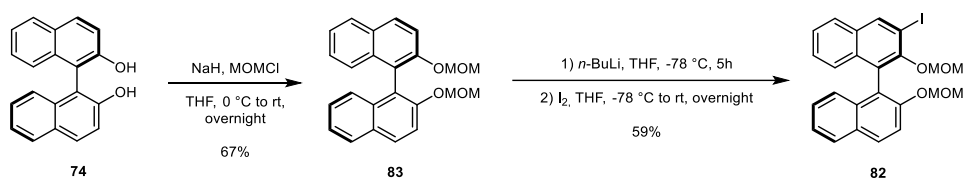


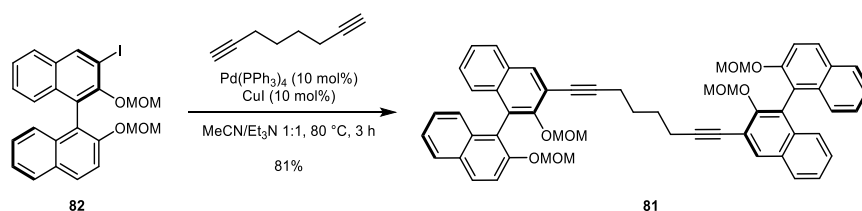
Figure 24. Structure of C_2 -symmetric dialkyne **81.**

Aryl iodide **82** could be easily accessed in just two steps starting from (*R*)-BINOL, whose OH groups were initially protected as MOM ethers to allow the following deprotonation/iodination step (Scheme 67).^[142] The methoxymethyl protecting groups were chosen to improve the yield of the iodination: deprotonation with *n*-BuLi is facilitated and selectively directed to position 3 on account of the chelating effect of the two oxygen atoms of the acetal group on the lithium cation.



Scheme 67. Synthesis of iodide 82.

For the coupling with 1,7-octadiyne, a methodology reported for the alkylation of **82** with Phenylacetylene was followed:^[143] the reaction was performed in a 1:1 mixture of acetonitrile and triethylamine with Pd(PPh₃)₄ and CuI, and afforded the desired product **81** in 81% yield (Scheme 68). The same coupling with 1,7-octadiyne in THF at room temperature with a lower amount of amine was less efficient, leading to the formation only of trace amounts of **81**. In this case, also the application of copper-free conditions (Pd(OAc)₂, SPhos and Cs₂CO₃ in toluene at 100 °C for 4 hours) did not result in major improvements.



Scheme 68. Synthesis of 81 through cross-coupling between 82 and 1,7-octadiyne.

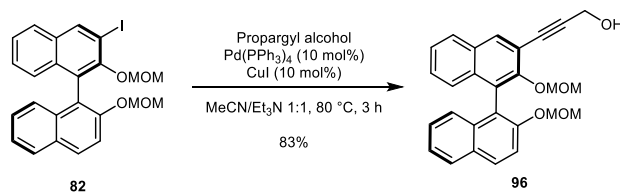
The synthesis of asymmetrically substituted 1,7-octadiynes containing the (*R*)-2,2'-bis(methoxymethoxy)-[1,1'-binaphthalen]-3-yl moiety on one end of the dialkyne chain was then undertaken.

The same conditions were applied to the reaction of **84** with 1,7-octadiyne derivatives already substituted on one of the two terminal positions, and led to the isolation of a small scope of *C*₁-symmetric 1,7-octadiynes functionalized on one end with a binaphthyl derivative and on the other end with aliphatic groups (Me, compound **84**), heteroatoms (SiMe₃, compound **85**), and aromatic rings (Phenyl, Mesityl, Pentafluorophenyl, and 2,6-Dimethoxyphenyl groups, **86-89**). The results of the cross-couplings are reported in Table 5.

Table 5. Sonogashira cross-coupling between 82 and alkynes 90-95.

Entry	Dialkyne substrate	Residue -R	Product	Yield (%)
1	90	-Me	84	74
2	91	-SiMe ₃	85	72
3	92	-Ph	86	75
4	93		87	65
5	94		88	77
6	95		89	80

Propargyl alcohol was also used as starting material in the same conditions. Compound **96** was isolated in 83% yield (Scheme 69) using two equivalents of the alkyne substrate.

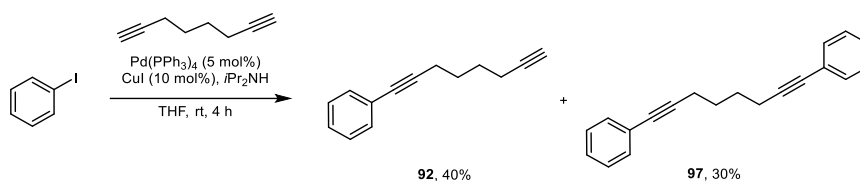


Scheme 69. Synthesis of alcohol 96.

2.6.4. Mono-substituted 1,7-octadiynes

While compounds **90** and **91** were prepared following literature-known procedures,^[110] the synthesis of the other alkynes used in the screening reported in Table 5 (**92-95**) was achieved in turn via Sonogashira coupling between 1,7-octadiyne and the corresponding aryl halides.

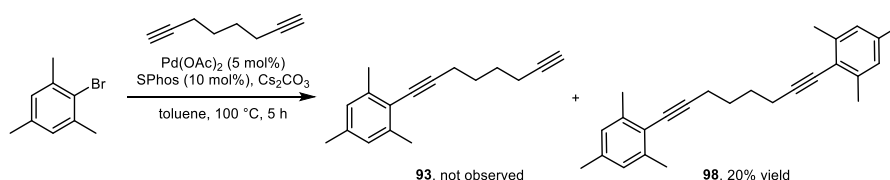
Examples of mono-substitution of 1,7-octadiyne can be found in the literature.^[144,145] Isolation of 1-Phenyl-1,7-octadiyne (**92**) was reported in 75% yield from iodobenzene and 1,7-octadiyne in THF at room temperature, using Pd(PPh₃)₄ and CuI as catalytic system, and diethylamine as base.^[144] Running the same reaction in the above mentioned conditions, just substituting diethylamine with diisopropylamine, led us to the formation of **92** in trace amounts, along with a 47% of di-substitution product **97**. 40% yield in **92** was achieved in higher dilution conditions and with 2 equivalents of 1,7-octadiyne, but still with a 30% of **97** (Scheme 70).



Scheme 70. Mono-functionalization of 1,7-octadiyne with iodobenzene. Concentration: 0.075 M

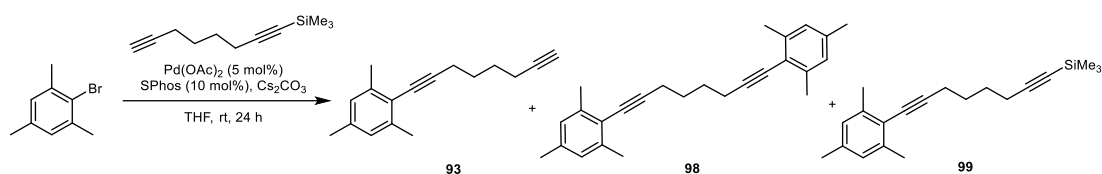
Treatment of iodobenzene with 3 equivalents of 1,7-octadiyne in copper-free conditions (toluene at 100 °C with Pd(OAc)₂, SPhos and Cs₂CO₃) led to analogous results.

Synthesis of 1,3,5-trimethyl-2-(octa-1,7-diyn-1-yl)benzene (**93**) was initially undertaken under classical Sonogashira conditions using 2-Bromomesitylene as starting material, but no reaction took place. Application of copper-free conditions (Scheme 71) resulted in the formation solely of the disubstitution product **98** in low yields.



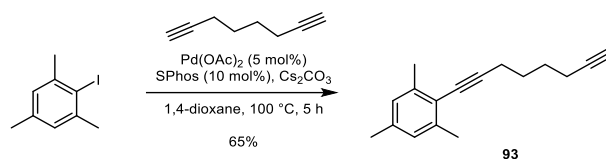
Scheme 71. Copper-free Sonogashira coupling between bromomesitylene and 1,7-octadiyne.

Aiming to avoid the formation of compound **98**, trimethyl(octa-1,7-diyn-1-yl)silane (**91**) was used in the coupling with 2-bromomesitylene: a first test was performed in THF at 60 °C, in the presence of PdCl₂(PPh₃)₂ and CuI, but no product was observed. Switching to copper free conditions (5 mol% of Pd(OAc)₂, 10 mol% of SPhos and Cs₂CO₃ as base) led to the isolation of a small amount of a mixture, from which pure products could not be separated, containing the coupling product **99**, desilylated compound **93**, and the product of double substitution **98** (Scheme 72), even though an excess of 1,7-octadiyne was used.



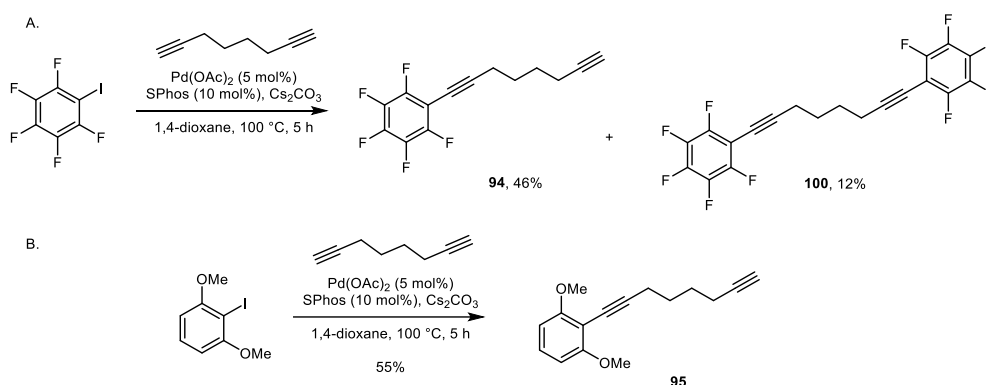
Scheme 72. Copper-free Sonogashira cross-coupling between **91 and bromomesitylene.**

Running the reaction again in refluxing 1,4-dioxane led to formation of the same mixture of products in higher yield. Use of the more active 2-iodomesitylene effectively improved the results, allowing the easier isolation of the desired alkylation products. Reaction with 3 equivalents of non-substituted 1,7-octadiyne in simple Sonogashira conditions (5 mol% of Pd(PPh₃)₄, 10 mol% of CuI and *i*Pr₂NH in THF at room temperature) afforded selectively product **93**, although only in 8% yield. Moving again to harsher copper-free conditions, 65% yield was reached (Scheme 73).



Scheme 73. Copper-free Sonogashira cross-coupling between iodomesitylene and 1,7-octadiyne.

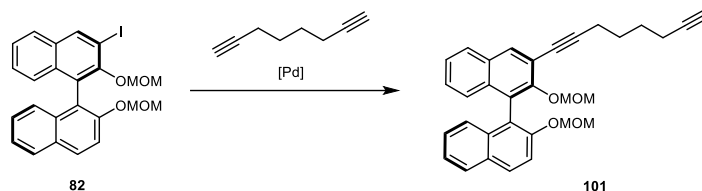
Products **94** and **95** were in turn prepared from the corresponding iodides and 1,7-octadiyne. **94** was isolated in 46% yield along with by-product **100** in 12% yield (Scheme 74A). **95** was isolated in 55% yield (Scheme 74B).



Scheme 74. A. Synthesis of alkyne **94; B. Synthesis of alkyne **95**.**

The mono-functionalization of 1,7-octadiyne was tested also on iodide **82**: Compound **101** (Table 6) could be directly obtained through coupling between equimolar amounts of 1,7-octadiyne and iodide **82**, even though the reaction showed some critical issues.

Table 6. Screening of conditions for the cross-coupling of **82 with one equivalent of 1,7-octadiyne.**



Entry	Catalytic system	Base	Solvent	Temp.	Alkyne [eq]	Time	Yield
1	Pd(PPh ₃) ₄ /CuI	Et ₃ N	MeCN	80 °C	1.1	2 h	27%
2	Pd(PPh ₃) ₄ /CuI	Et ₃ N	MeCN	80 °C	2	2 h	31%
3	Pd(OAc) ₂ /S-Phos	Cs ₂ CO ₃	toluene	110 °C	3	3.5 h	27%
4	Pd(OAc) ₂ /S-Phos	Cs ₂ CO ₃	toluene	80 °C	3	5.5 h	20%
5	Pd ₂ (dba) ₃ /S-Phos	Et ₃ N	THF	rt	3	16 h	/
6	Pd ₂ (dba) ₃ /S-Phos	Et ₃ N	THF	75 °C	3	3.5 h	10%

When the transformation was conducted in the conditions reported in entry 1, competitive formation of the doubly substituted product **81** (Scheme 68) was observed, and **101** was isolated in only 27% yield. The equivalents of 1,7-octadiyne were doubled, but yield remained limited to 31%, due to the presence of **81** and due to the generation of a Csp-Csp coupling by-products. Copper-free catalytic systems (Pd(OAc)₂/SPhos/Cs₂CO₃, entries 3 and 4) did not improve the conversion and the selectivity towards **84**: even though the amount of **81** was negligible, the isolated yield in **84** was never higher than 27%, in consequence probably of its degradation in the reaction conditions. Reaction with Pd₂(dba)₃ as catalyst stopped at low conversions when performed at room temperature (entry 5) but resulted in a mixture of product and byproducts at higher temperatures (entry 6).

2.7. Iron Complexes Containing 1,1'-Binaphthyl-based C₂-symmetric Cyclopentadienone Ligands

The dialkynes functionalized with 1,1'-binaphthyl residues described in the previous chapter were used as precursors for the synthesis of novel chiral (cyclopentadienone)iron tricarbonyl complexes. We decided to incorporate binaphthyl-based residues in the pre-catalysts object of this thesis since we figured that binding these atropisomeric moieties to positions 2 and 5 of the cyclopentadienone ring could lead to highly asymmetrically hindered ligands, with a robust and rigid conformation.

Two classes of chiral (cyclopentadienone)iron complexes were initially prepared starting from (*R*)-BINOL: complexes **102** and **103-106** (Figure 25).

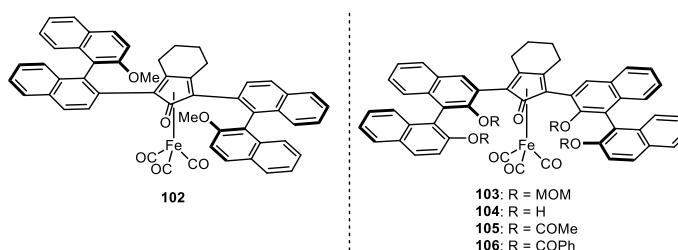


Figure 25. Structure of the new iron complexes described in this chapter.

102 and **103-106** show the same structural motif based on the substitution of both sides of the carbonyl group of the cyclopentadienone with identical binaphthyl residues. The symmetrical substitution imparts to the ligand a C₂-axial symmetry, which is essential to avoid the formation of multiple isomers of the product after the complexation step, as the two faces of the cyclopentadienone ring are homotopic.

The main difference between the two structures presented in Figure 25 resides in the position of the 1,1'-binaphthyl moieties to whom the cyclopentadienone ring is attached, namely position 2 for **102** and position 3 in the case of complexes **103-106**. Connection on position 2 was envisioned as a particularly good strategy for the synthesis of an enantioselective species, as it generates a conformationally locked and rigid molecular structure: we hypothesized that one of the two 2-methoxy-1,1'-binaphthyl residues would have occupied a portion of space close to the iron tricarbonyl moiety, while the second residue would have been placed on the free side of the ligand (Figure 26).

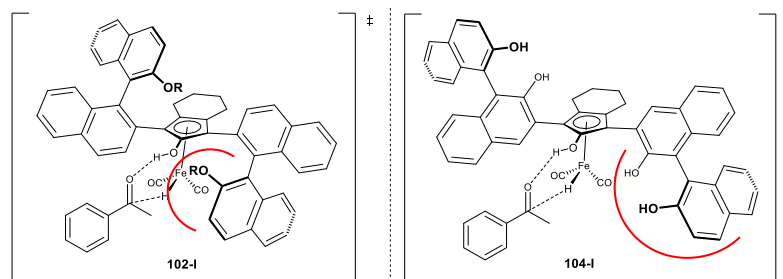
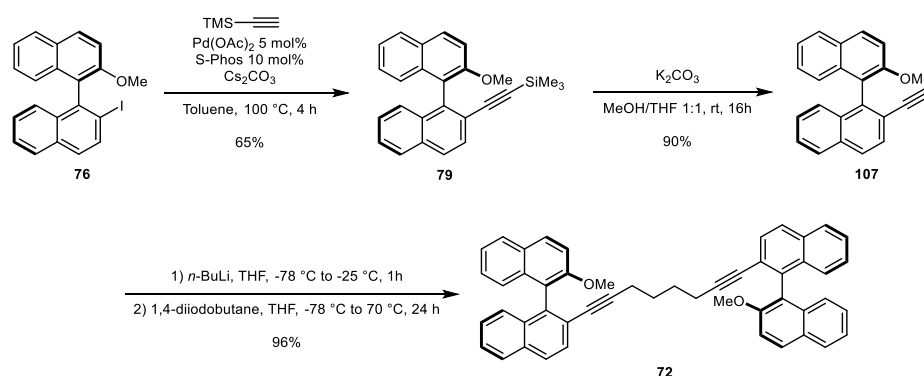


Figure 26. Suggested conformation for the transition states generated from interaction of acetophenone with **102** (**102-I**), and with **104** (**104-I**), highlighting the assumed asymmetric hindrance generated by the corresponding binaphthyl residues.

An analogous conformation was hypothesized for complexes **103-106**, even though the bond between positions 2 of the cyclopentadienone and position 3 of the 2,2'-disubstituted-1,1'-binaphthyl residues in these structures possibly leads to a less constrained conformation, due to the higher degree of freedom in its rotation. However, synthesis of compound **103** is much easier if compared to that of **102** and allowed us to investigate the effect of structural modifications of the complex on its reactivity and selectivity more in depth.

2.7.1. Synthesis of complex **102**

For the synthesis of complexes **102** and **103**, carbonylative cyclization of a 1,7-octadiyne derivatized on both extremities with the corresponding 1,1'-binaphthyl moieties was planned. Synthesis of complex **102** started from (*R*)-BINOL, from which iodide **76** was isolated in five steps (Scheme 75).

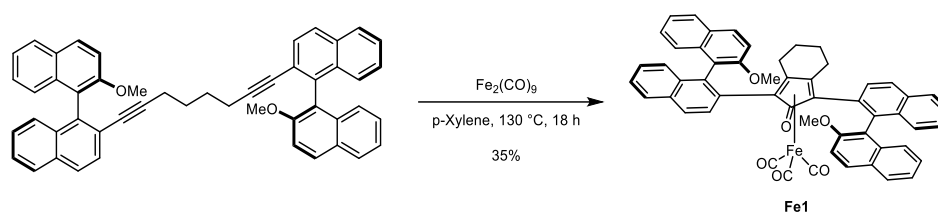


Scheme 75. Synthesis of diyne precursor **72**, used in the preparation of complex **102**.

As described above (see Section 2.6.2), the preparation of precursor **72** could not be directly achieved through Sonogashira coupling between 1,7-octadiyne and **76**. Coupling with

ethynyltrimethylsilane led instead to compound **79**. Cleavage of the trimethylsilyl protecting group in basic conditions afforded terminal alkyne **107**, which was finally deprotonated with *n*-BuLi and treated with 1,4-diiodobutane: this final step required an excess of intermediate **107** and to carefully control the temperature during the addition of the alkyl iodide. In this way, diyne **72** was isolated in 96% yield (calculated over 1,4-diiodobutane, the terminal alkyne in excess was recovered almost quantitatively after purification).

Carbonylative cyclization of **72** was initially conducted in toluene at 110 °C using diiron nonacarbonyl as iron source. Even though the formation of a product could be clearly spotted on TLC, isolation of the iron complex was not achieved. In further complexation tests a yellow solution was recovered after chromatographic column, but the obtained compound partially degraded before volatiles could be removed. Carefully removing the solvent after purification at room temperature and avoiding the contact with air, finally afforded the isolation of a pale-yellow compound in small amounts. Yield was further improved to 35% by performing the reaction in *m*-xylene at 130 °C (Scheme 76).

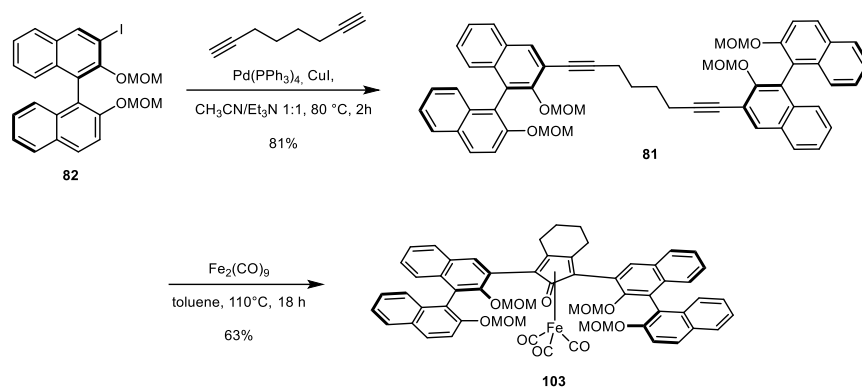


Scheme 76. Synthesis of chiral complex 102 through carbonylative cyclization of diyne 72.

The scarce stability of the isolated product made its characterization through NMR impossible (all spectra recorded were not well resolved). Nevertheless, the compound could be identified as pre-catalyst **102** through MS analysis.

2.7.2. Synthesis of Complexes 103-106

For the synthesis of complex **103**, diyne precursor **81** could be directly prepared via cross-coupling reaction between iodide **82** (Scheme 67, Section 2.6.3) and 1,7-octadiyne. Despite the possible lability of the MOM protecting groups, carbonylative cyclization was attempted, and complex **103** was isolated in 63% yield through reaction of **82** with diiron nonacarbonyl in toluene at 110 °C (Scheme 77).



Scheme 77. Synthesis of chiral complex 103.

Complex **103** was sufficiently stable and could be fully characterized: ^1H - and ^{13}C -NMR showed separate peaks for both the methylene and methyl groups of the MOM residues. In addition, crystals suitable for X-ray diffraction analysis could be grown via slow diffusion of *n*-hexane into a solution of **103** in ethyl acetate. The presence of suspected complex could unambiguously be identified with single crystal X-ray diffraction. The structure is reported in Figure 27. The complex crystallizes in the space group *I*2 with one symmetry independent molecule in the asymmetric unit (*Z* = 4). The space group was found to be enantiomorphous and thus only the isomer with the reported configuration was observed.

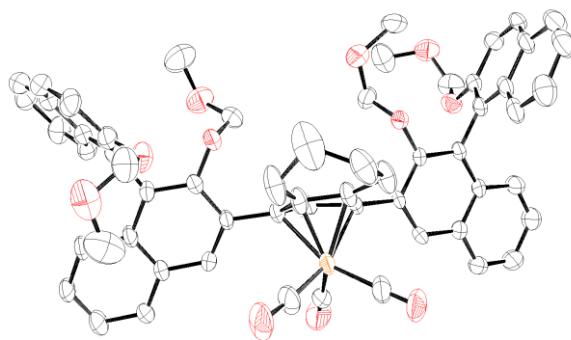
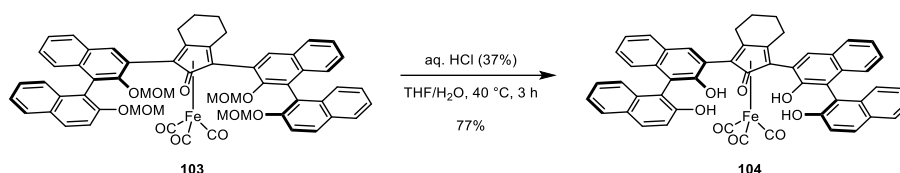


Figure 27. ORTEP representation of the molecular structure of complex 103. Thermal ellipsoids are represented at the 50% probability level.

The stability of the new iron complex to acidic conditions also allowed cleavage of the acetal protecting group using concentrated HCl, and the isolation of complex **104** (Scheme 78). Complex **104** showed a lower stability in air than **103** and required analogous care to those taken for **102** after the purification. However, it was successfully characterized and used in further synthetic steps.

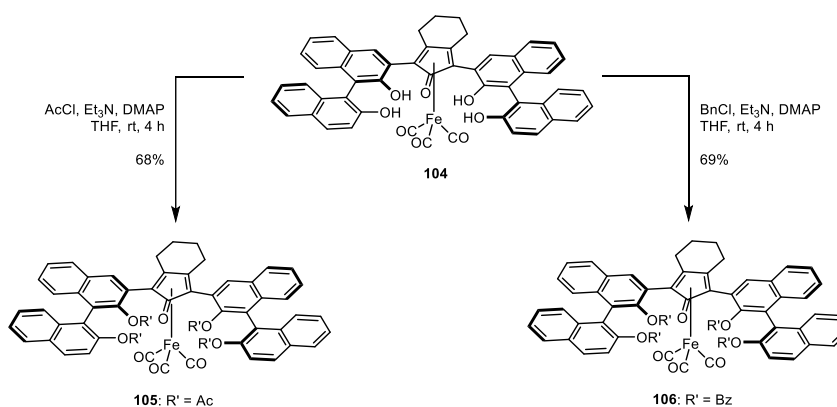


Scheme 78. Synthesis of chiral complex 104.

In order to test the dependence of activity and selectivity on the substituents installed on the binaphthyl moieties, the preparation of a small library of complexes was undertaken, using the fully deprotected compound **104** as starting material.

At first, functionalization of the four OH groups with alkyl groups was attempted. Methylation was tested using an excess of methyl iodide in the presence of K_2CO_3 as base in refluxing acetone, but only degradation of the substrate was observed. Treatment of **104** with benzyl bromide and K_2CO_3 in THF at 70 °C equally led to degradation. Benzylation was tested once more using an excess of benzyl bromide and sodium hydride in DMF at room temperature and resulted in the formation of a complex mixture containing products of incomplete functionalization.

We then proceeded to test acyl chlorides as electrophiles: fully acetylated product **105** was successfully obtained in 68% yield by reaction of **104** with acetyl chloride, triethylamine and a catalytic amount of *N,N*-dimethylaminopyridine in THF at room temperature. The same reaction conditions were applied to the functionalization with benzoyl chloride, affording **106** in 69% yield.



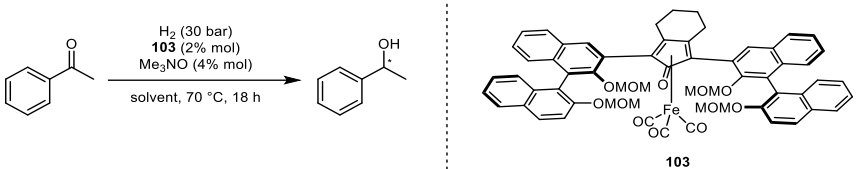
Scheme 79. Functionalization of the four oxygen atoms in complex 104 with acetyl and benzoyl groups.

2.7.3. Catalytic tests with complexes **102** and **103-106**

Complexes **102** and **103-106** were all tested in the reduction of acetophenone to evaluate their activity and selectivity. In all the reported reactions Me₃NO was used for the *in situ* oxidative activation of the pre-catalysts. Conversion and enantiomeric excess values were determined through GC analysis with a chiral stationary phase.

Pre-catalyst **103** was initially employed in the hydrogenation of acetophenone in a 5:2 mixture of isopropanol and water, which was identified as the solvent affording the best conversion values with other (cyclopentadienone)iron complexes.^[95,102,106] However, after 18 h at 70 °C under 30 bar of H₂, a modest 35% conversion was observed (Table 7, entry 1). A thick precipitate was observed at the end of the reaction, which led us to evaluate the use of other solvent systems: the reaction was performed again in the absence of water, and conversions up to 99% were achieved in isopropanol (Table 7, entry 4). To our disappointment, in all cases *ee* values were negligible.

Table 7. Screening of the solvents for the AH of acetophenone catalyzed by **103.**

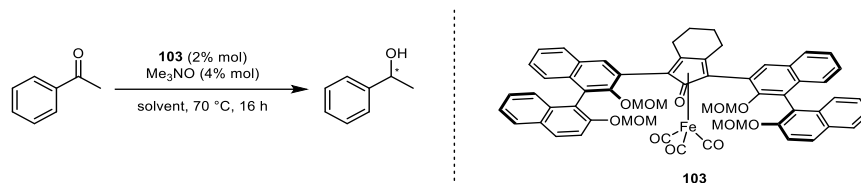


The reaction scheme shows acetophenone reacting with H₂ (30 bar), complex **103** (2% mol), and Me₃NO (4% mol) in a solvent at 70 °C for 18 h to yield 1-phenylethanol. The structure of complex **103** is a ferrocenyl iron complex with a cyclopentadienone ligand, a ferrocene backbone, and several MOMO and CO ligands.

Entry	Solvent	Conversion [%] ^[a]	<i>ee</i> [%] ^[a]
1	<i>i</i> PrOH/H ₂ O 5:2	35	<5
2	Toluene	98	<5
3	1,4-Dioxane	91	<5
4	<i>i</i> PrOH	99	<5

Reaction conditions: C₀(acetophenone) = 1.43 M; acetophenone/pre-catalyst/Me₃NO = 100:2:4, temperature: 70 °C, reaction time: 18 h; [a] Determined by GC equipped with a chiral capillary column (see Experimental Section, Paragraph 4.14.5).

Complex **102** was also tested in the ATH of acetophenone (Table 8). Reactions were conducted in different solvents at 70 °C for 16 h. The same relationship between conversion and solvent observed in the hydrogenation tests was found. Reaction in *i*PrOH/H₂O 5:2 led to a poor 4% conversion, while 60% conversion was reached in 100% *i*PrOH. Unfortunately, the milder conditions of the transfer hydrogenation process did not lead to improvements in the selectivity.

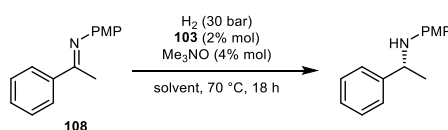
Table 8. Screening of the solvents for the AH of acetophenone catalyzed by 103.

Entry	pre-cat (mol%)	Solvent	Conversion [%] ^[a]	ee [%] ^[a]
1 ^[b]	2	<i>i</i> PrOH/H ₂ O 5:2	4	<5
2 ^[c]	2	<i>i</i> PrOH/toluene 1:1	36	<5
3 ^[d]	5	<i>i</i> PrOH/toluene 1:1	63	<5
4 ^[e]	2	<i>i</i> PrOH	60	<5
5 ^[e]	2	<i>i</i> PrOH/toluene 1:1	44	<5

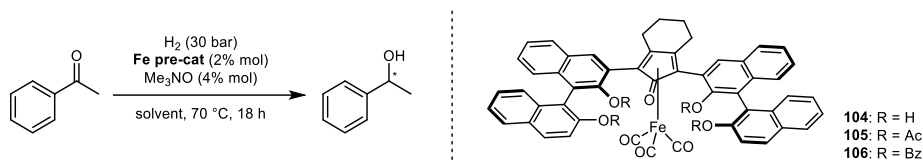
Reaction conditions: acetophenone/pre-catalyst/Me₃NO = 100:2:4, temperature: 70 °C, reaction time: 16 h; [a] Determined by GC equipped with a chiral capillary column (see Experimental Section, Paragraph 4.14.5); [b] C₀(acetophenone) = 0.7 M; [c] C₀(acetophenone) = 0.5 M; [d] C₀(acetophenone) = 0.5 M; acetophenone/pre-catalyst/Me₃NO = 100:5:10; [e] C₀(acetophenone) = 1.0 M.

An explanation to the low enantioselectivities was given by observing the molecular structure of **103** (Figure 27), which shows how the steric hindrance generated by the binaphthyl systems on both positions 2 and 5 of the ligand is positioned mostly over the upper face of the cyclopentadienone ring. The binaphthyl substituents do not substantially generate a chiral environment around the iron center.

103 was also used in the hydrogenation of imine **108** (Scheme 80), which was reduced to the (*R*)-configured enantiomer of the corresponding amine in 22% yield, with a poor 12% *ee*.

**Scheme 80. Hydrogenation of imine 108 catalyzed by chiral complex 103.**

Asymmetric hydrogenation of acetophenone was then studied also with pre-catalysts **104-106**, in the same conditions reported for **103**, using isopropanol or isopropanol/water as solvent (Table 9).

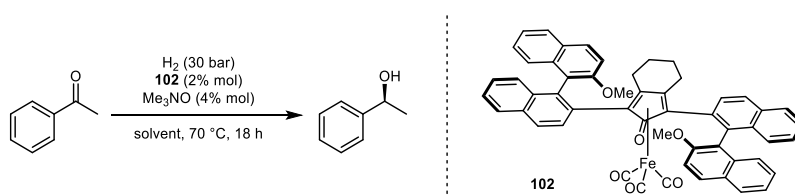
Table 9. Tests of the AH of acetophenone catalyzed by pre-catalysts 104-106.

Entry	pre-cat	Solvent	Conversion [%] ^[a]	ee [%] ^[a]
1	104	<i>i</i> PrOH	22	<5
2	104	<i>i</i> PrOH/H ₂ O 5:2	2	21 (<i>S</i>)
3	105	<i>i</i> PrOH	14	9 (<i>R</i>)
4	106	<i>i</i> PrOH	3	11 (<i>R</i>)
5	106	<i>i</i> PrOH/H ₂ O 5:2	10	22 (<i>R</i>)

Reaction conditions: C₀(acetophenone) = 1.43 M; acetophenone/pre-catalyst/Me₃NO = 100:2:4, temperature: 70 °C, reaction time: 18 h; [a] Determined by GC equipped with a chiral capillary column (see Experimental Section, Paragraph 4.14.5).

Hydrogenation catalyzed by **104** in *i*PrOH resulted in the formation of (±)-1-phenylethanol in 22% conversion (entry 1), while the same reduction performed in *i*PrOH/H₂O 5:2 gave a much lower yield of 2% along with 21% *ee* towards the (*S*)-enantiomer of the product (entry 2). The opposite enantiomer [(*R*)-1-phenylethanol] was obtained using complexes **105** and **106** (entries 3-5), but conversions were low and a maximum enantiomeric excess of 22% was reached with **106**.

Both hydrogenation and transfer hydrogenation were tested with complex **102**: acetophenone was not reduced at all in the ATH conducted in *i*PrOH at 70 °C overnight. Hydrogenation was performed in both *i*PrOH and *i*PrOH/H₂O 5:2 (Table 10).

Table 10. Tests of the AH of acetophenone catalyzed by pre-catalyst 102.

Entry	Solvent	Conversion [%] ^[a]	ee [%] ^[a]
1	<i>i</i> PrOH	11	36 (<i>S</i>)
2	<i>i</i> PrOH/H ₂ O 5:2	17	33 (<i>S</i>)

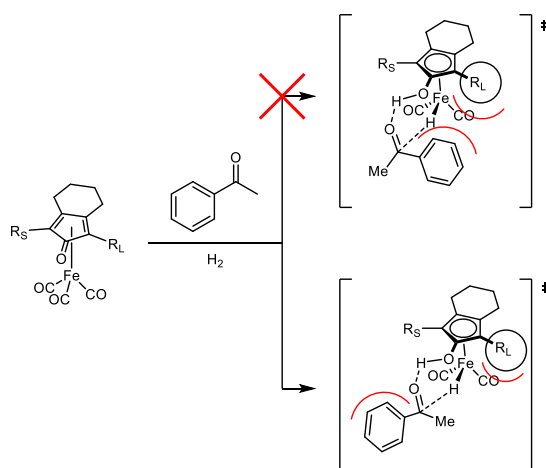
Reaction conditions: C₀(acetophenone) = 1.43 M; acetophenone/pre-catalyst/Me₃NO = 100:2:4, temperature: 70 °C, reaction time: 18 h; [a] Determined by GC equipped with a chiral capillary column (see Experimental Section, Paragraph 4.14.5).

While conversions remained low, both tests led to an excess in (*S*)-1-phenylethanol of more than 30%. Higher *ee*'s are in agreement with our expectations about pre-catalyst **102** and its more

rigid conformation. The enantiomer obtained in excess also seems to be in line with the hypothesis that we formulated on the structure of the complex and of the related transition state **102-I** (Figure 26). Unfortunately, the scarce stability of **102** did not allow to produce crystals suitable for X-ray analysis and to confirm the hypothesis. On the other hand, the poor conversions can be rationalized taking into account the stability issues of **102**, which is probably subject to degradation in the reaction environment.

2.8. Diastereoisomerically Pure Complexes containing 1,1'-Binaphthyl-based C_1 -Symmetric Cyclopentadienone Ligands

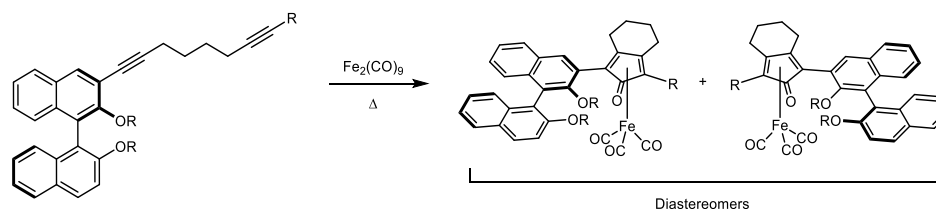
Observing that ligands with both sides of the carbonyl group occupied by identical binaphthyl-based residues could not generate a sufficiently stereoselective environment, we decided to investigate the preparation of complexes containing asymmetrically substituted ligands. At the base of this strategy there is the idea of optimizing the difference in steric hindrance between the two sides of the active site of the catalyst by placing a small substituent on position α to the carbonyl of the cyclopentadienone and a larger one on position α' , so that a prochiral ketone is forced to approach the catalyst only with one of its enantiofaces.



Scheme 81. Representation of the two possible transition states generated during the reduction of acetophenone with a complex containing an asymmetrically substituted cyclopentadienone.

Chiral (cyclopentadienone)iron tricarbonyl pre-catalysts with positions 2 and 5 of the ligand occupied by two different substituents have been recently developed by Gennari and coworkers in collaboration with our research group.^[110] Several complexes were prepared from achiral 1,7-octadiyne derivatives with different substituents attached to positions 1 and 8 or from achiral cyclopentadienones with differently functionalized positions 2 and 5. In these cases the complexation with the iron tricarbonyl moiety leads to the generation of a stereogenic plane, and thus to the formation of pairs of enantiomeric complexes. After testing all the racemic mixtures for their catalytic activity, two pairs of enantiopure pre-catalysts were isolated through separation via chiral semipreparative HPLC, characterized, and tested for enantioselectivity (complexes **60a** and **60b**, see Section 2.3.3. Scheme 51).

Our approach to the development of new chiral (cyclopentadienone)iron tricarbonyl complexes involved the synthesis of *chiral* C_1 -symmetric ligands: we embarked on the preparation of ligands bearing the same binaphthyl group contained in complex **103** on position 2 of the cyclopentadienone and substituents showing different steric effects on position 5 (Scheme 82).

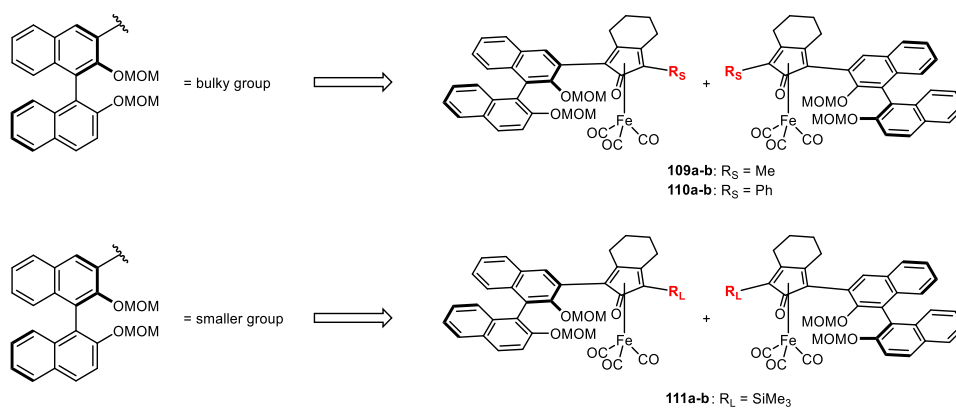


Scheme 82. Carbonylative cyclization/complexation of a 1,1'-binaphthyl-based C_1 -symmetric 1,7-octadiyne derivative.

The presence of the stereogenic axis of the 1,1'-binaphthyl moiety in the diyne pre-ligands leads to the formation of pairs of diastereomers, instead of enantiomers: a chiral stationary phase for the separation of the products of the complexation step is thus not necessary, with a clear advantage in terms of synthetic practicality.

3-iodo-2,2'-bis(methoxymethoxy)-1,1'-binaphthalene **82** was chosen as starting material for the construction of the asymmetrically disubstituted ligands despite its inability to generate enantiomeric discrimination, because it can be easily synthesized from commercially available (*R*)-BINOL in three steps. Furthermore, the presence of the MOM groups proved essential to obtain good conversions with the previously tested catalysts.

In a first instance, a methyl group and a phenyl group were chosen as substituents at the opposite end of the dialkyne chain, in order to decrease the steric hindrance with respect to the binaphthyl group. A trimethylsilyl residue was also installed to increase the steric hindrance with respect to the binaphthyl group (Scheme 83).



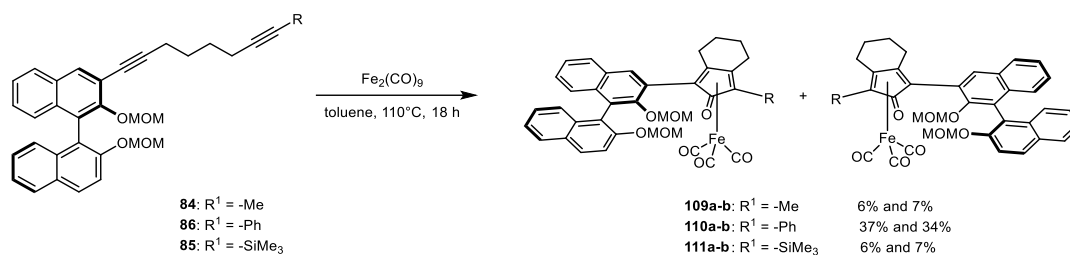
Scheme 83. Structure of complexes 109 and 110, containing the 1,1'-binaphthyl moiety as bulkier substituents and of complex 111, containing a trimethylsilyl moiety as bulkier substituent.

2.8.1. Synthesis and Catalytic Activity of Diastereoisomerically Pure (Cyclopentadienone)iron Tricarbonyl Complexes 109-111

For the preparation of the diyne precursors we decided to follow convergent synthetic pathways, involving firstly the isolation of iodide **82** and of mono-functionalized 1,7-octadiynes, and in second instance the coupling between the two products. Trimethyl(octa-1,7-diyne)silane and 1,7-nonadiyne were prepared through a literature-known procedure:^[110] 1,7-octadiyne was mono-deprotonated with lithium bis-(trimethylsilyl)amide and silylated with chlorotrimethylsilane, affording diyne **91**. Methylation with iodomethane followed by desilylation in basic conditions led to the isolation of **90**. 1-phenyl-1,7-octadiyne was directly prepared via coupling of 1,7-octadiyne and iodobenzene (see Section 2.6.4).

The target asymmetrically substituted diynes **84**, **85** and **86** (Table 5, Section 2.6.3) were obtained in good yields via Sonogashira coupling between the mono-substituted alkynes and iodide **82**.

Complexation reactions with diiron nonacarbonyl of **84**, **85** and **86** were performed in toluene at 110 °C (Scheme 84): in all cases two distinct spots could be observed in thin layer chromatography, and to our delight separation of the diastereomerically pure complexes through simple chromatographic column on silica gel could be achieved.



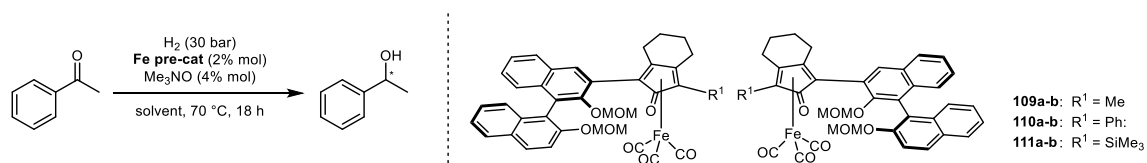
Scheme 84. Carbonylative cyclization/complexation of alkynes 85-86.

The two diastereomers of complexes **109** and **111** were obtained from the corresponding alkynes with low 6% and 7% yields, due to their low stability, which led to partial degradation during the isolation and required two consecutive purifications through chromatographic column. The two isomers of complex **110** were more easily isolated in 35% and 34% yield.

It must be pointed out that the absolute configuration of the stereogenic plane in the isolated isomers has not been assigned yet: the diastereoisomerically pure complexes described will thus be referred to as **a** and **b**, depending on their higher (**a**) or lower (**b**) R_f value.

The diastereoisomerically pure pre-catalysts **109-111** were tested in the asymmetric hydrogenation of acetophenone (Table 11). The reactions were conducted in isopropanol, since it was observed as the solvent in which **103** gave the highest conversions.

Table 11. Screening of pre-catalysts 109-111 in the hydrogenation of acetophenone.



Entry	pre-cat	Solvent	Conversion [%] ^[a]	ee [%] ^[a]
1	109a	<i>i</i> PrOH	2	-
2 ^[b]	109a	toluene	15	11 (<i>S</i>)
3	110a	<i>i</i> PrOH	98	38 (<i>R</i>)
4	110b	<i>i</i> PrOH	98	33 (<i>S</i>)
5	111a	<i>i</i> PrOH	<1	-
6	111b	<i>i</i> PrOH	<1	-

Reaction conditions: C₀(acetophenone) = 1.43 M; acetophenone/pre-catalyst/Me₃NO = 100:2:4, temperature: 70 °C, reaction time: 18 h; [a] Determined by GC equipped with a chiral capillary column (see Experimental Section, Paragraph 4.14.5); [b] The reaction was conducted in toluene at 110 °C.

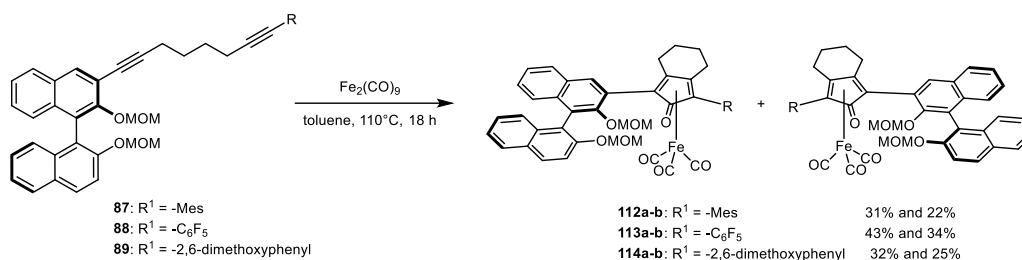
The complexes containing trimethylsilyl- and methyl-substituted cyclopentadienones were not active in catalysis in the usual AH conditions (entries 1, 5 and 6). Running the reaction with pre-

catalyst **109a** in toluene at 110 °C proved beneficial but led only to a low 15% conversion to (*S*)-1-phenylethanol and to a poor 11% *ee* (entry 2). Interesting results were observed with the two isomers of complex **110** (entries 3 and 4). Almost quantitative conversions were achieved, and an unexpectedly high >30% *ee* was reached with both pre-catalysts. The enantiomeric excess was overbalanced towards the opposite enantiomers in the two tests [i.e. (*R*)-1-phenylethanol was obtained in excess in the reaction catalyzed by **110a**, (*S*)-1-phenylethanol was the main product with **110b**], showing that the effect of the stereogenic plane on enantioselectivity was predominant. On the opposite hand, the similar *ee* values indicate the absence of a synergistic effect between the two stereogenic elements in determining the absolute configuration of the product. The fact that there are not “matched” and “mismatched” pairs can be considered as an interesting property of this class of complexes: both isomers can in principle be used at need to afford the formation of alcohols with opposite configuration.

2.8.2. Complexes Containing C_1 -Symmetric Cyclopentadienones Functionalized with Different Aromatic Systems

Based on the promising *ee* values reached with the isomers of the phenyl-substituted pre-catalysts **110a-b**, the use of aromatic systems in combination with the usual bis-MOM-protected binaphthyl system was studied more in depth. Use of a mesityl group was chosen to test the substitution with a bulkier residue. Aiming to examine also the possible effect of electronic properties on enantioselectivity, the screening was then extended to electron-rich 2,6-dimethoxyphenyl and electron-poor pentafluorophenyl groups.

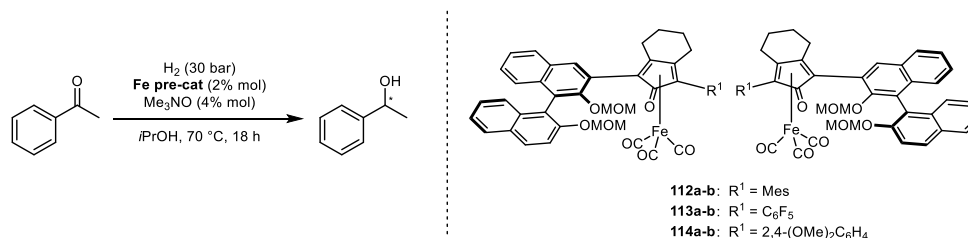
The three new pairs of diastereomeric complexes were prepared according to the strategy mentioned above: mono-aryl-substituted alkynes **93-95** were synthesized via copper-free Sonogashira reaction of iodoarenes with 1,7-octadiyne and subsequently coupled with iodide **82** (see Section 2.6.4). Carbonylative cyclization/complexation of the diyne precursors **87-89** in the presence of $Fe_2(CO)_9$ proceeded smoothly with yields between 53% and 77% over the two diastereomers (Scheme 85). The separation through chromatographic column of the products could always be performed. Nevertheless, we could observe a clear trend in the stability of the complexes: the electron-poor pentafluorophenyl resulted in stable complexes, while complexes containing electron-rich aromatic rings were subject to partial degradation during their isolation.



Scheme 85. Carbonylative cyclization/complexation of alkynes 87-89.

Results of the first reactivity screening on the stereoisomers of complexes **112-114** are reported in Table 12.

Table 12. Screening of pre-catalysts 112-114 in the hydrogenation of acetophenone.



Entry	pre-cat	Conversion [%] ^[a]	ee [%] ^[a]
1	112a	25	7 (<i>R</i>)
2	112b	18	10 (<i>S</i>)
3	113a	>99	5 (<i>R</i>)
4	113b	>99	5 (<i>S</i>)
5	114a	8	53 (<i>R</i>)
6	114b	2	54 (<i>S</i>)

Reaction conditions: C₀(acetophenone) = 1.43 M; acetophenone/pre-catalyst/Me₃NO = 100:2:4, temperature: 70 °C, reaction time: 18 h; [a] Determined by GC equipped with a chiral capillary column (see Experimental Section, Paragraph 4.14.5).

The use of the bulky mesityl residue led to a drop in both conversions and enantioselectivities (entries 1 and 2), while complexes bearing the pentafluorophenyl group showed excellent activity along with the worst selectivity among this series of structures. Low conversions to 1-phenylethanol were obtained using complexes **114a-b**, but along with 53% and 54% ee's (entries 5 and 6), which are among the highest achieved with cyclopentadienone iron complexes so far.

As already highlighted for the tests made on complexes **110a-b**, the two diastereomers of each couple of complexes lead to numerically comparable enantiomeric excesses, but to the opposite enantiomers of 1-phenylethanol. Furthermore, we observed a general trend in the formation of an excess of (*R*)-1-phenylethanol when the pre-catalyst employed was the first diastereomer

isolated through chromatographic column (the one with a higher R_f value in thin layer chromatography on silica gel, namely **112a-114a**). (*S*)-1-phenylethanol was the major enantiomer when the 2nd isomer (**112b-114b**) of the pre-catalysts was used.

2.8.3. Complexes Prepared from 1,1'-Binaphthyl-based Terminal Alkynes

Besides screening different aromatic rings as substituents on position α' of the cyclopentadienone ring, the preparation of complexes without any substituent on one side of the carbonyl group was also investigated (**115**, Figure 28). Combination of hydrogen and the 2,2'-bis(methoxymethoxy)-1,1'-binaphth-3-yl moiety was considered as a good way to achieve the highest disproportion in steric hindrance possible.

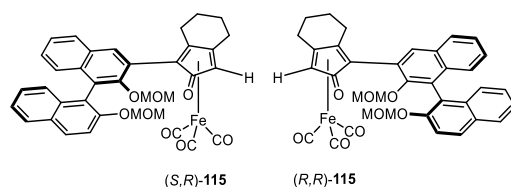
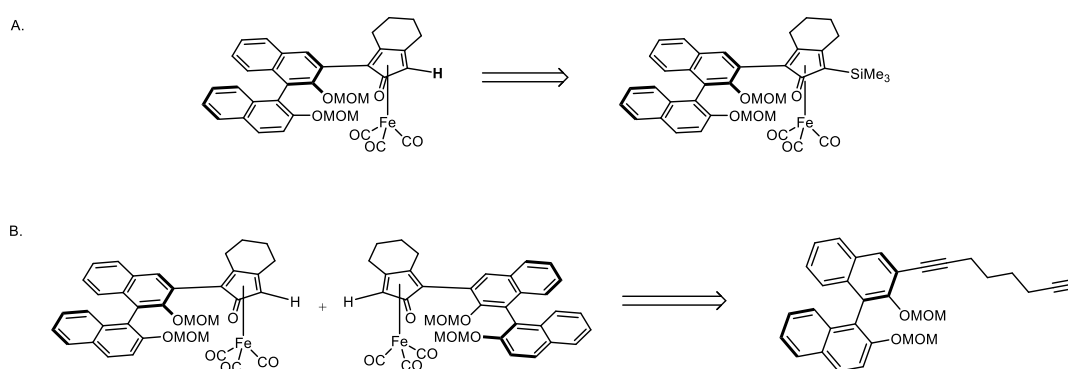


Figure 28. Structure of the two diastereomers of complex **115**.

However, only few examples of (cyclopentadienone)iron complex with a free position 2 on the ligand were reported in literature to our knowledge.^[66] The two synthetic strategies envisioned for the preparation of complexes (*S,R*)-**115** and (*R,R*)-**115** are reported in Scheme 86.

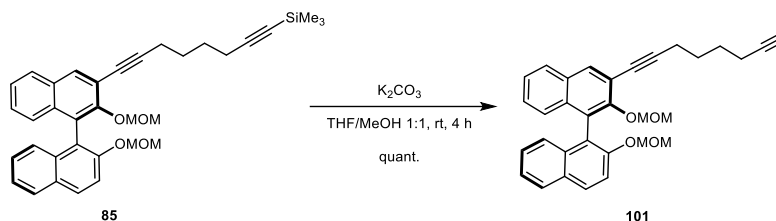


Scheme 86. Retrosynthetic approach to the synthesis of the isomers of complex **115**.

The first option (Scheme 8A) involves the removal of the trimethylsilyl group from the isolated isomers of complex **111**, but the stability issues observed during their isolation held us back from following this route. Moreover, desilylation on (cyclopentadienone)iron tricarbonyl complexes was already reported in literature, but the necessity of exchanging one of the CO ligands with

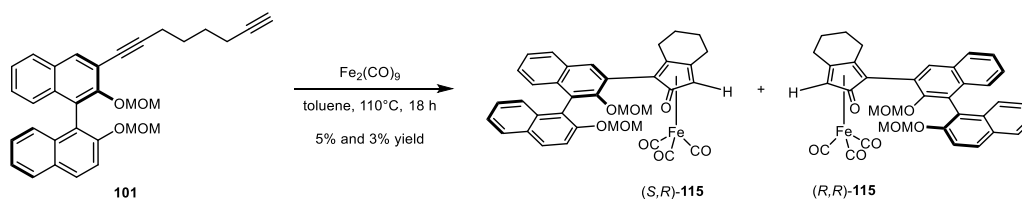
triphenylphosphine prior to treatment with fluorides was underlined.^[66] The second pathway, which was eventually followed, contemplated the preparation of a mono-functionalized 1,7-octadiyne and its cyclative carbonylation/complexation (Scheme 86B).

Diyne **101** could be obtained in modest yields via direct coupling between 1,7-octadiyne and iodide **82** (Table 6, Section 2.6.4) or by removing the trimethylsilyl group from diyne **85** (Scheme 87).



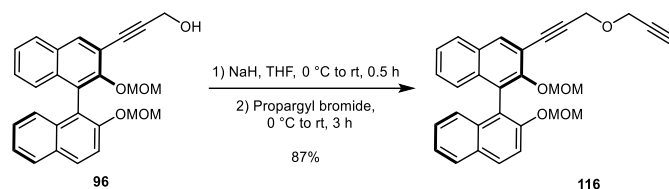
Scheme 87. Synthesis of diyne 101 through desilylation of 85.

Complex formation was tested in the usual conditions (with diiron nonacarbonyl in toluene at 110 °C, for 18 h). A complex mixture of products in small amounts was obtained. Complexes **115a** and **115b** were isolated in 5% and 3% yield respectively after column chromatography. Other fractions recovered after purification contained products of degradation, among which partially deprotected complexes were identified via MS analysis. We thus tried to run the reaction at lower temperatures to avoid formation of byproducts, but improvements were not observed.



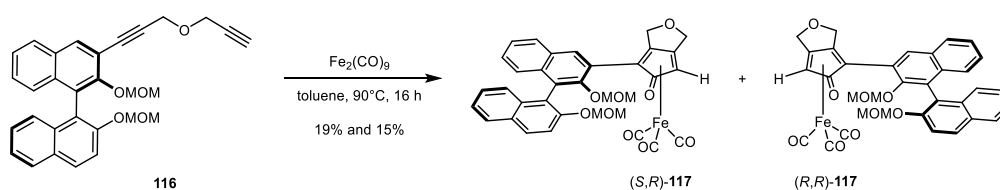
Scheme 88. Carbonylative cyclization of diyne 101.

In order to avoid the issues faced in the mono-functionalization of 1,7-octadiyne, we thus decided to pursue the synthesis of an analogous system with a hydrogen atom on one side of the carbonyl group, but with a five-membered ring fused to the cyclopentadienone ring. The formation of diyne pre-ligand **116** was achieved by cross-coupling between iodide **82** and propargyl alcohol (see Scheme 69, Section 2.6.3) and subsequent substitution reaction on propargyl bromide (Scheme 89).



Scheme 89. Synthesis of diyne precursor 116.

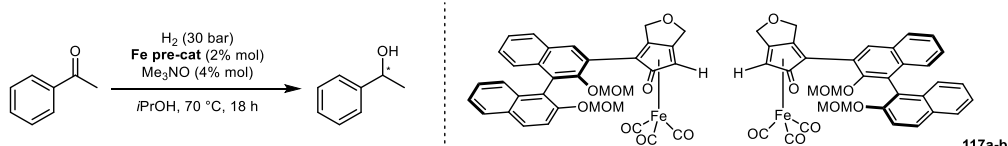
Reaction of **116** with diiron nonacarbonyl in refluxing toluene led to the formation of the two target iron complexes in about 10% yield. 19% and 15% yields were achieved by conducting the complexation at 90 °C (Scheme 90).



Scheme 90. Carbonylative cyclization/complexation of diyne precursor 116.

The catalytic activity of the two diastereomers of structure **115** could not be tested due to the small amounts that were isolated, while the results of a first screening of the activity and selectivity of *(S,R)*-**117** and *(R,R)*-**117** in the asymmetric hydrogenation of acetophenone is reported in Table 13.

Table 13. AH of acetophenone catalyzed by pre-catalysts 117a-b.



Entry	pre-cat	Conversion [%] ^[a]	ee [%] ^[a]
1	117a	19	39 (<i>R</i>)
2	117b	17	37 (<i>S</i>)

Reaction conditions: $C_0(\text{acetophenone}) = 1.43 \text{ M}$; acetophenone/pre-catalyst/ $\text{Me}_3\text{NO} = 100:2:4$, temperature: 70 °C, reaction time: 18 h; [a] Determined by GC equipped with a chiral capillary column (see Experimental Section, Paragraph 4.14.5).

The asymmetric hydrogenation test performed with **117a** resulted in the formation of (*R*)-1-phenylethanol in 39% ee. A comparable excess of 37% towards (*S*)-1-phenylethanol was observed using **117b**, in analogy with the trend observed in the tests with complexes **109-114**. However, conversions were low in both cases, and the ee's were similar to those achieved with

110a-b (Table 11), even though there is a larger difference in steric bulk between the two sides of the active site of **117a-b**.

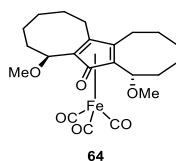
2.9. Conclusions and Outlook

The synthesis of new chiral (cyclopentadienone)iron tricarbonyl species and the study of their catalytic activity in asymmetric hydrogenation reactions has been described in this thesis elaborate.

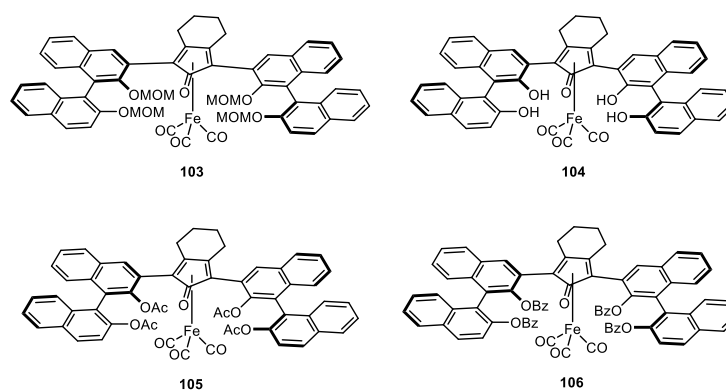
The interest in the isolation of iron complexes suitable for the use in catalytic transformations stems from the sustainable nature of iron, which is widely regarded as the optimal alternative to more expensive and toxic noble metals. Increasing attention has been drawn towards the development of new iron-based catalysts over the course of the last decades, but their application is often limited by their sensitivity to air and water, or by the long and elaborated syntheses of the ligands that are necessary to stabilize the metal center. (Cyclopentadienone)iron complexes are regarded as a possible solution to these issues, thanks to their peculiar stability, the relatively easy synthesis of cyclopentadienone ligands and their activity as catalysts for redox transformations. However, there is still plenty room for improvement in the field of enantioselective catalysis, where (cyclopentadienone)iron complexes haven't succeeded to afford synthetically useful results in terms of selectivity.

My research towards the synthesis of new chiral (cyclopentadienone)iron tricarbonyl complexes focused mainly on the modification of the structure of the ligand. More specifically, the focus was on the insertion of stereogenic elements as close as possible to the reactive portion of the catalytic system, namely the C=O double bond of the ligand and the iron center, in order to generate a chiral environment suitable for a good enantiodiscrimination.

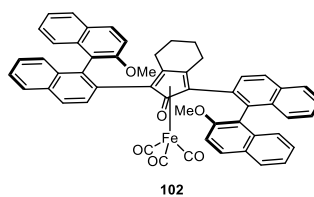
As a first approach, we aimed to synthesize complex **64** through the complexation of enantiopure 3-methoxycyclooctene. The structure of **64** resembles that of [bis(hexamethylene)cyclopentadienone]iron tricarbonyl, previously studied in our research group and identified as an outstanding catalyst for its activity. The synthesis of a chiral complex with the same backbone was thus considered a good strategy to have an efficient and selective catalyst. Unfortunately, we could not isolate the desired compound, due to the low-yielding carbonylative cyclization of the 3-substituted cyclooctyne, which moreover resulted in a poor regio- and stereo-selective outcome.



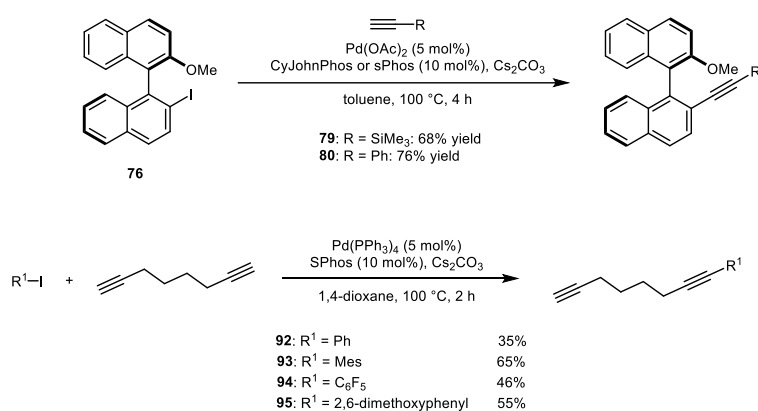
We shifted thus our attention to the synthesis complexes containing 1,1'-binaphthyl-based C_2 -symmetric cyclopentadienones, **102** and **103-106**. Chiral complex **103** was prepared from (*R*)-BINOL in four synthetic steps, with an overall yield of 20%. Cleavage of the MOM protecting groups allowed us to isolate complex **104** and further explore the effect of the substitution on the binaphthyl systems through functionalization with acetyl chloride (complex **105**) and benzoyl chloride (complex **106**). The four new structures were characterized and tested in the asymmetric hydrogenation of acetophenone. While **103** afforded quantitative conversion to 1-phenylethanol, pre-catalysts **104-106** proved poorly active. In all cases enantiomeric excesses were low.



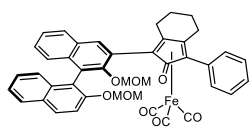
Complex **102** contains a cyclopentadienone substituted at positions 2 and 5 with 2-methoxy-1,1'-binaphth-2-yl residues. We envisaged that the conformation assumed by the ligand upon complexation to the (cyclopentadienone)iron moiety could be particularly adequate for the generation of a proper enantioselective environment. The preparation of **102** started again from (*R*)-BINOL, but required in this case a greater synthetic effort, mainly due to the difficulties encountered in the Sonogashira coupling required for the preparation of the diyne pre-ligand. Complex **102** was finally isolated in 12% yield after 9 synthetic steps. Hydrogenation of acetophenone catalyzed by **102** led to 36% *ee*, but it was accompanied by low conversions, probably due to easy degradation of the complex in the reaction environment.



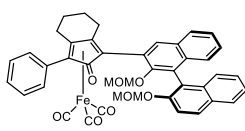
The problems faced while studying the cross-coupling between 2-iodo-2'-methoxy-1,1'-binaphthalene (**76**) and 1,7-octadiyne, along with the necessity to employ the Sonogashira cross coupling in the synthesis of most of the dialkyne precursors to our complexes, prompted us to investigate more in depth this synthetic methodology. From a screening of conditions on the coupling of the unactivated 2-iodo-2'-methoxy-1,1'-binaphthalene (**76**) with different alkynes, we found out that the alkynylation could be achieved only with alkynes without propargylic protons, and that yields could be improved through the use of "copper-free" conditions. Furthermore, the same copper free conditions were suitable for the selective mono-arylation of 1,7-octadiyne with aryl iodides with different steric and electronic properties.



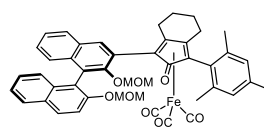
Finally, we synthesized a small library of *C*₂-symmetric disubstituted dialkynes through the coupling between 3-iodo-2,2'-bis(methoxymethoxy)-1,1'-binaphthalene (**82**) and mono-substituted diynes. Carbonylative cyclization/complexation of these compounds with diiron nonacarbonyl led to the formation of pairs of diastereomeric complexes (**109-115**, **117**). We were able to consistently isolate the corresponding diastereoisomerically pure pre-catalysts via simple purification through chromatographic column on silica gel. Activity and selectivity of this new class of chiral complexes was screened in the asymmetric hydrogenation of acetophenone, reaching *ee*'s as high as 54%. Remarkably, we also acknowledged the possibility of reducing ketones to both possible enantiomers of the corresponding alcohol with comparable enantioselectivities by employing the two diastereomers of the same catalyst. The research towards optimal conditions for the asymmetric hydrogenation of acetophenone catalyzed by complexes **109-115** and **117**, as well as their use in the reduction of other carbonyl compounds, is still under investigation.



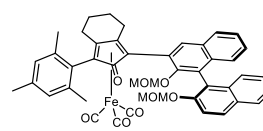
(S,R)-110



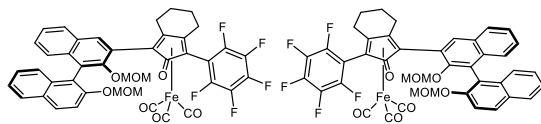
(R,R)-110



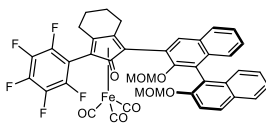
(S,R)-112



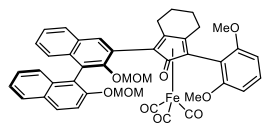
(R,R)-112



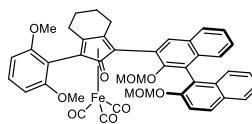
(R,R)-113



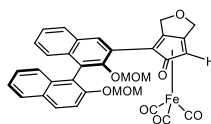
(S,R)-113



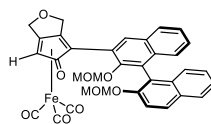
(R,R)-114



(S,R)-114



(S,R)-117



(R,R)-117

3. Part B.

Diastereoselective Epoxidation of Chiral Terminal Allylic Alcohols Catalyzed by a Titanium Salalen Complex

3.1. Titanium Complexes

Titanium is an element belonging to period 4 and group IV of the periodic table, with an electronic configuration of $[\text{Ar}]3d^24s^2$. It is the second most abundant transition metal on Earth's crust, where it is found in an oxidized form in minerals like anatase, brookite, ilmenite, perovskite, rutile, and titanite.

The oxidation state +4 is the most common for titanium compounds: TiO_2 is an ubiquitous species that finds many applications, particularly as a pigment, but nanosized TiO_2 is also widely employed in material sciences and in photocatalysis, thanks to its UV light absorption capability. Many other Ti^{IV} species, such as the halides, easily hydrolyze to form the chemically inert TiO_2 , due to the oxophilic nature of the metal.

Among the halides, TiCl_4 has a particularly relevant role in organic chemistry thanks to the strong Lewis acidity of the metal center. Examples of this reactivity are the Mukayama condensation^[146] and the methylenation promoted by Lombardo's reagent.^[147] TiCl_4 is also used as starting material in the synthesis of many Ti^{IV} coordination complexes.

$\text{Ti}(\text{O}i\text{Pr})_4$, readily prepared by reaction of TiCl_4 with isopropanol, is a moisture-sensitive transparent liquid, which has been used in organic synthesis for its Lewis acidic properties, as well as catalyst for redox reactions, radical processes and formation of C-C bonds.^[148] Most notably, combined with enantiopure tartrate esters, it played a key role in enantioselective synthesis, as catalyst in the Sharpless asymmetric epoxidation.^[149]

Other complexes containing titanium generally show a coordination number of 6 with an octahedral geometry, even though species like alkoxides or organotitanium complexes containing cyclopentadienyl or aryl ligands can assume tetrahedral geometries. The use of titanium complexes in catalysis is very attractive, given the low toxicity and the availability of the metal. However, their application is more limited than that of late transition metals, due to the lower tolerance of functional groups and other issues related to oxophilicity and strong Lewis acidity.

Nevertheless, Ti^{IV} -based catalysts have already found widespread applications in diverse organic transformations.^[150] Ti^{III} (d^1)^[151] and Ti^{II} (d^2)^[152] complexes are less frequently found, but have been applied to redox reactions, thanks to their easy oxidation to Ti^{IV} (d^0) species.^[153]

Organotitanium compounds have been studied as catalysts for polymerization reactions,^[154] as well as for hydrogenation^[155] and hydroamination reactions,^[156] cycloadditions,^[157] cyclopropanations,^[158] and other redox transformations.^[159]

Notable examples of titanium complexes employed in organic transformations (Figure 29) are titanocene dichloride (Cp_2TiCl_2), used as Ziegler-Natta catalysts for the syndiotactic polymerization of propylene, or the titanium complexes containing tethered cyclopentadienyl ligands known as Kaminsky catalysts.^[160] Well-established methods for alkenylation reactions are based on the use of titanium species like Tebbe's reagent, prepared from Cp_2TiCl_2 and AlMe_3 ,^[161] or the Petasis' reagent (Cp_2TiMe_2).^[162]

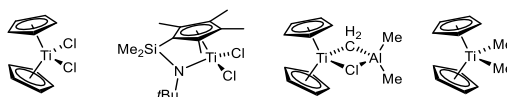


Figure 29. Selected examples of well-known titanium-based catalysts. From left to right: Cp_2TiCl_2 , Kaminsky catalyst, Tebbe's reagent, Petasis' reagent.

Complexes containing diverse and more elaborated ligands have been developed and extensively studied for their catalytic activity over the years.^[163]

Among the various compounds investigated for the coordination to titanium, chiral tetradentate *O-N-N-O* species (salen, salan and salalen ligands) have attracted great interest during the last decades, due to the ability of their complexes to catalyze asymmetric transformations.

3.2. Titanium Salalen Complexes

The first salen ligand was isolated in 1889. Since then, Schiff base ligands (Figure 2) have been looked at as very interesting ligands, due to their easy synthesis through condensation of two aldehyde units (usually salicylaldehyde derivatives) with a diamine, and due to their ability to stabilize various metal centers via chelation.

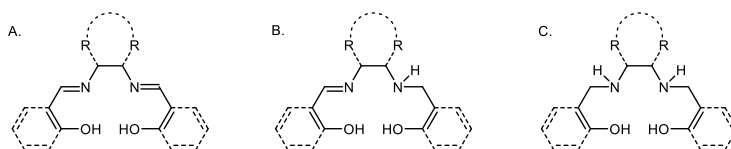


Figure 30. Exemplificative structure of: A. salen; B. salalen; C. salan ligands.

Furthermore, during the second half of the 20th century metal complexes containing properly designed chiral salen ligands have been studied as catalysts for diverse asymmetric transformations, including for instance enantioselective epoxidations, Baeyer-Villiger oxidations, hydroxylations, sulfoxidations, cyclopropanations, cycloadditions, and other processes.^[164]

A considerable contribution to this field of chemistry has been given by Tsutomu Katsuki, who developed optically active salen ligands used in several catalytic processes in combination with various metals, and put emphasis on the role of the coordination topology of this class of complexes on enantioselectivity.^[165] A *cis-β* configuration generates a better enantioselective environment by imparting a Λ or Δ helicity to the metal, while proper substitution on the ligand results in an asymmetrically hindered active site in the catalyst (Figure 32).^[166]

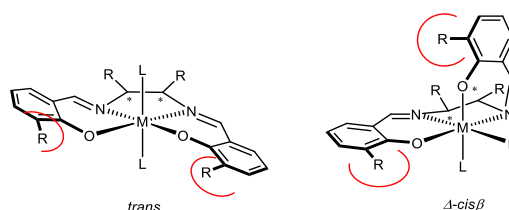


Figure 31. General structure of chiral metal salen complexes showing a *trans* configuration (left) and a *cis-β* configuration (right).

Among the reactions catalyzed by metal salen complexes, asymmetric epoxidation was achieved with promising results using manganese-based catalysts in the 1990's. Complexes such as **118**,^[165d] reported by Jacobsen, and **119**^[167], reported by Katsuki, led to the epoxidation of *cis*-disubstituted, trisubstituted and tetrasubstituted olefins with up to 98% *ee*, using *m*-CPBA, NaOCl or other oxidizing agents (Figure 33).^[168]

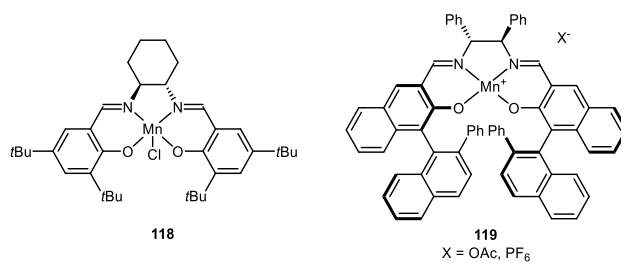
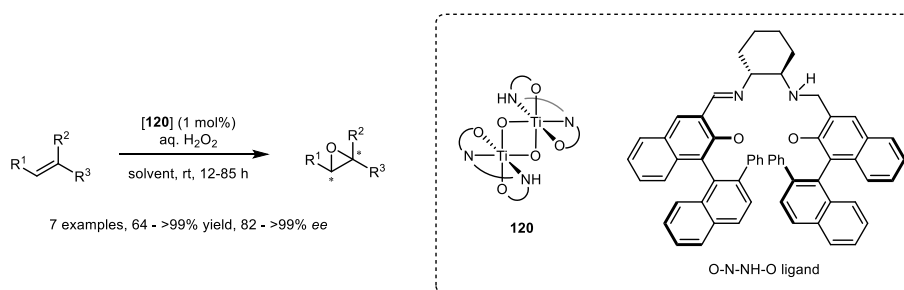


Figure 32. Structure of Mn-based catalysts for the asymmetric epoxidation of alkenes developed by Jacobsen and Katsuki.

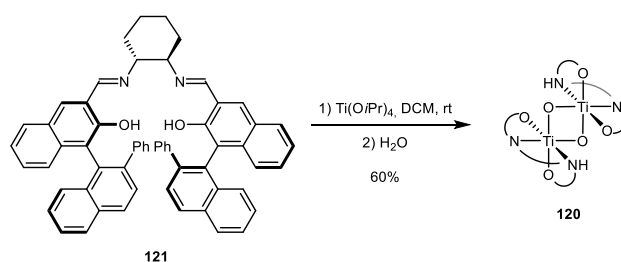
In 2005 Katsuki reported the asymmetric epoxidation of unfunctionalized trisubstituted olefins in the presence of benign hydrogen peroxide as terminal oxidant catalyzed by di- μ -oxo titanium complex **120**, which led to enantiomeric excesses as high as >99% (Scheme 91).^[169]



Scheme 91. Asymmetric epoxidation catalyzed by di- μ -oxo complex **120.**

Complex **120** was the first example of a titanium salen complex used in epoxidation reactions, and it must be pointed out that even unactivated unconjugated olefins could be oxidized in good yields and selectivities [e.g. 1-octene was converted to (*S*)-1,2-epoxyoctane in 85% yield and 82% ee].

Complex **120** was prepared from salen ligand **121** through coordination with a titanium center derived from Ti(O*i*Pr)₄. The resulting [Ti(**121**)(O*i*Pr)₂] intermediate spontaneously underwent Meerwein-Ponndorf-Verley reduction, through which one of the imine moieties was reduced to amine, and dimerization in the presence of water (Scheme 92).^[169]



Scheme 92. Synthesis of titanium salen complex **120 from ligand **121**.**

Complex **120** shows *cis*- β configurations on both metal centers, with Δ and Λ helicity respectively. This topology proved extremely beneficial for the enantioselective outcome of the reaction, while the semi-reduced ligand was essential for the catalytic activity. Indeed, dimeric salen complexes were previously reported to perform with better enantioselectivities than the corresponding monomer,^[170] and a titanium-based di- μ -oxo complex containing salen ligand **121** was prepared (complex **122**, Figure 33). However, **122** was not active as catalyst for epoxidation reactions.^[169]

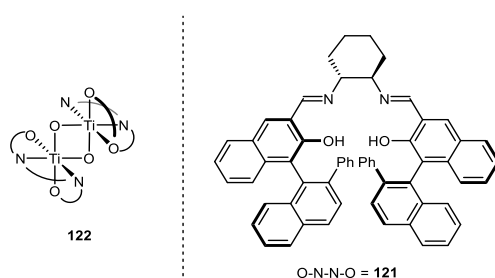
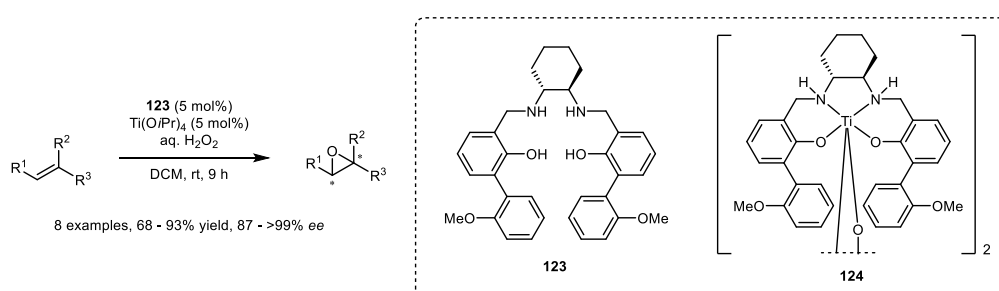


Figure 33. Structure of dimeric salen complex **122**, inactive in epoxidation of alkenes.

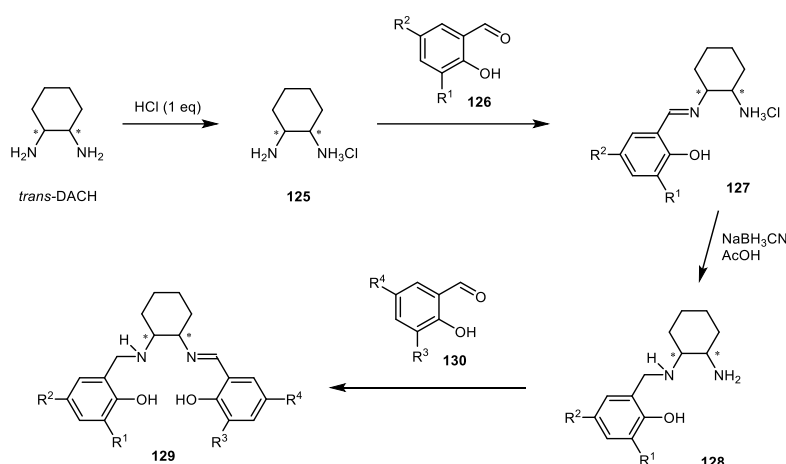
In 2006, the synthesis of chiral titanium salen ligand **123** (Scheme 93) was reported by Katsuki and coworkers. X-ray analysis confirmed also in this case the dimeric nature of the corresponding complex **124**, which shows a *cis*- β configuration, in analogy with the previously described salen and salalen titanium species. Use of **124** (generated *in situ*) as catalyst in the presence of hydrogen peroxide afforded the epoxidation of terminal, *cis*-disubstituted, and trisubstituted conjugated alkenes at room temperature, with good yields and up to >99% *ee*.^[171]



Scheme 93. Asymmetric epoxidation of alkenes promoted by titanium salen complex **124**.

Advantages in the use of catalyst **124** compared to **120** can be identified in its lower molecular weight, as well as in the easier synthesis of the ligand, and in the fact that the Meerwein-Ponndorf-Verley process that leads to the formation *in situ* of the semi-reduced salalen ligand in **120** could not be easily applied to other complexes.

A practical method for the synthesis of salalen ligands was reported in 2007 by Berkessel and coworkers (Scheme 94),^[172] involving the initial mono-protonation of a chiral diamine (*trans*-1,2-diaminocyclohexane), followed by condensation of the free amine in **125** with a salicylaldehyde derivative (**126**). The imine moiety in structure **127** is then reduced, affording intermediate **128**. The second imine bond in species **129** is formed through condensation with another equivalent of salicylaldehyde (**130**). The modularity of the synthesis allows the formation of symmetrically as well as the preparation of asymmetrical salalen ligands, when two different aldehydes are employed.



Scheme 94. General synthetic pathway for the preparation of salalen ligands.

This approach to the preparation of salalen ligands allowed to screen the effect of the substitution on the aromatic rings. The functionalization of the positions in *ortho* to the OH groups turned out to be essential for both yield and selectivity. Complex **131** (Figure 34) was identified as the optimal catalyst among the compounds studied, affording the epoxidation of conjugated *cis*-difunctionalized olefins in high yields and with enantioselectivities as high as 97%, even if its structure is far simpler than that of **120**. Nevertheless, epoxidation of unconjugated olefins was achieved in low conversions, probably due to competitive degradation of the catalyst in the reaction environment.^[173]

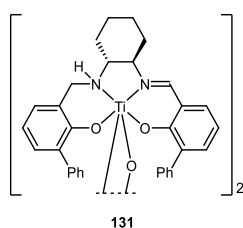
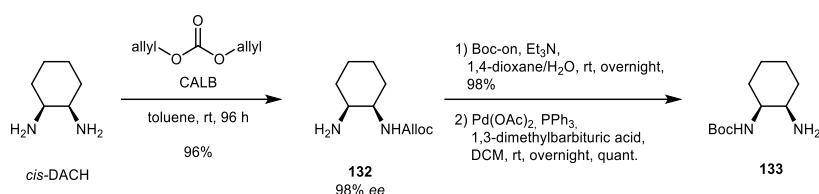


Figure 34. Structure of catalyst **131**.

A major turning point in the activity of chiral titanium salen catalysts was reached with the development of ligands based on *cis*-diaminocyclohexane (*cis*-DACH).

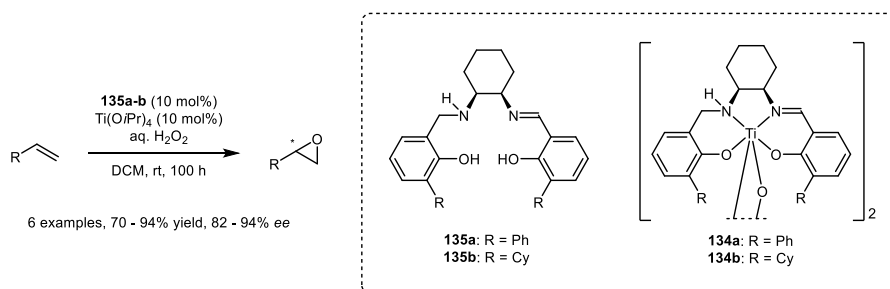
Due to the enantiotopic nature of the two nitrogen atoms, application of the sequential pathway shown in Scheme 94 to *cis*-DACH would lead to the formation of racemic salen ligands. However, an efficient method for the enantioselective mono-Alloc-protection of *cis*-DACH mediated by *Candida antarctica* lipase B was developed in Berkessel's research group (Scheme 95).^[174]



Scheme 95. Synthesis of enantiopure mono-protected *cis*-DACH derivatives **132** and **133**.

(*1R,2S*)-**132** was prepared in 98% *ee*. Protection of the second amine group in **132** followed by orthogonal cleavage of the Alloc group afforded (*1S,2R*)-**133** (Scheme 95), which could be used in turn to obtain the opposite enantiomers of the salen ligands. Both compounds could be used for the synthesis of new salen ligands by means of condensation with a first unit of salicylaldehyde, followed by reduction, removal of the allyloxy carbonyl protecting group and final formation of the second imine moiety.

Synthesis of *cis*-DACH-based salen ligands with various patterns of substitution on the aromatic rings was reported in 2013 by the same research group. Titanium complexes **134a-b**, containing ligands **135a-b**, presented the usual di- μ -oxo structure and *cis*- β configuration on both metal centers and were shown to be less prone to oxidative degradation than **131**. **134a** and **134b** were both tested in the H_2O_2 -mediated oxidation of unconjugated unactivated alkenes (Scheme 96), which could be converted to the corresponding epoxides in high yields and up to 94% *ee*.^[175]



Scheme 96. Epoxidation of unactivated alkenes catalyzed by *cis*-DACH-based complexes **134a** and **134b**.

However, epoxidations promoted by **134a-b** proceeded with a limited rate, requiring 10 mol% catalyst loadings and up to 100 hours of reaction time. Improvement in the activity was achieved with catalysts **136a-b** (Figure 35): epoxidation of 1-octene occurred in analogous reaction times, with catalyst loadings as low as 0.5% for **136a** (72% yield, 96% *ee*, solvent-free conditions) and 0.1% for **136b** (89% yield, 92% *ee* in DCE).^[176]

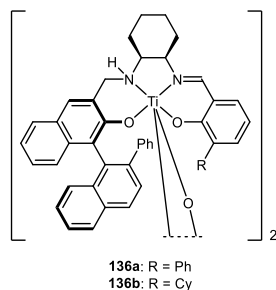


Figure 35. Structure of titanium salen complexes **136a-b**.

Finally, in 2017 Berkessel and coworkers reported the synthesis of ligand **137**, which reacts with $\text{Ti}(\text{O}i\text{Pr})_4$ and water to give di- μ -oxo complex **138** (Figure 36).^[177]

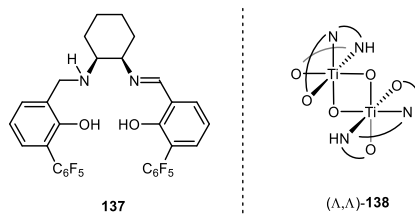
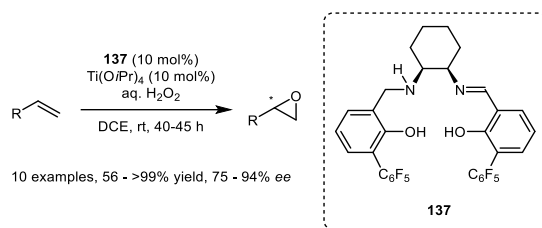


Figure 36. Structure of salalen ligand **137** and the corresponding dimeric titanium complex **138**.

To date, complex **138** afforded the best results as catalyst for H_2O_2 -mediated asymmetric epoxidation of unactivated alkenes. Both activity and selectivity of this new titanium species exceeded the results previously obtained: 1-octene was converted to (*S*)-1,2-octene epoxide in quantitative yield and 94% *ee* in 45 hours, and *ee*'s up to >99% were reported for other terminal alkenes and allyl ethers (Scheme 97). Moreover, **138** was proven sufficiently stable to often allow recycling of the catalyst.



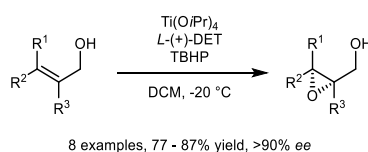
Scheme 97. Asymmetric epoxidation of alkenes catalyzed by complex 138.

The mechanism of the asymmetric epoxidation promoted by **138** was recently elucidated through X-ray Diffraction and NMR analyses, kinetic studies, and DFT computation. The key role of the pentafluorophenyl substituents in the activation of hydrogen peroxide was highlighted, along with the cooperative action of the hydrogen bonding donation from the amine moiety in the ligand and of the Lewis acidity of titanium.^[178]

3.3. Asymmetric Epoxidation of Allylic Alcohols

As the *syn*-selective epoxidation of chiral secondary allylic alcohol will be treated in this part of the elaborate, the most relevant catalytic methods reported to date for this asymmetric transformation will be briefly described.

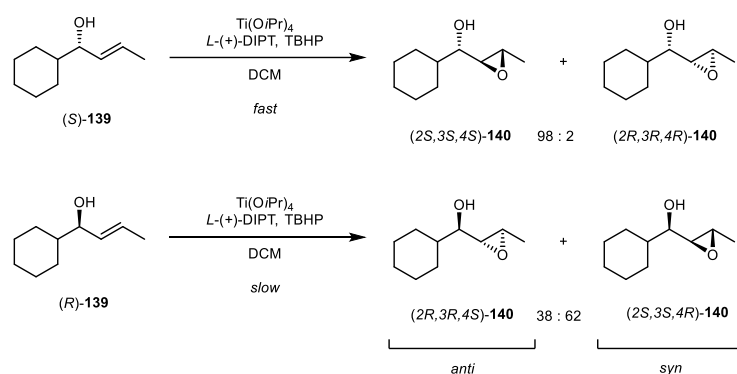
The first efficient metal-catalyzed method for the asymmetric epoxidation of allylic alcohols was reported by Sharpless in 1980. The reaction involved the use of *tert*-butyl hydroperoxide (TBHP) as terminal oxidant in the presence of stoichiometric amounts of Ti(O*i*Pr)₄ and enantiopure (+)- or (-)-diethyl tartrate (Scheme 98).^[149]



Scheme 98. Sharpless asymmetric epoxidation.

Key features of the Sharpless Asymmetric Epoxidation (SAE) are the uniformly high enantioselectivities that can be achieved with diverse allylic alcohols^[179] and the fact that the absolute configuration of the newly-generated stereocenters depends only on the enantiomer of tartrate employed, and not on the substitution pattern of the substrate. The method was subsequently found to be efficient also by using catalytic amounts of titanium isopropoxide and tartrate.^[180]

When applied to secondary allylic alcohols, the SAE gives different results depending on the configuration of the stereocenter already present on the alcohol combined with the enantiomer of the tartrate. Sharpless reported in 1981 the epoxidation of *rac*-1-cyclohexylbut-2-en-1-ol (**139**, Scheme 99) with *L*-(+)-diisopropyltartrate: reaction with enantiomer (*S*)-**139** occurred with a higher rate, affording the selective formation of the *anti*-epoxy alcohol product (*2S,3S,4S*)-**140** (*anti:syn dr* = 98:2), while oxidation of (*R*)-**139** was slower and less diastereoselective towards the *syn*-product (*2S,3S,4R*)-**140** (*syn:anti dr* 62:38).^[181]



Scheme 99. SAE performed on chiral allylic alcohol **139**.

Conditions for the kinetic resolution of chiral allylic alcohols based on the SAE were thus optimized. Use of *L*-(+)-diisopropyltartrate with several allylic alcohols afforded the selective recovering of the (*R*)-enantiomer of the starting material, with preferential formation in most cases of the *anti*-product deriving from the (*S*)-enantiomer of the starting material in high *dr*'s. Previous attempts to achieve *anti*-selective epoxidation of chiral allylic alcohols involving the use of an achiral catalytic system based on VO(acac)₂ and TBHP were reported, but *anti:syn* ratios were only moderate.^[181]

In 2000, Scettri and coworkers reported the unprecedented use of cyclopentadienyl complexes of titanium and zirconium (Figure 37) for the epoxidation of allylic alcohols and observed the tendency of these systems to consistently lead to excesses towards the *anti*-products, even though with lower *dr*'s than in the SAE.^[182]

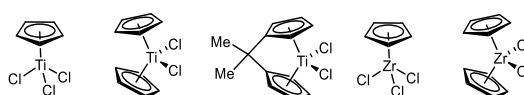
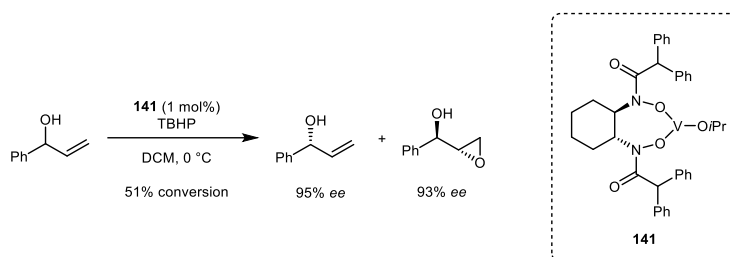


Figure 37. Titanocene and zirconocene complexes used by Scettri for the epoxidation of chiral allylic alcohols.

High preference towards the formation of *anti*-epoxy alcohols were reported also by Yamamoto and coworkers, who described the TBHP-mediated epoxidation of allylic alcohols catalyzed by complexes of vanadium containing chiral bishydroxamic acid ligands.^[183] Complex **141** was used in the kinetic resolution of chiral allylic alcohols (Scheme 100) with selectivities comparable to Sharpless' method.



Scheme 100. Kinetic resolution of 1-phenylprop-2-en-1-ol catalyzed by complex 141.

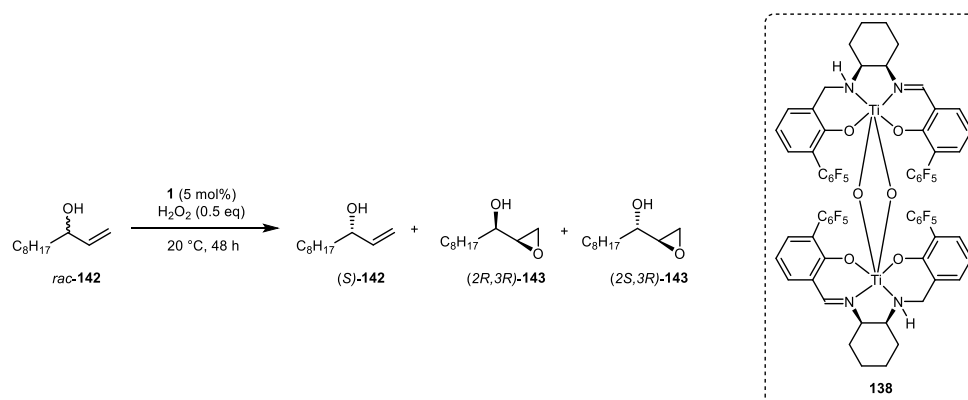
On the other hand, a catalytic method for the highly diastereoselective formation of *syn*-epoxy alcohols is not known yet. In 1996, Adam reported that the stereochemical outcome could be reversed, even though still with modest results, by employing titanium-containing zeolites (TS-1) in combination with hydrogen peroxide or the hydrogen peroxide-urea adduct.^[184] Furthermore, the nature of the alcohol and that of the oxidizing agent were reported to have a high influence on diastereoselectivity, leading in some cases to the preferential isolation of the *syn*-products in the absence of chiral catalytic systems.^[185] However, many substrates such as terminal allylic alcohols could never be converted to the corresponding *syn*-epoxy alcohols with synthetically useful diastereomeric excesses.

3.4. Results and Discussion

Given the good activity and high enantioselectivity shown by catalyst **138** in the asymmetric epoxidation of terminal alkenes, its application to the catalytic oxidation of a wider range of functionalized olefinic substrates was investigated more in depth.

Terminal secondary allylic alcohols were tested, in order to explore activity and selectivity of **138** in a procedure analogous to the Sharpless kinetic resolution. Epoxidation of racemic undec-1-en-3-ol (*rac*-**142**) was conducted in the presence of 5 mol% of **138** and 0.5 equivalents of hydrogen peroxide at 20 °C, both in dichloromethane and acetonitrile as solvents. The results obtained for the two tests are reported in Table 14.

Table 14. Tests on the kinetic resolution of *rac*-**142** catalyzed by titanium salalen complex **138**.



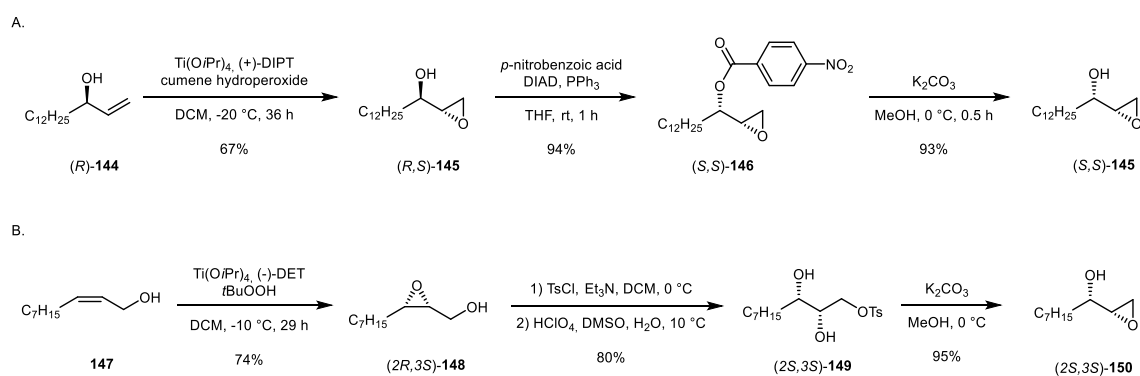
Entry	Solvent	Conversion [%] ^[a]	ee for (S)- 142 [%] ^[a]	Yield in (2R,3R)- 143 [%] ^[a]	ee for (2R,3R)- 143 [%] ^[a]	syn:anti dr ^[a]
1	DCM	41	42	32	97	7.9:1
2	MeCN	51	42	41	94	3.3:1

Reaction conditions: C₀(substrate) = 0.2 M, substrate/catalyst/H₂O₂ = 100:5:50, temperature = 20 °C, reaction time = 48 h; [a] Determined by GC analysis with a chiral capillary column, using Ph₂O as internal standard. The reactions were conducted by Dr. Fabian Severin.

In both dichloromethane and acetonitrile, almost half of the starting material was consumed after 48 hours, but the non-converted alcohol was recovered in only 42% ee. Even though a significant influence of the absolute configuration of the allylic alcohol on the conversion rates was not observed, the enantioselective behavior of the titanium salalen complex towards the epoxidation reaction was confirmed by the high ee values achieved for the newly generated stereocenters, which possess an (*R*) absolute configuration, in agreement with the data already collected for other terminal alkenes. Moreover, an interesting diastereoselective outcome was observed in the formation of the epoxy alcohol products, especially in the test performed in

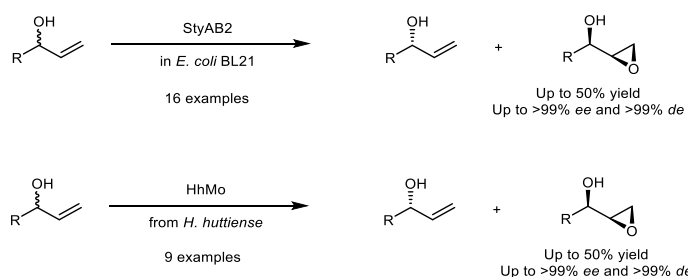
dichloromethane, which resulted in a diastereomeric ratio of 7.9:1 in favor of the *syn*-product (*2R,3R*)-**143**.

The preferential formation of the *syn*-configured product cannot be easily achieved by the employment of other catalytic systems, which usually lead mostly to an excess towards the *anti*-epoxy alcohol, as described in chapter 3.3. Synthesis of compounds with this stereochemistry is usually achieved through multiple synthetic steps, involving for instance the inversion of configuration of the alcohol stereocenter of an *anti*-epoxy alcohol through Mitsunobu reaction (Scheme 101A),^[186] or the acid-catalyzed ring opening of a tosylated 2,3-epoxy-1-alcohol, followed by formation of a new epoxide cycle on positions 1 and 2 in basic media (Scheme 101B).^[179,187]



Scheme 101. Preparation of *syn*-epoxy alcohols through: A. inversion of the configuration of position 2 via Mitsunobu reaction; B. intramolecular substitution reaction.

Alternatively, some *syn*-epoxy alcohols could be isolated from the corresponding racemic allylic alcohols via enzymatic kinetic resolution promoted by monooxygenases (Scheme 102).^[188,189]



Scheme 102. Enzymatic kinetic resolution of terminal allylic alcohols mediated by monooxygenases.

A deeper investigation of the reactivity of the Berkessel-Katsuki catalyst with terminal allylic alcohols was thus pursued, envisaging the possibility to develop an efficient and direct catalytic method for their *syn*-selective epoxidation. Specifically, the results of the first test performed on

rac-undec-1,2-en-3-ol suggested that the *syn*-configured product (*2R,3R*)-**143** could be obtained as single isomer from enantiopure (*R*)-undec-1,2-en-3-ol.

The study of the asymmetric epoxidation of enantiopure terminal allylic alcohols promoted by H₂O₂ and catalyzed by complex **138** was thus conducted and the results that were obtained are described in the following chapters.

3.4.1. Asymmetric Epoxidation of Enantiopure Terminal Allylic Alcohols

We decided to investigate the *syn*-selective epoxidation on a small library of enantiopure secondary alcohols bearing different alkyl residues. Besides the *n*-octyl chain contained in compound (*R*)-**142**, secondary, tertiary, and benzylic carbons were connected to position 3 of the allylic alcohol moiety (Figure 38), in order to test the applicability of the method to variously substituted substrates.

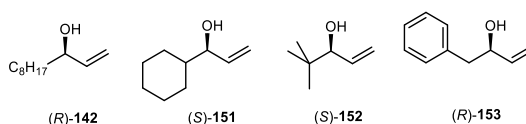
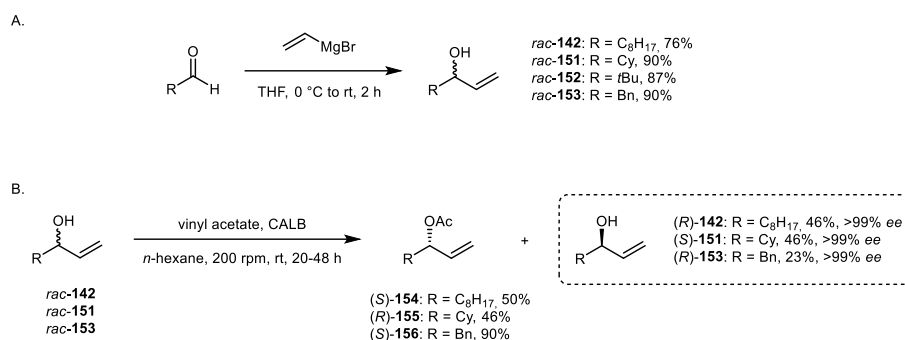


Figure 38. Library of alcohols employed as substrates in the *syn*-selective epoxidation catalyzed by **138**.

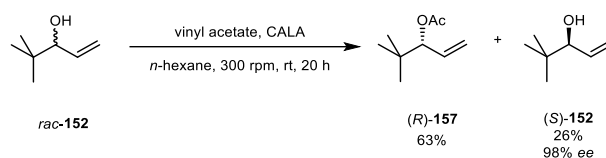
Enantiopure terminal allylic alcohols with the configuration required for the *syn*-selectivity can be easily and efficiently isolated from the corresponding racemic material through enzymatic kinetic resolution promoted by lipases.^[190]

The four allylic alcohols were firstly prepared as racemates by addition of vinylmagnesium bromide to the corresponding aldehydes (Scheme 103A). (*R*)-**142**, (*S*)-**151**, and (*R*)-**153** were then readily isolated in >99% *ee* by treatment with *Candida antarctica* lipase B (CALB) and vinyl acetate in *n*-hexane (Scheme 103B).



Scheme 103. Synthetic pathway for the preparation of: A. racemic alcohols *rac*-142, *rac*-151-153; B. enantiopure alcohols (*R*)-142, (*S*)-151, and (*R*)-153. Compounds (*R*)-142 and (*R*)-153 were synthesized by Dr. Fabian Severin.

Resolution of compound *rac*-152 required the use of *Candida antarctica* lipase A (CALA) and led to the isolation of (*S*)-152 in 98% ee in 26% yield (Scheme 104).



Scheme 104. Resolution of substrate *rac*-152 promoted by CALA.

The evaluation of proper conditions for the epoxidation reaction were undertaken on enantiopure substrate (*R*)-142. The catalytic tests were conducted in different solvents in the presence of 1.5 equivalents of hydrogen peroxide and complex **138** with a 5 mol% catalytic loading, at 20 °C for 48 hours (Table 15).

Table 15. Solvent screening for the titanium-catalyzed epoxidation performed on (*R*)-142.

Solvent	DCM	CHCl ₃	CHCl ₃ over K ₂ CO ₃	DCE	MeCN	Toluene	EtOH	HFIP	THF
Yield [%] ^[a]	88	91	87	87	74	47	12	80	67

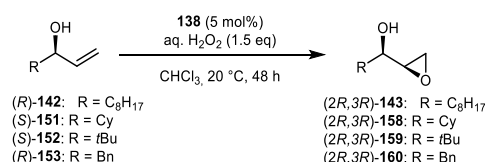
Reaction conditions: C₀(substrate) = 0.2 M, substrate/catalyst/H₂O₂ = 100:5:150, temperature = 20 °C, reaction time = 48 h; [a] Determined by GC analysis with a chiral capillary column, using Ph₂O as internal standard. The tests were conducted by Dr. Fabian Severin.

Screening of the solvent reported in Table 15 shows that **138** leads to generally good yields. The best results were achieved in halogenated solvents, reaching up to 91% yield in chloroform. Further tests involving the use of pentafluorobenzoic acid or 2,6-di-*tert*butylpyridine as additives

did not lead to major improvements. From these preliminary tests, we could also observe, to our delight, the formation of (*2R,3R*)-**143** in >99:1 *syn:anti* diastereoisomeric ratio, with preservation of the >99% *ee*.

Consequently, we proceeded to test substrates (*S*)-**151**, (*S*)-**152**, and (*R*)-**153** in the conditions described above. Results of the catalytic tests are reported in Table 16.

Table 16. Catalytic tests performed on substrates (*R*)-142**, (*S*)-**151**, (*S*)-**152**, and (*R*)-**152**.**



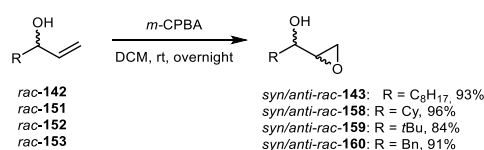
Entry	Substrate	138 [mol %]	H ₂ O ₂ [eq]	Yield [%] ^[a]	<i>syn:anti</i> <i>dr</i> ^[a]	<i>ee</i> [%] ^[a]
1	(<i>R</i>)- 142 , R = C ₈ H ₁₇	5	1.5	91	>99:1	>99
2	(<i>R</i>)- 142 , R = C ₈ H ₁₇	1	1.5	88	>99:1	>99
3	(<i>S</i>)- 151 , R = Cy	5	1.5	93	>99:1	>99
4	(<i>S</i>)- 151 , R = Cy	1	1.5	70	>99:1	>99
5	(<i>S</i>)- 151 , R = Cy	1	3 ^[b]	85	>99:1	>99
6 ^[c]	(<i>S</i>)- 151 , R = Cy	2	3 ^[b]	94 ^[d]	>99:1	>99
7	(<i>S</i>)- 152 , R = <i>t</i> Bu	5	1.5	85	93:1	99
8	(<i>S</i>)- 152 , R = <i>t</i> Bu	5	3 ^[b]	97	99:1	99
9	(<i>S</i>)- 152 , R = <i>t</i> Bu	10	1.5	97	99:1	99
10	(<i>R</i>)- 153 , R = Bn	5	1.5	86	>99:1	>99

Reaction conditions: C₀(substrate) = 0.2 M, substrate/catalyst/H₂O₂ = 100:5:150, solvent = CHCl₃, temperature = 20 °C, reaction time = 48 h; [a] Determined by GC with a chiral capillary column, using Ph₂O as internal standard (see Experimental Section, Paragraph 4.19). [b] The additional aliquot of 1.5 eq of H₂O₂ was added after the first 24 hours. Tests on substrates (*R*)-**142** and (*R*)-**153** were conducted by Dr. Fabian Severin; [c] Reaction performed on 2.57 mmol of (*S*)-**151**; [d] Isolated yield.

The tests were conducted in chloroform at 20 °C. All reactions proceeded smoothly and afforded the highly diastereoisomerically pure *syn*-epoxy alcohols (*2R,3R*)-**143**, (*2R,3R*)-**158**, (*2R,3R*)-**159**, and (*2R,3R*)-**160** in overall good yields after 48 hours. Substrates (*R*)-**142** and (*S*)-**151** were both converted to the corresponding *syn*-epoxy alcohols in >90% yields using 5 mol% of the catalyst and 1.5 equivalents of hydrogen peroxide, with *syn:anti* *dr*'s of >99:1 (entries 1 and 3). (*2R,3R*)-**158** was obtained in 88% yield even with a catalyst loading of 1%, maintaining the diastereoselectivity intact (entry 2). Lowering the amount of titanium complex to 1% led to 70% yield in the case of the cyclohexyl-substituted substrate (entry 4); however, the yield could be increased to 85% by addition of a second portion of hydrogen peroxide (1.5 equivalents) after

the first 24 hours, without any erosion of the *syn:anti dr. tert*-Butyl substituted epoxy alcohol (*R,R*)-**159** was obtained in 85% yield in the standard reaction conditions (entry 6), and in 97% yield both by adding more H₂O₂ over time (entry 7) or by enhancing the catalyst loading to 10 mol % (entry 8). In the tests performed on alcohol **152** traces of (*2R,3S*)-**159** [deriving from the oxidation of (*R*)-**152**] were observed, due to the <99% *ee* of the starting material. Moreover, formation of minor amounts of (*2S,3R*)-**159** was also observed. However, the registered *syn:anti* ratios were always high. Finally, (*R*)-**153** was converted to (*2R,3R*)-**160** in 87% yield and >99:1 *syn:anti dr.*

Conversions and stereoselectivities were monitored by analyzing samples taken from the reactions through GC equipped with chiral capillary columns (diphenyl ether was added to the reaction mixture as internal standard). The stereoselective outcome was verified by comparison of the chromatograms of the diastereopure products with those of the racemic compounds *syn/anti-rac-143* and *syn/anti-rac-158-160*, which were prepared by epoxidation of the corresponding racemic alcohols with *m*-CPBA (Scheme 105).



Scheme 105. Epoxidation of racemic substrates *rac*-142 and *rac*-151-153 promoted by *m*-CPBA.

Assignment of the *syn/anti* configurations of the epoxy alcohol products was done via analysis of the chemical shift patterns of ¹H-NMR spectra of the pure compounds (see Experimental Section, Paragraph 4.19.2).^[191] Moreover, crystals suitable for X-ray diffraction analysis of (*R,R*)-**158** were grown by slow evaporation of a *n*-pentane solution of the product: the molecular structure confirms the (*R*)-configuration of both stereocenters (Figure 39).

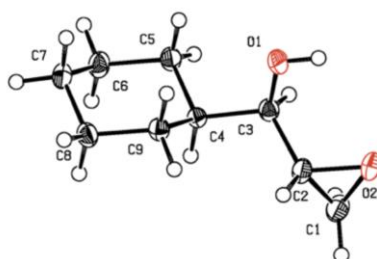
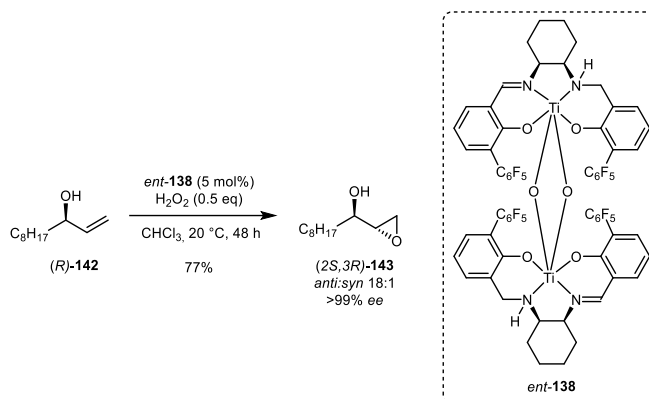


Figure 39. ORTEP diagram (CCDC 2132886) for the molecular structure of epoxy alcohol (*2R,3R*)-158**.**

To demonstrate the possibility of achieving also *anti*-configured products by means of the application of our methodology, the epoxidation of substrate (*R*)-**142** was conducted in the presence of the enantiomer of complex **138** (*ent*-**138**, Scheme 106).

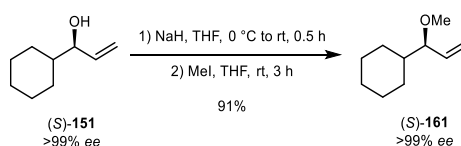


Scheme 106. Anti-selective epoxidation of substrate (*R*)-142** catalyzed by *ent*-**138**.**

The same conditions used in the previous tests (Table 16) were applied, with a 5 mol% catalyst loading, and (*2S,3R*)-**143** was formed in 77% yield. As expected, the absolute configuration of the stereocenter generated upon epoxidation was opposite to what would have been afforded with **138**, and 18:1 *anti:syn* *dr* was observed. Both the conversion and the excess towards the major isomer were good, but lower than the ones previously reported: these results can be rationalized by looking at the combination of (*R*)-**142** and **138** as a “matched pair”, for which diastereoselectivity, as well as the reaction rate, are higher, resulting in overall better results.

3.4.2. Asymmetric Epoxidation of a Chiral Allyl Ether

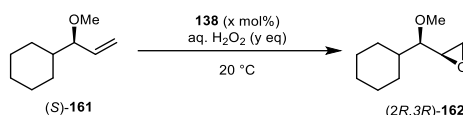
To further explore whether the *syn*-selectivity of asymmetric epoxidation catalyzed by **138** were independent of the presence of the alcohol moiety, and thus to lay the foundations for its application to a wider spectrum of substrates, we embarked on testing the reaction on an allylic ether. Compound (*S*)-**161** was readily synthesized from enantiopure alcohol (*S*)-**151** via methylation with iodomethane (Scheme 107).



Scheme 107. Preparation of methyl ether (*S*)-161**.**

We then proceeded to test the epoxidation under the previously optimized conditions, namely working in chloroform at 20 °C with 1.5 equivalents of H₂O₂ and 5 mol% of **138**. The hoped-for syn product (2*R*,3*R*)-**162** was obtained with excellent diastereoselectivity, even though accompanied by a low 24% yield after 48 hours (Table 17, entry 1).

Table 17. Catalytic asymmetric epoxidation of methyl ether (S)-161.

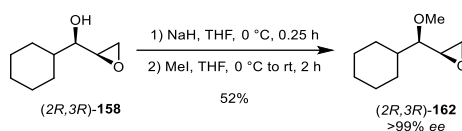


Entry	138 [mol%]	Solvent	H ₂ O ₂ [eq]	Time [h]	Yield [%] ^[a]	<i>syn:anti dr</i> ^[a]	<i>ee</i> [%] ^[a]
1	5	CHCl ₃	1.5	48	24	>99:1	>99
2	5	CHCl ₃	3 ^[b] 7.5 ^[b]	48 168	33 49	>99:1	>99
3 ^[c]	10	CHCl ₃	1.5 3 ^[c]	48 168	46 48	>99:1	>99
4	5	DCE	1.5 3 ^[c]	48 168	59 71	>99:1	>99

Reaction conditions: C₀(substrate) = 0.2 M, substrate/catalyst/H₂O₂ = 100:5:150, temperature = 20 °C; [a] Determined by GC with a chiral capillary column, using Ph₂O as internal standard. [b] Addition of 1.5 eq of H₂O₂ was performed every 24 hours. [c] substrate/catalyst/H₂O₂ = 100:10:150; [d] A second aliquot of H₂O₂ was added after 48 hours.

Aiming to increase the yield, the transformation was repeated with the addition of a higher amount of hydrogen peroxide over time (entry 2), but a maximum of 49% yield was reached after seven days and a total of 7.5 equivalents of hydrogen peroxide. Employment of a higher catalyst loading (10%, entry 3) led to an initial increase in the rate of the reaction, but the reaction substantially stopped at about 48% yield. A major improvement was achieved by performing the reaction in 1,2-dichloroethane (entry 4): 59% yield was observed after 48 hours, and 71% yield was afforded after seven days. All the tests showed >99:1 *syn:anti dr*.

The progress of the reactions and the stereochemical outcome were monitored via chiral GC analysis, using Ph₂O as internal standard also in this case. Furthermore, we could verify the absolute configuration of the two stereocenters of the product (2*R*,3*R*)-**162** by synthesizing the same compound through methylation of epoxy alcohol (2*R*,3*R*)-**158** (Scheme 18).



Scheme 108. Synthesis of epoxy ether (2R,3R)-162 through methylation of enantiopure epoxy alcohol (2R,3R)-158.

Comparison between the $^1\text{H-NMR}$ spectra and the chromatograms of the epoxy ethers obtained through the two methods confirmed the nature of the product of epoxidation and the validity of our procedure for the asymmetric epoxidation.

3.4.3. Synthetic Application: Preparation of a Subunit of Montanacin D

Given the outstanding results obtained for the small library of compounds that were tested, we also planned to employ the newly developed *syn*-selective epoxidation method to the gram-scale synthesis of a portion of a biologically active molecule. The structure targeted for this purpose is the 2,5-bis(hydroxyalkyl)tetrahydrofuran subunit contained in natural products like Montanacin D (Figure 40).^[192]

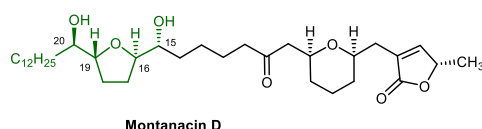
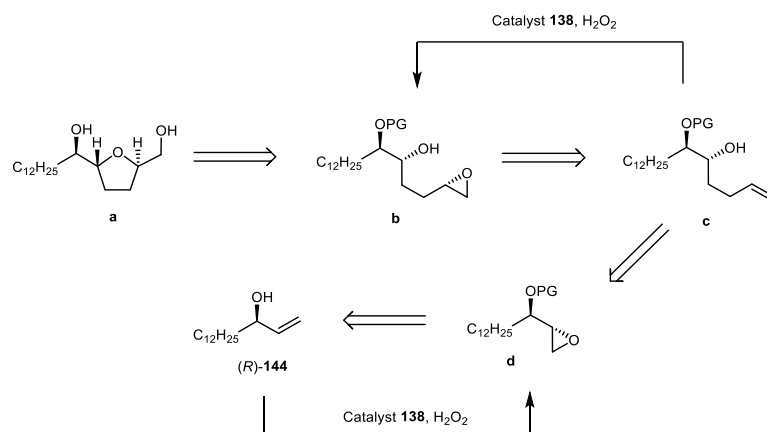


Figure 40. Structure of Montanacin D. The portion of the molecule targeted by our synthesis is highlighted in green.

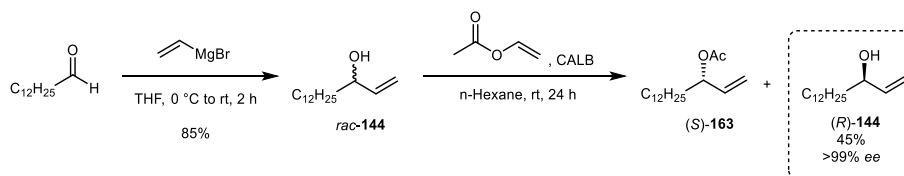
Montanacin D is an *annonaceous acetogenine* that can be isolated through extraction from the leaves of *Annona montana*. It contains a tetrahydropyran ring connected to a nonadjacent tetrahydrofuran ring. The *syn-trans-syn* motif of the latter portion was recognized as a pattern that could be built through the asymmetric epoxidation catalyzed by **138**.



Scheme 109. Retrosynthetic pathway proposed for the preparation of the tetrahydrofuran subunit of Montanacin D.

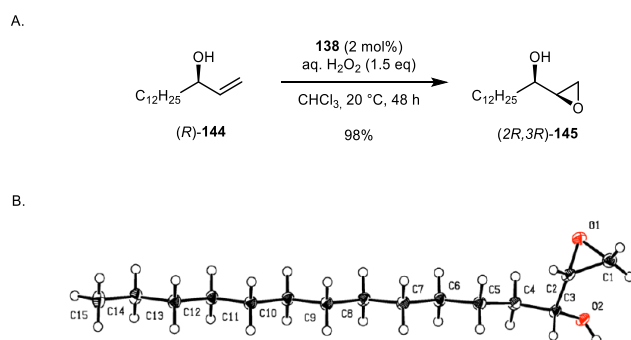
The proposed retrosynthetic pathway, reported in Scheme 109, involves the use of catalyst **138** in two steps: firstly, in the *syn*-selective epoxidation of (*R*)-pentadec-1-en-3-ol [(*R*)-**144**], and then in the asymmetric epoxidation of the terminal double bond of compound **c**.

We thus proceeded to the synthesis of fragment **a**, starting from alcohol (*R*)-**144**, which was prepared in analogous fashion to the previously isolated enantiopure allylic alcohols (Scheme 110).



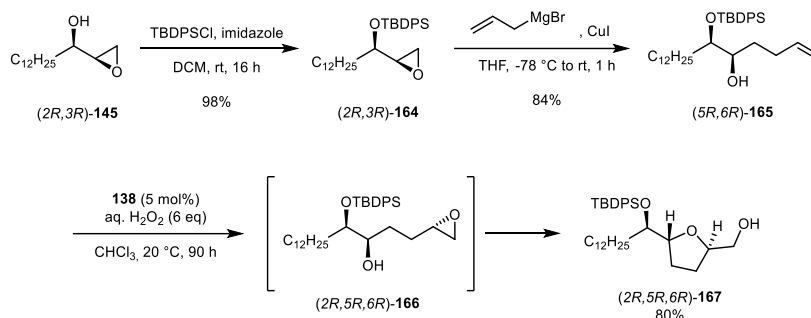
Scheme 110. Synthesis of enantiopure allylic alcohol (*R*)-144**. Kinetic resolution of *rac*-**144** was performed by Sarwar Aziz.**

Epoxy alcohol (*2R,3R*)-**145** was then obtained in 98% yield through epoxidation of (*R*)-**144** promoted by hydrogen peroxide and catalyzed by 2 mol% of **138** (Scheme 111A). Slow evaporation of a solution of (*2R,3R*)-**145** in *n*-pentane afforded crystals suitable for X-ray analysis, which uniquely confirmed the *syn*-configuration of the product of epoxidation (Scheme 111B)



Scheme 111. A. *syn*-selective epoxidation of alcohol (*R*)-144 catalyzed by complex **138; B. ORTEP diagram (CCDC 2132887) for the molecular structure of epoxy alcohol (*2R,3R*)-145.**

Protection of the free OH group was then performed with *tert*-butyl(chloro)diphenylsilane and imidazole in DCM (Scheme 112). The epoxide ring of the TBDPS-protected epoxy alcohol (*2R,3R*)-**164** was subsequently opened with allylmagnesium bromide in the presence of catalytic copper iodide, affording product (*5R,6R*)-**165** in 84% yield.



Scheme 112. Synthesis of the protected subunit of Montanacin D 167 from *syn*-epoxy alcohol 145.

The epoxidation of (*5R,6R*)-**165** catalyzed by titanium complex **138** (5 mol%) was conducted in chloroform at 20 °C and required the addition of 6 equivalents of H₂O₂ over time to reach full conversion after 90 hours. However, (*2R,5R,6R*)-**167** was directly isolated in 80% yield. Formation of the epoxide could be observed by monitoring the reaction through ¹H-NMR spectroscopy (Figure 41), but formation of the five-membered cycle spontaneously occurred in the reaction conditions, probably due to the acidic environment generated by hydrogen peroxide. Building block (*2R,5R,6R*)-**167** was thus successfully prepared from enantiopure terminal allylic alcohol (*R*)-**144** in four synthetic steps with an overall 64% yield.

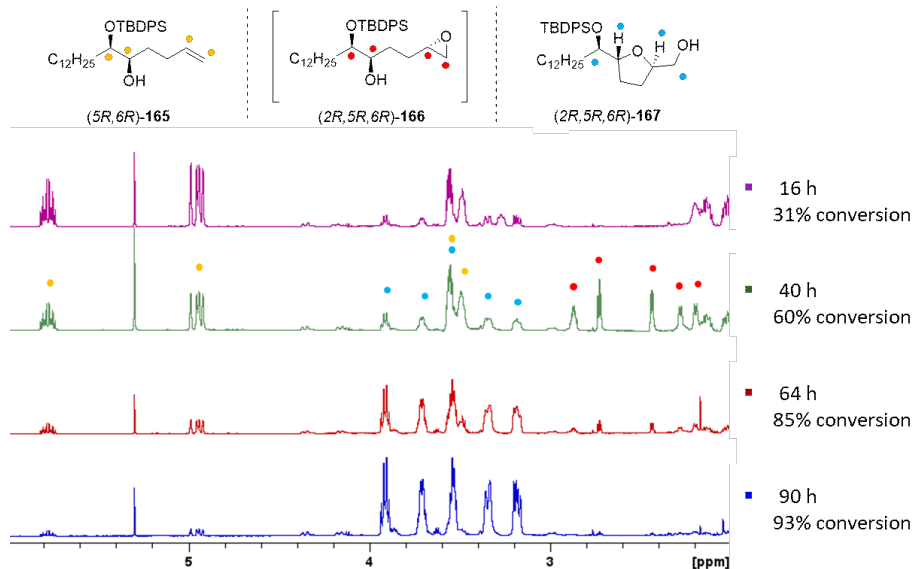
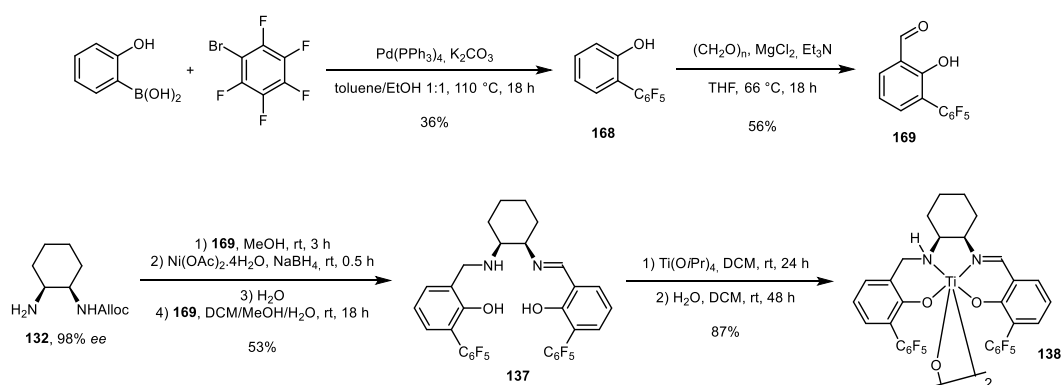


Figure 41. Compared $^1\text{H-NMR}$ spectra (500 MHz, CDCl_3) of samples taken from the epoxidation reaction of (5R,6R)-164 after 16, 40, 64, and 90 hours.

3.4.4. Synthesis of Titanium Salalen Complex **138**

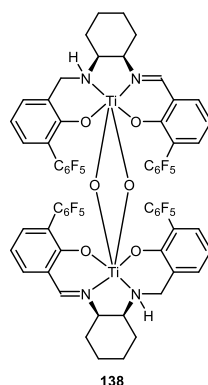
Complex **138** was prepared through a modified literature procedure, as described in Scheme 113. Suzuki coupling between 2-phenylboronic acid and bromopentafluorobenzene catalyzed by $\text{Pd}(\text{PPh}_3)_4$ afforded pentafluorophenyl-substituted phenol **168**, which was formylated in *ortho*-position with paraformaldehyde in the presence of MgCl_2 , leading to salicylaldehyde derivative **169**. Enantiopure salalen ligand **137** was prepared in a one-pot process from mono-protected *cis*-DACH and **169**.^[193] Finally, complex formation was achieved by stirring the ligand in dichloromethane with $\text{Ti}(\text{O}i\text{Pr})_4$ and subsequently adding water to the resulting solution.



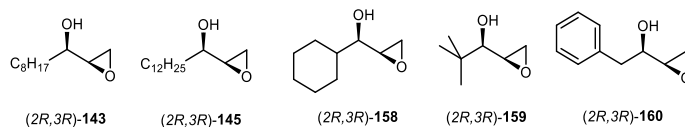
Scheme 113. Synthetic pathway followed for the preparation of titanium salalen complex **138**.

3.5. Conclusions and Outlook

The project described in this section of my PhD thesis aimed to develop a novel method for the H_2O_2 -mediated *syn*-selective epoxidation of chiral terminal allylic alcohols catalyzed by titanium salalen complex **138**, previously developed in Prof. Berkessel's research group, and studied for its outstanding performance in the enantioselective epoxidation of unactivated olefins.

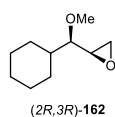


In preliminary tests the catalyst showed excellent activity and diastereoselectivity when used in combination with (*R*)-undec-1-en-3-ol, thus our attention has been directed towards the epoxidation of substrates with the same configuration. A small library of enantiopure terminal allylic alcohols was prepared and tested: all the reactions led to the selective formation of the *syn*-configured epoxy alcohols, in yields as high as 97% and >99:1 *dr*'s throughout. The configuration of the newly generated stereocenter could be undoubtedly confirmed by XRD analysis of epoxy alcohols (*R,R*)-**145** and (*R,R*)-**158**.

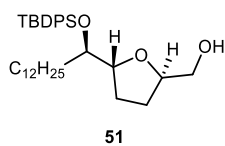


Remarkably, catalyst loadings as low as 1% were sufficient to achieve full conversions. Complex **138** was thus shown to be an overall excellent catalyst in the transformation object of our investigation, whose diastereoselective outcome cannot be easily achieved otherwise.

We were also able to demonstrate that the newly developed strategy for the *syn*-selective epoxidation is not limited to substrates containing free OH groups: performing the reaction on allylic ether as substrate, the *syn*-epoxy ether was successfully obtained in up to 71% yield and >99:1 *syn:anti dr*.



Finally, the elegant and efficient synthesis of building block **167**, suitable for the use in the synthesis of biologically active compounds such as Montanacin D, gave us a further demonstration of the synthetical practicality of the new method: gram-scale preparation of enantiomerically pure **167** was readily performed starting from (*R*)-pentadec-1-en-3-ol in four synthetic steps, two of which involved the use of catalyst **138** in epoxidation processes.



4. 4. Experimental Section

4.1. Materials and Methods

All reactions were carried out in anhydrous solvents in flame-dried glassware with magnetic stirring under nitrogen or argon atmosphere, unless otherwise stated.

The solvents for reactions were either purchased from commercial suppliers (Sigma Aldrich: THF, DMF, toluene, 1,4-dioxane, CCl₄; Carlo Erba: DCM, THF, toluene) and stored under argon over molecular sieves or distilled over the following drying agents and transferred under argon atmosphere: DCM (CaH₂), MeOH (CaH₂), THF (Na), Et₃N (CaH₂).

The reactions were monitored by analytical thin-layer chromatography (TLC) using silica gel 60 F254 pre-coated glass or aluminum plates (0.25 mm thickness). Visualization was accomplished by irradiation with a UV lamp and/or by treatment with staining agents (potassium permanganate alkaline solution, vanillin/H₂SO₄ ethanolic solution, or phosphomolybdic acid ethanolic solution). Purifications through flash column chromatography were performed using silica gel (60 Å, particle size 40-64 μm) as stationary phase phase, following the procedure by Still and co-workers.^[194]

Commercially available reagents were purchased from commercial suppliers (TCI Chemicals, Fluorochem, Sigma Aldrich) and were used as received.

4.2. Instrumentations

¹H-NMR spectra were recorded on Bruker spectrometers operating at 300, 400, or 500 MHz. Proton chemical shifts are reported in ppm (δ) using solvent signal is used as reference (CDCl₃ δ = 7.26 ppm; CD₂Cl₂ δ = 5.32 ppm; (CD₃)₂CO δ = 2.05 ppm). The following abbreviations are used to describe spin multiplicity: s = singlet, d = doublet, t = triplet, q = quartet, m = multiplet, br s = broad signal, dd = doublet-doublet, td = triplet-doublet, ddd = doublet- doublet- doublet. Coupling constant values are reported in Hz. ¹³C-NMR spectra were recorded on on Bruker spectrometers operating at 75, 100, or 125 MHz, with complete proton decoupling. Carbon chemical shifts are reported in ppm (δ) using solvent signal is used as reference (CDCl₃ δ = 77.16 ppm; CD₂Cl₂ δ = 54.00 ppm; (CD₃)₂CO δ = 29.84 ppm, 206.26 ppm). Infrared spectra were recorded on standard FT/IR spectrometers. Wave numbers were reported in cm⁻¹ and the intensities of absorption bands are indicated by the following abbreviations: s = strong, m =

medium, w = weak, br = broad. Optical rotation values were measured on an automatic polarimeter with a 1 dm cell at the sodium D line ($\lambda = 589$ nm).

GC-MS analysis was done on an Agilent Technologies 7890A instrument with injector and autosampler, and an Agilent Technologies 5975C Triple-Axis Detector. A HP-5 MS column (length: 30.0 m, inner diameter: 0.25 mm, film thickness: 0.25 μm) was used with H_2 as carrier gas and the following temperature program 50 $^\circ\text{C}$, 5 min, 20 $^\circ\text{C}/\text{min}$ to 280 $^\circ\text{C}$, 10 min.

High resolution mass spectra (HRMS) were recorded on a Thermo Scientific Exactive GC with an Orbitrap Analyser or on a Fourier Transform Ion Cyclotron Resonance (FT-ICR) Mass Spectrometer APEX II & Xmass software (Bruker Daltonics) – 4.7 T Magnet (MagneX) equipped with ESI source, available at CIGA (Centro Interdipartimentale Grandi Apparecchiature) c/o Università degli Studi di Milano.

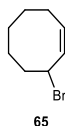
Elemental analyses were performed on a Perkin Elmer Series II CHNS/O Analyzer 2000 n or on an Elementar Vario MICRO cube from Elementar Analysensysteme GmbH. X-ray intensity data were collected with a Bruker Apex II CCD area detector by using graphite monochromated Mo-K α radiation.

Melting points were determined on a Büchi B-540 instrument.

Chiral GC analyses were performed on an Agilent Technologies 6890N instrument with injector 7683B and a Chirasil-Dex CB column (length: 25.0 m, inner diameter: 250 μm , film thickness: 0.25 μm), on an HP 6890 instrument with injector 6890, autosampler and a Lipodex A (length: 25.0 m, inner diameter: 250 μm , film thickness: 0.25 μm), and on a Perkin Elmer Clarus 590 instrument equipped with a flame ionization detector and a MEGADEX DACTBS β capillary column (0.25 μm ; diameter = 0.25 mm; length = 25 m).

4.3. Synthesis and Carbonylative Cyclization of *rac*-3-Methoxycyclooctyne

4.3.1. *rac*-3-Bromocyclooctene (**65**)



cis-cyclooctene (5 mL, 4.22 g, 38.4 mmol, 1 eq) was dissolved in dry CCl₄ (20 mL) under nitrogen atmosphere. NBS (6.84 g, 38.4 mmol, 1 eq) and AIBN (6.6 mg, 0.04 mmol, 0.001 eq) were then added. The mixture was heated to reflux for 2 hours, then cooled to 0 °C. The white precipitate was filtered off through celite, washing with hexane. The solvents were removed under reduced pressure. *rac*-3-Bromocyclooctene **65** was isolated via distillation (40-50 °C, 1 mbar) as a colorless liquid.

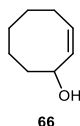
Yield: 4.55 g (24.1 mmol, 62%).

Characterization data are in agreement with the literature.^[195]

R_f = 0.73 (SiO₂, DCM/EDP 1:4)

¹H-NMR (400 MHz, CDCl₃) δ [ppm] = 5.83 – 5.75 (m, 1H), 5.65 – 5.54 (m, 1H), 4.99 – 4.89 (m, 1H), 2.30 – 2.15 (m, 2H), 2.15 – 2.06 (m, 1H) 2.06 – 1.94 (m, 1H), 1.76 – 1.64 (m, 2H), 1.60 – 1.50 (m, 2H), 1.43 – 1.29 (m, 2H).

4.3.2. *rac*-Cyclooct-2-en-3-ol (**66**)



Compound **65** (12.47 g, 66.0 mmol, 1eq) was dissolved in acetone (90 mL). A solution of NaHCO₃ (16.63 g, 197.9 mmol, 3 eq) in water (45 mL) was added and the mixture was heated to reflux for 1 hour. The mixture was then cooled to rt and filtered. Acetone was removed under reduced pressure and the residue was extracted with Et₂O (3 x 40 mL). The collected organic layers were dried over sodium sulphate, filtered and concentrated under reduced pressure. *rac*-Cyclooct-2-en-3-ol **66** was isolated as a colorless liquid and used without further purification.

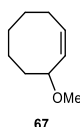
Yield: 7.82 g (62.0 mmol, 94%).

Characterization data are in agreement with the literature.^[196]

R_f = 0.21 (SiO₂, EtOAc/EDP 1:4)

¹H-NMR (400 MHz, CDCl₃) δ [ppm] = 5.67 – 5.58 (m, 1H), 5.58 – 5.50 (m, 1H), 4.72 – 4.60 (m, 1H), 2.24 – 2.04 (m, 2H), 1.97 – 1.87 (m, 1H), 1.72 – 1.34 (m, 7H).

4.3.3. *rac*-3-Methoxycyclooctene (**67**)



Compound **66** (4.00 g, 31.7 mmol, 1 eq) was dissolved in dry Et₂O (25 mL) under nitrogen atmosphere. NaH (60% in mineral oil, 1.14 g, 47.5 mmol, 1.5 eq) was added and the mixture was stirred at rt for 30 minutes. MeI (3.35 mL, 7.65 g, 53.9 mmol, 1.7 eq) was then added and the reaction mixture was stirred at rt for 24 hours. The crude was washed with water (30 mL), then the aqueous layer was extracted with diethyl ether (2 x 30 mL). The collected organic layers were dried over sodium sulphate, filtered and concentrated under reduced pressure. *rac*-3-Methoxycyclooctene **67** was obtained as a colorless liquid and used without further purification.

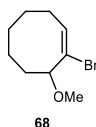
Yield: 4.44 g (31.7 mmol, quantitative).

Characterization data are in agreement with the literature.^[117]

R_f = 0.38 (SiO₂, DCM/*n*-Hexane 4:1)

¹H-NMR (400 MHz, CDCl₃) δ [ppm] = 5.76 – 5.67 (m, 1H), 5.47 (ddd, *J* = 10.8, 7.1, 0.9 Hz, 1H), 4.20 – 4.08 (m, 1H), 3.32 (s, 3H), 2.26 – 2.02 (m, 2H), 1.98 – 1.87 (m, 1H), 1.72 – 1.32 (m, 7H).

4.3.4. *rac*-2-Bromo-3-methoxycyclooctene (**68**)



Compound **67** (10.00 g, 71.3 mmol, 1 eq) was dissolved in dry DCM (40 mL) under inert atmosphere and the solution was cooled to $-40\text{ }^{\circ}\text{C}$. A solution of bromine (3.65 mL, 11.40 g, 71.30 mmol, 1 eq) in DCM (10 mL) was added dropwise at the same temperature. After the addition, the mixture was allowed to reach rt. The reaction was quenched with $\text{Na}_2\text{S}_2\text{O}_3$ (10% aq solution, 40 mL) and the crude was extracted with DCM (2 x 30 mL). The solution was dried over sodium sulphate, filtered, and concentrated under reduced pressure. The residue was dissolved in dry THF (45 mL) and the solution was cooled to $-40\text{ }^{\circ}\text{C}$. KOtBu (11.30 g, 100.7 mmol, 1.4 eq) was added in 3 portions, then the reaction was allowed to reach rt. After stirring at rt for 90 minutes water (30 mL) was added at $0\text{ }^{\circ}\text{C}$ and the crude was extracted with diethyl ether (3 x 30 mL). The organic layer was washed with brine, dried over sodium sulphate, filtered, and concentrated under reduced pressure. The residue was purified through fractioned distillation ($65\text{ }^{\circ}\text{C}$, 1 mbar). *rac*-2-Bromo-3-methoxycyclooctene **68** was isolated as a colorless liquid.

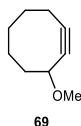
Yield: 10.83 g (49.4 mmol, 69%).

Characterization data are in agreement with the literature.^[117]

$R_f = 0.50$ (SiO_2 , DCM/*n*-Hexane 7:3)

$^1\text{H-NMR}$ (400 MHz, CDCl_3) δ [ppm] = 6.32 (t, $^3J = 8.8$ Hz, 1H), 4.22 (dd, $^3J = 10.4$, $^3J = 5.3$ Hz, 1H), 3.33 (s, 3H), 2.24 – 2.16 (m, 2H), 1.87 – 1.59 (m, 5H), 1.43 – 1.22 (m, 3H).

4.3.5. *rac*-3-Methoxycyclooctyne (**69**)



A solution of LDA in THF was prepared by dropwise addition of *n*BuLi (1.6 M in hexane, 11 mL, 17.5 mmol, 0.57 eq) to diisopropylamine (2.5 mL, 1.77 g, 17.5 mmol, 0.57 eq) in dry THF (10 mL) at $-25\text{ }^{\circ}\text{C}$. The mixture was stirred at $-25\text{ }^{\circ}\text{C}$ for 10 minutes. **68** (6.70 g, 30.6 mmol, 1 eq) was

dissolved in dry THF (4 mL) and added dropwise to the LDA solution at -25 °C. The reaction was allowed to slowly reach rt and it was stirred for 2 more hours. The reaction was quenched with aq. 1 M HCl (20 mL), then extracted with pentane (3 x 20 mL). The organic layer was washed with brine, dried over sodium sulphate, filtered, and concentrated under reduced pressure. The residue was purified through distillation (30 °C, 1 mbar), followed by chromatographic column on silica gel (Et₂O/*n*-Hexane 1:14). *rac*-3-Methoxycyclooctyne **69** was isolated as a colorless liquid.

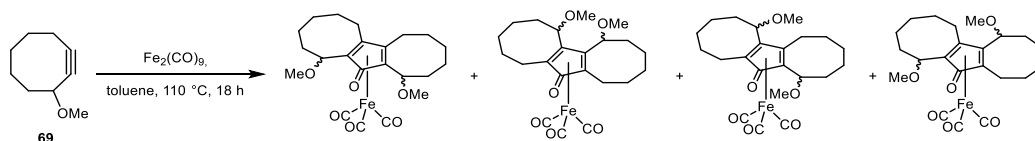
Yield: 798 mg (5.77 mmol, 33%).

Characterization data are in agreement with the literature.^[117]

R_f = 0.47 (SiO₂, Et₂O/*n*-Hexane 1:9)

¹H-NMR (400 MHz, CDCl₃) δ [ppm] = 4.09 – 4.04 (m, 1H), 3.31 (s, 3H), 2.31 – 2.05 (m, 3H), 2.01 – 1.74 (m, 4H), 1.70 – 1.57 (m, 2H), 1.53 – 1.41 (m, 1H).

4.3.6. Carbonylative Cyclization/Complexation of *rac*-3-Methoxycyclooctyne (**69**)



rac-3-Methoxycyclooctyne **69** (150 mg, 1.08 mmol, 1eq) was dissolved in dry toluene (2.5 mL) in a 10 mL Schlenk tube under nitrogen atmosphere. Diiron noncarbonyl (790 mg, 2.17 mmol, 2 eq) was added and the reaction was heated to 110 °C. After 18 hours the reaction was filtered through celite, rinsing with AcOEt. The crude mixture was purified through chromatographic column (AcOEt/EDP 1:4 to 1:1). Four fractions were isolated.

1st fraction: 5.6 mg (0.013 mmol, 2.3%)

MS (ESI+): m/z 467.09 [M+Na]⁺ (calculated for C₂₃H₃₁FeO₆Na: 467.11)

2nd fraction: 10.7 mg (0.024 mmol, 4.4%)

MS (ESI+): m/z 467.07 [M+Na]⁺ (calculated for C₂₃H₃₁FeO₆Na: 467.11)

3rd fraction: 4.9 mg (0.011 mmol, 2.0%)

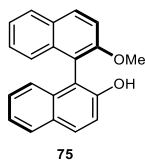
MS (ESI+): m/z 445.05 [M+H]⁺ (calculated for C₂₃H₃₂FeO₆: 445.13)

4th fraction: 5.7 mg (0.013 mmol, 2.3%)

MS (ESI+): m/z 467.13 [M+Na]⁺ (calculated for C₂₃H₃₁FeO₆Na: 467.11)

4.4. Synthesis of (*R*)-2-iodo-2'-methoxy-1,1'-binaphthalene (76)

4.4.1. (*R*)-2-Methoxy-[1,1'-binaphthalen]-2-ol (75)



K_2CO_3 (1.74 g, 12.59 mmol, 1.2 eq) was added to a solution of (*R*)-BINOL (3.00 g, 10.48 mmol, 1 eq) in acetone (105 mL). The mixture was stirred at room temperature for 30 minutes. MeI (645 μ L, 1.49 g, 10.48 mmol, 1 eq) was added, and the reaction was heated to reflux for 6 hours. The solvent was then removed under reduced pressure. Water (30 mL) was added. The crude was extracted with DCM (30 mL), then washed with water (2 x 30 mL) and with brine. The collected organic layers were dried over sodium sulphate, filtered, and concentrated under reduced pressure. The product was purified through chromatographic column on silica gel (DCM/EDP 3:2 to 7:3). **75** was isolated as a white solid.

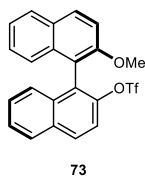
Yield: 2.83 g (9.42 mmol, 90%).

Characterization data are in agreement with the literature.^[197]

R_f = 0.42 (SiO₂, DCM/EDP 7:3)

¹H-NMR (400 MHz, CDCl₃) δ [ppm] = 8.06 (d, ³ J = 9.1 Hz, 1H), 7.90 (d, ³ J = 8.7 Hz, 2H), 7.86 (d, ³ J = 8.1 Hz, 1H), 7.49 (d, ³ J = 9.1 Hz, 1H), 7.40 – 7.15 (m, 6H), 7.04 (d, ³ J = 8.4 Hz, 1H), 3.81 (s, 3H).

4.4.2. (*R*)-2'-Methoxy-[1,1'-binaphthalen]-2-yl trifluoromethanesulfonate (73)



Compound **75** (1.62 g, 5.39 mmol, 1 eq) was dissolved in dry DCM (16.5 mL). Pyridine (522 μ L, 512 mg, 6.47 mmol, 1.2 eq) was added. Trifluoromethanesulfonic anhydride (1.1 mL, 1.83 g, 6.47 mmol, 1.2 eq) was slowly added at 0 °C. The reaction mixture was stirred at 0 °C for 2 hours, then at room temperature for 3 more hours. The reaction was quenched with water (20 mL).

The DCM layer was separated and washed with 4 M aqueous HCl (20 mL), sat. aq. NaHCO₃ (20 mL), and brine. The organic layer was dried over Na₂SO₄, filtered, and concentrated under reduced pressure. The product was used without further purification. **73** was isolated as a pale-yellow solid.

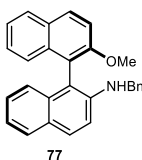
Yield: 2.16 g (5.00 mmol, 93%).

Characterization data are in agreement with the literature.^[198]

R_f = 0.44 (SiO₂, EtOAc/EDP 1:4)

¹H-NMR (400 MHz, CDCl₃) δ [ppm] = 8.09 – 8.00 (m, 2H), 7.98 (d, ³J = 8.2 Hz, 1H), 7.89 (d, ³J = 8.2 Hz, 1H), 7.60 – 7.50 (m, 2H), 7.46 (d, ³J = 9.1 Hz, 1H), 7.40 – 7.28 (m, 3H), 7.28 – 7.20 (m, 1H), 7.01 (d, ³J = 8.5 Hz, 1H), 3.82 (s, 3H).

4.4.3. (*R*)-*N*-Benzyl-2'-methoxy-[1,1'-binaphthalen]-2-amine (**77**)



Compound **73** (3.11 g, 7.19 mmol, 1 eq) and benzylamine (2.75 mL, 2.70 g, 25.2 mmol, 3.5 eq) were dissolved in dry 1,4- dioxane (43 mL) under nitrogen atmosphere. Cesium carbonate (8.20 g, 25.16 mmol, 3.5 eq) and rac-BINAP (895 mg, 1.44 mmol, 0.2 eq) were added, then palladium acetate (231 mg, 1.03 mmol, 0.14 eq) was added, and the mixture was heated to 105 °C overnight. After cooling to rt, the reaction was filtered through celite, rinsing with DCM. The product was purified through chromatographic column (AcOEt/EDP 1:9). **77** was isolated as transparent oil.

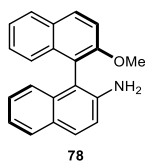
Yield: 2.67 g (6.86 mmol, 95%).

Characterization data are in agreement with the literature.^[199]

R_f = 0.23 (SiO₂, EtOAc/EDP 1:9)

¹H-NMR (400 MHz, CDCl₃) δ [ppm] = 8.03 (d, ³J = 9.1 Hz, 1H), 7.90 (d, ³J = 8.1 Hz, 1H), 7.83 (d, ³J = 8.9 Hz, 1H), 7.78 (d, ³J = 8.0 Hz, 1H), 7.48 (d, ³J = 9.1 Hz, 1H), 7.40 – 7.09 (m, 11H), 6.95 (d, ³J = 8.3 Hz, 1H), 4.44 (d, ²J = 15.3 Hz, 1H), 4.34 (d, ²J = 15.4 Hz, 1H), 3.80 (s, 3H).

4.4.4. (*R*)-2'-Methoxy-[1,1'-binaphthalen]-2-amine (**78**)



Compound **77** (792 mg, 2.03 mmol, 1 eq) was dissolved in EtOAc (9.5 mL) in a round bottom flask. The solution was purged with nitrogen. Pd/C (10% Pd on activated carbon, 10.8 mg of Pd, 0.01 mmol, 0.05 eq) was added, and hydrogen was charged. The reaction mixture was heated to 60 °C for 3 hours, then it was allowed to cool down to rt. The flask was flushed with nitrogen, and the mixture was filtered through celite and concentrated in vacuo. The product was purified through crystallization from an oversaturated EtOAc/hexane solution. **78** was isolated as a colorless crystalline solid.

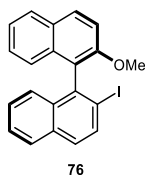
Yield: 593 mg (1.98 mmol, 97%).

Characterization data are in agreement with the literature.^[199]

R_f = 0.37 (SiO₂, EtOAc/EDP 1:4)

¹H-NMR (400 MHz, CDCl₃) δ [ppm] = 8.01 (d, ³J = 9.0 Hz, 1H), 7.89 (d, ³J = 8.1 Hz, 1H), 7.85 – 7.75 (m, 2H), 7.47 (d, ³J = 9.0 Hz, 1H), 7.35 (dd, ³J = 7.3 Hz, 1H), 7.30 – 7.13 (m, 5H), 6.99 (d, ³J = 8.3 Hz, 1H), 3.78 (s, 3H), 3.11 (br s, 2H, NH₂).

4.4.5. (*R*)-2-Iodo-2'-methoxy-1,1'-binaphthalene (**76**)



Compound **78** (786 mg, 2.63 mmol, 1 eq) was suspended in concentrated HCl (3 mL). A solution of NaNO₂ (398 mg, 5.78 mmol, 2.2 eq) in water (22 mL) was added dropwise at 0 °C. The obtained red solution was then allowed to warm up to rt. After 2.5 h, the solution was cooled to 0 °C, and EtOAc (10 mL) was added. A solution of KI (4.46 g, 26.9 mmol, 10 eq) in water (25 mL) was added dropwise, and the reaction was left under stirring at room temperature overnight. The reaction was quenched with 15 mL of saturated Na₂SO₃, then extracted with DCM (3 x 30

mL). The organic layer was washed with brine, dried over Na₂SO₄, filtered, and concentrated under reduced pressure. The product was purified through chromatographic column (DCM/EDP 1:9). **76** was isolated as a white crystalline solid.

Yield: 900 mg (2.19 mmol, 83%).

Characterization data are in agreement with the literature.^[199]

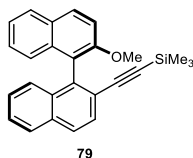
R_f = 0.60 (SiO₂, EtOAc/EDP 1:4)

¹H-NMR (400 MHz, CDCl₃) δ [ppm] = 8.09 – 8.01 (m, 2H), 7.93 – 7.87 (m, 2H), 7.67 (d, ³J = 8.7 Hz, 1H), 7.50 – 7.42 (m, 2H), 7.35 (t, ³J = 7.3 Hz, 1H), 7.29 – 7.17 (m, 3H), 6.98 (d, ³J = 8.5 Hz, 1H), 3.83 (s, 3H).

¹³C-NMR (100 MHz, CDCl₃) δ [ppm] = 154.4 (1C), 139.9 (1C), 135.8 (1C), 134.0 (1C), 133.1 (1C), 133.1 (1C), 130.3 (1C), 129.2 (1C), 129.2 (1C), 128.2 (1C), 128.2 (1C), 127.0 (2C), 127.0 (1C), 126.3 (1C), 125.9 (1C), 124.8 (1C), 123.9 (1C), 114.0 (1C), 100.6 (1C), 56.8 (1C).

4.5. Sonogashira Cross-Coupling Reactions on Iodide **76**

4.5.1. (*R*)-((2'-Methoxy-[1,1'-binaphthalen]-2-yl)ethynyl)trimethylsilane (**79**)



Iodide **76** (910 mg, 2.22 mmol, 1 eq) was dissolved in dry toluene (22 mL). Cs₂CO₃ (2.89 g, 8.87 mmol, 4 eq) was added, and the suspension was degassed with a nitrogen stream. Ethynyltrimethylsilane (436 mg, 4.44 mmol, 2 eq), SPhos (91 mg, 0.22 mmol, 0.1 eq), and Pd(OAc)₂ (27 mg, 0.11, 0.05 eq) were added. The reaction mixture was heated to 100 °C for 4 hours. The reaction was allowed to cool down to room temperature, and it was filtered through celite, rinsing with DCM. The product was purified through chromatographic column (DCM/EDP 1:9 to 1:4). **79** was isolated as a yellow oil.

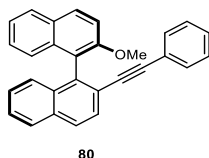
Yield: 550 mg (1.45 mmol, 65%).

R_f = 0.20 (SiO₂, DCM/EDP 1:4)

$^1\text{H-NMR}$ (400 MHz, CDCl_3) δ [ppm] = 8.01 (d, $^3J = 9.0$ Hz, 1H), 7.95 – 7.86 (m, 3H), 7.70 (d, $^3J = 8.5$ Hz, 1H), 7.53 – 7.43 (m, 2H), 7.41 – 7.28 (m, 3H), 7.25 (dd, $^3J = 9.8$ Hz, 1H), 7.10 (d, $^3J = 8.5$ Hz, 1H), 3.79 (s, 3H), -0.21 (s, 9H).

$^{13}\text{C-NMR}$ (100 MHz, CDCl_3) δ [ppm] = 154.9 (1C), 139.6 (1C), 133.9 (1C), 133.3 (1C), 133.0 (1C), 129.7 (1C), 129.4 (1C), 128.3 (1C), 128.2 (1C), 127.8 (1C), 127.7 (1C), 126.7 (1C), 126.6 (1C), 126.6 (1C), 126.5 (1C), 125.3 (1C), 123.6 (1C), 122.3 (1C), 121.7 (1C), 114.2 (1C), 105.3 (1C), 97.8 (1C), 57.1 (1C), -0.4 (3C).

4.5.2. (*R*)-2-Methoxy-2'-(phenylethynyl)-1,1'-binaphthalene (**80**)



Iodide **76** (100 mg, 0.244 mmol, 1 eq) was dissolved in dry toluene (2.4 mL). Cs_2CO_3 (318 mg, 0.976 mmol, 4 eq) was added, and the suspension was degassed with a nitrogen stream. Phenylacetylene (27 μL , 25 mg, 0.244 mmol, 1 eq), CyJohnPhos (8.4 mg, 0.024 mmol, 0.1 eq), and $\text{Pd}(\text{OAc})_2$ (2.7 mg, 0.012, 0.05 eq) were added. The reaction mixture was heated to 100 $^\circ\text{C}$ for 16 hours. The reaction was allowed to cool down to room temperature, and it was filtered through celite, rinsing with DCM. The product was purified through chromatographic column (EtOAc/EDP 1:10). **80** was isolated as a yellow solid.

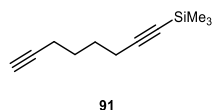
Yield: 71 mg (0.185 mmol, 76%).

$^1\text{H-NMR}$ (400 MHz, CDCl_3) δ [ppm] = 8.06 (d, $^3J = 9.0$ Hz, 1H), 7.99 – 7.89 (m, 3H), 7.80 (d, $^3J = 8.5$ Hz, 1H), 7.53 – 7.46 (m, 2H), 7.40 – 7.30 (m, 4H), 7.30 – 7.25 (m, 1H), 7.18 – 7.12 (m, 3H), 6.85 (d, $^3J = 6.4$ Hz, 2H), 3.81 (s, 3H).

$^{13}\text{C-NMR}$ (100 MHz, CDCl_3) δ [ppm] = 155.1 (1C), 138.5 (1C), 134.0 (1C), 133.2 (1C), 133.1 (1C), 131.4 (2C), 129.9 (1C), 129.3 (1C), 128.5 (1C), 128.2 (1C), 128.1 (2C), 128.0 (1C), 127.9 (1C), 127.8 (1C), 126.7 (2C), 126.7 (1C), 126.5 (1C), 125.5 (1C), 123.7 (1C), 123.5 (1C), 122.2 (1C), 121.9 (1C), 114.2 (1C), 92.9 (1C), 89.9 (1C), 57.1 (1C).

4.6. Synthesis of mono-Substituted 1,7-Octadiynes 91-95

4.6.1. Trimethyl(octa-1,7-diyn-1-yl)silane (91)



n-BuLi (1.6 M in hexanes, 4.7 mL, 7.54 mmol, 1 eq) was added to a solution of hexamethyldisilazane (1.22 g, 7.54 mmol, 1 eq) in THF (4 mL) at -78 °C. The mixture was allowed to reach 0 °C and stirred for 30 minutes. The resulting LiHMDS solution was cooled to -78 °C and then added to a solution of 1,7-octadiyne (1 mL, 800 mg, 7.54 mmol, 1 eq) in THF (11 mL). After 0.5 hours at -78 °C, chlorotrimethylsilane (19.1 mL, 820 mg, 958 μ L, 7.54 mmol, 1 eq) was added dropwise. The mixture was stirred for 10 minutes at -78 °C and then it was allowed to reach rt. After 2 more hours, the reaction was quenched with water (10 mL). The mixture was extracted with *n*-pentane (3 \times 10 mL). The combined organic layers were then washed with 1 M aq. HCl (10 mL) and brine, dried over Na₂SO₄, filtered, and concentrated under reduced pressure. **91** was isolated as a colorless oil and used without further purification.

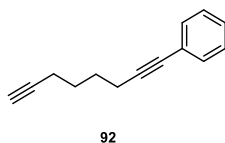
Yield: 1.34 g (7.54 mmol, quantitative).

Characterization data are in agreement with the literature.^[110]

R_f = 0.42 (SiO₂, DCM/EDP 1:9)

¹H-NMR (400 MHz, CDCl₃) δ [ppm] = 2.20 – 2.17 (m, 4H), 1.90 (t, ³J = 2.68 Hz, 1H), 1.61 – 1.57 (m, 4H), 0.10 (s, 9H).

4.6.2. 1-Phenyl-1,7-octadiyne (92)



Iodobenzene (200 μ L, 365 mg, 1.79 mmol, 1 eq) and 1,7-octadiyne (474 μ L, 380 mg, 3.57 mmol, 2 eq) were dissolved in dry THF (24 mL) under inert atmosphere. Degassed *i*PrNH₂ (751 μ L, 5.36 mmol, 3 eq) was added and the solution was purged with nitrogen. Pd(PPh₃)₄ (103 mg, 0.089

mmol, 0.05 eq) and CuI (34 mg, 0.179 mmol, 0.1 eq) were added and the reaction was left under stirring at rt for 4 hours. The reaction was quenched with sat. aq. NH₄Cl (5 mL) and THF was removed under reduced pressure. The residue was extracted with DCM (2 x 10 mL). The collected organic layers were washed with water (10 mL), brine, dried over Na₂SO₄, filtered, and concentrated under reduced pressure. The product was purified through chromatographic column (DCM/EDP 1:10 to 1:9). **92** was isolated as a colorless oil.

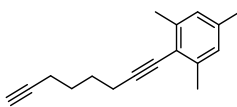
Yield: 130 mg (0.72 mmol, 40%).

Characterization data are in agreement with the literature.^[144]

R_f = 0.42 (SiO₂, DCM/EDP 1:9)

¹H-NMR (400 MHz, CDCl₃) δ [ppm] = 7.47 – 7.35 (m, 2H), 7.35 – 7.20 (m, 3H), 2.52 – 2.38 (m, 2H), 2.32 – 2.22 (m, 2H), 1.99 – 1.93 (m, 1H), 1.80 – 1.67 (m, 4H).

4.6.3. 1-Mesityl-1,7-octadiyne (**93**)



93

1,7-octadiyne (243 μL, 194 mg, 1.83 mmol, 3 eq) and iodomesitylene (150 mg, 0.61 mmol, 1 eq) were dissolved in dry 1,4-dioxane (8 mL). Cs₂CO₃ (794 mg, 2.44 mmol, 4 eq) was added, and the suspension was degassed with an argon stream. SPhos (25 mg, 0.061 mmol, 0.1 eq), and Pd(OAc)₂ (7.5 mg, 0.031 mmol, 0.05 eq) were added. The reaction mixture was heated to 100 °C for 4 hours. The reaction was allowed to cool to room temperature, and it was filtered through celite, rinsing with DCM. The product was purified through chromatographic column (DCM/EDP 1:9). **93** was isolated as a yellowish oil.

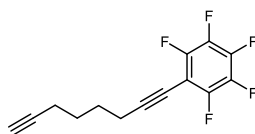
Yield: 89 mg (0.397 mmol, 65%)

R_f = 0.53 (SiO₂, DCM/EDP 1:9)

¹H-NMR (400 MHz, CDCl₃) δ [ppm] = 6.84 (s, 2H), 2.57 – 2.50 (m, 2H), 2.37 (s, 6H), 2.31 – 2.22 (m, 2H), 2.25 (s, 3H), 1.96 (t, ⁴J = 2.6 Hz, 1H), 1.79 – 1.72 (m, 4H).

¹³C-NMR (100 MHz, CDCl₃) δ [ppm] = 140.0 (1C), 136.9 (2C), 127.6 (2C), 120.8 (1C), 97.3 (1C), 84.3 (1C), 78.7 (1C), 68.6 (1C), 28.1 (1C), 27.7 (1C), 21.4 (1C), 21.2 (2C), 19.3 (1C), 18.1 (1C).

4.6.4. 1,2,3,4,5-Pentafluoro-6-(octa-1,7-diyn-1-yl)benzene (94)



94

1,7-octadiyne (332 μL , 265 mg, 2.50 mmol, 2.5 eq) and pentafluoriodobenzene (133 μL , 294 mg, 1.00 mmol, 1 eq) were dissolved in dry 1,4-dioxane (13 mL). Cs_2CO_3 (1.41 g, 4.00 mmol, 4 eq) was added, and the suspension was degassed with a stream of argon. SPhos (41 mg, 0.10 mmol, 0.1 eq), and $\text{Pd}(\text{OAc})_2$ (11 mg, 0.05 mmol, 0.05 eq) were added. The reaction mixture was heated to 100 $^\circ\text{C}$ for 2 hours. The reaction was allowed to cool to room temperature, and it was filtered through celite, rinsing with DCM. The product was purified through chromatographic column (DCM/EDP 1:15). **94** was isolated as a colorless liquid.

Yield: 128 mg (0.47 mmol, 47%)

R_f = 0.48 (SiO_2 , DCM/EDP 1:15)

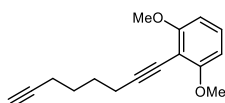
$^1\text{H-NMR}$ (400 MHz, CDCl_3) δ [ppm] = 2.54 (t, 3J = 6.6 Hz, 2H), 2.26 (td, 3J = 6.5 Hz, 4J = 2.3 Hz, 2H), 1.97 (t, 4J = 2.4 Hz, 1H), 1.86 – 1.62 (m, 4H).

$^{13}\text{C-NMR}$ (100 MHz, CDCl_3) δ [ppm] = 149.1 – 146.1 (m, 2C), 142.7 – 139.5 (m, 1C), 139.2 – 136.2 (m, 2C), 103.6 – 103.3 (m, 1C), 101.0 – 100.0 (m, 1C), 84.0 (1C), 68.8 (1C), 65.4 – 65.0 (m, 1C), 27.5 (1C), 27.2 (1C), 19.5 (1C), 18.1 (1C).

$^{19}\text{F-NMR}$ (377 MHz, CDCl_3) δ [ppm] = -136.99 – -137.26 (m, 2F), -154.20 (t, 3J = 20.8 Hz, 1F), -162.33 – -162.51 (m, 2F).

IR (neat): $\tilde{\nu}$ [cm^{-1}] = 2949.4 (s), 2868.0 (m), 2666.2 (w), 2438.1 (w), 2247.9 (s), 2119.2 (w), 1737.3 (w), 1649.4 (w), 1626.7 (w), 1518.6 (s), 1496.9 (s), 1459.7 (m), 1430.5 (m), 1374.2 (m), 1320.7 (m), 1273.9 (w), 1176.6 (w), 1148.5 (w), 1048.7 (s), 989.4 (s), 923.1 (w), 838.3 (w), 816.9 (w), 793.2 (w).

4.6.5. 1,3-Dimethoxy-2-(octa-1,7-diyn-1-yl)benzene (95)



95

1,7-octadiyne (302 μ L, 241 mg, 2.27 mmol, 3 eq) and iodomesitylene (200 mg, 0.757 mmol, 1 eq) were dissolved in dry 1,4-dioxane (10 mL). Cs_2CO_3 (987 mg, 3.03 mmol, 4 eq) was added, and the suspension was degassed with a stream of argon. SPhos (31 mg, 0.076 mmol, 0.1 eq), and $\text{Pd}(\text{OAc})_2$ (9.3 mg, 0.038 mmol, 0.05 eq) were added. The reaction mixture was heated to 100 $^\circ\text{C}$ for 2 hours. The reaction was allowed to cool to room temperature, and it was filtered through celite, rinsing with DCM. The product was purified through chromatographic column (DCM/EDP 1:4 to 2:3). **95** was isolated as a yellowish oil.

Yield: 101 mg (0.417 mmol, 55%)

R_f = 0.15 (SiO_2 , DCM/EDP 1:4)

$^1\text{H-NMR}$ (400 MHz, CDCl_3) δ [ppm] = 7.17 (t, 3J = 8.4 Hz, 1H), 6.51 (d, 3J = 8.4 Hz, 2H), 3.87 (s, 6H), 2.60 – 2.54 (m, 2H), 2.33 – 2.21 (m, 2H), 1.95 (t, 4J = 2.6 Hz, 1H), 1.86 – 1.69 (m, 4H).

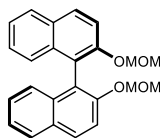
$^{13}\text{C-NMR}$ (100 MHz, CDCl_3) δ [ppm] = 161.6 (2C), 128.9 (1C), 103.6 (2C), 98.6 (1C), 84.6 (1C), 73.1 (1C), 68.4 (1C), 56.2 (2C), 27.9 (1C), 27.7 (1C), 19.8 (1C), 18.2 (1C).

IR (neat): $\tilde{\nu}$ [cm^{-1}] = 3286.4 (s, $\text{C}\equiv\text{CH}$), 3003.1 (m), 2933.3 (s), 2837.8 (s), 2538.8 (w), 2229.8 (w), 2188.7 (w), 2115.2 (w), 1927.2 (w), 1713.6 (w), 1583.5 (s), 1473.9 (s), 1432.2 (s), 1329.1 (m), 1300.8 (m), 1252.7 (s), 1173.5 (w), 1110.6 (s), 1033.3 (s), 958.4 (w), 902.2 (w), 776.9 (s), 725.8 (s).

HRMS (ESI+): m/z 243.1358 [$\text{M}+\text{H}$] $^+$, 265.1205 [$\text{M}+\text{Na}$] $^+$ (calculated for $\text{C}_{16}\text{H}_{19}\text{O}_2^+$ = 243.1358, $\text{C}_{16}\text{H}_{18}\text{O}_2\text{Na}^+$ = 265.1204).

4.7. Synthesis of 3-iodo-2,2'-bis(methoxymethoxy)-1,1'-binaphthalene (82)

4.7.1. (*R*)-2,2'-Bis(methoxymethoxy)-1,1'-binaphthalene (83)



83

(*R*)-BINOL (1.00 g, 3.49 mmol, 1 eq) was dissolved in dry THF (18 mL). NaH (209 mg, 8.73 mmol, 2.5 eq) was added in one portion at 0 °C. The mixture was allowed to reach room temperature, and it was left under stirring for 1 hour. Chloromethyl methyl ether (647 mg, 8.03 mmol, 2.3 eq) was added at 0 °C, and the reaction was stirred at room temperature overnight. The product was purified through precipitation from $i\text{Pr}_2\text{O}$. **83** was isolated as a white crystalline solid.

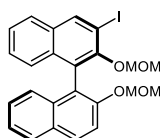
Yield: 880 mg (2.35 mmol, 67%).

Characterization data are in agreement with the literature.^[200]

$R_f = 0.53$ (SiO_2 , EtOAc/EDP 1:4)

$^1\text{H-NMR}$ (400 MHz, CDCl_3) δ [ppm] = 7.99 (d, $^3J = 9.0$ Hz, 2H), 7.91 (d, $^3J = 8.2$ Hz, 2H), 7.61 (d, $^3J = 9.0$ Hz, 2H), 7.41 – 7.34 (m, 2H), 7.29-7.24 (m, 2H), 7.19 (d, $^3J = 8.4$ Hz, 2H), 5.12 (d, $^2J = 6.8$ Hz, 2H), 5.01 (d, $^2J = 6.8$ Hz, 2H), 3.18 (s, 6H).

4.7.2. (*R*)-3-Iodo-2,2'-bis(methoxymethoxy)-1,1'-binaphthalene (82)



82

Compound **83** (500 mg, 1.34 mmol, 1 eq) was dissolved in dry THF (19 mL) under nitrogen atmosphere. The solution was cooled to -78 °C, then *n*-BuLi (1.6 M in hexane, 1 mL) was added dropwise. The mixture was stirred at -78 °C for 5 hours. A solution of iodine (407 mg, 1.60 mmol, 1.2 eq) in THF (2 mL) was added dropwise. After 1 more hour at -78 °C the reaction was allowed

to slowly warm up to rt and it was left under stirring overnight. The reaction was quenched with a 5% aqueous solution of Na₂SO₃ (7 mL). After 2 hours THF was removed under reduced pressure and the residue was extracted with AcOEt (2 x 15 mL). The organic layer was dried over anhydrous Na₂SO₄. The product was purified through chromatographic column (AcOEt/EDP 1:10, then 1:9). **82** was isolated as a white crystalline solid.

Yield: 391 mg (0.78 mmol, 59%).

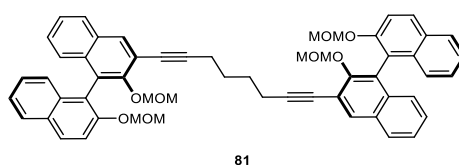
Characterization data are in agreement with the literature.^[201]

R_f = 0.47 (SiO₂, EtOAc/EDP 1:9)

¹H-NMR (400 MHz, CDCl₃) δ [ppm] = 8.52 (s, 1H), 7.97 (d, ³J = 9.1 Hz, 1H), 7.86 (d, ³J = 8.1 Hz, 1H), 7.78 (d, ³J = 8.2 Hz, 1H), 7.58 (d, ³J = 8.2 Hz, 1H), 7.41 – 7.34 (m, 2H), 7.29 – 7.23 (m, 2H), 7.20 – 7.13 (m, 2H), 5.14 (d, ²J = 6.9 Hz, 1H), 5.04 (d, ²J = 6.9 Hz, 1H), 4.73 (d, ²J = 5.2 Hz, 1H), 4.49 (d, ²J = 5.2 Hz, 1H), 3.20 (s, 3H), 2.72 (s, 3H).

4.8. Sonogashira Cross-Coupling Reactions on Iodide **82**

4.4.3. 1,8-Bis((*R*)-2,2'-bis(methoxymethoxy)-[1,1'-binaphthalen]-3-yl)octa-1,7-diyne (**81**)



Iodide **82** (807 mg, 1.61 mmol, 1 eq) was dissolved in a 1:1 mixture of Et₃N (6.5 mL) and MeCN (6.5 mL). The solution was degassed with a stream of argon, then 1,7-octadiyne (107 μL, 86 mg, 0.81 mmol, 1 eq), CuI (15 mg, 0.08 mmol, 0.1 eq), and Pd(PPh₃)₄ (94 mg, 0.08 mmol, 0.1 eq) were added. The mixture was heated to 80 °C for 2 hours. The reaction was allowed to cool down to rt, and volatiles were removed under reduced pressure. The crude was purified through chromatographic column on silica gel (EtOAc/EDP 1:9). **81** was isolated as a white crystalline solid.

Yield: 556 mg (0.65 mmol, 81%).

R_f = 0.42 (SiO₂, EtOAc/EDP 1:4)

m.p. = 147-149 °C

$^1\text{H-NMR}$ (400 MHz, CDCl_3) δ [ppm] = 8.08 (s, 2H), 7.94 (d, $^3J = 9.0$ Hz, 2H), 7.85 (d, $^3J = 8.1$ Hz, 2H), 7.78 (d, $^3J = 8.2$ Hz, 2H), 7.56 (d, $^3J = 9.0$ Hz, 2H), 7.38 – 7.32 (m, 4H), 7.26 – 7.13 (m, 8H), 5.13 (d, $^2J = 6.8$ Hz, 2H), 4.97 (d, $^2J = 6.2$ Hz, 4H), 4.87 (d, $^2J = 5.7$ Hz, 2H), 3.14 (s, 6H), 2.61 – 2.54 (s, 10H), 1.89 – 1.84 (m, 4H).

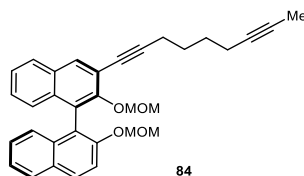
$^{13}\text{C-NMR}$ (100 MHz, CDCl_3) δ [ppm] = 153.1 (2C), 152.9 (2C), 134.2 (2C), 133.9 (2C), 133.5 (2C), 130.6 (2C), 129.8 (2C), 129.8 (2C), 127.8 (2C), 127.6 (2C), 126.8 (2C), 126.6 (2C), 126.2 (2C), 126.1 (2C), 125.9 (2C), 125.4 (2C), 124.2 (2C), 120.8 (2C), 118.2 (2C), 116.8 (2C), 98.7 (2C), 95.2 (2C), 94.1 (2C), 78.2 (2C), 56.2 (2C), 56.0 (2C), 28.0 (2C), 19.5 (2C).

IR (nujol): $\tilde{\nu}$ [cm^{-1}] = 1616.4 (w), 1592.0 (m), 1507.2 (m), 1259.2 (s), 1242.6 (s), 1152.0 (s), 1073.4 (m), 1034.3 (s), 1013.0 (m), 983.7 (m), 922.6 (m), 896.7 (m), 809.3 (m), 763.5 (m).

4.8.2. General Procedure for the Coupling of Iodide **82** with Alkynes **90-95** (A)

Iodide **82** (1 eq) and the mono-substituted diyne substrate (1 eq) were dissolved in a 1:1 mixture of MeCN and triethylamine ($C_0[\mathbf{82}]$: 0.1 M). The solution was degassed with a stream of argon. CuI (0.1 eq) and $\text{Pd}(\text{PPh}_3)_4$ (0.05 eq) were added, and the reaction was heated to 80 °C for 2 hours. Volatiles were removed and the crude was suspended in a saturated solution of NH_4Cl . The residue was extracted with DCM. The collected organic layers were washed with brine, dried over Na_2SO_4 , filtered, and concentrated under reduced pressure. Products **84-89** were purified through chromatographic column on silica gel.

4.8.3. (*R*)-2,2'-Bis(methoxymethoxy)-3-(nona-1,7-diyne-1-yl)-1,1'-binaphthalene (**84**)



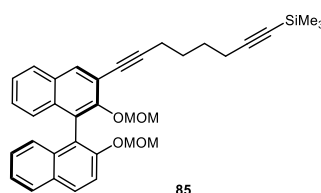
Compound **84** was prepared according to general procedure A, starting from 167 mg (1.39 mmol) of diyne **90**. **84** was isolated through chromatographic column on silica gel (EtOAc/EDP 5:95 to 1:9) as a yellowish oil.

Yield: 427 mg (0.86 mmol, 74%)

$R_f = 0.50$ (SiO_2 , EtOAc/EDP 3:7)

$^1\text{H-NMR}$ (400 MHz, CDCl_3) δ [ppm] = 8.07 (s, 1H), 7.94 (d, $^3J = 9.0$ Hz, 1H), 7.85 (d, $^3J = 8.1$ Hz, 1H), 7.81 (d, $^3J = 8.2$ Hz, 1H), 7.57 (d, $^3J = 9.0$ Hz, 1H), 7.41 – 7.31 (m, 2H), 7.29 – 7.11 (m, 4H), 5.14 (d, $^2J = 6.9$ Hz, 1H), 5.02 – 4.95 (m, 2H), 4.87 (d, $^2J = 5.8$ Hz, 1H), 3.15 (s, 3H), 2.57 (s, 3H), 2.51 (t, $^3J = 6.8$ Hz, 2H), 2.24 – 2.16 (m, 2H), 1.78 (t, $^4J = 2.4$ Hz, 3H), 1.81 – 1.63 (m, 4H).

4.8.4. (R)-(8-(2,2'-Bis(methoxymethoxy)-[1,1'-binaphthalen]-3-yl)octa-1,7-diyne-1-yl)-trimethylsilane (85)



Compound **85** was prepared according to general procedure A, starting from 57 mg (0.32 mmol) of diyne **91**. **85** was isolated through chromatographic column on silica gel (EtOAc/EDP 1:4) as a yellowish oil.

Yield: 128 mg (0.23 mmol, 73%)

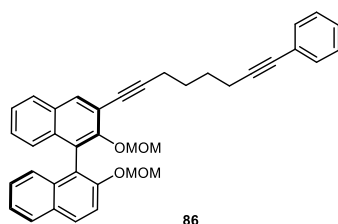
$R_f = 0.67$ (SiO_2 , EtOAc/EDP 1:4)

$^1\text{H-NMR}$ (400 MHz, CDCl_3) δ [ppm] = 8.08 (s, 1H), 7.94 (d, $^3J = 9.0$ Hz, 1H), 7.85 (d, $^3J = 8.1$ Hz, 1H), 7.81 (d, $^3J = 8.2$ Hz, 1H), 7.57 (d, $^3J = 9.0$ Hz, 1H), 7.40 – 7.31 (m, 2H), 7.31 – 7.11 (m, 4H), 5.14 (d, $^2J = 6.9$ Hz, 1H), 5.04 – 4.94 (m, 2H), 4.87 (d, $^2J = 5.7$ Hz, 1H), 3.16 (s, 3H), 2.58 (s, 3H), 2.52 (t, $^3J = 6.5$ Hz, 2H), 2.30 (t, $^3J = 6.5$ Hz, 2H), 1.84 – 1.66 (m, 4H), 0.15 (s, 9H).

$^{13}\text{C-NMR}$ (100 MHz, CDCl_3) δ [ppm] = 153.1 (1C), 152.9 (1C), 134.2 (1C), 133.9 (1C), 133.5 (1C), 130.6 (1C), 129.8 (1C), 129.8 (1C), 127.8 (1C), 127.6 (1C), 126.8 (1C), 126.6 (1C), 126.2 (1C), 126.1 (1C), 126.0 (1C), 125.4 (1C), 124.2 (1C), 120.8 (1C), 118.2 (1C), 116.9 (1C), 107.1 (1C), 98.7 (1C), 95.2 (1C), 94.2 (1C), 85.0 (1C), 78.1 (1C), 56.2 (1C), 56.0 (1C), 28.0 (1C), 27.9 (1C), 19.6 (1C), 19.5 (1C), -0.3 (3C).

IR (nujol): $\tilde{\nu}$ [cm^{-1}] = 3058.2 (m), 3007.4 (m), 2954.7 (s), 2864.4 (m), 2827.9 (m), 2227.6 (w), 2172.6 (s), 1946.9 (w), 1672.7 (w), 1622.3 (s), 1594.4 (s), 1509.9 (s), 1494.9 (m), 1470.4 (m), 1427.7 (s), 1393.2 (m), 1357.9 (m), 1334.9 (m), 1306.7 (w), 1261.0 (m), 1243.4 (s), 1215.9 (m), 1199.3 (m), 1156.6 (s), 1122.9 (w), 1070.5 (m), 1034.6 (s), 1015.1 (s), 979.2 (s), 924.3 (s), 905.9 (m), 843.0 (s), 810.8 (w), 756.3 (s), 698.1 (w).

4.8.5. (*R*)-2,2'-Bis(methoxymethoxy)-3-(8-phenylocta-1,7-diyn-1-yl)-1,1'-binaphthalene (86)



Compound **86** was prepared according to general procedure A, starting from 55 mg (0.30 mmol) of diyne **92**. **86** was isolated through chromatographic column on silica gel (EtOAc/EDP 1:9 to 1:4) as a thick yellowish oil.

Yield: 125 mg (0.23 mmol, 75%)

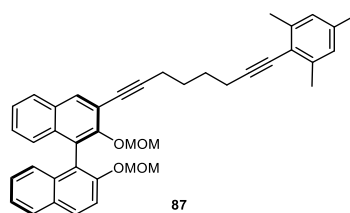
R_f = 0.61 (SiO₂, EtOAc/EDP 1:4)

¹H-NMR (400 MHz, CDCl₃) δ [ppm] = 8.09 (s, 1H), 7.95 (d, ³J = 9.0 Hz, 1H), 7.85 (d, ³J = 8.2 Hz, 1H), 7.81 (d, ³J = 8.2 Hz, 1H), 7.57 (d, ³J = 9.0 Hz, 1H), 7.43 – 7.31 (m, 4H), 7.31 – 7.23 (m, 4H), 7.23 – 7.13 (m, 3H), 5.14 (d, ²J = 6.9 Hz, 1H), 4.99 (d, ²J = 7.0 Hz, 1H), 4.99 (d, ²J = 5.7 Hz, 1H), 4.88 (d, ²J = 5.7 Hz, 1H), 3.16 (s, 3H), 2.57 (s, 3H), 2.62 – 2.53 (m, 2H), 2.53 – 2.46 (m, 2H), 1.94 – 1.75 (m, 4H).

¹³C-NMR (100 MHz, CDCl₃) δ [ppm] = 153.1 (1C), 152.9 (1C), 134.2 (1C), 133.9 (1C), 133.5 (1C), 131.7 (2C), 130.6 (1C), 129.8 (1C), 129.8 (1C), 128.3 (2C), 127.8 (1C), 127.7 (1C), 127.6 (1C), 126.8 (1C), 126.6 (1C), 126.2 (1C), 126.1 (1C), 126.0 (1C), 125.4 (1C), 124.2 (1C), 124.1 (1C), 120.8 (1C), 118.2 (1C), 116.9 (1C), 98.7 (1C), 95.2 (1C), 94.2 (1C), 89.9 (1C), 81.2 (1C), 78.2 (1C), 56.2 (1C), 56.0 (1C), 28.1 (1C), 28.0 (1C), 19.5 (1C), 19.2 (1C).

HRMS (ESI⁺): m/z 577.2355 [M+Na]⁺ (calcd. for C₃₈H₃₄NaO₄⁺: 577.2355).

4.8.6. (R)-3-(8-Mesitylocta-1,7-diyn-1-yl)-2,2'-bis(methoxymethoxy)-1,1'-binaphthalene (87)



Compound **87** was prepared according to general procedure A, starting from 80 mg (0.36 mmol) of diyne **93**. **87** was isolated through chromatographic column on silica gel (EtOAc/EDP 1:9) as a yellowish oil.

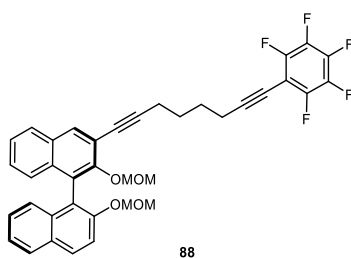
Yield: 139 mg (0.233 mmol, 65%)

R_f = 0.71 (SiO₂, EtOAc/EDP 1:4)

¹H-NMR (400 MHz, CDCl₃) δ [ppm] = 8.07 (s, 1H), 7.94 (d, ³J = 9.1 Hz, 1H), 7.85 (d, ³J = 8.1 Hz, 1H), 7.80 (d, ³J = 8.1 Hz, 1H), 7.57 (d, ³J = 9.0 Hz, 1H), 7.41 – 7.31 (m, 2H), 7.30 – 7.12 (m, 4H), 6.83 (s, 2H), 5.14 (d, ²J = 6.9 Hz, 1H), 5.02 – 4.93 (m, 2H), 4.87 (d, ²J = 5.7 Hz, 1H), 3.15 (s, 3H), 2.63 – 2.50 (m, 7H), 2.37 (s, 6H), 2.25 (s, 3H), 1.93 – 1.77 (m, 4H).

¹³C-NMR (100 MHz, CDCl₃) δ [ppm] = 153.1 (1C), 152.9 (1C), 140.0 (1C), 136.9 (2C), 134.2 (1C), 133.9 (1C), 133.5 (1C), 130.6 (1C), 129.8 (1C), 129.8 (1C), 127.8 (1C), 127.6 (1C), 127.6 (2C), 126.2 (1C), 126.1 (1C), 126.0 (1C), 125.4 (1C), 124.2(1C), 120.9 (1C), 120.8 (1C), 118.3 (1C), 116.9 (1C), 98.7 (1C), 97.4 (1C), 95.2 (1C), 94.3 (1C), 78.8 (1C), 78.1 (1C), 56.2 (1C), 56.0 (1C), 28.4 (1C), 28.0 (1C), 21.4 (1C), 21.2 (2C), 19.5 (1C), 19.4 (1C).

4.8.7. (R)-2,2'-Bis(methoxymethoxy)-3-(8-(perfluorophenyl)octa-1,7-diyn-1-yl)-1,1'-binaphthalene (88)



Compound **88** was prepared according to general procedure A, starting from 56 mg (0.21 mmol) of diyne **94**. **88** was isolated through chromatographic column on silica gel (EtOAc/*n*-hexane 1:9) as a yellowish oil.

Yield: 102 mg (0.16 mmol, 77%)

R_f = 0.26 (SiO₂, EtOAc/EDP 1:9)

¹H-NMR (400 MHz, CDCl₃) δ [ppm] = 8.08 (s, 1H), 7.94 (d, ³J = 9.0 Hz, 1H), 7.85 (d, ³J = 8.1 Hz, 1H), 7.81 (d, ³J = 8.2 Hz, 1H), 7.57 (d, ³J = 9.0 Hz, 1H), 7.42 – 7.30 (m, 2H), 7.30 – 7.11 (m, 4H), 5.14 (d, ²J = 6.9 Hz, 1H), 5.03 – 4.93 (m, 2H), 4.86 (d, ²J = 5.7 Hz, 1H), 3.15 (s, 3H), 2.65 – 2.50 (m, 4H), 2.57 (s, 3H), 1.94 – 1.74 (m, 4H).

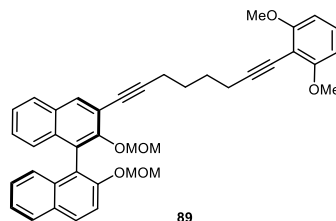
¹³C-NMR (100 MHz, CDCl₃) δ [ppm] = 153.1 (1C), 152.9 (1C), 149.0 – 146.2 (m, 2C), 142.7 – 139.5 (m, 1C), 139.2 – 136.2 (m, 2C), 134.2 (1C), 133.9 (1C), 133.5 (1C), 130.6 (1C), 129.8 (1C), 129.8 (1C), 127.9 (1C), 127.6 (1C), 126.8 (1C), 126.6 (1C), 126.2 (1C), 126.1 (1C), 125.9 (1C), 125.4 (1C), 124.2 (1C), 120.8 (1C), 118.1 (1C), 116.9 (1C), 103.6 – 103.4 (m, 1C), 100.9 – 100.4 (m, 1C), 98.7 (1C), 95.2 (1C), 93.8 (1C), 78.3 (1C), 65.4 – 65.2 (m, 1C), 56.2 (1C), 56.0 (1C), 27.8 (1C), 27.5 (1C), 19.5 (1C), 19.4 (1C).

¹⁹F-NMR (377 MHz, CDCl₃) δ [ppm] = -136.95 – -137.13 (m, 2F), -154.18 (t, ³J = 20.8 Hz, 1F), -162.27 – -162.51 (m, 2F).

IR (neat): $\tilde{\nu}$ [cm⁻¹] = 1612.8 (w), 1594.0 (w), 1334.7 (w), 1260.8 (w), 1241.9 (m), 1214.8 (w), 1155.7 (m), 1069.8 (m), 1033.8 (m), 1014.3 (m), 976.5 (m), 923.1 (w), 809.1 (w), 761.2 (s), 691.1 (w).

HRMS (ESI+): m/z 667.1884 [M+Na]⁺ (calculated for C₃₈H₂₉O₄NaF₅⁺ = 667.1884).

4.8.8. (R)-3-(8-(2,6-Dimethoxyphenyl)octa-1,7-diyn-1-yl)-2,2'-bis(methoxymethoxy)-1,1'-binaphthalene (89)



Compound **89** was prepared according to general procedure A, starting from 77 mg (0.32 mmol) of diyne **95**. **89** was isolated through chromatographic column on silica gel (EtOAc/EDP 1:4 to 3:7) as a yellow solid.

Yield: 152 mg (0.247 mmol, 78%)

$R_f = 0.39$ (SiO₂, EtOAc/EDP 1:4)

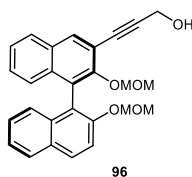
¹H-NMR (400 MHz, CDCl₃) δ [ppm] = 8.07 (s, 1H), 7.94 (d, ³J = 9.1 Hz, 1H), 7.85 (d, ³J = 8.1 Hz, 1H), 7.80 (d, ³J = 8.2 Hz, 1H), 7.57 (d, ³J = 9.0 Hz, 1H), 7.41 – 7.30 (m, 2H), 7.30 – 7.10 (m, 5H), 6.51 (d, ³J = 8.4 Hz, 2H), 5.14 (d, ²J = 6.9 Hz, 1H), 5.01 – 4.94 (m, 2H), 4.87 (d, ²J = 5.8 Hz, 1H), 3.86 (s, 6H), 3.16 (s, 3H), 2.68 – 2.51 (m, 4H), 2.56 (s, 3H), 1.97 – 1.79 (m, 4H).

¹³C-NMR (100 MHz, CDCl₃) δ [ppm] = 161.6 (2C), 153.1 (1C), 153.0 (1C), 134.2 (1C), 133.9 (1C), 133.5 (1C), 130.6 (1C), 129.8 (1C), 128.9 (1C), 127.8 (1C), 127.6 (1C), 127.8 (1C), 127.6 (1C), 126.8 (1C), 126.6 (1C), 126.1 (1C), 126.0 (1C), 125.3 (1C), 124.2 (1C), 120.9 (1C), 118.3 (1C), 116.9 (1C), 103.6 (2C), 98.7 (1C), 98.6 (1C), 95.2 (1C), 94.6 (1C), 78.0 (1C), 73.2 (1C), 56.2 (2C), 56.2 (1C), 56.0 (1C), 28.2 (1C), 27.9 (1C), 19.9 (1C), 19.6 (1C).

IR (nujol): $\tilde{\nu}$ [cm⁻¹] = 3058.4 (w), 3007.4 (m), 2934.7 (s), 2836.7 (m), 2227.0 (w, C≡C), 2191.1 (w, C≡C), 1711.5 (w), 1622.1 (w), 1529.6 (s), 1584.1 (s), 1473.4 (s), 1432.3 (s), 1393.1 (w), 1357.7 (w), 1334.5 (w), 1301.7 (w), 1253.8 (s), 1217.2 (w), 1199.4 (w), 1155.8 (s), 1112.6 (s), 1071.3 (m), 1033.9 (s), 1014.3 (s), 978.5 (s), 923.5 (m), 904.9 (m), 810.9 (w), 752.9 (s), 725.3 (m).

HRMS (ESI⁺): m/z 637.2565 [M+Na]⁺ (calculated for C₄₀H₃₈O₆Na⁺ = 637.2566).

4.8.1. (*R*)-3-(2,2'-bis(methoxymethoxy)-[1,1'-binaphthalen]-3-yl)prop-2-yn-1-ol (**96**)



Iodide **82** (500 mg, 1.00 mmol, 1 eq) was dissolved in a 1:1 mixture of MeCN (5 mL) and triethylamine (5 mL). The solution was degassed with a stream of argon. CuI (19 mg, 0.10 mmol, 0.1 eq), Pd(PPh₃)₄ (115 mg, 0.10 mmol, 0.1 eq), and propargyl alcohol (116 μL, 112 mg, 2.00 mmol, 2 eq) were added. The reaction was heated to 80 °C for 2 hours. Volatiles were removed, and the residue was suspended in a saturated solution of NH₄Cl (15 mL). The crude was extracted with DCM (2 x 15 mL). The collected organic layers were washed with brine, dried over Na₂SO₄, filtered, and concentrated under reduced pressure. The product was purified through chromatographic column on silica gel (EtOAc/EDP 2:3). **96** was isolated as a pale-yellow solid.

Yield: 355 mg (0.83 mmol, 83%)

R_f = 0.41 (SiO₂, EtOAc/EDP 2:3)

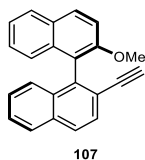
¹H-NMR (400 MHz, CDCl₃) δ [ppm] = 8.12 (s, 1H), 7.96 (d, ³J = 9.0 Hz, 1H), 7.89 – 7.80 (m, 2H), 7.58 (d, ³J = 9.0 Hz, 1H), 7.44 – 7.32 (m, 2H), 7.30 – 7.22 (m, 2H), 7.20 – 7.13 (m, 2H), 5.14 (d, ²J = 6.9 Hz, 1H), 5.00 (d, ²J = 6.9 Hz, 1H), 4.90 (d, ²J = 5.6 Hz, 1H), 4.82 (d, ²J = 5.6 Hz, 1H), 4.55 (d, ³J = 3.5 Hz, 2H), 3.16 (s, 3H), 2.71 (s, 3H), 1.91 (br s, 1H, OH).

¹³C-NMR (100 MHz, CDCl₃) δ [ppm] = 153.1 (1C), 152.8 (1C), 134.2 (1C), 134.1 (1C), 134.0 (1C), 130.5 (1C), 130.0 (1C), 129.8 (1C), 127.9 (1C), 127.9 (1C), 127.3 (1C), 126.8 (1C), 126.4 (1C), 126.2 (1C), 125.7 (1C), 125.6 (1C), 124.3 (1C), 120.4 (1C), 117.0 (1C), 116.8 (1C), 99.0 (1C), 95.2 (1C), 91.5 (1C), 83.1 (1C), 56.5 (1C), 56.1 (1C), 52.0 (1C).

IR (nujol): $\tilde{\nu}$ [cm⁻¹] = 3417.4 (br, OH), 2226.9 (w, C≡C), 1621.7 (m), 1593.5 (m), 1261.1 (w), 1241.7 (m), 1214.9 (m), 1154.5 (m), 1120.5 (w), 1068.4 (m), 1032.7 (m), 1013.7 (m), 974.0 (m), 921.3 (m), 864.4 (w), 809.5 (w), 761.4 (s).

4.9. Synthesis of Iron Complex 102

4.9.1. (*R*)-2-ethynyl-2'-methoxy-1,1'-binaphthalene (107)



Alkyne **79** (250 mg, 0.66 mmol, 1 eq) was dissolved in 1:1 mixture of methanol (3.3 mL) and THF (3.3 mL). K_2CO_3 (908 mg, 6.57 mmol, 10 eq) was added, and the suspension was left under stirring overnight. After 16 hours, the reaction mixture was filtered. Volatiles were removed under reduced pressure. The residue was suspended in water (10 mL) and extracted with DCM (4 x 10 mL). The collected organic layers were washed with brine, dried over Na_2SO_4 , filtered, and concentrated in vacuo. The product was used without further purification. **107** was isolated as a crystalline yellowish solid.

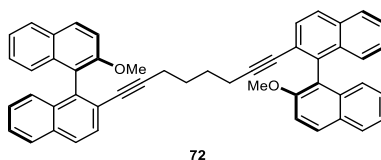
Yield: 183 mg (0.59 mmol, 90%).

Characterization data are in agreement with the literature.^[137]

R_f = 0.34 (SiO_2 , EtOAc/EDP 5:95)

1H -NMR (400 MHz, $CDCl_3$) δ [ppm] = 8.01 (d, 3J = 9.0 Hz, 1H), 7.94 – 7.84 (m, 3H), 7.72 (d, 3J = 8.5 Hz, 1H), 7.54 – 7.41 (m, 2H), 7.33 (dd, 3J = 7.5 Hz, 1H), 7.30 – 7.17 (m, 3H), 7.03 (d, 3J = 8.5 Hz, 1H), 3.79 (s, 3H), 2.76 (s, 1H).

4.9.2. 1,8-bis((*R*)-2'-methoxy-[1,1'-binaphthalen]-2-yl)octa-1,7-diyne (72)



Alkyne **107** (403 mg, 1.307 mmol, 4 eq) was dissolved in dry THF (3.5 mL) under inert atmosphere. The solution was cooled to -78 °C and *n*-BuLi (1.6 M in hexanes, 785 μ L, 1.25 mmol, 3.8 eq) was added. The mixture was allowed to slowly warm up to -25 °C, and it was kept between -30 °C and -25 °C for 1 hour. After cooling to -78 °C, a solution of 1,4-diiodobutane (102

mg, 0.33 mmol, 1 eq) in dry THF (2 mL) was added via cannula. The reaction mixture was warmed up to room temperature and it was heated to 70 °C for 6 hours. The reaction was allowed to cool to rt, and it was quenched with sat. aq. NH₄Cl (5 mL). The crude was extracted with DCM (4 x 5 mL). The collected organic layers were washed with brine, dried over Na₂SO₄, filtered, and concentrated under reduced pressure. The product was purified through chromatographic column (Acetone/EDP 1:9 to 1:4). **72** was isolated as a yellowish oil. 180 mg of **107** (0.58 mmol, 45%) were recovered.

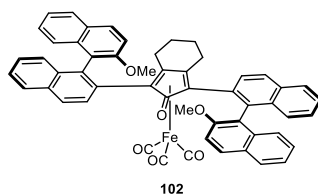
Yield: 212 mg (0.32 mmol, 96%, calculated on 1,4-diiodobutane).

R_f = 0.27 (SiO₂, EtOAc/EDP 1:9)

¹H-NMR (400 MHz, CDCl₃) δ [ppm] = 7.93 – 7.84 (m, 6H), 7.78 (d, ³J = 8.1 Hz, 2H), 7.63 (d, ³J = 8.5 Hz, 2H), 7.48 – 7.40 (m, 2H), 7.37 (d, ³J = 9.0 Hz, 2H), 7.30 – 7.19 (m, 6H), 7.15 (dd, ³J = 11.0 Hz, 2H), 7.02 (d, ³J = 8.4 Hz, 2H), 3.73 (s, 6H), 1.70 – 1.61 (m, 4H), 0.46 – 0.31 (m, 4H).

¹³C-NMR (100 MHz, CDCl₃) δ [ppm] = 154.9 (2C), 137.6 (2C), 133.9 (2C), 133.0 (2C), 132.9 (2C), 129.6 (2C), 129.2 (2C), 128.9 (2C), 128.1 (2C), 127.8 (2C), 127.7 (2C), 126.5 (2C), 126.5 (2C), 126.4 (2C), 126.1 (2C), 125.3 (2C), 123.6 (2C), 122.6 (2C), 122.5 (2C), 114.3 (2C), 93.4 (2C), 80.9 (2C), 57.1 (2C), 26.2 (2C), 18.6 (2C).

4.9.3. Complex 102



Diene **72** (91.5 mg, 0.136 mmol, 1 eq) and Fe₂(CO)₉ (100 mg, 0.273 mmol, 2 eq) were charged in a Schlenk tube under argon atmosphere. Dry *p*-Xylene (1.4 mL) was added, and the mixture was heated to 130 °C for 18 hours. The reaction was allowed to cool to room temperature, and it was filtered through celite, rinsing with DCM. The product was purified through chromatographic column (Et₂O/EDP 1:1 to 3:2). To avoid degradation of the product after purification, the solvents were slowly removed at room temperature. **102** was isolated as a pale-yellow solid.

Yield: 40 mg (0.048 mmol, 35%).

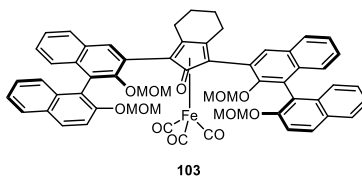
R_f = 0.42 (SiO₂, EtOAc/EDP 3:7)

¹H-NMR and ¹³C-NMR spectra were not well resolved.

MS (ESI⁺): m/z = 840.7 [M+H⁺] (calculated for C₅₄H₃₉FeO₆ = 839.2).

4.10. Synthesis of Complexes 103-106

4.10.1. Complex 103



Diiron nonacarbonyl (521 mg, 1.43 mmol, 2 eq) and **81** (610 mg, 0.72 mmol, 1 eq) were charged in a dried Schlenk under inert atmosphere. Dry toluene (7 mL) was added, the Schlenk was sealed, and the mixture was heated to 110 °C for 18 h. The reaction was allowed to cool to room temperature and filtered through celite, rinsing with DCM. The product was purified through chromatographic column on silica gel (EtOAc/EDP 1:4 to 3:7). **103** was isolated as a yellow crystalline solid.

Yield: 466 mg (0.46 mmol, 64%).

R_f = 0.39 (SiO₂, EtOAc/EDP 3:7)

m.p. = 245-250 °C (dec.)

¹H-NMR (400 MHz, CDCl₃) δ [ppm] = 8.08 – 7.90 (m, 6H), 7.85 (t, ³ J = 9.1 Hz, 2H), 7.62 (d, ³ J = 9.1 Hz, 1H), 7.57 (d, ³ J = 9.0 Hz, 1H), 7.49 – 7.41 (m, 2H), 7.40 – 7.19 (m, 10H), 7.17 (d, ³ J = 8.4 Hz, 1H), 5.14 – 4.97 (m, 4H), 4.69 (d, ² J = 4.8 Hz, 1H), 4.63 (d, ² J = 5.0 Hz, 1H), 4.54 (d, ² J = 4.8 Hz, 1H), 4.40 (d, ² J = 4.2 Hz, 1H), 3.23 (s, 3H), 3.19 (s, 3H), 3.03 – 2.81 (m, 2H), 2.53 – 2.33 (m, 5H), 2.28 (s, 3H), 1.98 – 1.80 (m, 4H).

¹³C-NMR (100 MHz, CDCl₃) δ [ppm] = 209.2 (3C), 171.6 (1C), 153.6 (1C), 153.0 (1C), 152.3 (1C), 152.1 (1C), 136.2 (1C), 136.1 (1C), 134.4 (1C), 134.3 (1C), 134.2 (1C), 134.0 (1C), 131.2 (1C), 131.1 (1C), 129.9 (1C), 129.8 (1C), 129.8 (1C), 129.5 (1C), 128.4 (2C), 128.1 (1C), 127.7 (1C), 126.9 (1C), 126.7 (1C), 126.6 (1C), 126.6 (1C), 126.5 (1C), 126.3 (1C), 126.2 (1C), 126.1 (1C), 125.8 (1C), 125.4 (1C), 125.4 (1C), 125.2 (1C), 125.0 (1C), 124.9 (1C), 124.3 (1C), 123.9 (1C), 121.1 (1C), 120.0 (1C), 117.1 (1C), 115.9 (1C), 106.0 (1C), 105.2 (1C), 99.4 (1C), 99.4 (1C), 95.5 (1C), 94.6 (1C), 84.0 (1C), 83.8 (1C), 56.2 (1C), 56.1 (1C), 55.8 (2C), 22.5 (1C), 22.4 (1C), 22.3 (1C), 22.1 (1C).

IR (nujol): $\tilde{\nu}$ [cm⁻¹] = 2060 (s, Fe(CO)₃), 2013 (s, Fe(CO)₃), 1978 (s, Fe(CO)₃), 1731 (m), 1639 (s, C=O), 1591 (m), 1305.8 (w), 1239.3 (s), 1196.1 (w), 1147.8 (m), 1084.7 (w), 1039.5 (m), 1008.0 (s), 924.1 (w), 901.0 (w), 811.4 (w), 744.2 (m), 722.0 (m).

HRMS (ESI+): m/z 1019.2739 [M+H]⁺ (calculated for C₆₀H₅₁⁵⁶FeO₁₂⁺ = 1019.2724).

X-Ray Crystal Structure Analysis of Complex 103

Crystals suitable for X-ray diffraction analysis were obtained by slow diffusion of *n*-hexane into a EtOAc solution of **103**. Crystal data and details of data collection and refinement are reported in Table 18. Data reduction was performed using the software package CrysAlisPro.^[202] The absorption corrections were carried out semi-empirically. The structure was solved by dual space methods with SHELXT-2017^[203] and refined with SHELXL-2018^[204] using the WinGX program suite.^[205] Structure refinement was done using full-matrix least-square routines against F^2 . All hydrogen atoms were calculated on idealized positions.

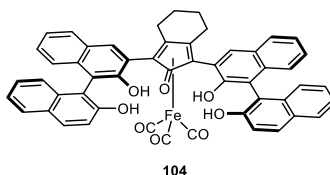
Table 18. Crystal data and structure refinement for complex 103.

Empirical formula	C ₁₀ H ₈ Fe _{0.16} O _{1.92}
Formula weight	167.82
Temperature	295(2) K
Wavelength	0.71073 Å
Crystal system, space group	Monoclinic, I 2
Unit cell dimensions	a = 25.7074(18) Å alpha = 90° b = 8.2601(6) Å beta = 103.171(7)° c = 27.8632(19) Å gamma = 90°
Volume	5761.0(7) Å ³
Z, Calculated density	25, 1.209 Mg/m ³
Absorption coefficient	0.321 mm ⁻¹
F(000)	2188
Crystal size	0.10 x 0.05 x 0.05 mm
Theta range for data collection	1.627 to 25.345 deg.
Limiting indices	-30 ≤ h ≤ 30, -9 ≤ k ≤ 9, -33 ≤ l ≤ 33
Reflections collected / unique	27972 / 10510 [R(int) = 0.0401]
Completeness to theta = 25.242	99.9 %
Absorption correction	Semi-empirical from equivalents
Max. and min. transmission	1.00000 and 0.74093
Refinement method	Full-matrix least-squares on F^2
Data / restraints / parameters	10510 / 1 / 662
Goodness-of-fit on F^2	1.087
Final R indices [I > 2σ(I)]	R1 = 0.1011, wR2 = 0.2639
R indices (all data)	R1 = 0.1380, wR2 = 0.2915

Absolute structure parameter	0.039(11)
Extinction coefficient	n/a
Largest diff. peak and hole	1.487 and -0.435 e ⁻³

The complex crystallizes in the space group *I*2 with one symmetry independent molecule in the asymmetric unit (*Z* = 4). The space group is enantiomorphous (Flack parameter χ = 0.039(11)) and thus only the atropisomer with the shown configuration is observed. The absolute structure was determined by anomalous dispersion effects. Beside the complex, a hexane molecule in general position and a twofold axis could be detected, thus 1.5 solvent molecules per complex molecule (**103**·1.5*n*-hexane).

4.10.2. Complex 104



Complex **103** (156 mg, 0.15 mmol, 1 eq) was dissolved in THF (1.2 mL). Concentrated aqueous HCl (0.9 mL) was added, and the mixture was heated to 40 °C for 3 hours. The solution was diluted with water (5 mL) and extracted with Et₂O (2 x 5 mL). The organic phase was dried over Na₂SO₄, filtered, and concentrated in vacuo. The product was purified through chromatographic column on silica gel (EtOAc/EDP 3:7). **104** was isolated as a yellow solid.

Yield: 100 mg (0.12 mmol, 77%).

R_f = 0.36 (SiO₂, EtOAc/EDP 2:3)

m.p. = 311-313 °C (dec.)

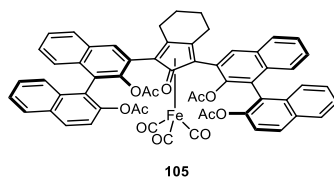
¹H-NMR (400 MHz, (CD₃)₂CO) δ [ppm] = 9.72 (s, 1H), 9.41 (s, 1H), 8.30 (d, ³*J* = 10.9 Hz, 2H), 8.01 – 7.82 (m, 8H), 7.42 – 7.15 (m, 10H), 7.15 – 7.01 (m, 4H), 3.24 – 3.09 (m, 1H), 3.04 – 2.90 (m, 3H), 2.17 – 1.88 (m, 4H).

¹³C-NMR (100 MHz, (CD₃)₂CO) δ [ppm] = 209.9 (3C), 166.9 (1C), 154.7 (1C), 154.3 (1C), 154.3 (1C), 153.7 (1C), 135.7 (1C), 135.7 (1C), 135.7 (1C), 135.7 (1C), 135.6 (1C), 133.5 (1C), 132.6 (1C), 130.8 (1C), 130.5 (1C), 130.2 (1C), 130.1 (1C), 129.5 (1C), 129.5 (1C), 129.3 (2C), 129.1 (1C), 129.0 (1C), 127.9 (1C), 127.8 (1C), 127.3 (1C), 127.1 (1C), 125.7 (1C), 125.6 (1C), 125.5 (1C), 124.5 (1C), 124.5 (1C), 123.8 (1C), 123.7 (1C), 122.2 (1C), 121.6 (1C), 119.7 (1C), 119.6 (1C), 118.4 (1C), 117.9 (1C), 116.1 (1C), 115.5 (1C), 104.9 (1C), 102.4 (1C), 85.4 (1C), 83.9 (1C), 25.3 (1C), 24.2 (1C), 23.2 (1C), 23.1 (1C).

IR (nujol): $\tilde{\nu}$ [cm^{-1}] = 2853 (s), 2074 (s, $\text{Fe}(\text{CO})_3$), 2019 (br, $\text{Fe}(\text{CO})_3$), 1620 (s, C=O), 1596, 1512 (w), 1500 (w), 1345 (m), 1210 (w), 1148 (w), 817 (w), 749 (m), 722 (m).

MS (ESI+): m/z = 843.00 [$\text{M}+\text{H}^+$], 864.95 [$\text{M}+\text{Na}^+$] (calculated for $\text{C}_{52}\text{H}_{35}\text{FeO}_8$ = 843.17, $\text{C}_{52}\text{H}_{35}\text{FeO}_8\text{Na}$ = 865.15).

4.10.3. Complex 105



Complex **104** (30 mg, 0.036 mmol, 1 eq) was dissolved in dry THF (0.7 mL). 4-dimethylaminopyridine (0.9 mg, 0.007 mmol, 0.2 eq), triethylamine (40 μL , 29 mg, 0.29 mmol, 8 eq), and acetyl chloride (15 μL , 17 mg, 0.21 mmol, 6 eq) were added. The mixture was stirred at room temperature for 4 hours. The reaction was quenched with water (5 mL) and extracted with Et_2O (2 x 5 mL). The organic phase was washed with a 0.5 M HCl solution (5 mL), water (5 mL), and brine, then dried over Na_2SO_4 , filtered, and concentrated under reduced pressure. The product was purified through chromatographic column on silica gel (EtOAc/EDP 3:7). **105** was isolated as a pale yellow solid.

Yield: 24.8 mg (0.024 mmol, 68%).

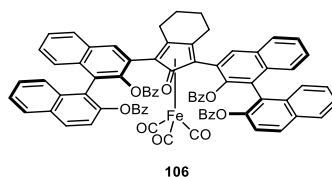
R_f = 0.29 (SiO_2 , EtOAc/EDP 3:7)

m.p. = 180 $^\circ\text{C}$ (dec.)

$^1\text{H-NMR}$ (400 MHz, $(\text{CD}_3)_2\text{CO}$) δ [ppm] = 8.24 (s, 1H), 8.22 – 8.13 (m, 3H), 8.13 – 8.04 (m, 2H), 8.04 – 7.95 (m, 2H), 7.62 – 7.42 (m, 6H), 7.40 – 7.26 (m, 2H), 7.26 – 7.18 (m, 2H), 7.09 (d, 3J = 8.4 Hz, 1H), 7.03 (d, 3J = 8.4 Hz, 1H), 3.04 – 2.88 (m, 1H), 2.69 – 2.43 (m, 3H), 2.02 – 1.73 (m, 4H), 1.94 (s, 3H), 1.90 (s, 3H), 1.66 (s, 3H), 1.60 (s, 3H).

$^{13}\text{C-NMR}$ (100 MHz, $(\text{CD}_3)_2\text{CO}$) δ [ppm] = 210.4 (3C), 171.2 (1C), 170.1 (1C), 169.5 (1C), 169.3 (1C), 168.3 (1C), 148.1 (1C), 148.0 (1C), 147.8 (1C), 147.5 (1C), 136.7 (1C), 136.0 (1C), 134.4 (1C), 134.2 (1C), 134.1 (2C), 132.7 (1C), 132.6 (1C), 132.6 (1C), 132.5 (1C), 130.7 (1C), 130.4 (1C), 129.4 (1C), 129.3 (1C), 129.1 (1C), 129.0 (1C), 128.2 (1C), 128.2 (1C), 127.8 (1C), 127.8 (1C), 127.6 (1C), 127.3 (1C), 127.3 (1C), 127.2 (1C), 126.9 (2C), 126.7 (1C), 126.6 (1C), 126.2 (1C), 125.5 (1C), 125.4 (1C), 124.2 (1C), 123.7 (1C), 123.7 (1C), 123.2 (1C), 105.2 (1C), 103.7 (1C), 84.3 (1C), 83.4 (1C), 24.0 (1C), 23.2 (1C), 23.2 (1C), 22.8 (1C), 21.1 (1C), 20.9 (1C), 20.8 (1C), 20.6 (1C).

4.10.4. Complex 106



Complex **104** (39 mg, 0.046 mmol, 1 eq) was dissolved in dry THF (1.2 mL). 4-dimethylaminopyridine (1.1 mg, 0.009 mmol, 0.2 eq), triethylamine (52 μ L, 38 mg, 0.37 mmol, 8 eq), and benzoyl chloride (32 μ L, 39 mg, 0.28 mmol, 6 eq) were added. The mixture was stirred at room temperature for 4 hours. The reaction was quenched with water (5 mL) and extracted with Et₂O (2 x 5 mL). The organic phase was washed with a 0.5 M HCl solution (5 mL), water (5 mL), and brine, then dried over Na₂SO₄, filtered, and concentrated under reduced pressure. The product was purified through chromatographic column on silica gel (EtOAc/EDP 1:3). **105** was isolated as a yellow solid.

Yield: 24.8 mg (0.024 mmol, 68%).

R_f = 0.51 (SiO₂, EtOAc/EDP 3:7)

m.p. = 176-182 °C (dec.)

¹H-NMR (400 MHz, CD₂Cl₂) δ [ppm] = 8.02 – 7.69 (m, 12H), 7.54 – 7.21 (m, 26H), 7.08 (dd, ³J = 7.6 Hz, 2H), 6.99 (dd, ³J = 7.1 Hz, 2H), 2.48 (ddd, ³J = 17.1 Hz, ³J = ²J = 6.6 Hz, 1H), 2.39 – 2.25 (m, 2H), 2.03 – 1.89 (m, 1H), 1.75 – 1.60 (m, 1H), 1.54 – 1.39 (m, 2H), 1.39 – 1.29 (m, 1H).

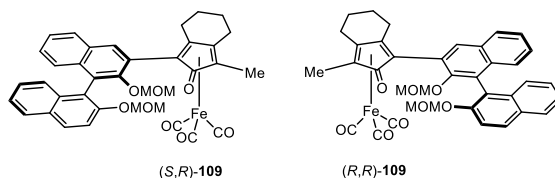
¹³C-NMR (100 MHz, (CD₂Cl₂) δ [ppm] = 209.3 (3C), 169.7 (1C), 165.4 (1C), 165.3 (1C), 165.1 (1C), 164.3 (1C), 147.7 (2C), 147.6 (1C), 147.1 (1C), 135.8 (br s), 134.6 (br s), 133.9 (1C), 133.8 (1C), 133.8 (1C), 133.7 (1C), 133.6 (1C), 133.6 (1C), 133.5 (1C), 132.1 (2C), 132.0 (1C), 131.8 (1C), 130.8 (CH), 130.4 (CH), 130.3 (CH), 130.1 (CH), 130.1 (CH), 130.1 (CH), 129.9 (1C), 129.6 (1C), 129.4 (1C), 129.3 (1C), 129.1 (CH), 129.0 (CH), 128.9 (1C), 128.8 (1C), 128.7 (1C), 128.6 (CH), 128.5 (CH), 128.5 (CH), 128.4 (1C), 128.3 (1C), 127.8 (1C), 127.7 (1C), 127.3 (1C), 127.2 (1C), 127.0 (CH), 126.7 (1C), 126.6 (1C), 126.4 (CH), 126.2 (1C), 126.1 (1C), 125.8 (1C), 125.8 (1C), 124.9 (1C), 124.5 (1C), 124.1 (1C), 124.0 (1C), 122.2 (1C), 122.1 (1C), 83.5 (1C), 83.2 (1C), 23.7 (br s), 22.8 (1C), 22.6 (1C), 22.0 (br s).

4.11. Synthesis of Iron Complexes 109-114

4.11.1. General Procedure for the Carbonylative Cyclization of Alkynes 84-89 (B)

Diironnonacarbonyl (2 eq) and the diyne pre-ligands **84-89** (1 eq) were charged in a dried Schlenk tube under inert atmosphere. Dry toluene (concentration: 0.14 M) was added, the tube was sealed, and the mixture was heated to 110 °C for 18 h. The reaction was allowed to cool to room temperature and filtered through celite, rinsing with DCM. The corresponding diastereoisomerically pure complexes **109-114** were isolated through chromatographic column on silica gel.

4.11.2. Complexes 109a-b



Complexes **109a-b** were prepared according to general procedure B, starting from 100 mg (0.203 mmol) of **84**. **109a** and **109b** were isolated through chromatographic column on silica gel (Et₂O/EDP 1:2) as yellow solids.

Complex 109a

Yield: 7.5 mg (0.011 mmol, 6%)

R_f = 0.58 (SiO₂, EtOAc/EDP 1:4)

¹H-NMR and ¹³C-NMR analyses resulted in badly resolved spectra.

MS (ESI⁺): m/z = 683.37 [M+Na⁺] (calculated for C₃₇H₃₂FeO₈Na = 683.13).

Complex 109b

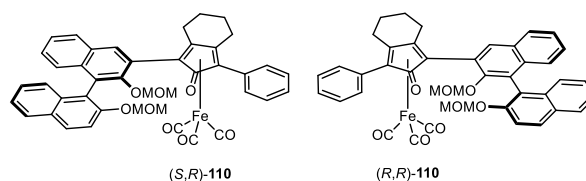
Yield: 9.4 mg (0.014 mmol, 7%)

R_f = 0.49 (SiO₂, EtOAc/EDP 1:4)

¹H-NMR and ¹³C-NMR analyses resulted in badly resolved spectra.

MS (ESI⁺): m/z = 683.25 [M+Na⁺] (calculated for C₃₇H₃₂FeO₈Na = 683.13).

4.11.3. Complexes 110a-b



Complexes **110a-b** were prepared according to general procedure B, starting from 125 mg (0.225 mmol) of **86**. **110a** and **110b** were isolated through chromatographic column on silica gel (Et₂O/EDP 1:1 to 3:2) as yellow solids.

Complex 110a

Yield: 59 mg (0.082 mmol, 36%)

R_f = 0.34 (SiO₂, Et₂O/EDP 3:2)

¹H-NMR (400 MHz, CD₂Cl₂) δ [ppm] = 8.03 – 7.97 (m, 2H), 7.94 – 7.87 (m, 2H), 7.77 – 7.72 (m, 2H), 7.63 (d, ³J = 9.1 Hz, 1H), 7.50 – 7.44 (m, 1H), 7.44 – 7.31 (m, 4H), 7.31 – 7.22 (m, 2H), 7.19 (d, ³J = 8.5 Hz, 1H), 7.13 (d, ³J = 8.5 Hz, 1H), 5.14 – 5.08 (m, 2H), 4.50 (d, ²J = 5.1 Hz, 1H), 4.34 (d, ²J = 5.1 Hz, 1H), 3.24 (s, 3H), 2.95 – 2.78 (m, 2H), 2.78 – 2.65 (m, 1H), 2.72 (s, 3H), 2.39 (ddd, ³J = 17.0 Hz, ³J = ²J = 5.3 Hz, 1H), 2.01 – 1.80 (m, 4H).

¹³C-NMR (100 MHz, CD₂Cl₂) δ [ppm] = 209.8 (3C), 171.4 (1C), 153.5 (1C), 153.1 (1C), 153.9 (1C), 134.7 (1C), 134.7 (1C), 132.3 (1C), 131.5 (1C), 130.5 (1C), 130.3 (1C), 130.2 (2C), 129.0 (2C), 128.7 (1C), 128.5 (1C), 128.5 (1C), 127.4 (1C), 127.3 (1C), 126.6 (1C), 126.4 (1C), 126.3 (1C), 125.9 (1C), 125.7 (1C), 124.7 (1C), 120.9 (1C), 117.4 (1C), 105.3 (1C), 101.8 (1C), 99.9 (1C), 95.9 (1C), 85.7 (1C), 81.2 (1C), 56.7 (1C), 56.2 (1C), 24.0 (1C), 23.2 (1C), 22.9 (1C), 22.6 (1C).

IR (nujol): $\tilde{\nu}$ [cm⁻¹] = 2059.7 (s, Fe(CO)₃), 1984.9 (br, Fe(CO)₃), 1639.7 (s, C=O), 1592.6 (w), 1240.9 (m), 1197.8 (w), 1148.4 (s), 1074.8 (w), 1034.1 (m), 1013.7 (m), 965.6 (m), 925.0 (w), 749.7 (m), 721.5 (s).

MS (ESI⁺): m/z = 723.28 [M+H⁺], 745.27 [M+Na⁺], 1466.40 (calculated for C₄₂H₃₅FeO₈⁺ = 723.17, C₄₂H₃₄FeO₈Na⁺ = 745.15).

HRMS (ESI⁺): m/z 723.1678 [M+H⁺]⁺, 745.1500 [M+Na⁺]⁺ (calculated for C₄₂H₃₅⁵⁶FeO₈⁺ = 723.1676, C₄₂H₃₄⁵⁶FeO₈Na⁺ = 745.1495).

Complex 110b

Yield: 56 mg (0.077 mmol, 34%)

R_f = 0.21 (SiO₂, Et₂O/EDP 3:2)

¹H-NMR (400 MHz, CD₂Cl₂) δ [ppm] = 8.05 – 7.97 (m, 2H), 7.95 – 7.89 (m, 2H), 7.78 – 7.72 (m, 2H), 7.67 (d, ³J = 9.1 Hz, 1H), 7.50 – 7.45 (m, 1H), 7.45 – 7.27 (m, 6H), 7.24 (d, ³J = 8.5 Hz, 1H), 7.15 (d, ³J = 8.5 Hz, 1H), 5.19 (d, ²J = 7.1 Hz, 1H), 5.10 (d, ²J = 7.1 Hz, 1H), 4.69 (d, ²J = 5.1 Hz, 1H), 4.53 (d, ²J = 5.1 Hz, 1H), 3.25 (s, 3H), 2.91 – 2.76 (m, 3H), 2.87 (s, 3H), 2.76 – 2.65 (m, 1H), 2.48 – 2.36 (m, 1H), 2.00 – 1.78 (m, 4H).

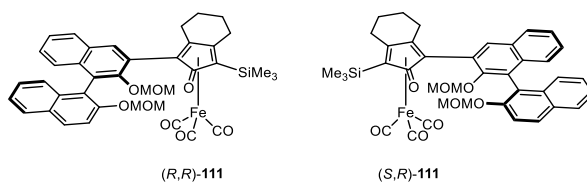
¹³C-NMR (100 MHz, CD₂Cl₂) δ [ppm] = 209.8 (3C), 171.6 (1C), 153.8 (1C), 152.8 (1C), 136.1 (1C), 134.6 (1C), 134.3 (1C), 132.3 (1C), 131.6 (1C), 130.6 (1C), 130.2 (2C), 130.2 (1C), 129.0 (2C), 128.8 (1C), 128.7 (1C), 128.5 (1C), 127.4 (1C), 127.2 (1C), 126.9 (1C), 126.0 (1C), 126.0 (1C), 125.7 (1C), 125.4 (1C), 124.6 (1C), 120.2 (1C), 116.4 (1C), 105.5 (1C), 101.9 (1C), 100.0 (1C), 95.2 (1C), 85.5 (s, 1C), 81.2 (1C), 57.0 (1C), 56.6 (1C), 23.8 (1C), 23.2 (1C), 22.9 (1C), 22.6 (1C).

IR (nujol): $\tilde{\nu}$ [cm⁻¹] = 2059.5 (s, Fe(CO)₃), 1984.9 (br, Fe(CO)₃), 1640.5 (s, C=O), 1592.6 (w), 1258.8 (w), 1241.4 (m), 1197.7 (w), 1148.1 (s), 1062.3 (w), 1032.9 (m), 1012.1 (m), 964.8 (m), 924.2 (w), 749.7 (m), 721.0 (s).

MS (ESI⁺): m/z = 723.25 [M+H⁺], 745.25 [M+Na⁺], 1466.54 (calculated for C₄₂H₃₅FeO₈ = 723.17, C₄₂H₃₄FeO₈Na = 745.15).

HRMS (ESI⁺): m/z 723.1677 [M+H]⁺, 745.1500 [M+Na]⁺ (calculated for C₄₂H₃₅⁵⁶FeO₈⁺ = 723.1676, C₄₂H₃₄⁵⁶FeO₈Na⁺ = 745.1495).

4.11.4. Complexes 111a-b



Complexes **111a-b** were prepared according to general procedure B, starting from 128 mg (0.232 mmol) of **85**. **111a** and **111b** were isolated through chromatographic column on silica gel (Et₂O/EDP 1:2) as brown solids.

Complex 111a

Yield: 9.9 mg (0.014 mmol, 6%)

R_f = 0.52 (SiO₂, EtOAc/EDP 3:7)

¹H-NMR (400 MHz, CD₂Cl₂) δ [ppm] = 7.98 (d, ³J = 9.1 Hz, 1H), 7.94 (d, ³J = 8.4 Hz, 1H), 7.88 (d, ³J = 8.1 Hz, 1H), 7.77 (s, 1H), 7.60 (d, ³J = 9.0 Hz, 1H), 7.45 – 7.39 (m, 1H), 7.35 (t, ³J = 7.1 Hz, 1H), 7.26 – 7.21 (m, 2H), 7.13 (d, ³J = 8.5 Hz, 1H), 7.07 (d, ³J = 8.5 Hz, 12H), 5.07 (s, 2H), 4.40 (d, ²J = 4.9 Hz, 1H), 4.28 (d, ²J = 5.0 Hz, 1H), 3.21 (s, 3H), 2.87 – 2.72 (m, 4H), 2.72 – 2.61 (m, 1H), 2.61 – 2.50 (m, 1H), 2.35 – 2.25 (m, 1H), 1.91 – 1.74 (m, 4H), 0.30 (s, 9H).

¹³C-NMR (100 MHz, CD₂Cl₂) δ [ppm] = 209.9 (3C), 153.3 (1C), 152.9 (1C), 135.6 (1C), 134.7 (1C), 134.6 (1C), 131.4 (1C), 130.4 (1C), 130.3 (1C), 128.6 (1C), 128.5 (1C), 127.3 (1C), 127.2 (1C), 126.4 (1C), 126.3 (1C), 126.2 (1C), 125.8 (1C), 124.7 (1C), 120.9 (1C), 118.8 (1C), 117.4 (1C), 110.1 (1C), 107.5 (1C), 99.7 (1C), 95.9 (1C), 88.7 (1C), 67.5 (1C), 56.8 (1C), 56.2 (1C), 24.8 (1C), 23.4 (1C), 23.3 (1C), 22.7 (1C), -0.1 (1C).

Complex 111b

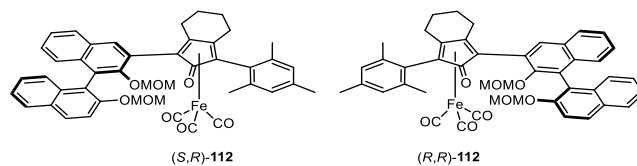
Yield: 11 mg (0.015 mmol, 7%)

R_f = 0.42 (SiO₂, EtOAc/EDP 3:7)

¹H-NMR (400 MHz, CD₂Cl₂) δ [ppm] = 8.00 (d, ³J = 9.1 Hz, 1H), 7.95 (d, ³J = 8.3 Hz, 1H), 7.91 (d, ³J = 7.9 Hz, 1H), 7.79 (s, 1H), 7.64 (d, ³J = 8.8 Hz, 1H), 7.48 – 7.42 (m, 1H), 7.41 – 7.34 (m, 1H), 7.33 – 7.25 (m, 2H), 7.20 (d, ³J = 8.6 Hz, 1H), 7.12 (d, ³J = 8.4 Hz, 1H), 5.17 (d, ²J = 7.1 Hz, 1H), 5.08 (d, ²J = 7.1 Hz, 1H), 4.61 (d, ²J = 4.7 Hz, 1H), 4.49 (d, ²J = 4.7 Hz, 1H), 3.22 (s, 3H), 2.90 (s, 3H), 2.87 – 2.49 (m, 3H), 2.38 – 2.28 (m, 1H), 1.98 – 1.60 (m, 4H), 0.32 (s, 9H).

¹³C-NMR (100 MHz, CD₂Cl₂) δ [ppm] = 209.9 (3C), 177.0 (1C), 153.8 (1C), 152.4 (1C), 135.9 (1C), 134.4 (1C), 134.2 (1C), 131.6 (1C), 130.5 (1C), 130.2 (1C), 128.7 (1C), 128.6 (1C), 127.2 (1C), 127.1 (1C), 126.7 (1C), 126.2 (1C), 125.9 (1C), 125.4 (1C), 124.6 (1C), 120.2 (1C), 116.4 (1C), 110.3 (1C), 107.6 (1C), 99.9 (1C), 95.2 (1C), 88.5 (1C), 67.5 (1C), 57.2 (1C), 56.6 (1C), 24.6 (1C), 23.5 (1C), 23.3 (1C), 22.6 (1C), -0.1 (1C).

4.11.5. Complexes 112a-b



Complexes **112a-b** were prepared according to general procedure B, starting from 112 mg (0.19 mmol) of **87**. **112a** and **112b** were isolated through chromatographic column on silica gel (Et₂O/*n*-hexane 2:3 to 3:2) as yellow solids.

Complex 112a

Yield: 45 mg (0.058 mmol, 31%)

R_f = 0.30 (SiO₂, EtOAc/EDP 1:4)

¹H-NMR (400 MHz, CD₂Cl₂) δ [ppm] = 7.99 (d, ³J = 9.2 Hz, 2H), 7.93 (s, 1H), 7.89 (d, ³J = 8.2 Hz, 1H), 7.62 (d, ³J = 9.0 Hz, 1H), 7.46 (Ψ-t, ³J = 7.4 Hz, 1H), 7.37 (Ψ-t, ³J = 7.3 Hz, 1H), 7.32 – 7.16 (m, 3H), 7.12 (d, ³J = 8.5 Hz, 1H), 6.98 (s, 1H), 6.94 (s, 1H), 5.10 (s, 2H), 4.59 (d, ²J = 4.8 Hz, 1H), 4.35 (d, ²J = 4.7 Hz, 1H), 3.23 (s, 3H), 3.04 – 2.91 (m, 1H), 2.62 (s, 3H), 2.47 – 2.35 (m, 4H), 2.34 – 2.21 (m, 5H), 2.11 (s, 3H), 2.00 – 1.73 (m, 4H).

¹³C-NMR (100 MHz, CD₂Cl₂) δ [ppm] = 210.2 (3C), 171.0 (1C), 153.7 (1C), 152.6 (1C), 138.6 (1C), 138.2 (1C), 137.2 (1C), 136.1 (1C), 131.4 (1C), 130.4 (1C), 130.3 (1C), 129.8 (1C), 128.7 (1C), 128.3 (1C), 127.3 (1C), 127.1 (1C), 126.8 (1C), 126.6 (1C), 126.5 (1C), 126.4 (1C), 125.9 (1C), 125.7 (1C), 124.7 (1C), 121.2 (1C), 117.5 (1C), 105.5 (1C), 103.0 (1C), 99.8 (1C), 96.1 (1C), 86.4 (1C), 85.6 (1C), 56.4 (1C), 56.2 (1C), 23.3 (1C), 23.2 (1C), 23.2 (1C), 23.1 (1C), 22.9 (1C), 21.4 (1C), 21.1 (1C).

IR (nujol): $\tilde{\nu}$ [cm⁻¹] = 2060.8 (s, Fe(CO)₃), 2008.4 (s, Fe(CO)₃), 1987.5 (s, Fe(CO)₃), 1644.0 (br, C=O), 1240.5 (w), 1151.4 (m), 1084.4 (w), 1035.9 (w), 1014.8 (w), 969.9 (w), 925.6 (w), 721.5 (m).

HRMS (ESI⁺): m/z 765.2145 [M+H]⁺, 787.1967 [M+Na]⁺ (calculated for C₄₅H₄₁⁵⁶FeO₈⁺ = 765.2145, C₄₅H₄₀⁵⁶FeO₈Na⁺ = 787.1965).

Complex 112b

Yield: 32 mg (0.041 mmol, 22%)

R_f = 0.16 (SiO₂, EtOAc/EDP 1:4)

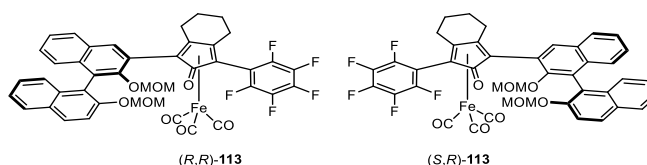
$^1\text{H-NMR}$ (400 MHz, CD_2Cl_2) δ [ppm] = 8.01 (d, $^3J = 9.2$ Hz, 1H), 7.98 (d, $^3J = 8.4$ Hz, 1H), 7.93 (s, 1H), 7.91 (d, $^3J = 8.2$ Hz, 1H), 7.67 (d, $^3J = 9.1$ Hz, 1H), 7.52 – 7.43 (m, 1H), 7.38 (Ψ -t, $^3J = 7.0$ Hz, 1H), 7.35 – 7.26 (m, 3H), 7.21 (d, $^3J = 8.4$ Hz, 1H), 6.98 (s, 1H), 6.95 (s, 1H), 5.16 (d, $^2J = 7.2$ Hz, 1H), 5.11 (d, $^2J = 7.2$ Hz, 1H), 4.70 (d, $^2J = 4.7$ Hz, 1H), 4.51 (d, $^2J = 4.7$ Hz, 1H), 3.26 (s, 3H), 2.97 – 2.84 (m, 1H), 2.63 (s, 3H), 2.54 – 2.41 (m, 4H), 2.35 – 2.21 (m, 5H), 2.11 (s, 3H), 2.05 – 1.84 (m, 2H), 1.84 – 1.65 (m, 2H).

$^{13}\text{C-NMR}$ (100 MHz, CD_2Cl_2) δ [ppm] = 210.2 (3C), 171.2 (1C), 154.1 (1C), 152.1 (1C), 138.5 (1C), 138.2 (1C), 137.3 (1C), 136.1 (1C), 134.5 (1C), 134.4 (1C), 131.5 (1C), 130.5 (1C), 130.3 (1C), 130.1 (1C), 129.8 (1C), 128.7 (1C), 128.6 (1C), 127.3 (1C), 127.1 (1C), 126.8 (1C), 126.5 (1C), 126.1 (1C), 126.0 (1C), 125.8 (1C), 125.4 (1C), 124.4 (1C), 120.1 (1C), 116.3 (1C), 105.9 (1C), 102.7 (1C), 99.9 (t, 1C), 95.2 (1C), 86.2 (1C), 85.7 (1C), 56.7 (1C), 56.6 (1C), 23.3 (1C), 23.3 (t, 1C), 23.1 (1C), 23.1 (1C), 22.9 (1C), 21.4 (1C), 21.1 (1C).

IR (nujol): $\tilde{\nu}$ [cm^{-1}] = 2060.6 (s, $\text{Fe}(\text{CO})_3$), 2004.0 (s, $\text{Fe}(\text{CO})_3$), 1989.5 (s, $\text{Fe}(\text{CO})_3$), 1642.6 (br, C=O), 1241.6 (w), 1148.3 (m), 1032.7 (w), 1012.2 (w), 963.6 (w), 925.6 (w), 721.4 (m).

HRMS (ESI+): m/z 765.2144 [$\text{M}+\text{H}$] $^+$, 787.1966 [$\text{M}+\text{Na}$] $^+$ (calculated for $\text{C}_{45}\text{H}_{41}^{56}\text{FeO}_8^+$ = 765.2145, $\text{C}_{45}\text{H}_{40}^{56}\text{FeO}_8\text{Na}^+$ = 787.1965).

4.11.6. Complexes 113a-b



Complexes **113a-b** were prepared according to general procedure B, starting from 95 mg (0.147 mmol) of **88**. **113a** and **113b** were isolated through chromatographic column on silica gel ($\text{Et}_2\text{O}/n$ -hexane 35:65) as yellow solids.

Complex 113a

Yield: 51 mg (0.063 mmol, 43%)

R_f = 0.32 (SiO_2 , $\text{Et}_2\text{O}/n$ -hexane 2:3)

$^1\text{H-NMR}$ (400 MHz, CD_2Cl_2) δ [ppm] = 8.04 – 7.96 (m, 2H), 7.93 – 7.85 (m, 2H), 7.63 (d, $^3J = 9.1$ Hz, 1H), 7.51 – 7.43 (m, 1H), 7.40 – 7.33 (m, 1H), 7.33 – 7.21 (m, 2H), 7.20 – 7.10 (m, 2H), 5.17 – 5.07

(m, 2H), 4.41 (d, $^2J = 5.2$ Hz, 1H), 4.37 (d, $^2J = 5.2$ Hz, 1H), 3.25 (s, 3H), 2.97 – 2.87 (m, 1H), 2.84 (s, 3H), 2.72 – 2.59 (m, 1H), 2.50 – 2.34 (m, 2H), 2.08 – 1.73 (m, 4H).

$^{13}\text{C-NMR}$ (100 MHz, CD_2Cl_2) δ [ppm] = 208.7 (3C), 169.8 (1C), 153.5 (1C), 153.2 (1C), 144.0 – 140.0 (m, 1C), 140.0 – 136.5 (m, 2C), 135.5 (1C), 134.8 (1C), 134.6 (1C), 131.4 (1C), 130.6 (1C), 130.3 (1C), 128.7 (1C), 128.5 (1C), 127.5 (1C), 127.3 (1C), 126.6 (1C), 126.3 (1C), 126.2 (1C), 126.0 (1C), 125.0 (1C), 124.8 (1C), 120.6 (1C), 117.2 (1C), 107.7 (1C), 106.6 (m, 1C), 101.4 (1C), 100.0 (1C), 95.8 (1C), 86.7 (1C), 67.2 (1C), 56.9 (1C), 56.2 (1C), 23.3 (1C), 22.9 (1C), 22.7 (1C), 22.2 (1C).

$^{19}\text{F-NMR}$ (377 MHz, CD_2Cl_2) δ [ppm] = -133.78 (br s, 1F), -137.62 (br s, 1F), -153.81 (t, $^3J = 20.7$ Hz), -161.58 (br s, 1F), -162.72 (br s, 1F).

IR (nujol): $\tilde{\nu}$ [cm^{-1}] = 2060.7 (s, $\text{Fe}(\text{CO})_3$), 2010 (s, $\text{Fe}(\text{CO})_3$), 1996.3 (s, $\text{Fe}(\text{CO})_3$), 1648.2 (br, C=O), 1525.6 (m), 1241.2 (w), 1150.9 (s), 1077.4 (m), 1034.6 (w), 1012.8 (m), 988.7 (m), 967.3 (m), 721.2 (m).

HRMS (ESI+): m/z 813.1205 $[\text{M}+\text{H}]^+$, 835.1029 $[\text{M}+\text{Na}]^+$ (calculated for $\text{C}_{42}\text{H}_{30}\text{F}_5^{56}\text{FeO}_8^+$ = 813.1205, $\text{C}_{42}\text{H}_{29}\text{F}_5^{56}\text{FeO}_8\text{Na}^+$ = 835.1024).

Complex 113b

Yield: 40.6 mg (0.050 mmol, 34%)

$R_f = 0.25$ (SiO_2 , $\text{Et}_2\text{O}/n$ -hexane 2:3)

$^1\text{H-NMR}$ (400 MHz, CD_2Cl_2) δ [ppm] = 8.05 – 7.96 (m, 2H), 7.95 – 7.86 (m, 2H), 7.66 (d, $^3J = 9.1$ Hz, 1H), 7.52 – 7.43 (m, 1H), 7.43 – 7.36 (m, 1H), 7.36 – 7.27 (m, 2H), 7.22 (d, $^3J = 8.5$ Hz, 1H), 7.13 (d, $^3J = 8.5$ Hz, 1H), 5.17 (d, $^2J = 7.1$ Hz, 1H), 5.08 (d, $^2J = 7.1$ Hz, 1H), 4.61 (d, $^2J = 5.1$ Hz, 1H), 4.50 (d, $^2J = 5.1$ Hz, 1H), 3.23 (s, 3H), 3.00 – 2.79 (m, 1H), 2.95 (s, 3H), 2.69 – 2.57 (m, 1H), 2.52 – 2.32 (m, 2H), 2.05 – 1.77 (m, 4H).

$^{13}\text{C-NMR}$ (100 MHz, CD_2Cl_2) δ [ppm] = 208.7 (3C), 169.9 (1C), 153.8 (1C), 152.7 (1C), 143.6 – 140.3 (m, 1C), 140.3 – 136.7 (m, 2C), 135.8 (1C), 134.7 (1C), 134.2 (1C), 131.5 (1C), 130.7 (1C), 130.2 (1C), 128.8 (1C), 128.7 (1C), 127.6 (1C), 127.2 (1C), 126.9 (1C), 126.1 (1C), 126.0 (1C), 125.3 (1C), 125.0 (1C), 124.6 (1C), 120.0 (1C), 116.5 (1C), 108.0 (1C), 106.6 (m, 1C), 101.5 (1C), 100.1 (1C), 95.2 (1C), 86.3 (1C), 57.2 (1C), 56.6 (1C), 23.2 (1C), 22.9 (1C), 22.7 (1C), 22.2 (1C).

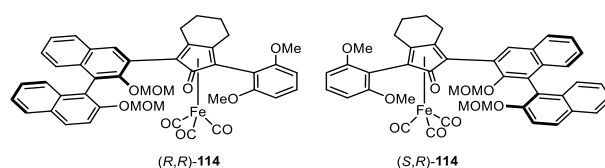
$^{19}\text{F-NMR}$ (377 MHz, CD_2Cl_2) δ [ppm] = -133.70 (br s, 1F), -137.61 (br s, 1F), -153.80 (t, $^3J = 21.0$ Hz), -161.53 (br s, 1F), -162.63 (br s, 1F).

IR (nujol): $\tilde{\nu}$ [cm^{-1}] = 2071.4 (s, $\text{Fe}(\text{CO})_3$), 2021.1 (s, $\text{Fe}(\text{CO})_3$), 1995.6 (s, $\text{Fe}(\text{CO})_3$), 1651.4 (br, C=O), 1592.4 (m), 1524.7 (s), 1493.2 (s), 1258.4 (w), 1241.5 (m), 1198.7 (w), 1148.1 (s), 1097.2 (m),

1077.8 (s), 1033.6 (s), 1012.8 (s), 989.1 (s), 967.4 (s), 921.6 (m), 811.2 (m), 802.1 (m), 746.7 (s), 721.8 (w), 666.61 (w).

HRMS (ESI+): m/z 813.1204 $[M+H]^+$, 835.1028 $[M+Na]^+$ (calculated for $C_{42}H_{30}F_5^{56}FeO_8^+$ = 813.1205, $C_{42}H_{29}F_5^{56}FeO_8Na^+$ = 835.1024).

4.11.7. Complexes 114a-b



Complexes **114a-b** were prepared according to general procedure B, starting from 145 mg (0.236 mmol) of **89**. **114a** and **114b** were isolated through chromatographic column on silica gel (Et_2O/n -hexane 4:1 to 100% Et_2O).

Complex 114a

Yellow solid.

Yield: 61 mg (0.076 mmol, 32%)

R_f = 0.30 (SiO_2 , $EtOAc/n$ -hexane 1:1)

1H -NMR (400 MHz, CD_2Cl_2) δ [ppm] = 8.02 – 7.96 (m, 2H), 7.92 (s, 1H), 7.88 (d, 3J = 8.1 Hz, 1H), 7.63 (d, 3J = 9.1 Hz, 1H), 7.48 – 7.41 (m, 1H), 7.39 – 7.30 (m, 2H), 7.30 – 7.21 (m, 2H), 7.21 – 7.15 (m, 1H), 7.12 (d, 3J = 8.2 Hz, 1H), 6.69 (d, 3J = 8.1 Hz, 1H), 6.61 (d, 3J = 8.1 Hz, 1H), 5.11 (s, 2H), 4.58 (d, 2J = 4.9 Hz, 1H), 4.39 (d, 2J = 4.9 Hz, 1H), 3.94 (s, 3H), 3.68 (s, 3H), 3.25 (s, 3H), 2.98 – 2.84 (m, 1H), 2.59 (s, 3H), 2.52 – 2.42 (m, 1H), 2.37 (ddd, 3J = 12.1 Hz, 3J = 2J = 5.8 Hz, 1H), 2.27 (ddd, 3J = 16.6 Hz, 3J = 2J = 5.2 Hz, 1H), 1.92 – 1.73 (m, 4H).

^{13}C -NMR (100 MHz, CD_2Cl_2) δ [ppm] = 210.4 (3C), 171.0 (1C), 159.7 (1C), 157.7 (1C), 153.6 (1C), 152.8 (1C), 136.1 (1C), 134.8 (1C), 134.6 (1C), 131.5 (1C), 130.4 (1C), 130.3 (1C), 130.3 (1C), 128.7 (1C), 128.3 (1C), 127.2 (1C), 127.1 (1C), 126.6 (1C), 126.5 (1C), 126.4 (1C), 126.3 (1C), 125.7 (1C), 124.7 (1C), 121.2 (1C), 117.5 (1C), 107.5 (1C), 104.8 (1C), 104.7 (1C), 104.1 (1C), 104.1 (1C), 99.7 (1C), 95.9 (1C), 86.3 (1C), 75.6 (1C), 56.6 (1C), 56.2 (1C), 56.2 (1C), 55.5 (1C), 23.2 (1C), 23.0 (2C), 22.5 (1C).

IR (nujol): $\tilde{\nu}$ [cm⁻¹] = 2059.7 (s, Fe(CO)₃), 2012.3 (m, Fe(CO)₃), 1988.7 (s, Fe(CO)₃), 1655.0 (s, C=O), 1593.0 (m), 1251.0 (m), 1149.4 (m), 1109.2 (m), 1030.5 (w), 1005.5 (m), 721.7 (m).

MS (ESI+): m/z = 783.50 [M+H⁺], 805.23 [M+Na⁺] (calculated for C₄₄H₃₉FeO₁₀ = 783.19, C₄₄H₃₈FeO₁₀Na = 805.17).

HRMS (ESI+): m/z 783.1885 [M+H⁺], 805.1707 [M+Na⁺] (calculated for C₄₄H₃₉⁵⁶FeO₁₀⁺ = 783.1887, C₄₄H₃₈⁵⁶FeO₁₀Na⁺ = 805.1707).

Complex 114b

Pale-yellow solid.

Yield: 46 mg (0.058 mmol, 25%)

R_f = 0.12 (SiO₂, EtOAc/*n*-hexane 1:1)

¹H-NMR (400 MHz, CD₂Cl₂) δ [ppm] = 8.04 – 7.96 (m, 2H), 7.93 (s, 1H), 7.91 (d, ³J = 8.2 Hz, 1H), 7.66 (d, ³J = 9.1 Hz, 1H), 7.50 – 7.42 (m, 1H), 7.42 – 7.27 (m, 4H), 7.24 (d, ³J = 8.3 Hz, 1H), 7.19 (d, ³J = 8.4 Hz, 1H), 6.70 (d, ³J = 8.4 Hz, 1H), 6.62 (d, ³J = 8.3 Hz, 1H), 5.17 (d, ²J = 7.2 Hz, 1H), 5.09 (d, ²J = 7.2 Hz, 1H), 4.68 (d, ²J = 4.7 Hz, 1H), 4.58 (d, ²J = 4.7 Hz, 1H), 3.95 (s, 3H), 3.70 (s, 3H), 3.25 (s, 3H), 2.86 (ddd, ³J = 17.4 Hz, ³J = ²J = 6.3 Hz, 1H), 2.79 (s, 3H), 2.54 – 2.35 (m, 2H), 2.26 (ddd, ³J = 17.2 Hz, ³J = ²J = 6.3 Hz, 1H), 1.95 – 1.74 (m, 4H).

¹³C-NMR (100 MHz, CD₂Cl₂) δ [ppm] = 210.4 (3C), 171.1 (1C), 159.6 (1C), 157.7 (1C), 153.9 (1C), 152.3 (1C), 136.3 (1C), 134.4 (1C), 134.4 (1C), 131.6 (1C), 130.4 (2C), 130.1 (1C), 128.7 (1C), 128.6 (1C), 127.1 (1C), 127.1 (1C), 126.8 (1C), 126.4 (1C), 126.0 (1C), 125.8 (1C), 125.5 (1C), 124.4 (1C), 120.3 (1C), 116.4 (1C), 107.4 (1C), 105.3 (1C), 104.8 (1C), 104.0 (1C), 103.9 (1C), 99.9 (1C), 95.2 (1C), 86.0 (1C), 75.6 (1C), 57.0 (1C), 56.6 (1C), 56.2 (1C), 55.5 (1C), 23.1 (1C), 23.1 (1C), 23.0 (1C), 22.6 (1C).

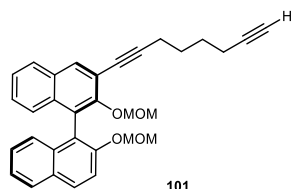
IR (nujol): $\tilde{\nu}$ [cm⁻¹] = 2060.7 (s, Fe(CO)₃), 2000.4 (s, Fe(CO)₃), 1991.4 (s, Fe(CO)₃), 1733.1 (w), 1636.0 (s, C=O), 1253.8 (s), 1244.9 (m), 1162.0 (m), 1150.3 (m), 1106.2 (s), 1058.6 (w), 1031.8 (w), 1012.9 (s), 989.8 (w), 964.9 (m), 932.7 (w), 721.0 (m).

MS (ESI+): m/z = 783.28 [M+H⁺], 805.21 [M+Na⁺] (calculated for C₄₄H₃₉FeO₁₀ = 783.19, C₄₄H₃₈FeO₁₀Na = 805.17).

HRMS (ESI+): m/z 783.1885 [M+H⁺], 805.1708 [M+Na⁺] (calculated for C₄₄H₃₉⁵⁶FeO₁₀⁺ = 783.1887, C₄₄H₃₈⁵⁶FeO₁₀Na⁺ = 805.1707).

4.12. Synthesis of Iron Complexes 115a-b

4.12.1. (*R*)-2,2'-bis(methoxymethoxy)-3-(octa-1,7-diyn-1-yl)-1,1'-binaphthalene (**101**)



Iodide **82** (145 mg, 0.26 mmol, 1 eq) was dissolved in a 1:1 mixture of THF (1.3 mL) and MeOH (1.3 mL). K_2CO_3 (363 mg, 2.62 mmol, 10 eq) was added. The reaction was left under stirring at rt for 4 hours. Volatiles were removed under reduced pressure. The residue was suspended in DCM (5 mL) and filtered. Product **101** was isolated as a yellowish oil and used without further purification.

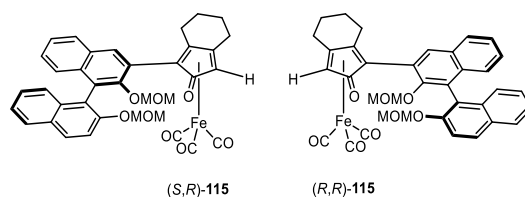
Yield: 127 mg (0.26 mmol, 99%)

R_f = 0.51 (SiO_2 , EtOAc/EDP 15:85)

1H -NMR (400 MHz, $CDCl_3$) δ [ppm] = 8.08 (s, 1H), 7.95 (d, 3J = 9.0 Hz, 1H), 7.85 (d, 3J = 8.2 Hz, 1H), 7.81 (d, 3J = 8.2 Hz, 1H), 7.57 (d, 3J = 9.0 Hz, 1H), 7.43 – 7.30 (m, 2H), 7.30 – 7.11 (m, 4H), 5.14 (d, 2J = 6.9 Hz, 1H), 5.02 – 4.94 (m, 2H), 4.87 (d, 2J = 5.7 Hz, 1H), 3.16 (s, 3H), 2.58 (s, 3H), 2.53 (t, 3J = 6.6 Hz, 2H), 2.27 (td, 3J = 6.5 Hz, 4J = 2.6 Hz, 2H), 1.96 (t, 4J = 2.6 Hz, 1H), 1.85 – 1.68 (m, 4H).

^{13}C -NMR (100 MHz, $CDCl_3$) δ [ppm] = 153.1 (1C), 152.9 (1C), 134.2 (1C), 133.9 (1C), 133.5 (1C), 130.6 (1C), 129.8 (1C), 129.8 (1C), 127.9 (1C), 127.6 (1C), 126.8 (1C), 126.7 (1C), 126.2 (1C), 126.1 (1C), 125.9 (1C), 125.9 (1C), 125.4 (1C), 124.2 (1C), 120.8 (1C), 118.2 (1C), 116.9 (1C), 98.7 (1C), 95.2 (1C), 94.1 (1C), 84.2 (1C), 78.2 (1C), 68.7 (1C), 56.2 (1C), 56.0 (1C), 27.8 (2C), 19.5 (1C), 18.2 (1C).

4.12.2. Complexes 115a-b



Complexes **115a-b** were prepared according to general procedure B, starting from 60 mg (0.125 mmol) of **101**. **115a** and **115b** were isolated through chromatographic column on silica gel (EtOAc/*n*-hexane 7:3 to 4:1) as yellow solids.

Complex 115a

Yield: 4 mg (0.006 mmol, 5%)

R_f = 0.29 (SiO₂, EtOAc/EDP 7:3)

¹H-NMR (400 MHz, CD₂Cl₂) δ [ppm] = 8.02 – 7.92 (m, 2H), 7.89 (d, ³J = 8.1 Hz, 1H), 7.81 (s, 1H), 7.61 (d, ³J = 9.1 Hz, 1H), 7.44 (t, ³J = 7.4 Hz, 1H), 7.40 – 7.32 (m, 1H), 7.30 – 7.20 (m, 2H), 7.19 – 7.06 (m, 2H), 5.15 – 5.03 (m, 2H), 4.46 (br s, 1H), 4.32 (br s, 1H), 3.97 (br s, 1H), 3.22 (s, 3H), 2.88 – 2.74 (m, 1H), 2.68 (s, 3H), 2.65 – 2.49 (m, 2H), 2.39 – 2.21 (m, 1H), 1.95 – 1.75 (m, 3H).

¹³C-NMR could not be recorded.

IR (nujol): $\tilde{\nu}$ [cm⁻¹] = 2065.3 (s, Fe(CO)₃), 2008.4 (s, Fe(CO)₃), 1995.5 (s, Fe(CO)₃), 1648.4 (s, C=O), 1264.4 (w), 1242.2 (w), 1150.6 (m), 1033.3 (w), 1014.3 (w), 721.0 (m).

LC-MS (ESI+): m/z = 564.09 [M-(CO)₃]⁺, 592.08 [M-(CO)₂]⁺, 605.35 [M-C₂H₅O]⁺, 616.25 [M-CO]⁺, 646.42 [M]⁺, 670.46 [M+Na]⁺ (calculated for C₃₆H₃₀FeO₈ = 646.13).

Complex 115b

Yield: 2.5 mg (0.004 mmol, 3%)

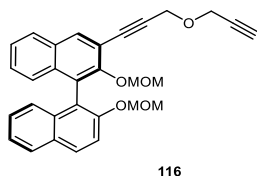
R_f = 0.14 (SiO₂, EtOAc/EDP 7:3)

¹H-NMR (400 MHz, CD₂Cl₂) δ [ppm] = 8.05 – 7.85 (m, 2H), 7.83 (s, 1H), 7.68 – 7.18 (m, 7H), 7.12 (d, ³J = 8.5 Hz, 1H), 5.17 (d, ²J = 7.1 Hz, 1H), 5.08 (d, ²J = 7.2 Hz, 1H), 4.63 (d, ²J = 5.0 Hz, 1H), 4.48 (d, ²J = 5.0 Hz, 1H), 3.97 (s, 1H), 3.23 (s, 3H), 2.83 (s, 3H), 2.80 – 2.67 (m, 1H), 2.66 – 2.51 (m, 2H), 2.43 – 2.29 (m, 1H), 1.92 – 1.76 (m, 4H).

¹³C-NMR could not be recorded.

4.13. Synthesis of Iron Complexes 117a-b

4.13.1. (*R*)-2,2'-bis(methoxymethoxy)-3-(3-(prop-2-yn-1-yloxy)prop-1-yn-1-yl)-1,1'-binaphthalene (116)



NaH (60% suspension in mineral oil, 16.6 mg, 0.693 mmol, 1.5 eq) was suspended in dry THF (3 mL). **96** (198 mg, 0.462 mmol, 1 eq) was dissolved in dry THF (1.6 mL). The solution of **96** was slowly added to the suspension of NaH under argon atmosphere at 0 °C. The mixture was left under stirring at room temperature for 0.5 hours. The reaction was cooled again to 0 °C and propargyl bromide (80% in toluene, 77 μ L, 82.5 mg, 0.693 mmol, 1.5 eq) was added. The mixture was stirred at room temperature for 3 hours. The reaction was quenched with sat. aq. NH₄Cl (10 mL). The crude was extracted with EtOAc (3 x 10 mL). The collected organic layers were washed with brine, dried over Na₂SO₄, filtered, and concentrated under reduced pressure. The product was purified through chromatographic column on silica gel (EtOAc/*n*-hexane 1:9 to 1:4). **116** was isolated as a thick yellowish oil.

Yield: 188 mg (0.40 mmol, 87%)

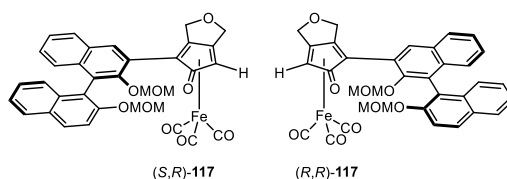
R_f = 0.56 (SiO₂, EtOAc/EDP 1:4)

¹H-NMR (400 MHz, CDCl₃) δ [ppm] = 8.14 (s, 1H), 7.96 (d, ³J = 9.1 Hz, 1H), 7.89 – 7.80 (m, 2H), 7.58 (d, ³J = 9.1 Hz, 1H), 7.48 – 7.31 (m, 2H), 7.31 – 7.20 (m, 2H), 7.20 – 7.13 (m, 2H), 5.14 (d, ²J = 6.9 Hz, 1H), 5.00 (d, ²J = 6.9 Hz, 1H), 4.93 (d, ²J = 5.7 Hz, 1H), 4.82 (d, ²J = 5.7 Hz, 1H), 4.57 (s, 2H), 4.37 (d, ⁴J = 2.3 Hz, 2H), 3.16 (s, 3H), 2.66 (s, 3H), 2.47 (t, ⁴J = 2.3 Hz, 1H).

¹³C-NMR (100 MHz, CDCl₃) δ [ppm] = 153.1 (1C), 152.9 (1C), 134.5 (1C), 134.1 (1C), 134.1 (1C), 130.5 (1C), 130.0 (1C), 129.8 (1C), 127.9 (1C), 127.9 (1C), 127.3 (1C), 126.8 (1C), 126.4 (1C), 126.2 (1C), 125.8 (1C), 125.6 (1C), 124.3 (1C), 120.4 (1C), 116.9 (1C), 116.7 (1C), 99.0 (1C), 95.2 (1C), 88.2 (1C), 84.3 (1C), 79.1 (1C), 75.2 (1C), 57.6 (1C), 56.7 (1C), 56.4 (1C), 56.1 (1C).

HRMS (ESI⁺): m/z 489.1676 [M+Na]⁺ (calculated for C₃₀H₂₆O₅Na⁺ = 489.1672).

4.13.2. Complexes 117a-b



Complexes **117a-b** were prepared according to general procedure B, starting from 74 mg (0.158 mmol) of **116**. **117a** and **117b** were isolated through chromatographic column on silica gel (EtOAc/*n*-hexane 7:3 to 4:1) as yellow solids.

Complex 117a

Yield: 18.7 mg (0.029 mmol, 19%)

R_f = 0.37 (SiO₂, EtOAc/*n*-hexane 7:3)

¹H-NMR (400 MHz, CD₂Cl₂) δ [ppm] = 8.39 (s, 1H), 8.03 – 7.94 (m, 2H), 7.90 (d, ³J = 8.1 Hz, 1H), 7.61 (d, ³J = 9.1 Hz, 1H), 7.44 (Ψ-t, ³J = 7.5 Hz, 1H), 7.37 (Ψ-t, ³J = 7.4 Hz, 1H), 7.29 – 7.22 (m, 2H), 7.13 (d, ³J = 8.4 Hz, 1H), 7.09 (d, ³J = 8.5 Hz, 1H), 5.10 – 5.02 (m, 3H), 4.80 (d, ²J = 13.4 Hz, 1H), 4.76 (s, 2H), 4.47 (d, ²J = 4.9 Hz, 1H), 4.35 (s, 1H), 4.23 (d, ²J = 4.9 Hz, 1H), 3.21 (s, 3H), 2.59 (s, 3H).

¹³C-NMR (100 MHz, CD₂Cl₂) δ [ppm] = 208.5 (3C), 173.1 (1C), 153.8 (1C), 151.3 (1C), 134.9 (1C), 134.7 (1C), 134.6 (1C), 134.3 (1C), 131.3 (1C), 130.6 (1C), 130.3 (1C), 128.9 (1C), 128.6 (1C), 127.6 (1C), 127.3 (1C), 126.3 (1C), 126.2 (1C), 126.1 (1C), 124.7 (1C), 124.5 (1C), 120.6 (1C), 117.6 (1C), 107.4 (1C), 103.9 (1C), 99.8 (1C), 95.9 (1C), 80.1 (1C), 69.9 (1C), 67.8 (1C), 57.4 (1C), 57.2 (1C), 56.2 (1C).

MS (ESI⁺): m/z = 635.29 [M+H⁺], 657.13 [M+Na⁺], 1290.27 (calculated for C₃₄H₂₇FeO₉ = 635.10, C₃₄H₂₆FeO₉Na = 657.08).

HRMS (ESI⁺): m/z 635.0999 [M+H]⁺, 657.0823 [M+Na]⁺ (calculated for C₃₄H₂₇⁵⁶FeO₉⁺ = 635.0999, C₃₄H₂₆⁵⁶FeO₉Na⁺ = 657.0818).

Complex 117b

Pale-yellow solid.

Yield: 15.1 mg (0.024 mmol, 15%)

R_f = 0.24 (SiO₂, EtOAc/*n*-hexane 7:3)

$^1\text{H-NMR}$ (400 MHz, CD_2Cl_2) δ [ppm] = 8.41 (s, 1H), 8.01 (d, $^3J = 8.7$ Hz, 1H), 7.97 (d, $^3J = 8.2$ Hz, 1H), 7.90 (d, $^3J = 8.1$ Hz, 1H), 7.65 (d, $^3J = 8.6$ Hz, 1H), 7.45 (Ψ -t, $^3J = 7.3$ Hz, 1H), 7.38 (Ψ -t, $^3J = 7.1$ Hz, 1H), 7.34 – 7.21 (m, 3H), 7.13 (d, $^3J = 8.5$ Hz, 1H), 5.20 – 5.08 (m, 2H), 4.97 (d, $^2J = 13.6$ Hz, 1H), 4.76 (d, $^2J = 13.7$ Hz, 1H), 4.74 (s, 2H), 4.67 (d, $^2J = 4.9$ Hz, 1H), 4.42 (d, $^2J = 4.9$ Hz, 1H), 4.36 (s, 1H), 3.24 (s, 3H), 2.73 (s, 3H).

$^{13}\text{C-NMR}$ (100 MHz, CD_2Cl_2) δ [ppm] = 208.6 (3C), 173.1 (1C), 153.7 (1C), 151.1 (1C), 134.9 (1C), 134.2 (1C), 134.1 (1C), 130.8 (1C), 130.2 (1C), 128.9 (1C), 128.6 (1C), 127.5 (1C), 127.3 (1C), 126.4 (1C), 126.2 (1C), 126.0 (1C), 125.2 (1C), 124.7 (1C), 124.5 (1C), 119.8 (1C), 116.1 (1C), 107.7 (1C), 103.9 (1C), 100.1 (1C), 95.2 (1C), 79.9 (1C), 69.9 (1C), 67.8 (1C), 57.5 (1C), 57.4 (1C), 56.7 (1C).

MS (ESI+): $m/z = 635.25$ [$\text{M}+\text{H}^+$], 657.11 [$\text{M}+\text{Na}^+$], 1290.31 (calculated for $\text{C}_{34}\text{H}_{27}\text{FeO}_9 = 635.10$, $\text{C}_{34}\text{H}_{26}\text{FeO}_9\text{Na} = 657.08$).

HRMS (ESI+): m/z 635.1002 [$\text{M}+\text{H}^+$], 657.0824 [$\text{M}+\text{Na}^+$] (calculated for $\text{C}_{34}\text{H}_{27}^{56}\text{FeO}_9^+ = 635.0999$, $\text{C}_{34}\text{H}_{26}^{56}\text{FeO}_9\text{Na}^+ = 657.0818$).

4.14. AH and ATH tests

4.14.1. General Procedure for AH of Acetophenone

The (cyclopentadienone)iron tricarbonyl pre-catalyst (0.010 mmol, 0.02 eq) was weighted in a 3 mL glass vial. A magnetic stirring bar was added, and the vial was charged in an autoclave. The system was purged with argon and the reaction solvent (0.35 mL) was added. Me_3NO (1.5 mg, 0.020 mmol, 0.04 eq) was added and the mixture was stirred for 5 minutes under argon (when water was used as cosolvent, 0.15 mL of a 0.2 M stock solution of Me_3NO were added instead). Acetophenone (58 μL , 60 mg, 0.497 mmol, 1 eq) was added. The autoclave was sealed and, after purging 2 times with hydrogen, it was charged with H_2 (30 bar). The reaction was heated to 70 $^\circ\text{C}$ for 18 h. After 18 h the reaction was allowed to cool to rt. Hydrogen was removed, and the reaction mixture was filtered through celite, rinsing with AcOEt/EDP 1:1. Conversion was evaluated through $^1\text{H-NMR}$ analysis and chiral GC analysis. Enantiomeric excesses were evaluated through GC analysis with a chiral column.

4.14.2. General Procedure for ATH of Acetophenone

The (cyclopentadienone)iron tricarbonyl pre-catalyst (0.010 mmol, 0.02 eq) was dissolved in the reaction solvent (0.35 mL) in a 10 mL Schlenk tube under argon atmosphere. Me₃NO (1.5 mg, 0.020 mmol, 0.04 eq) was added and the mixture was stirred for 5 minutes under argon (when water was used as cosolvent, 0.15 mL of a 0.2 M stock solution of Me₃NO were added instead). Acetophenone (58 μL, 60 mg, 0.497 mmol, 1 eq) was added and the tube was sealed. The reaction was heated to 70 °C for 18 h. After 18 h the reaction was allowed to cool to rt, and the reaction mixture was filtered through celite, rinsing with AcOEt/EDP 1:1. Conversion was evaluated through ¹H-NMR analysis and chiral GC analysis. Enantiomeric excesses were evaluated through GC analysis with a chiral column.

4.14.3. Conditions for the Determination of Conversion and ee Values

Conversion of acetophenone to 1-phenylethanol was determined by ¹H-NMR analysis of the crude reaction mixture through comparison of the areas of the peaks corresponding to the CH₃ groups of acetophenone (s, 2.61 ppm) and of 1-phenylethanol (d, 1.51 ppm).

Conversions and ee values were determined through GC analysis with a chiral MEGADEx DACTBSβ column (diacetyl-*tert*-butylsilyl-β-cyclodextrin 0.25 μm; diameter = 0.25 mm; length = 25 m); carrier gas: hydrogen; inlet pressure: 1 bar; oven temperature: 95 °C for 20 min. τ_R(substrate) = 6.0 min; τ_R[(*R*)-1-phenylethanol] = 13.2 min; τ_R[(*S*)-1-phenylethanol] = 15.1 min. The absolute configuration of the two enantiomers of the product were determined through comparison with literature data.^[206]

All GC analyses were performed by Tommaso Gandini at the University of Milano.

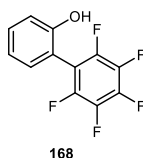
4.14.4. Hydrogenation of *N*-(4-methoxyphenyl)-1-phenylethan-1-imine

The (cyclopentadienone)iron tricarbonyl pre-catalyst (0.010 mmol, 0.02 eq) was weighed in a 3 mL glass vial. A magnetic stirring bar was added, and the vial was charged in an autoclave. The system was purged with argon and *i*PrOH (0.25 mL) was added. Me₃NO (1.5 mg, 0.020 mmol, 0.04 eq) was added and the mixture was stirred for 5 minutes under argon (a change in color was generally observed). *N*-(4-methoxyphenyl)-1-phenylethan-1-imine (113 mg, 0.500 mmol, 1 eq) was added. The autoclave was sealed and, after purging 2 times with hydrogen, it was charged with H₂ (30 bar). The reaction was heated to 70 °C for 18 h. After 18 h the reaction was

allowed to cool to rt. Hydrogen was removed, and the reaction mixture was filtered through celite, rinsing with DCM. Conversion was determined through $^1\text{H-NMR}$ analysis of the reaction crude, by comparing the areas of the peaks corresponding to the CH_3 groups of *N*-(4-methoxyphenyl)-1-phenylethan-1-imine (s, 2.26 ppm) and 4-methoxy-*N*-(1-phenylethyl)aniline (d, 1.54 ppm). Enantiomeric excesses were evaluated through HPLC analysis with a chiral Chiralpak AD-H column (0.8 mL/min, 97:3 hexane/*i*PrOH, $\lambda = 210$). $\tau_{\text{R}}(\text{R}) = 11.79$ min (major), $\tau_{\text{R}}(\text{S}) = 13.40$ min.

4.15. Synthesis of Titanium Complex 138

4.15.1. 2',3',4',5',6'-pentafluoro-[1,1'-biphenyl]-2-ol (168)



2-Hydroxyphenylboronic acid (8.01 g, 58.1 mmol, 1.2 eq), K_2CO_3 (12.23 g, 88.5 mmol, 1.8 eq) and $\text{Pd}(\text{PPh}_3)_4$ (554 mg, 0.478 mmol, 0.01 eq) were dissolved/suspended in a 1:1 mixture of dry ethanol (70 mL) and dry toluene (70 mL) under argon atmosphere. Bromopentafluorobenzene (6.1 mL, 12.1 g, 48.9 mmol, 1 eq) was added and argon was bubbled into the mixture for 5 minutes. The reaction was heated to reflux for 48 hours. After cooling to rt, ethanol was removed under reduced pressure and 2 M HCl (100 mL) was added. The crude was extracted with Et_2O (3 x 80 mL). The collected organic layers were washed with brine, dried over MgSO_4 , filtered, and concentrated under reduced pressure. The product was purified through chromatographic column on silica gel ($\text{EtOAc}/c\text{-hexane}$ 1:9), followed by recrystallization from cyclohexane. **168** was isolated as a white solid.

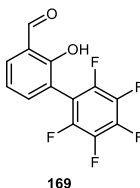
Yield: 4.64 g (17.8 mmol, 36%)

Characterization data are in agreement with the literature.^[177]

$R_f = 0.20$ (SiO_2 , $\text{EtOAc}/c\text{-hexane}$ 1:9)

$^1\text{H-NMR}$ (500 MHz, CDCl_3) δ [ppm] = 7.37 (td, $^3J = 8.1$ Hz, $^4J = 1.7$ Hz, 1H), 7.23 (d, $^3J = 7.5$ Hz, 1H), 7.06 (td, $^3J = 7.5$ Hz, $^4J = 1.0$ Hz, 1H), 6.94 (dd, $^3J = 8.2$ Hz, $^4J = 0.8$ Hz, 1H), 4.78 (s, 1H).

4.15.2. 2',3',4',5',6'-pentafluoro-2-hydroxy-[1,1'-biphenyl]-3-carbaldehyde (**169**)



Compound **168** (4.63 g, 17.8 mmol, 1 eq), *p*-formaldehyde (1.60 g, 53.4 mmol, 3 eq) and MgCl₂ (5.08 g, 53.4 mmol, 3 eq) were dissolved/suspended in dry THF (75 mL) under argon atmosphere. Dry Et₃N (5 mL, 3.60 g, 35.6 mmol, 2 eq) was added and the reaction was heated to reflux overnight. After cooling to rt, THF was removed under reduced pressure and 2 M HCl (60 mL) was added to the residue, which was extracted with DCM (4 x 50 mL). The collected organic layers were dried over Na₂SO₄, filtered, and concentrated under reduced pressure. The product was purified through chromatographic column on silica gel (toluene/*c*-hexane 1:3). **169** was isolated as a white solid. 1.42 g of **168** (5.45 mmol, 31%) were recovered.

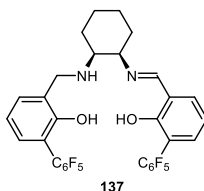
Yield: 2.85 g (9.90 mmol, 56%)

Characterization data are in agreement with the literature.^[177]

R_f = 0.27 (SiO₂, toluene/*c*-hexane 2:3)

¹H-NMR (300 MHz, CDCl₃) δ [ppm] = 11.45 (s, 1H), 9.98 (s, 1H), 7.73 (dd, ³J = 7.7 Hz, ⁴J = 1.6 Hz, 1H), 7.53 (d, ³J = 7.5 Hz, 1H), 7.17 (t, ³J = 7.7 Hz, 1H).

4.15.3. Ligand **137**



Allyl ((1*R*,2*S*)-2-aminocyclohexyl)carbamate (**132**, 500 mg, 2.52 mmol, 1 eq) and **169** (727 mg, 2.52 mmol, 1 eq) were dissolved in MeOH (5 mL). The solution was stirred for 3 hours, then Ni(OAc)₂ tetrahydrate (63 mg, 0.252 mmol, 0.1 eq) was added. After all the nickel acetate had dissolved, NaBH₄ (573 mg, 15.1 mmol, 6eq) was added quickly in one portion. Strong bubbling was observed, and the mixture turned to a grey color. 5 mL of MeOH were added and, after 30

minutes, water (20 mL) was added. DCM (6 mL) was added to dissolve the precipitate that formed, and the second portion of **169** (727 mg, 2.52 mmol, 1 eq) was added. The biphasic mixture was stirred at rt overnight. The aqueous layer was separated and extracted with DCM (3 x20 mL). The combined organic layers were washed with brine, dried over Na₂SO₄, filtered, and concentrated under reduced pressure. The product was purified through chromatographic column on silica gel (EtOAc/c-hexane 1:4), followed by recrystallization from cyclohexane. **137** was isolated as a bright yellow solid.

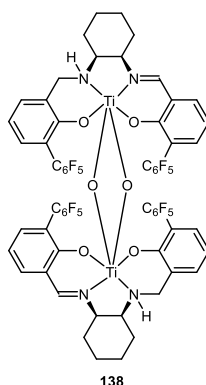
Yield: 1.01 g (1.54 mmol, 61%)

Characterization data are in agreement with the literature.^[177]

R_f = 0.30 (SiO₂, EtOAc/c-hexane 1:4)

¹H-NMR (500 MHz, CDCl₃) δ [ppm] = 13.98 (s, 1H), 8.53 (s, 1H), 7.44 (dd, ³J = 7.6 Hz, ⁴J = 1.2 Hz, 1H), 7.31 (d, ³J = 7.4 Hz, 1H), 7.14 (d, ³J = 7.6 Hz, 1H), 7.10 (d, ³J = 7.3 Hz, 1H), 7.02 (t, ³J = 7.6 Hz, 1H), 6.88 (t, ³J = 7.6 Hz, 1H), 4.13 (d, ²J = 14.2 Hz, 1H), 4.03 (d, ²J = 14.2 Hz, 1H), 3.74 (s, 1H), 2.84 (d, ³J = 10.9 Hz, 1H), 1.98 (dd, ³J = 8.7, 3.9 Hz, 1H), 1.93 – 1.79 (m, 2H), 1.79 – 1.68 (m, 1H), 1.68 – 1.48 (m, 3H), 1.46 – 1.32 (m, 2H).

4.15.4. Complex **138**



Ligand **137** (809 mg, 1.23 mmol, 1 eq) was dissolved in dry DCM (3 mL) under argon atmosphere. Ti(O*i*Pr)₄ (350 mg, 1.23 mmol, 1 eq) was dissolved in dry DCM (1.5 mL). The titanium solution was added to the ligand solution under argon atmosphere and the flask was washed with DCM (1.5 mL). The resulting mixture was stirred for 24 hours under inert atmosphere, then H₂O (44 μL, 44 mg, 2.47 mmol, 2 eq) was added. After 48 hours the reaction was filtered, rinsing with DCM. The product was purified via recrystallization from cyclohexane. **138** was isolated as a bright yellow solid.

Yield: 776 mg (0.538 mmol, 87%)

Characterization data are in agreement with the literature.^[178]

¹H-NMR (500 MHz, CDCl₃) δ [ppm] = 8.17 (s, 1H), 7.50 (dd, ³J = 7.7 Hz, ⁴J = 1.6 Hz, 1H), 7.34 (dd, ³J = 7.5 Hz, ⁴J = 1.2 Hz, 1H), 7.04 (t, ³J = 7.6 Hz, 1H), 6.95 (d, ³J = 7.4 Hz, 1H), 6.81 (d, ³J = 7.2 Hz, 1H), 6.69 (t, ³J = 7.5 Hz, 1H), 4.36 (d, ³J = 12.0 Hz, 1H), 4.24 (d, ²J = 13.9 Hz, 1H), 3.52 – 3.40 (m, 1H), 3.13 – 2.95 (m, 2H), 2.36 (ddt, ³J = 13.5 Hz, ⁴J = 3.6 Hz, 1H), 1.82 (d, ³J = 14.9 Hz, 1H), 1.68 (d, ³J = 12.9 Hz, 1H), 1.60 – 1.48 (m, 1H), 1.47 – 1.38 (m, 1H), 1.37 – 1.27 (m, 1H), 1.23 – 1.11 (m, 1H), 1.00 – 0.84 (m, 1H).

¹³C-NMR (100 MHz, CDCl₃) δ [ppm] = 162.5 (2C), 160.1 (2C), 159.1 (2C), 145.1 (2C), 144.3 (4C), 144.2 (2C), 144.0 (2C), 140.6 (2C), 139.6 (2C), 137.9 (2C), 137.5 (2C), 137.4 (2C), 136.6 (2C), 136.4 (2C), 136.3 (2C), 130.8 (2C), 130.2 (2C), 122.9 (2C), 122.5 (2C), 118.7 (2C), 117.4 (2C), 115.0 (2C), 114.6 (2C), 114.0 (2C), 113.6 (2C), 73.2 (2C), 53.7 (2C), 49.3 (2C), 29.4 (2C), 24.4 (2C), 23.4 (2C), 18.4 (2C).

4.16. Synthesis and Resolution of Allylic Alcohols **142**, **144** and **151-153**

4.16.1. Synthesis of Racemic Allylic Alcohols *rac*-**142**, *rac*-**144** and *rac*-**151-153**

Racemic allylic alcohols **142** and **151-153** were synthesized through addition of vinylmagnesium bromide to the corresponding aldehydes following the literature procedure reported by Breit and Grünanger.^[207] Characterization data for *rac*-**142**,^[207] *rac*-**151**,^[208] *rac*-**152**,^[209] *rac*-**153**,^[208] and *rac*-**144**^[186] are in agreement with the data reported in the cited literature.

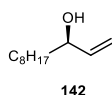
4.16.2. General Procedure for the Enzymatic Kinetic Resolution of Allylic Alcohols **142**, **144** and **151-153 (C)**

The racemic allylic alcohol (1 eq) was weighted in an Erlenmeyer flask, and it was dissolved in *n*-hexane (concentration: 0.1 M). *Candida antarctica* lipase B (Novozyme 435, 1590 U/g, 50 mg/mmol) and vinyl acetate (1.1 eq) were added, and the reaction was kept under agitation at 150-200 rpm until complete consumption of one enantiomer of the alcohol, then the suspension was filtered, rinsing with cyclohexane. The reaction was monitored through GC analysis with a chiral capillary column. Enantiomeric excesses of allylic alcohols (*R*)-**142**, (*R*)-**144**, (*S*)-**151**, (*S*)-**152**, and (*R*)-**153** were determined via GC analysis with a chiral column. Enantiomeric excesses of

the acetylated byproducts were determined via GC analysis with a chiral column after hydrolysis in basic methanol to the corresponding free alcohols.

4.16.3. (*R*)-Undec-1-en-ol, (*R*)-**142**

(*R*)-**142** was prepared following general procedure C starting from 641 mg (3.77 mmol) of *rac*-**142**. (*R*)-**142** and the acetylated product (*S*)-**154** were isolated through chromatographic column (EtOAc/*c*-hexane 1:6) as colorless liquids.



Yield: 296 mg (1.74 mmol, 46%)

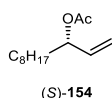
ee: >99%

Chiral GC: Lipodex A; 93 °C isothermal 45 min, 10 °C/min to 130 °C, isothermal 30 min, 10 °C/min to 180 °C isothermal 5 min; flow 1.0 mL/min; τ_R [(*S*)-**142**] (minor) = 39.2 min; τ_R [(*R*)-**142**] (major) = 40.3 min.

Characterization data are in agreement with the literature.^[207]

R_f = 0.26 (SiO₂, EtOAc/*c*-hexane 1:6)

¹H-NMR (300 MHz, CDCl₃) δ [ppm] = 5.87 (ddd, ³*J* = 16.9, 10.4, 6.2 Hz, 1H), 5.22 (ddd, ³*J* = 17.2 Hz, ²*J* = ⁴*J* = 1.5 Hz, 1H), 5.10 (ddd, ³*J* = 10.4 Hz, ²*J* = ⁴*J* = 1.4 Hz, 1H), 4.10 (q, ³*J* = 6.4 Hz, 1H), 1.60 – 1.20 (m, 14H), 0.93 – 0.83 (m, 3H).



Yield: 400 mg (1.88 mmol, 50%)

ee: 94%

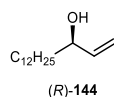
Characterization data are in agreement with the literature.^[210]

R_f = 0.80 (SiO₂, EtOAc/*c*-hexane 1:6)

¹H-NMR (300 MHz, CDCl₃) δ [ppm] = 5.77 (ddd, ³*J* = 17.0, 10.5, 6.3 Hz, 1H), 5.32 – 5.11 (m, 3H), 2.06 (s, 3H), 1.73 – 1.48 (m, 2H), 1.40 – 1.16 (m, 12H), 0.94 – 0.81 (m, 3H).

4.16.4. (*R*)-Pentadec-1-en-3-ol, (*R*)-144

(*R*)-144 was prepared following general procedure C starting from 2.65 g (11.7 mmol) of rac-144. (*R*)-144 and the acetylated product (*S*)-163 were isolated through chromatographic column (EtOAc/*c*-hexane 1:6).



White solid

m.p. = 33-35°C

Yield: 1.21 mg (5.34 mmol, 46%)

ee: >99%

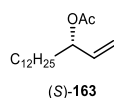
The enantiomeric excess was determined by chiral HPLC after derivatization with 3,5-dinitrobenzoyl chloride (Daicel Chiracel OD-H; *n*-hexane:isopropanol = 98:2; flow = 1.0 mL/min, 18 °C, fixed 210 nm); τ_R (*R*) (major) = 13.8 min; τ_R (*S*) (minor) = 18.3 min.

Characterization data are in agreement with the literature.^[186]

R_f = 0.30 (SiO₂, EtOAc/*c*-hexane 1:6)

¹H-NMR (300 MHz, CDCl₃) δ [ppm] = 5.86 (ddd, ³*J* = 16.9, 10.4, 6.2 Hz, 1H), 5.21 (dΨ-t, ³*J* = 17.2 Hz, ²*J* = ³*J* = 1.4 Hz, 1H), 5.09 (dΨ-t, ³*J* = 10.3 Hz, ²*J* = ³*J* = 1.2 Hz, 1H), 4.09 (dt, ³*J* = 6.3 Hz, 1H), 1.59 – 1.45 (m, 2H), 1.45 – 1.14 (m, 21H), 0.87 (t, ³*J* = 6.7 Hz, 3H).

¹³C-NMR (75 MHz, CDCl₃) δ [ppm] = 141.5 (1C), 114.6 (1C), 73.4 (1C), 37.2 (1C), 32.1 (1C), 29.8 (CH₂), 29.8 (CH₂), 29.7 (CH₂), 29.5 (CH₂), 25.5 (1C), 22.8 (1C), 14.3 (1C).



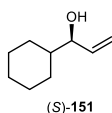
Colorless oil.

R_f = 0.56 (SiO₂, EtOAc/*c*-hexane 1:6)

¹H-NMR (500 MHz, CDCl₃) δ [ppm] = 5.82 – 5.72 (m, 1H), 5.27 – 5.18 (m, 2H), 5.15 (d, ³*J* = 10.5 Hz, 1H), 2.06 (s, 3H), 1.76 – 1.50 (m, 2H), 1.37 – 1.21 (m, 20H), 0.88 (t, ³*J* = 7.0 Hz, 3H).

4.16.5. (S)-1-Cyclohexylprop-2-en-1-ol, (S)-151

(S)-151 was prepared following general procedure C starting from 141 mg (1.00 mmol) of *rac*-151. The reaction was stopped after 20 hours. (S)-151 and the acetylated product (R)-155 were isolated through chromatographic column (EtOAc/*c*-hexane 1:10 to 1:9) as colorless liquids.



Yield: 64 mg (0.46 mmol, 46%)

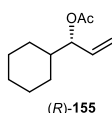
ee: >99%

Chiral GC: Chirasil-DEX CB; 85 °C isothermal 45 min, 10 °C/min to 140 °C isothermal 20 min, 10 °C/min to 180 °C isothermal 5 min; flow 1.2 mL/min; τ_R [(R)-151] (minor) = 40.6 min; τ_R [(S)-151] (major) = 42.2 min.

Characterization data are in agreement with the literature.^[212]

R_f = 0.25 (SiO₂, EtOAc/*c*-hexane 1:9)

¹H-NMR (500 MHz, CDCl₃) δ [ppm] = 5.87 (ddd, ³*J* = 17.1, 10.4, 6.6 Hz), 5.20 (ddd, ³*J* = 17.3 Hz, ²*J* = ⁴*J* = 1.5 Hz, 1H), 5.14 (ddd, ³*J* = 10.4 Hz, ²*J* = ⁴*J* = 1.5 Hz, 1H), 3.85 (m, 1H), 1.91 – 1.60 (m, 5H), 1.49 – 1.33 (m, 2H), 1.32 – 0.91 (m, 5H).



Yield: 85 mg (0.47 mmol, 46%)

ee: >99%

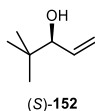
Characterization data are in agreement with the literature.^[211]

R_f = 0.44 (SiO₂, EtOAc/*c*-hexane 1:10)

¹H-NMR (500 MHz, CDCl₃) δ [ppm] = 5.75 (ddd, ³*J* = 17.3, 10.5, 6.9 Hz, 1H), 5.24 – 5.15 (m, 2H), 5.04 (t, ³*J* = 6.8 Hz, 1H), 2.06 (s, 3H), 1.80 – 1.61 (m, 5H), 1.61 – 1.47 (m, 1H), 1.32 – 1.06 (m, 3H), 1.06 – 0.91 (m, 2H).

4.16.6. (S)-4,4-Dimethylpent-1-en-3-ol, (S)-152

(S)-152 was prepared following general procedure C (using *Candida antarctica* lipase A, 350 mg, 200 mg/mmol) starting from 200 mg (1.75 mmol) of *rac*-152. The reaction was stopped after 18 hours. (S)-152 and the acetylated product (R)-157 were isolated through chromatographic column (100% DCM) as colorless liquids.



Yield: 52 mg (0.46 mmol, 26%)

ee: 98%

Chiral GC: Chiralsil-DEX CB; 50 °C isothermal 38 min, 10 °C/min to 140 °C isothermal 20 min, 10 °C/min to 180 °C isothermal 5 min; flow 1.5 mL/min; τ_R [(R)-152] (minor) = 29.7 min; τ_R [(S)-152] (major) = 31.6 min.

Characterization data are in agreement with the literature.^[209]

R_f = 0.39 (SiO₂, Et₂O/*n*-pentane 1:4)

¹H-NMR (500 MHz, CDCl₃) δ [ppm] = 5.93 (ddd, ³*J* = 17.2, 10.5, 6.7 Hz, 1H), 5.26 – 5.20 (m, 1H), 5.20 – 5.14 (m, 1H), 3.75 (dt, ³*J* = 6.7, 1.1 Hz, 1H), 0.91 (s, 9H).



Yield: 171 mg (1.09 mmol, 63%)

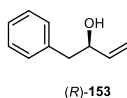
ee: 70%

R_f = 0.70 (SiO₂, EtOAc/*c*-hexane 1:10)

¹H-NMR (500 MHz, CDCl₃) δ [ppm] = 5.85 – 5.73 (m, 1H), 5.25 – 5.21 (m, 1H), 5.21 – 5.17 (m, 1H), 5.00 – 4.96 (m, 1H), 2.08 (s, 3H), 0.92 (s, 9H).

4.16.7. (R)-1-Phenylbut-3-en-2-ol, (R)-153

(R)-153 was prepared following general procedure C starting from 162 mg (1.09 mmol) of *rac*-153. (R)-153 and the acetylated product (S)-156 were isolated through chromatographic column (Et₂O/*n*-pentane 1:6) as colorless liquids.



Yield: 37 mg (0.25 mmol, 23%)

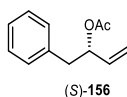
ee: >99%

Chiral GC: Chiralsil-DEX CB; 100 °C isothermal 30 min, 10 °C/min to 180 °C isothermal 5 min; flow 2.0 mL/min; τ_R [(*R*)-**153**] (major) = 20.5 min; τ_R [(*S*)-**153**] (minor) = 22.1 min.

Characterization data are in agreement with the literature.^[208]

R_f = 0.17 (SiO₂, Et₂O/*n*-pentane 1:6)

¹H-NMR (300 MHz, CDCl₃) δ [ppm] = 7.36 – 7.28 (m, 2H), 7.28 – 7.20 (m, 3H), 5.94 (ddd, ³*J* = 17.2, 10.5, 5.8 Hz, 1H), 5.25 (dt, ³*J* = 17.2 Hz, ²*J* = ⁴*J* = 1.4 Hz, 1H), 5.13 (dt, ³*J* = 10.5 Hz, ²*J* = ⁴*J* = 1.4 Hz, 1H), 4.36 (dtd, ³*J* = 7.9, 5.6, 4.0 Hz, 1H), 2.89 (dd, ³*J* = 13.6, 5.2 Hz, 1H), 2.79 (dd, ³*J* = 13.6, 7.9 Hz, 1H), 1.61 (d, ³*J* = 4.0 Hz, 1H)



Yield: 118 mg (0.62 mmol, 57%)

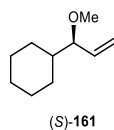
ee: 45%

Characterization data are in agreement with the literature.^[213]

R_f = 0.61 (SiO₂, Et₂O/*n*-pentane 1:6)

¹H-NMR (500 MHz, CDCl₃) δ [ppm] = 7.32 – 7.24 (m, 2H), 7.24 – 7.15 (m, 3H), 5.81 (ddd, ³*J* = 17.0, 10.5, 6.2 Hz, 1H), 5.51 – 5.42 (m, 1H), 5.20 (dt, ³*J* = 17.2 Hz, ²*J* = ⁴*J* = 1.3 Hz, 1H), 5.15 (dt, ³*J* = 10.5 Hz, ²*J* = ⁴*J* = 1.2 Hz, 1H), 2.96 (dd, ³*J* = 13.7, 7.4 Hz, 1H), 2.88 (dd, ³*J* = 13.7, 6.3 Hz, 1H), 2.01 (s, 3H).

4.17. (S)-(1-Methoxyallyl)cyclohexane, (S)-161



(S)-**151** (140 mg, 1.00 mmol, 1 eq) was dissolved in anhydrous THF (2 mL) under argon atmosphere. NaH (60% dispersion in mineral oil, 48 mg, 2.00 mmol, 2 eq) was added at 0 °C, and the mixture was stirred at rt for 30 minutes. MeI (93 μ L, 213 mg, 1.50 mmol, 1.5 eq) was added. The reaction mixture was stirred at rt for 3 hours. The reaction was quenched with 10 mL of sat. aq. NH₄Cl, and the crude was extracted with DCM (3 x 10 mL). The combined organic layers were washed with brine, dried over MgSO₄, filtered, and concentrated under reduced pressure. The product was purified through chromatographic column on silica gel (DCM/c-Hex 3:7 to 100% DCM). (S)-**161** was isolated as a colorless liquid.

Yield: 140 mg (0.91 mmol, 91%)

ee: >99%

Chiral GC: Chiralsil-DEX CB; 70 °C isothermal 45 min, 10 °C/min to 140 °C isothermal 20 min, 10 °C/min to 180 °C isothermal 5 min; flow 1.3 mL/min; τ_R [(S)-**161**] (major) = 40.6 min; τ_R [(R)-**161**] (minor) = 20.3 min.

R_f = 0.56 (SiO₂, EtOAc/c-hexane 1:10)

¹H-NMR (500 MHz, CDCl₃) δ [ppm] = 5.63 (ddd, ³J = 17.3, 10.3, 8.1 Hz, 1H), 5.22 (dd, ³J = 10.3 Hz, ²J = 1.9 Hz, 1H), 5.14 (ddd, ³J = 17.2 Hz, ²J = 1.9 Hz, ⁴J = 0.7 Hz, 1H), 3.25 (s, 3H), 3.23 – 3.19 (m, 1H), 1.89 – 1.83 (m, 1H), 1.77 – 1.68 (m, 2H), 1.68 – 1.59 (m, 2H), 1.48 – 1.38 (m, 1H), 1.28 – 1.07 (m, 3H), 1.01 – 0.89 (m, 2H).

¹³C-NMR (125 MHz, CDCl₃) δ [ppm] = 137.5 (1C), 117.9 (1C), 88.1 (1C), 56.6 (1C), 42.5 (1C), 29.3 (1C), 28.9 (1C), 26.8 (1C), 26.3 (1C), 26.3 (1C).

ATR: $\tilde{\nu}$ [cm⁻¹] = 3077 (w), 2979 (w), 2923 (s), 2853 (s), 2819 (w), 1642 (w), 1450 (s), 1420 (w), 1327 (w), 1263 (w), 1231 (w), 1195 (w), 1174 (w), 1117 (s), 1101 (s), 1086 (s), 995 (s), 971 (m), 922 (s), 888 (m), 885.2(w), 841.7 (w), 691.0 (w).

GC-MS (ESI⁺): m/z = 153.3 [M-H]⁺, 122.1 [M-CH₄O]⁺, 107.2, 94.1, 79.1, 71.1 [M-C₆H₁₁]⁺, 67.1, 55.1.

HR-GC-MS: measured: m/z = 122.10891, calculated: m/z 122.10955 [M-CH₄O].

4.18. Synthesis of the Racemic Epoxides

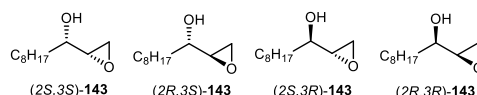
4.18.1. General Procedure for the Epoxidation with *m*-CPBA (D)

The racemic/enantiopure olefin substrate (**142**, **144**, **151-153**, **161**, 1 eq) was dissolved in DCM (concentration: 0.4M). *m*-CPBA ($\leq 77\%$ purity, 1.25 eq) was added, and the mixture was stirred at rt overnight, monitoring the conversion via TLC. The reaction was quenched by addition of sat. aq. NaHCO₃ and sat. aq. Na₂S₂O₃ (or alternatively sat. aq. Na₂SO₃). The crude was extracted with DCM, and the combined organic layers were washed with brine, dried over MgSO₄, filtered, and concentrated under reduced pressure.

4.18.2. Determination of the Absolute Configurations and of the *syn/anti* Ratios for Epoxides **143**, **145**, **158-160**, **162**

The *syn/anti* configurations was attributed by analysis of the chemical shift patterns of ¹H-NMR spectra of the pure compounds:^[191] The characteristic signals used for the assignment are highlighted in blue. *syn/anti* configuration associated with the GC peaks was determined by comparison of the ratios between the areas with the ratios of the areas of ¹H-NMR signals. The absolute configurations were assigned by GC analysis of the mixture of diastereomers obtained from epoxidation of the enantiopure alcohol substrates with *m*-CPBA according to general procedure D.

4.18.3. 1,2-Epoxyundecan-3-ol (**143**)



Epoxy alcohol *syn/anti-rac-143* was prepared following general procedure D starting from 300 mg (1.76 mmol) of *rac-142*. The mixture of the four stereoisomers of **143** was isolated through chromatographic column (EtOAc/*c*-hexane 1:6) as a colorless liquid with a ratio of the *syn/anti*-racemates of 56:44.

Yield: 304 mg (1.63 mmol, 93%)

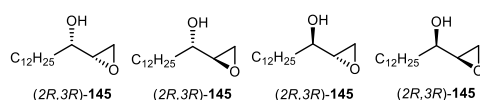
Characterization data are in agreement with the literature.^[214]

R_f = 0.13 (SiO₂, EtOAc/c-hexane 1:6)

¹H-NMR (300 MHz, CDCl₃) δ [ppm] = 3.84 (ddt, *J* = 7.4, 4.9, 2.8 Hz, 1H, *anti*), 3.44 (dq, *J* = 7.4, 5.7 Hz, 1H, *syn*), 3.02 (q, *J* = 3.3 Hz, 1H, *anti*), 2.98 (td, *J* = 4.5, 2.7 Hz, 1H, *syn*), 2.86 – 2.79 (m, 2H, *syn* + *anti*), 2.76 – 2.69 (m, 2H, *syn* + *anti*), 1.84 (dt, *J* = 6.0, 1.6 Hz, 1H, *syn*), 1.79 (d, *J* = 2.4 Hz, 1H, *anti*), 1.67 – 1.20 (m, 28H, *syn* + *anti*), 0.88 (t, *J* = 6.9 Hz, 6H, *syn* + *anti*).

Chiral GC: Lipodex A split = 50:1; split flow = 50 mL/min, N₂; flow 1.0 mL/min; 93 °C isothermal 45 min, 10 °C/min to 130 °C isothermal 30 min, 10 °C/min to 180 °C isothermal 5 min; τ_R[(2*S*,3*S*)-**143**] = 59.5 min; τ_R[(2*R*,3*S*)-**143**] = 59.9 min; τ_R[(2*S*,3*R*)-**143**] = 60.5 min; τ_R[(2*R*,3*R*)-**143**] = 61.3 min.

4.18.4. 1,2-Epoxy-pentadecan-3-ol (**145**)



Epoxy alcohol *syn/anti-rac-145* was prepared following general procedure D starting from 362 mg (1.60 mmol) of *rac-144*. The mixture of the four stereoisomers of **145** was isolated through chromatographic column (EtOAc/c-hexane 1:4) as a colorless liquid with a ratio of the *syn/anti*-racemates of 56:44.

Yield: 304 mg (1.63 mmol, 93%)

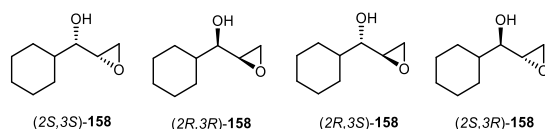
Characterization data are in agreement with the literature.^[214]

R_f = 0.13 (SiO₂, EtOAc/c-hexane 1:6)

¹H-NMR (300 MHz, CDCl₃) δ [ppm] = 3.84 (ddt, *J* = 7.4, 4.9, 2.7 Hz, 1H, *anti*), 3.48 – 3.38 (m, 1H, *syn*), 3.02 (q, *J* = 3.3 Hz, 1H, *anti*), 2.98 (td, *J* = 4.5, 2.7 Hz, 1H, *syn*), 2.84 – 2.79 (m, 2H, *syn* + *anti*), 2.75 – 2.71 (m, 2H, *syn* + *anti*), 1.90 – 1.84 (m, 1H, *syn*), 1.83 – 1.79 (m, 1H, *anti*), 1.66 – 1.19 (m, 44H, *syn* + *anti*), 0.88 (t, *J* = 6.9 Hz, 6H, *syn* + *anti*).

The four isomers could not be resolved through chiral GC analysis.

4.18.5. 3-Cyclohexyl-1,2-epoxypropan-3-ol (**158**)



Epoxy alcohol *syn/anti-rac-158* was prepared following general procedure D starting from 140 mg (1.00 mmol) of *rac-151*. The mixture of the four stereoisomers of **158** was isolated as a colorless liquid without purification through chromatography with a ratio of the *syn/anti*-racemates of 57:43.

Yield: 150 mg (0.96 mmol, 96%)

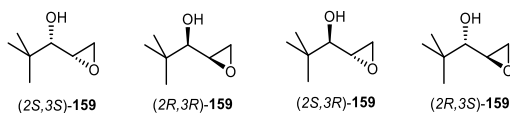
Characterization data are in agreement with the literature.^[190]

R_f = 0.19 (SiO₂, EtOAc/*c*-hexane 1:4)

¹H-NMR (500 MHz, CDCl₃) δ [ppm] = 3.66 (m, 1H, *anti*), 3.19 (dd, *J* = 11.7, 5.8 Hz, 1H, *syn*), 3.11 – 3.07 (m, 1H, *anti*), 3.07 – 3.02 (m, 1H, *syn*), 2.85 (dt, *J* = 5.3, 3.3 Hz, 2H, *syn* + *anti*), 2.77 (dd, *J* = 5.0, 4.1 Hz, 1H, *anti*), 2.72 (dd, *J* = 5.0, 2.8 Hz, 1H, *syn*), 1.98 – 1.63 (m, 10H, *syn* + *anti*), 1.64 – 1.51 (m, 2H, *syn* + *anti*), 1.35 – 1.01 (m, 10H, *syn* + *anti*).

Chiral GC: Chirasil-Dex CB split = 80:1; split flow = 125.3 mL/min, N₂; flow 1.6 mL/min; 100 °C isothermal 55 min, 10 °C/min to 180 °C isothermal 5 min; τ_R[(2S,3S)-**158**] = 43.3 min; τ_R[(2R,3R)-**158**] = τ_R[(2R,3S)-**158**] = 47.1 min; τ_R[(2S,3R)-**158**] = 51.1 min.

4.18.6. 4,4-Dimethyl-1,2-epoxypentan-3-ol (**159**)



Epoxy alcohol *syn/anti-rac-159* was prepared following general procedure D starting from 75 mg (0.66 mmol) of *rac-152*. The mixture of the four stereoisomers of **159** was isolated as a yellowish liquid without purification through chromatography with a ratio of the *syn/anti*-racemates of 48:52.

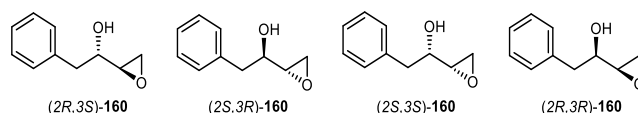
Yield: 72 mg (0.56 mmol, 84%)

R_f = 0.23 (SiO₂, EtOAc/*c*-hexane 1:4)

$^1\text{H-NMR}$ (500 MHz, CDCl_3) δ [ppm] = 3.52 (d, J = 2.9 Hz, 1H, *anti*), 3.17 – 3.03 (m, 3H, *syn + anti*), 2.87 – 2.80 (m, 2H, *syn + anti*), 2.76 (dd, J = 5.1, 4.0 Hz, 1H, *anti*), 2.70 (dd, J = 5.0, 2.6 Hz, 1H, *syn*), 1.73 (brs, 2H, *syn + anti*), 1.00 (s, 18H, *syn + anti*).

Chiral GC: Chirasil-Dex CB split = 80:1; split flow = 100.2 mL/min, N_2 ; flow 1.3 mL/min; 80 °C isothermal 30 min, 10 °C/min to 100 °C isothermal 25 min, 10 °C/min to 180 °C isothermal 5 min; $\tau_{\text{R}}[(2\text{S},3\text{S})\text{-159}]$ = 16.4 min; $\tau_{\text{R}}[(2\text{R},3\text{R})\text{-159}]$ = 17.8 min; $\tau_{\text{R}}[(2\text{R},3\text{S})\text{-159}]$ = 19.8 min; $\tau_{\text{R}}[(2\text{S},3\text{R})\text{-159}]$ = 21.6 min.

4.18.7. 4-Phenyl-1,2-epoxybutan-3-ol (**160**)



Epoxy alcohol *syn/anti-rac-160* was prepared following general procedure D starting from 290 mg (1.96 mmol) of *rac-153*. The mixture of the four stereoisomers of **160** was isolated through chromatographic column ($\text{Et}_2\text{O}/n\text{-pentane}$ 1:6) as a colorless liquid with a ratio of the *syn/anti*-racemates of 59:41.

Yield: 292 mg (1.78 mmol, 91%)

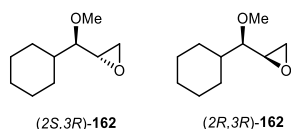
R_f = 0.17 (SiO_2 , $\text{Et}_2\text{O}/n\text{-pentane}$ 1:6)

Characterization data are in agreement with the literature.^[215]

$^1\text{H-NMR}$ (300 MHz, CDCl_3) δ [ppm] = 7.36 – 7.28 (m, 4H, *syn + anti*), 7.28 – 7.21 (m, 6H, *syn + anti*), 4.01 (ddt, J = 7.9, 4.5, 2.9 Hz, 1H, *anti*), 3.72 (dtd, J = 7.3, 6.2, 4.6 Hz, 1H, *syn*), 3.06 – 3.02 (m, 2H, *syn + anti*), 2.99 – 2.82 (m, 4H, *syn + anti*), 2.80 (dd, J = 5.0, 2.7 Hz, 1H, *anti*), 2.75 (dd, J = 4.9, 4.0 Hz, 2H, *syn + anti*), 2.62 (dd, J = 4.9, 2.7 Hz, 1H, *syn*), 1.97 (m, 1H, *syn*), 1.89 – 1.85 (m, 1H, *anti*).

Chiral GC: Lipodex A split = 50:1; split flow = 50 mL/min, N_2 ; flow 1.0 mL/min; 120 °C isothermal 32 min, 10 °C/min to 180 °C isothermal 5 min; $\tau_{\text{R}}[(2\text{R},3\text{S})\text{-160}]$ = 28.1 min; $\tau_{\text{R}}[(2\text{S},3\text{R})\text{-160}]$ = $\tau_{\text{R}}[(2\text{S},3\text{S})\text{-160}]$ = 28.7 min; $\tau_{\text{R}}[(2\text{R},3\text{R})\text{-160}]$ = 30.2 min.

4.18.8. 3-Cyclohexyl-3-methoxy-1,2-epoxypropane (**162**)



Epoxide *syn/anti*-(3*R*)-**162** was prepared following general procedure D starting from 51 mg (0.33 mmol) of (*S*)-**161**. The mixture of the two diastereoisomers of **162** was isolated as a colorless liquid without purification through chromatography in a *syn/anti* ratio of 42:58.

Yield: 36 mg (0.21 mmol, 63%)

R_f = 0.25 (SiO₂, EtOAc/*c*-hexane 1:10)

¹H-NMR (500 MHz, CDCl₃) δ [ppm] = 3.47 (s, 3H, *syn*), 3.38 (s, 3H, *anti*), 3.00 – 2.92 (m, 2H, *syn + anti*), 2.82 – 2.72 (m, 4H, *syn + anti*), 2.57 – 2.51 (m, 1H, *syn*), 2.51 – 2.46 (m, 1H, *syn*), 1.92 – 1.52 (m, 12H, *syn + anti*), 1.32 – 1.00 (m, 10H, *syn + anti*).

Chiral GC: Chirasil-Dex CB split = 80:1; split flow = 97.9 mL/min, N₂; flow 1.2 mL/min; 85 °C isothermal 50 min, 10 °C/min to 100 °C isothermal 16 min, 10 °C/min to 180 °C isothermal 5 min; τ_R [(2*S*,3*R*)-**162**] = 41.5 min; τ_R [(2*R*,3*R*)-**162**] = 44.0 min.

4.19. Epoxidation Tests

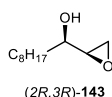
4.19.1. General Procedure for the Asymmetric Epoxidation Catalyzed by **138**

The enantiopure substrates (0.100 mmol, 1 eq), the titanium catalyst (7.2 mg, 0.005 mmol, 0.05 eq), and Ph₂O (0.100 mmol, 1 eq) were weighted in a 10 mL test tube. A stirring bar and CHCl₃ (0.5 mL) were added, and the temperature of the mixture was set to 20 °C. Aqueous H₂O₂ (50% solution, 8.5 μ L, 0.150 mmol, 1.5 eq) was added, and the reaction mixture was stirred at 20 °C. The reaction was monitored through chiral GC analysis. When the reaction was complete or conversion of the substrate was not observed anymore, the mixture was filtered over MgSO₄ and MnO₂, rinsing with DCM. The solvents were removed under reduced pressure, and the products were purified through chromatographic column.

4.19.2. Determination of the *ee*, of the *syn/anti dr*, and of the Absolute Configuration of the Epoxidation Products

Enantiomeric excesses and diastereomeric ratios were determined via GC analysis of samples taken from the reactions with a chiral capillary column. Absolute configurations were determined by comparison with the data previously collected for the mixtures of stereoisomers obtained from epoxidation with *m*-CPBA. Absolute configuration of compounds (2*R*,3*R*)-**145** and (2*R*,3*R*)-**158** could be confirmed by X-ray diffraction analysis. Absolute configuration of compound (2*R*,3*R*)-**162** was verified by preparing the diastereoisomerically pure product through methylation of (2*R*,3*R*)-**158**.

4.19.3. (2*R*,3*R*)-1,2-Epoxyundecan-3-ol, (2*R*,3*R*)-**143**



Colorless liquid

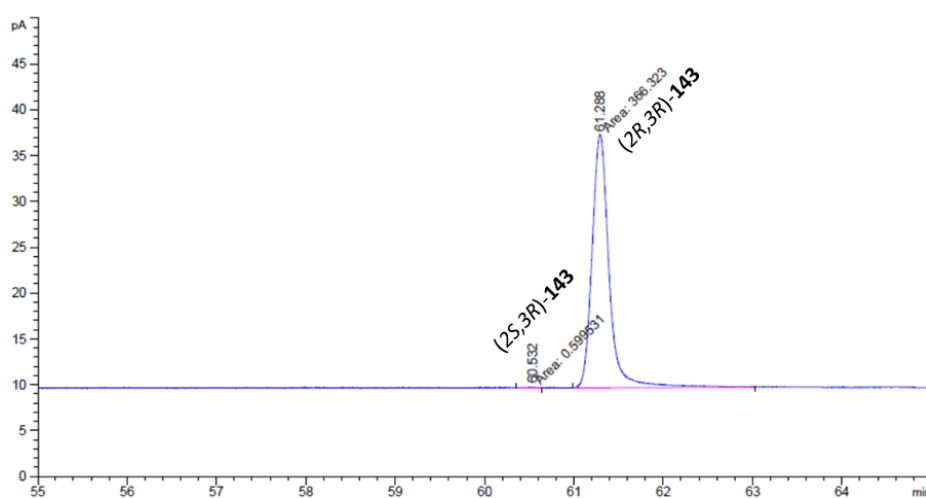
Characterization data are in agreement with the literature.^[214]

$R_f = 0.13$ (SiO₂, EtOAc/*c*-hexane 1:6)

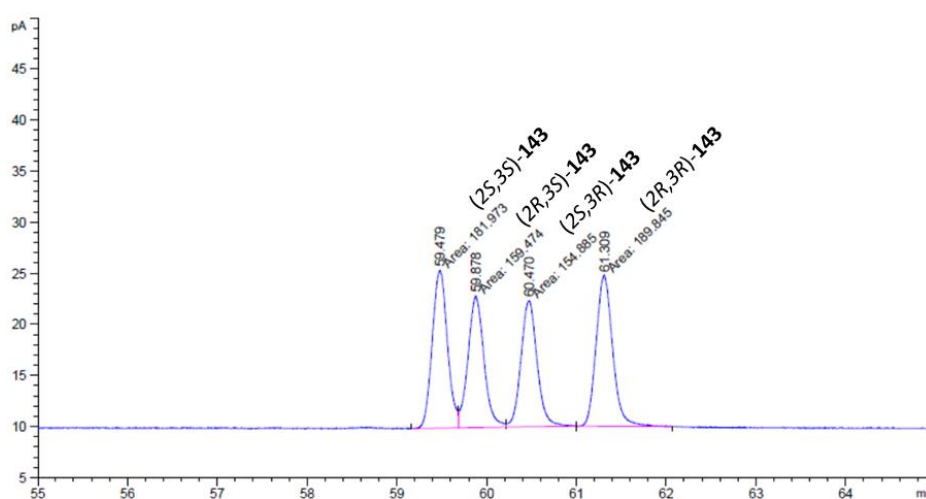
¹H-NMR (300 MHz, CDCl₃) δ [ppm] = 3.44 (dq, $J = 7.4, 5.7$ Hz, 1H), 2.98 (td, $J = 4.5, 2.7$ Hz, 1H), 2.86 – 2.79 (m, 1H), 2.76 – 2.69 (m, 1H), 1.84 (dt, $J = 6.0, 1.6$ Hz, 1H), 1.67 – 1.20 (m, 14H), 0.88 (t, $J = 6.9$ Hz, 3H).

Chiral GC: Lipodex A split = 50:1; split flow = 50 mL/min, N₂; flow 1.0 mL/min; 93 °C isothermal 45 min, 10 °C/min to 130 °C isothermal 30 min, 10 °C/min to 180 °C isothermal 5 min; τ_R [(2*R*,3*R*)-**143**] = 61.3 min.

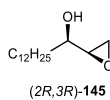
GC obtained from the catalytic test reported in entry 1 of Table 16 (epoxy alcohol region).



GC obtained from epoxidation of *rac*-142 with *m*-CPBA (epoxy alcohol region).



4.19.4. (2R,3R)-Pentadecan-3-ol, (2R,3R)-145



White solid.

$R_f = 0.19$ (SiO_2 , EtOAc/*c*-hexane 1:4)

m.p. = 48-49 °C

$^1\text{H-NMR}$ (500 MHz, CDCl_3) δ [ppm] = 3.42 (br s, 1H), 2.97 (ddd, $^3J = 5.1, 4.1, 2.8$ Hz, 1H), 2.81 (dd, $^2J = 4.9$ Hz, $^3J = 4.1$ Hz, 1H), 2.71 (dd, $^2J = 4.9$ Hz, $^3J = 2.8$ Hz, 1H), 1.95 (br s, 1H), 1.64 – 1.53 (m, 2H), 1.52 – 1.41 (m, 1H), 1.41 – 1.18 (m, 19H), 0.87 (t, $^3J = 7.0$ Hz, 3H).

$^{13}\text{C-NMR}$ (125 MHz, CDCl_3) δ [ppm] = 71.8 (1C), 55.5 (1C), 45.3 (1C), 34.6 (1C), 32.1 (1C), 29.8 (CH_2), 29.8 (CH_2), 29.7 (CH_2), 29.5 (CH_2), 25.4 (1C), 22.8 (1C), 14.3 (1C).

ATR: $\tilde{\nu}$ [cm^{-1}] = 3662 (w), 3362 (br), 3291 (br), 2962 (w), 2916 (s), 2849 (s), 1473 (s), 1463 (s), 1404 (m), 1338 (w), 1255 (w), 1125 (m), 1068 (m), 1031 (w), 963 (s), 889 (s), 874 (s), 824 (w), 791 (w), 752 (s), 729 (s), 720 (s), 664 (m), 648 (m), 541 (w), 509 (w).

GC-MS (ESI+): $m/z = 208.3, 199.1$ [$\text{M-C}_3\text{H}_7$] $^+$ / [$\text{M-C}_2\text{H}_3\text{O}$] $^+$, 166.2, 152.1, 137.3, 125.1 [$\text{C}_8\text{H}_{13}\text{O}$] $^+$, 111.2 [$\text{C}_7\text{H}_{11}\text{O}$] $^+$, 97.1 [$\text{C}_6\text{H}_9\text{O}$] $^+$, 83.1 [$\text{C}_5\text{H}_7\text{O}$] $^+$, 69.1 [$\text{C}_4\text{H}_5\text{O}$] $^+$, 55.1.

X-Ray Crystal Structure Analysis of (2R,3R)-145

Crystals suitable for X-ray diffraction analysis were obtained by slow evaporation of a saturated solution of (2R,3R)-145 in *n*-pentane.

Table 19. Crystal data and structure refinement for (2R,3R)-145.

CCDC registry number	2132887
Empirical formula	$\text{C}_{15}\text{H}_{30}\text{O}_2$
Moiety formula	$\text{C}_{15}\text{H}_{30}\text{O}_2$
Formula weight	242.39
Temperature	100(2) K
Wavelength	1.54178 Å
Crystal system	Monoclinic
Space group	P2_1
Unit cell dimensions	$a = 8.8612(5)$ Å $b = 4.8888(4)$ Å $c = 33.909(2)$ Å
Volume	$1468.95(17)$ Å ³
Z	4
Density (calculated)	1.096 mg/m^3
Absorption coefficient	0.538 mm^{-1}
F(000)	544
Crystal size	0.500 x 0.100 x 0.020 mm^3
Theta range for data collection	2.606 to 72.205°
Index ranges	$-10 \leq h \leq 10, -5 \leq k \leq 6, -41 \leq l \leq 41$
Reflections collected	28259

Independent reflections	5640 [R(int) = 0.0658]
Completeness to theta = 67.679°	99.9%
Absorption correction	Semi-empirical from equivalents
Max. and min. transmission	0.7536 and 0.5828
Refinement method	Full-matrix least-squares on F ²
Data / restraints / parameters	5640 / 1 / 317
Goodness-of-fit on F ²	1.068
Final R indices [I>2sigma(I)]	R1 = 0.0398, wR2 = 0.1072
R indices (all data)	R1 = 0.0429, wR2 = 0.1093
Absolute structure parameter	0.10(10)
Extinction coefficient	n/a
Largest diff. peak and hole	0.226 and -0.206 e•Å ⁻³

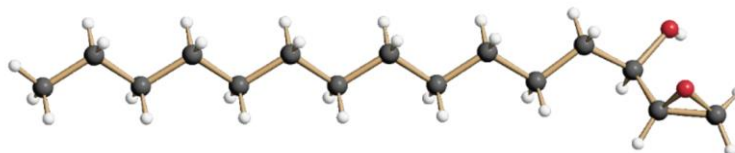
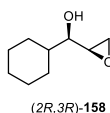


Figure 42. Molecular structure of (2*R*,3*R*)-145.

4.19.5. (2*R*,3*R*)-3-Cyclohexyl-1,2-epoxypropan-3-ol, (2*R*,3*R*)-158



White solid.

Characterization data are in agreement with the literature.^[190]

R_f = 0.19 (SiO₂, EtOAc/*c*-hexane 1:4)

¹H-NMR (500 MHz, CDCl₃) δ [ppm] = 3.13 (ddd, ³J = 5.7 Hz, 1H), 3.06 – 2.99 (m, 1H), 2.82 (dd, ²J = 4.9 Hz, ³J = 4.1 Hz, 1H), 2.68 (dd, ²J = 4.9 Hz, ³J = 2.8 Hz, 1H), 2.09 (br s, 1H), 1.99 – 1.85 (m, 1H), 1.83 – 1.62 (m, 4H), 1.62 – 1.46 (m, 1H), 1.34 – 0.95 (m, 5H).

¹³C-NMR (75 MHz, CDCl₃) δ [ppm] = 76.0 (1C), 54.2 (1C), 45.5 (1C), 42.4 (1C), 28.9 (1C), 28.7 (1C), 26.5 (1C), 26.2 (1C), 26.1 (1C).

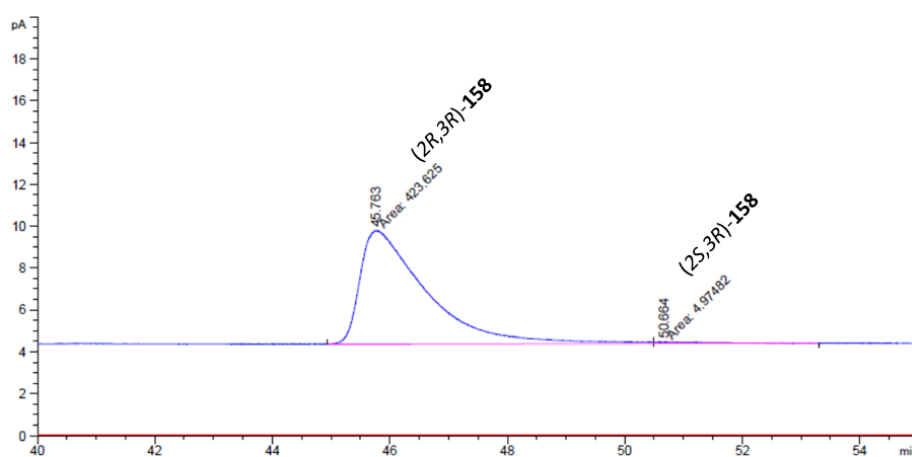
ATR: $\tilde{\nu}$ [cm⁻¹] = 3434 (br), 3401 (br), 3072 (w), 3030 (w), 2999 (w), 2956 (w), 2926 (s), 2853 (s), 2660 (w), 1480 (w), 1453 (s), 1420 (m), 1396 (w), 1345 (w), 1313 (m), 1259 (s), 1190 (w), 1137

(w), 1107 (s), 1089 (m), 1053 (m), 1038 (s), 991 (w), 962 (m), 923 (s), 889 (s), 875 (m), 853 (s), 841 (m), 799 (m), 779 (s), 683 (m), 588 (s), 545 (s), 536 (s).

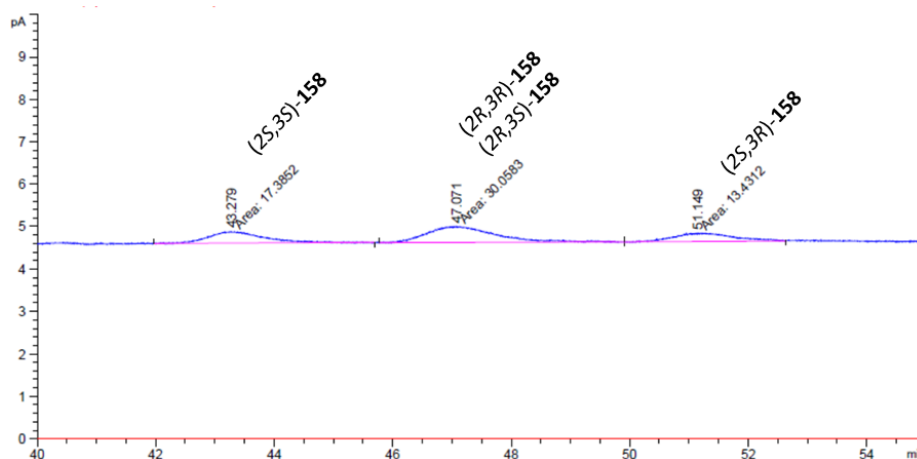
GC-MS (ESI+): $m/z = 155.9 [M]^+$, 137.0, 122.9, 109.1, 95.1, 83.1 $[C_6H_{11}]^+$, 67.1, 55.1.

Chiral GC: Chirasil-Dex CB split = 80:1; split flow = 125.3 mL/min, N_2 ; flow 1.6 mL/min; 100 °C isothermal 55 min, 10 °C/min to 180 °C isothermal 5 min; $\tau_R[(2R,3R)\text{-158}] = 47.1$ min.

GC obtained from the catalytic test reported in entry 3 of Table 16 (epoxy alcohol region).



GC obtained from epoxidation of *rac*-151 with *m*-CPBA(epoxy alcohol region).



X-Ray Crystal Structure Analysis of (2R,3R)-158

Crystals suitable for X-ray diffraction analysis were obtained by slow evaporation of a saturated solution of (2R,3R)-158 in *n*-pentane.

Table 20. Crystal data and structure refinement for (2R,3R)-158.

CCDC registry number	2132886
Empirical formula	$C_9H_{16}O_2$

Moiety formula	C ₉ H ₁₆ O ₂
Formula weight	156.22
Temperature	150(2) K
Wavelength	1.54178 Å
Crystal system	Monoclinic
Space group	P2 ₁
Unit cell dimensions	a = 5.2366(2) Å α = 90° b = 31.8952(10) Å β = 90.3810(10)° c = 10.4186(3) Å γ = 90°
Volume	1740.10(10) Å ³
Z	8
Density (calculated)	1.193 mg/m ³
Absorption coefficient	0.656 mm ⁻¹
F(000)	688
Crystal size	2.000 x 0.200 x 0.040 mm ³
Theta range for data collection	4.243 to 72.235°
Index ranges	-5 ≤ h ≤ 6, -39 ≤ k ≤ 39, -12 ≤ l ≤ 12
Reflections collected	35958
Independent reflections	6833 [R(int) = 0.0388]
Completeness to theta = 67.679°	99.7%
Absorption correction	Semi-empirical from equivalents
Max. and min. transmission	0.7536 and 0.6502
Refinement method	Full-matrix least-squares on F ²
Data / restraints / parameters	6833 / 1 / 405
Goodness-of-fit on F ²	1.053
Final R indices [I > 2σ(I)]	R1 = 0.0269, wR2 = 0.0726
R indices (all data)	R1 = 0.0273, wR2 = 0.0728
Absolute structure parameter	0.00(3)
Extinction coefficient	n/a
Largest diff. peak and hole	0.170 and -0.135 e•Å ⁻³

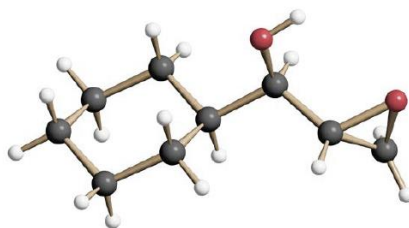
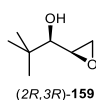


Figure 43. Molecular structure of epoxy alcohol (2*R*,3*R*)-158.

4.19.6. (2*R*,3*R*)-4,4-Dimethyl-1,2-epoxypentan-3-ol, (2*R*,3*R*)-159



Yellowish oil

$R_f = 0.29$ (SiO₂, Et₂O/*n*-pentane 3:7)

¹H-NMR (500 MHz, CDCl₃) δ [ppm] = 3.13 – 3.09 (m, 1H), 3.09 – 3.05 (m, 1H), 2.82 (dd, ²*J* = 5.0 Hz, ³*J* = 4.0 Hz, 1H), 2.69 (dd, ²*J* = 5.0, ³*J* = 2.8 Hz, 1H), 1.99 (s, 1H), 1.00 (s, 9H).

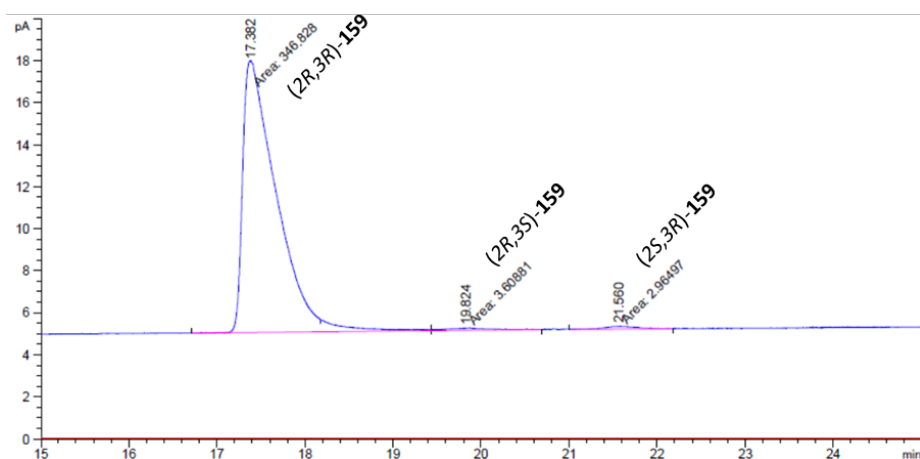
¹³C-NMR (125 MHz, CDCl₃) δ [ppm] = 78.4 (1C), 52.1 (1C), 45.4 (1C), 34.9 (1C), 25.8 (3C).

ATR: $\tilde{\nu}$ [cm⁻¹] = 3461 (br), 2956 (s), 2871 (s), 1704 (w), 1481 (s), 1417 (w), 1397 (m), 1365 (s), 1287 (w), 1256 (s), 1187 (s), 1135 (w), 1107 (s), 1061 (s), 1011 (s), 990 (w), 928 (s), 904 (s), 880 (s), 846 (s), 809 (m), 767 (m), 745 (m), 672 (m), 526 (s).

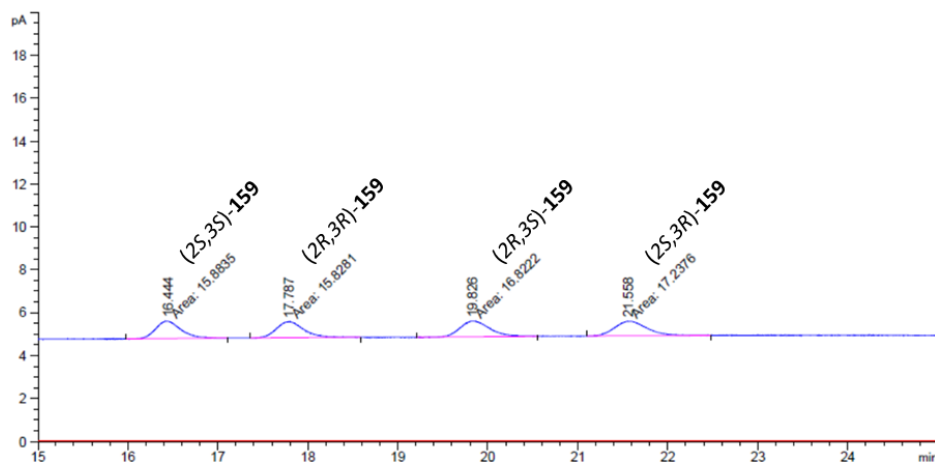
GC-MS (ESI+): *m/z* = 129.9 [M]⁺, 115.1 [M-CH₃]⁺, 98.1 [M-CH₄O]⁺, 85.1, 74.1, 69.1, 57.1 [C₄H₉]⁺.

Chiral GC: Chirasil-Dex CB split = 80:1; split flow = 100.2 mL/min, N₂; flow 1.3 mL/min; 80 °C isothermal 30 min, 10 °C/min to 100 °C isothermal 25 min, 10 °C/min to 180 °C isothermal 5 min; τ_R [(2*R*,3*R*)-159] = 17.4 min.

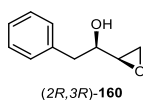
GC obtained from the catalytic test reported in entry 8 of Table 16 (epoxy alcohol region).



GC obtained from epoxidation of *rac*-152 with *m*-CPBA (epoxy alcohol region).



4.19.7. (2R,3R)-4-Phenyl-1,2-epoxybutan-3-ol, (2R,3R)-160



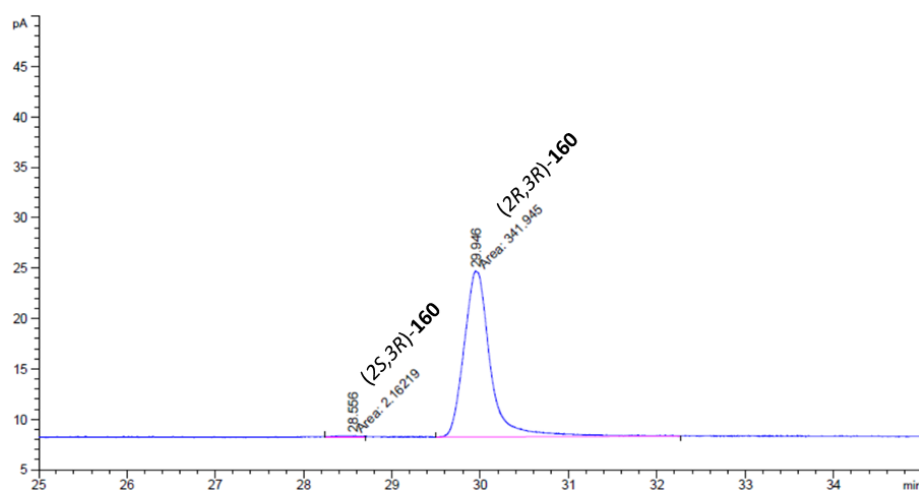
Colorless oil

$R_f = 0.17$ (SiO₂, Et₂O/*n*-pentane 1:6)

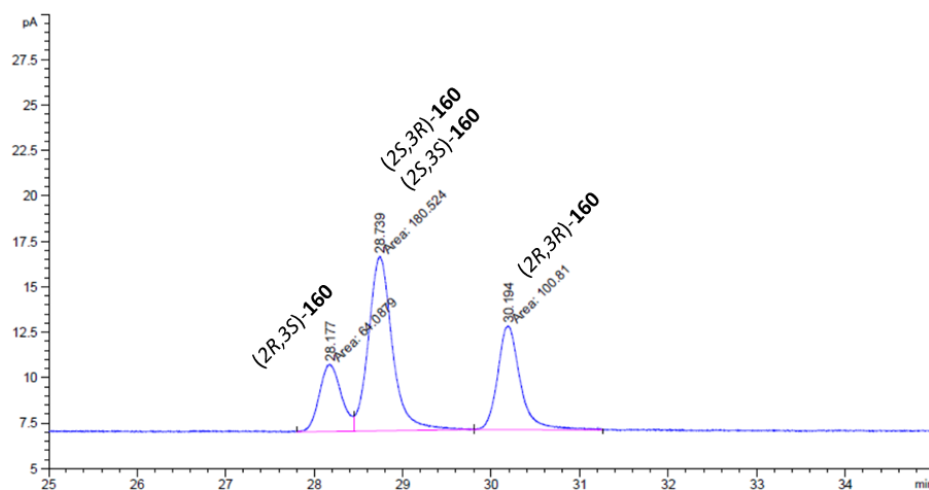
Characterization data are in agreement with the literature.^[215]

Chiral GC: Lipodex A split = 50:1; split flow = 50 mL/min, N₂; flow 1.0 mL/min; 120 °C isothermal 32 min, 10 °C/min to 180 °C isothermal 5 min; $\tau_R[(2R,3R)\text{-160}] = 29.9$ min.

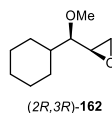
GC obtained from the catalytic test reported in entry 10 of Table 16 (epoxy alcohol region).



GC obtained from epoxidation of *rac*-153 with *m*-CPBA (epoxy alcohol region).



4.19.8. (2R,3R)-3-Cyclohexyl-3-methoxy-1,2-epoxypropan-3-ol, (2R,3R)-162



Yellowish oil

R_f = 0.25 (SiO₂, EtOAc/*c*-hexane 1:10)

$^1\text{H-NMR}$ (500 MHz, CDCl_3) δ [ppm] = 3.46 (s, 3H), 2.96 (ddd, $^3J = 7.2, 4.2, 2.8$ Hz, 1H), 2.77 (dd, $^2J = 4.9$ Hz, $^3J = 4.3$ Hz, 1H), 2.55 – 2.50 (m, 1H), 2.48 (dd, $^2J = 4.9$ Hz, $^3J = 2.8$ Hz, 1H), 1.89 – 1.82 (m, 1H), 1.78 – 1.69 (m, 3H), 1.69 – 1.6 (m, 1H), 1.62 – 1.50 (m, 1H), 1.29 – 0.99 (m, 5H).

$^{13}\text{C-NMR}$ (125 MHz, CDCl_3) δ [ppm] = 87.1 (1C), 58.6 (1C), 53.7 (1C), 43.6 (1C), 41.4 (1C), 29.3 (1C), 29.2 (1C), 26.6 (1C), 26.4 (1C), 26.3 (1C).

ATR: $\tilde{\nu}$ [cm^{-1}] = 3046 (w), 2980 (w), 2924 (s), 2853 (s), 2826 (m), 1450 (s), 1410 (w), 1310 (w), 1255 (w), 1185 (w), 1144 (w), 1102 (s), 1085 (s), 976 (m), 967 (m), 912 (s), 886 (s), 854 (s), 838 (s), 815 (s), 795 (w), 690 (w), 671 (w), 618 (m), 515 (s).

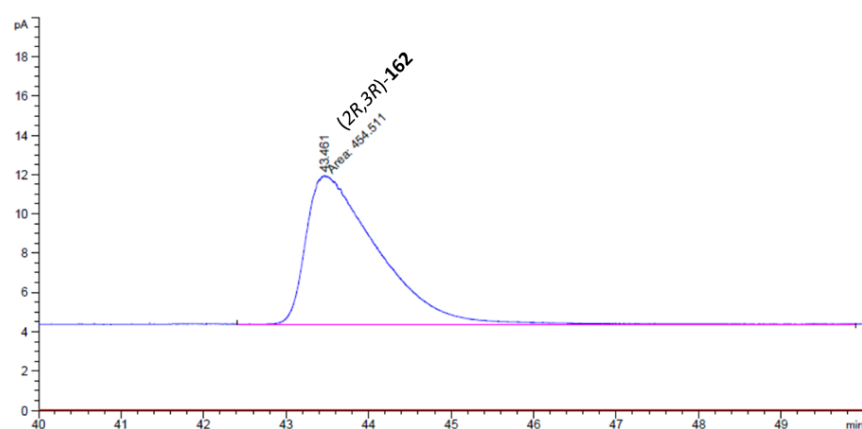
GC-MS (ESI+): m/z = 152.0 $[\text{M-H}_2\text{O}]^+$, 138.1 $[\text{M-CH}_4\text{O}]^+$, 127.1 $[\text{M-C}_2\text{H}_3\text{O}]^+$, 95.1, 87.0 $[\text{M-C}_6\text{H}_{11}]^+$, 79.1, 67.1, 55.1.

HR-GC-MS (ESI+): measured: m/z = 127.11160, theoretical: m/z 122.11229 $[\text{M-C}_2\text{H}_3\text{O}]^+$

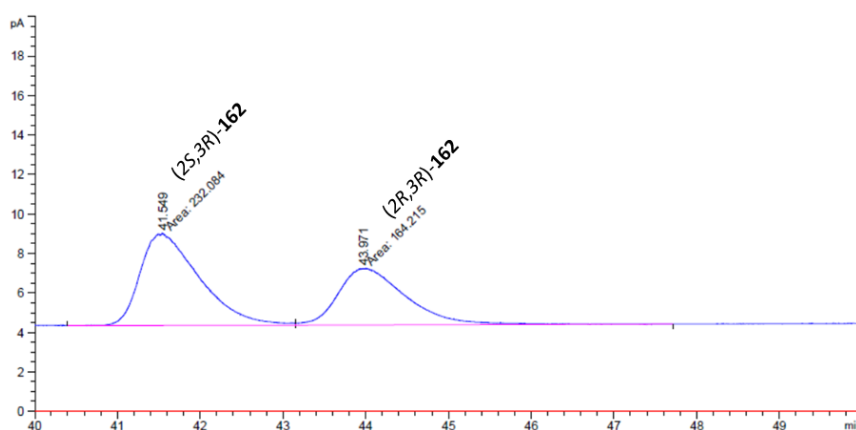
Elemental analysis: calcd (%) for $\text{C}_{10}\text{H}_{18}\text{O}_2$: C = 70.55; H = 10.66; found: C = 70.38; H = 10.55.

Chiral GC: Chirasil-Dex CB split = 80:1; split flow = 97.9 mL/min, N_2 ; flow 1.2 mL/min; 85 °C isothermal 50 min, 10 °C/min to 100 °C isothermal 16 min, 10 °C/min to 180 °C isothermal 5 min; $\tau_{\text{R}}[(2R,3R)\text{-162}] = 43.5$ min.

GC obtained from the catalytic test reported in entry 4 of Table 17 (epoxide region).



GC obtained from epoxidation of (*S*)-**161** with *m*-CPBA (epoxide region).



4.19.9. Synthesis of (2*R*,3*R*)-**162** through Methylation of (2*R*,3*R*)-**158**

Epoxy alcohol (2*R*,3*R*)-**158** (220 mg, 1.41 mmol, 1 eq) was dissolved in dry THF under argon atmosphere. NaH (60% in mineral oil, 37 mg, 1.55 mmol, 1.1 eq) was added in one portion at 0 °C, and the mixture was stirred at 0 °C for 15 minutes. MeI (97 μ L, 220 mg, 1.55 mmol, 1.1 eq) was added at 0 °C. The reaction was stirred at rt for 2 hours. The reaction was quenched with sat. aq. NH₄Cl (5 mL), then the crude was extracted with Et₂O (2 x 5 mL). The organic layers were dried over MgSO₄, filtered and concentrated under reduced pressure. The product was purified through chromatographic column (Et₂O/*n*-pentane 1:10 to 1:4). (2*R*,3*R*)-**162** was isolated as a colorless liquid.

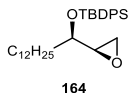
Yield: 125 mg (0.73 mmol, 52%).

Characterization data are in agreement with those shown in the previous paragraph.

Chiral GC: Chirasil-Dex CB split = 80:1; split flow = 97.9 mL/min, N₂; flow 1.2 mL/min; 85 °C isothermal 50 min, 10 °C/min to 100 °C isothermal 16 min, 10 °C/min to 180 °C isothermal 5 min; $\tau_R[(2*R*,3*R*)-\mathbf{162}] = 43.2$ min.

4.20. Synthesis of Building Block 167

4.20.1. *tert*-Butyl[*((R)*-1-[(*R*)-oxiran-2-yl]tridecyl)oxy]diphenylsilane (**164**)



Epoxy alcohol **145** (408 mg, 1.68 mmol, 1 eq) was dissolved in DCM (7 mL). The solution was cooled to 0 °C, and imidazole (344 mg, 5.05 mmol, 3 eq) and *tert*-butyl(chloro)diphenylsilane (525 μ L, 555 mg, 2.02 mmol, 1.2 eq) were added. The reaction mixture was left under stirring at rt overnight. The mixture was diluted with DCM (20 mL) and washed with water (20 mL). The aqueous phase was extracted again with DCM (2 x 10 mL). The combined organic layers were washed with brine, dried over MgSO₄, filtered, and concentrated under reduced pressure. Product **164** was isolated as a colorless oil and used without further purification.

Yield: 784 mg (1.63 mmol, 97%)

R_f = 0.26 (SiO₂, DCM/*c*-hexane 3:7)

¹H-NMR (500 MHz, CDCl₃) δ [ppm] = 7.77 – 7.64 (m, 4H), 7.46 – 7.40 (m, 2H), 7.40 – 7.32 (m, 4H), 3.36 (dd, ³J = 6.3 Hz, 1H), 3.05 (ddd, ³J = 6.7, 4.1, 2.7 Hz, 1H), 2.72 (dd, ²J = 4.9 Hz, ³J = 4.2 Hz, 1H), 2.47 (dd, ²J = 4.9 Hz, ³J = 2.7 Hz, 1H), 1.55 – 1.42 (m, 2H), 1.38 – 1.00 (m, 20H), 1.10 (s, 9H), 0.90 (t, ³J = 7.0 Hz, 3H).

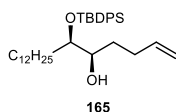
¹³C-NMR (125 MHz, CDCl₃) δ [ppm] = 136.1 (2C), 136.1 (2C), 134.4 (1C), 134.1 (1C), 129.7 (1C), 129.7 (1C), 127.6 (2C), 127.5 (2C), 75.3 (1C), 55.8 (1C), 45.0 (1C), 34.9 (1C), 32.1 (1C), 29.8 (1C), 29.8 (1C), 29.8 (1C), 29.7 (1C), 29.7 (1C), 29.6 (1C), 29.5 (1C), 27.2 (3C), 25.0 (1C), 22.9 (1C), 19.6 (1C), 14.3 (1C).

ATR: $\tilde{\nu}$ [cm⁻¹] = 3662 (w), 3072 (w), 3049 (w), 2924 (s), 2854 (s), 1958 (w), 1891 (w), 1823 (w), 1590 (w), 1464 (m), 1428 (s), 1391 (w), 1362 (w), 1308 (w), 1257 (w), 1105 (s), 1071 (s), 999 (w), 929 (br), 844 (w), 822 (m), 739 (m), 700 (s), 611 (s), 507 (s).

GC-MS (ESI+): m/z = 03.1, 465.3 [M-CH₃]⁺, 423.3 [M-C₄H₉]⁺, 393.3, 345.2, 225.1 [M-C₁₆H₁₉OSi]⁺, 199.1, 165.0, 139.0.

Elemental analysis: calcd. (%) for C₃₁H₄₈O₂Si: C = 77.44; H = 10.06; found: C = 77.45; H = 10.08.

4.20.2. (5*R*,6*R*)-6-[(*tert*-butyldiphenylsilyl)oxy]octadec-1-en-5-ol (**165**)



Compound **164** (723 mg, 1.50 mmol, 1 eq) was dissolved in dry THF (15 mL) under argon atmosphere. CuI (50 mg, 0.26 mmol, 0.17 eq) was added and the suspension was cooled to -78 °C. Allylmagnesium bromide (1 M solution in Et₂O, 4.5 mL, 4.51 mmol, 3 eq) was added dropwise. The reaction mixture was allowed to warm up to rt and left under stirring at rt for 1 hour. The reaction was cooled to 0 °C and quenched with sat. aq. NH₄Cl (20 mL). The organic phase was separated, and the aqueous layer was extracted with Et₂O (2 x 20 mL). The combined organic layers were washed with brine, dried over MgSO₄, filtered, and concentrated under reduced pressure. Product **165** was isolated through chromatographic column on silica gel (Et₂O/*c*-hexane 4:96) as a colorless oil.

Yield: 662 mg (1.27 mmol, 84%)

R_f = 0.30 (SiO₂, Et₂O/*c*-hexane 4:96)

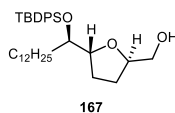
¹H-NMR (500 MHz, CDCl₃) δ [ppm] = 7.72 – 7.66 (m, 4H), 7.46 – 7.41 (m, 2H), 7.41 – 7.34 (m, 4H), 5.79 (ddt, ³J = 16.9, 10.2, 6.6 Hz, 1H), 5.01 – 4.96 (m, 1H), 4.96 – 4.92 (m, 1H), 3.61 – 3.54 (m, 1H), 3.54 – 3.46 (m, 1H), 2.22 (d, ³J = 7.1 Hz, 1H), 2.20 – 2.11 (m, 1H), 2.08 – 1.97 (m, 1H), 1.64 – 1.53 (m, 2H), 1.53 – 1.40 (m, 1H), 1.39 – 0.93 (m, 21H), 1.08 (s, 9H), 0.90 (t, ³J = 7.0 Hz, 3H).

¹³C-NMR (125 MHz, CDCl₃) δ [ppm] = 138.5 (1C), 136.0 (2C), 135.9 (2C), 134.1 (1C), 133.5 (1C), 129.8 (1C), 129.7 (1C), 127.7 (2C), 127.5 (2C), 114.6 (1C), 76.3 (1C), 72.2 (1C), 33.4 (1C), 33.2 (1C), 32.0 (1C), 30.1 (1C), 29.8 (CH₂), 29.8 (CH₂), 29.7 (CH₂), 29.6 (CH₂), 29.6 (CH₂), 29.5 (CH₂), 29.5 (CH₂), 27.3 (3C), 25.0 (1C), 22.8 (1C), 19.6 (1C), 14.2 (1C).

ATR: $\tilde{\nu}$ [cm⁻¹] = 3578 (w), 3073 (w), 3051 (w), 2924 (s), 2854 (s), 1957 (w), 1889 (w), 1823 (w), 1641 (w), 1590 (w), 1464 (m), 1428 (s), 1390 (w), 1378 (w), 1362 (w), 1306 (w), 1261 (w), 1190 (w), 1110 (s), 1074 (br), 998 (m), 910 (m), 821 (m), 739 (m), 700 (s), 608 (m), 505 (s).

GC-MS (ESI⁺): m/z = 490.3, 465.3 [M-C₄H₉]⁺, 437.4 [M-C₅H₉O]⁺, 409.3 [M-C₈H₁₇]⁺, 387.3, 355.2, 325.4, 281.0, 249.3, 199.1, 139.0, 109.1, 81.1, 57.1.

4.20.3. (2*R*,5*R*)-5-[(*R*)-1-[(*tert*-butyldiphenylsilyl)oxy]tridecyl]tetrahydrofuran-2-yl]methanol (167**)**



Compound **165** (1.69 g, 3.23 mmol, 1 eq) and titanium complex **138** (233 mg, 0.16 mmol, 0.05 eq) were dissolved in CHCl₃ (16.2 mL) in a 100 mL round bottom flask. The temperature was set to 20 °C, and H₂O₂ (50% solution in water, 275 μL, 4.85 mmol, 1.5 eq) was added. The reaction mixture was left under stirring at 20 °C and it was monitored through ¹H-NMR analysis. After 24 hours, 48 hours, and 72 hours, portions of 1.5 eq of H₂O₂ were added. After 96 hours, the reaction was filtered through MnO₂ and MgSO₄, rinsing with CHCl₃. The product was purified through two consecutive chromatographic columns on silica gel (EtOAc/c-Hex 1:9 to 1:4, and 100% DCM). Product **167** was isolated as a colorless liquid.

Yield: 1.38 g (2.57 mmol, 80%)

R_f = 0.42 (SiO₂, EtOAc/c-hexane 1:4)

¹H-NMR (500 MHz, CDCl₃) δ [ppm] = 7.80 – 7.65 (m, 4H), 7.45 – 7.39 (m, 2H), 7.39 – 7.33 (m, 4H), 3.93 (d^ψ-t, ³J = 7.9, 6.8 Hz, 1H), 3.76 – 3.68 (m, 1H), 3.61 – 3.50 (m, 1H), 3.36 (dd, ²J = 11.5 Hz, ³J = 3.0 Hz, 1H), 3.20 (dd, ²J = 11.5 Hz, ³J = 6.5 Hz, 1H), 1.96 – 1.70 (m, 2H), 1.57 – 1.45 (m, 2H), 1.45 – 1.09 (m, 22H), 1.05 (s, 9H), 0.90 (t, ³J = 6.9 Hz, 3H).

¹³C-NMR (125 MHz, CDCl₃) δ [ppm] = 136.3 (2C), 135.9 (2C), 135.6 (1C), 134.3 (1C), 129.4 (1C), 129.3 (1C), 127.4 (2C), 127.2 (2C), 82.2 (1C), 79.2 (1C), 76.6 (1C), 65.1 (1C), 33.4 (1C), 32.1 (1C), 29.8 (CH₂), 29.8 (CH₂), 29.8 (CH₂), 29.8 (CH₂), 29.7 (CH₂), 29.7 (CH₂), 29.5 (CH₂), 28.6 (1C), 27.8 (1C), 27.3 (3C), 25.3 (1C), 22.8 (1C), 19.8 (1C), 14.3 (1C).

ATR: $\tilde{\nu}$ [cm⁻¹] = 3571 (w), 3453 (br), 3071 (w), 3049 (w), 1957 (w), 1889 (w), 1823 (w), 1590 (w), 1464 (m), 1428 (m), 1389 (w), 1378 (w), 1361 (w), 1329 (w), 1261 (w), 1190 (w), 1110 (s), 1051 (s), 998 (w), 939 (w), 889 (w), 822 (m), 739 (m), 700 (s), 609 (m), 507 (s).

GC-MS (ESI+): m/z = 507.3 [M-CH₃O]⁺, 481.4 [M-C₄H₉]⁺, 461.0, 437.4 [M-C₅H₉O₂]⁺, 403.4, 379.1, 355.2, 281.1, 239.1 [C₁₆H₁₉Si]⁺, 199.1, 167.1, 135.1, 78.1, 57.1.

5. References

- [1] *IUPAC Compendium of Chemical Terminology*, Oxford: Blackwell Scientific Publications, **2009**.
- [2] a) M. Beller, C. Bolm, *Transition Metals for Organic Synthesis: Building Blocks and Fine Chemicals, Second Revised and Enlarged Edition*, WILEY-VCH, **2004** b) R. H. Crabtree, *The Organometallic Chemistry of the Transition Metals*, John Wiley & Sons, Inc., **2014** c) B. Roderick, *Organic Synthesis Using Transition Metals, 2nd ed.*, John Wiley & Sons, Inc., New York, **2012**.
- [3] The prices were obtained from: <http://www.infomine.com/investment/metal-prices/>; <https://tradingeconomics.com/commodities>; <http://www.sunsirs.com/commodity-price/>.
- [4] P. Anastas, N. Eghbali, *Chem. Soc. Rev.* **2010**, *39*, 301–312.
- [5] R. M. Bullock, *Catalysis without Precious Metals*, Wiley-VCH, **2010**.
- [6] For representative examples, see: a) J. F. Kirner, W. Dow, W. R. Scheidt, *Inorg. Chem.* **1976**, *15*, 1685; b) M. E. Silver, J. A. Ibers, *J. Am. Chem. Soc.* **1983**, *105*, 4108. c) S. H. Strauss, M. E. Silver, K. M. Long, R. G. Thompson, R. A. Hudgens, K. Spartalian, J. A. Ibers, *J. Am. Chem. Soc.* **1985**, *107*, 4207. d) R.A. Ghiladi, R. M. Kretzer, I. Guzei, A. L. Rheingold, Y.-M. Neuhold, K. R. Hatwell, A. D. Zuberbuhler, K. D. Karlin, *Inorg. Chem.* **2001**, *40*, 5754. e) D. Jacoby, C. Floriani, A. Chiesi-Villa, C. Rizzoli, *Chem. Commun.* **1991**, 220.
- [7] a) R. G. Pearson, *J. Am. Chem. Soc.* **1963**, *85*, 3533 – 3539; b) R. G. Pearson, *J. Chem. Educ.* **1968**, *45*, 581 – 586; c) R. G. Pearson, *J. Chem. Educ.* **1968**, *45*, 643 – 648.
- [8] a) B. Plietker, A. Dieskau, *Eur. J. Org. Chem.* **2009**, 775 – 787; b) O. G. Manchegno, *Angew. Chem. Int. Ed.* **2011**, *50*, 2216 – 2218; c) I. Bauer, H.-J. Knolker, *Chem. Rev.* **2015**, *115*, 3170 – 3387.
- [9] a) B. Plietker, *Iron Catalysis in Organic Chemistry*, Wiley-VCH Verlag, Weinheim, **2008**.
- [10] a) J. L. Pierre, M. Fontecave, *BioMetals* **1999**, *12*, 195–199; b) R. R. Crichton, *Inorganic Biochemistry of Iron Metabolism*, Ellis Horwood, Chichester, **1991**.
- [11] a) S. Blanchard, E. Derat, M. Desage-El Murr, L. Fensterbank, M. Malacria, V. Mouriès-Mansuy, *Eur. J. Inorg. Chem.* **2012**, 376–389; b) K. Hindson, *Eur. J. Inorg. Chem.* **2012**, 340.
- [12] H. Grützmacher, *Angew. Chem. Int. Ed.* **2008**, *47*, 1814–1818.
- [13] a) F. D. Toste, S. L. You, *Organometallics* **2019**, *38*, 3899–3901; b) S. Shaaban, C. Davies, H. Waldmann, *Eur. J. Org. Chem.* **2020**, *2020*, 6512–6524; c) I. Ojima, N. Clòs, C. Bastos, *Tetrahedron* **1989**, *45*, 6901–6939.
- [14] H. Brunner, *Angew. Chem. Int. Ed.* **1999**, *38*, 1194–1208.
- [15] M. Fontecave, O. Hamelin, S. Ménage, *Top. Organomet. Chem.* **2005**, *15*, 271–288.
- [16] S. J. Malcolmson, S. J. Meek, E. S. Sattely, R. R. Schrock, A. H. Hoveyda, *Nature* **2008**, *456*, 933–937.
- [17] a) E. B. Bauer, *Chem. Soc. Rev.* **2012**, *41*, 3153–3167; b) E. C. Constable, *Chem. Soc. Rev.* **2013**, *42*, 1637–1651.
- [18] a) T. Mukherjee, S. K. Ghosh, T. Wititsuwannakul, N. Bhuvanesh, J. A. Gladysz, *Organometallics* **2020**, *39*, 1163–1175; b) F. Santoro, M. Althaus, C. Bonaccorsi, S. Gischig, A. Mezzetti, *Organometallics* **2008**, *27*, 3866–3878; c) M. Lasa, P. Lopez, C. Cativiela, D. Carmona, L. A. Oro, *J. Mol. Catal.* **2005**, *234*, 129–135. d) H. Huo, C. Fu, K. Harms, E. Meggers *J. Am. Chem. Soc.* **2014**, *136*, 2990–2993; e) H. Huo, X. Shen, C. Wang, L. Zhang, P. Röse, L.-A. Chen, K. Harms, M. Marsch,

- G. Hilt, E. Meggers, *Nature* **2014**, *515*, 100–103; f) J. W. Feller, J. T. Nguyen, W. Ellis, M. R. Mazziere *Organometallics* **1993**, *12*, 1434–1438; g) G. Wang, Z. Zhou, X. Shen, S. Ivlev, E. Meggers *Chem. Commun.* **2020**, *56*, 7714–7717; h) F. Seidel, J. A. Gladysz, *Synlett* **2007**, *6*, 986–988; i) H. Huo, K. Harms, E. Meggers, *J. Am. Chem. Soc.* **2016**, *138*, 6936–6939; b) K. Kromm, P. L. Osburn, J. A. Gladysz, *Organometallics* **2002**, *21*, 4275–4280.
- [19] Y. Hong, L. Jarrige, K. Harms, E. Meggers, *J. Am. Chem. Soc.* **2019**, *141*, 4569–4572.
- [20] P. D. Knight, P. Scott, *Coord. Chem. Rev.* **2003**, *242*, 125–143.
- [21] E. J. Hawrelak, W. H. Bernskoetter, E. Lobkovsky, G. T. Yee, E. Bill, P. J. Chirik, *Inorg. Chem.* **2005**, *44*, 3103–3111.
- [22] H. Brunner, *Angew. Chem. Int. Ed.* **1971**, *10*, 249–260.
- [23] a) Z.-H. Yan, D. Li, X.-B. Yin, *Sci. Bull.* **2017**, *62*, 1344–1354; b) D. Carmona, R. Medrano, I. T. Dobrinovich, F. J. Lahoz, J. Ferrer, L. A. Oro, *J. Organomet. Chem.* **2006**, *691*, 5560–5566; c) H. Brunner, K. Fisch, P. G. Jones, J. Salbeck, *Angew. Chem. Int. Ed.* **1989**, *28*, 1521–1523.
- [24] a) H. Pellissier, *Coord. Chem. Rev.* **2019**, *386*, 1–31; b) L. Zhang, E. Meggers, *Chem. Asian J.* **2017**, *12*, 2335–2342.
- [25] a) H. Wen, G. Liu, Z. Huang, *Coord. Chem. Rev.* **2019**, *386*, 138–153; b) P. J. Chirik, *Acc. Chem. Res.* **2015**, *48*, 1687–1695.
- [26] a) L. Markó, M. A. Radhi, Irma Otvos, *J. Organomet. Chem.* **1981**, *218*, 369–376; b) M. A. Radhi, L. Marká, *J. Organomet. Chem.* **1984**, *262*, 359–364.
- [27] J.-S. Chen, L.-L. Chen, Y. Xing, G. Chen, W.-Y. Shen, Z.-R. Dong, Y.-Y. Li, J.-X. Gao *Acta Chim. Sin.* **2004**, *62*, 1745–1750.
- [28] S. Yu, W. Shen, Y. Li, Z. Dong, Y. Xu, Q. Li, J. Zhang, J. Gao, *Adv. Synth. Catal.* **2012**, *354*, 818–822.
- [29] Y. Y. Li, S. L. Yu, W. Y. Shen, J. X. Gao, *Acc. Chem. Res.* **2015**, *48*, 2587–2598.
- [30] A. Naik, T. Maji, O. Reiser, *Chem. Commun.* **2010**, *46*, 4475–4477.
- [31] a) C. Sui-Seng, F. Freutel, A. J. Lough, R. H. Morris, *Angew. Chem. Int. Ed.* **2008**, *47*, 940–943; b) N. Meyer, A. J. Lough, R. H. Morris, *Chem. Eur. J.* **2009**, *15*, 5605–5610. c) A. Mikhailine, A. J. Lough, R. H. Morris, *J. Am. Chem. Soc.* **2009**, *131*, 1394–1395; d) A. Mikhailine, M. I. Maishan, A. J. Lough, R. H. Morris, *J. Am. Chem. Soc.* **2012**, *134*, 12266–12280.
- [32] a) W. Zuo, A. J. Lough, Y. F. Li, R. H. Morris, *Science*, **2013**, *342*, 1080–1084; b) S. A. M. Smith, R. H. Morris, *Synthesis* **2015**, *47*, 1775–1779; c) K. Z. Demmans, C. S. G. Seo, A. J. Lough, R. H. Morris, *Chem. Sci.* **2017**, *8*, 6531–6541.
- [33] S. A. M. Smith, D. E. Prokopchuk, R. H. Morris, *Isr. J. Chem.* **2017**, *57*, 1204–1215.
- [34] A. Zirakzadeh, K. Kirchner, A. Roller, B. Stöger, M. Widhalm, R. H. Morris, *Organometallics* **2016**, *35*, 3781–3787.
- [35] a) J. F. Sonnenberg, K. Y. Wan, P. E. Sues, R. H. Morris, *ACS Catal.* **2017**, *7*, 316–326; b) S. A. M. Smith, P. O. Lagaditis, A. Lüpke, A. J. Lough, R. H. Morris, *Chem. Eur. J.* **2017**, *23*, 7212–7216.
- [36] R. Bigler, E. Otth, A. Mezzetti, *Organometallics* **2014**, *33*, 4086–4099.
- [37] R. Bigler, A. Mezzetti, *Org. Lett.* **2014**, *16*, 6460–6463.
- [38] a) R. Bigler, R. Huber, M. Stöckli, A. Mezzetti, *ACS Catal.* **2016**, *6*, 6455–6464; b) A. Mezzetti, *Isr. J. Chem.* **2017**, *57*, 1090–1105.
- [39] L. De Luca, A. Mezzetti, *Angew. Chem. Int. Ed.* **2017**, *56*, 11949–11953.

- [40] a) T. Cruchter, V. A. Larionov, *Coord. Chem. Rev.* **2018**, *376*, 95–113; b) K. P. Bryliakov, *Chem. Rev.* **2017**, *117*, 11406–11459.
- [41] a) G. Olivo, O. Cussó, M. Costas, *Chem. Asian J.* **2016**, *11*, 3148–3158; b) P. C. A. Bruijninx, G. Van Koten, R. J. M. Klein Gebbink, *Chem. Soc. Rev.* **2008**, *37*, 2716–2744.
- [42] M. Costas, A. K. Tipton, K. Chen, D. H. Jo, J. Que L., *J. Am. Chem. Soc.* **2001**, *123*, 6722–6723.
- [43] K. Suzuki, P. D. Oldenburg, L. Que, *Angew. Chem. Int. Ed.* **2008**, *47*, 1887–1889.
- [44] C. Zang, Y. Liu, Z.-J. Xu, C.-W. Tse, X. Guan, J. Wei, J.-S. Huang, C.-M. Che, *Angew. Chem. Int. Ed.* **2016**, *55*, 10253–10257.
- [45] M. Costas, L. Que, *Angew. Chem. Int. Ed.* **2002**, *41*, 2179–2181.
- [46] Y. Nishikawa, H. Yamamoto, *J. Am. Chem. Soc.* **2011**, *133*, 8432–8435.
- [47] M. Wu, C. X. Miao, S. Wang, X. Hu, C. Xia, F. E. Kühn, W. Sun, *Adv. Synth. Catal.* **2011**, *353*, 3014–3022.
- [48] B. Wang, S. Wang, C. Xia, W. Sun, *Chem. Eur. J.* **2012**, *18*, 7332–7335.
- [49] a) A. M. Zima, O. Y. Lyakin, R. V. Ottenbacher, K. P. Bryliakov, E. P. Talsi, *ACS Catal.* **2017**, *7*, 60–69; b) R. Mas-Ballesté, L. Que, *J. Am. Chem. Soc.* **2007**, *129*, 15964–15972.
- [50] a) Y. Wang, D. Janardanan, D. Usharani, K. Han, L. Que, S. Shaik, *ACS Catal.* **2013**, *3*, 1334–1341; b) O. Cussó, I. Garcia-Bosch, X. Ribas, J. Lloret-Fillol, M. Costas, *J. Am. Chem. Soc.* **2013**, *135*, 14871–14878.
- [51] W. Wang, Q. Sun, D. Xu, C. Xia, W. Sun, *ChemCatChem* **2017**, *9*, 420–424.
- [52] O. Cussó, M. Cianfanelli, X. Ribas, R. J. M. Klein Gebbink, M. Costas, *J. Am. Chem. Soc.* **2016**, *138*, 2732–2738.
- [53] a) A. Jalba, N. Régnier, T. Ollevier, *Eur. J. Org. Chem.* **2017**, *2017*, 1628–1637; b) J. Legros, C. Bolm, *Angew. Chem. Int. Ed.* **2004**, *43*, 4225–4228; c) J. Legros, C. Bolm, *Chem. Eur. J.* **2005**, *11*, 1086–1092; d) H. Egami, T. Katsuki, *J. Am. Chem. Soc.* **2007**, *129*, 8940–8941.
- [54] C. Duboc-Toia, S. Ménage, C. Lambeaux, M. Fontecave, *Tetrahedron Lett.* **1997**, *38*, 3727–3730.
- [55] F. Wang, L. Feng, S. Dong, X. Liu, X. Feng, *Chem. Commun.* **2020**, *56*, 3233–3236.
- [56] a) S. G. Davies, *Aldrichimica Acta* **1990**, *23*, 31–37; b) H. Brunner, B. Hammer, I. Bernal, M. Draux, *Organometallics* **1983**, *2*, 1595–1603.
- [57] S. G. Davies, *Pure Appl. Chem.* **1988**, *60*, 13–20.
- [58] a) S. G. Davies, J. C. Walker, **1986**, *03*, 609–610; b) K. Broadly, S. G. Davies, *Tetrahedron Lett.* **1984**, *25*, 1743–1744; c) S. G. Davies, N. Aktogu, H. Felkin, *J. Chem. Soc. Chem. Commun.* **1982**, 1303–1304; d) G. J. Baird, J. A. Bandy, S. G. Davies, K. Prout, *J. Chem. Soc. Chem. Commun.* **1983**, 1202–1203; e) H. Brunner, *Angew. Chem. Int. Ed.* **1999**, *38*, 1194–1208.
- [59] P. W. Ambler, S. G. Davies, *Tetrahedron Lett.* **1988**, *29*, 6983–6984.
- [60] a) M. Brookhart, Y. Liu, R. C. Buck, *J. Am. Chem. Soc.* **1988**, *110*, 2337–2339; b) M. Brookhart, R. C. Buck, *J. Organomet. Chem.* **1989**, *370*, 111–127.
- [61] J. Wei, B. Cao, C. W. Tse, X. Y. Chang, C. Y. Zhou, C. M. Che, *Chem. Sci.* **2020**, *11*, 684–693.
- [62] Y. Hong, T. Cui, S. Ivlev, X. Xie, E. Meggers, *Chem. Eur. J.* **2021**, *27*, 8557–8563.
- [63] W. Reppe, H. Vetter, *Justus Liebigs Ann. Chem.* **1953**, *582*, 133–161.
- [64] G. N. Schrauzer, *J. Am. Chem. Soc.* **1959**, *81*, 5307–5310.
- [65] a) H. J. Knölker, J. Heber, *Synlett* **1993**, 924–926; b) H. J. Knölker, E. Baum, J. Heber, *Tetrahedron*

- Lett.* **1995**, *36*, 7647–7650; c) H.-J. Knoelker, J. Heber, C. H. Mahler, *Synlett* **1992**, 1002–1004.
- [66] a) A. J. Pearson, R. J. Shivley Jr., R. A. Dubbert, *Organometallics* **1992**, *11*, 4096–4104; b) A. J. Pearson, R. J. Shively, *Organometallics*, **1994**, *13*, 578–584; c) A. J. Pearson, A. Perosa, *Organometallics* **1995**, *14*, 5178–5183; d) A. J. Pearson, X. Yao, *Synlett* **1997**, 1281–1282; e) A. J. Pearson, R. A. Dubbert, *J. Chem. Soc. Chem. Commun.* **1991**, *4*, 202–203.
- [67] H. J. Knölker, E. Baum, H. Goesmann, R. Klauss, *Angew. Chem. Int. Ed.* **1999**, *38*, 2064–2066.
- [68] W. Hieber, F. Leutert, *Z. Anorg. Allg. Chem.* **1931**, *204*, 145–164.
- [69] a) C. P. Casey, H. Guan, *J. Am. Chem. Soc.* **2007**, *129*, 5816–5817; b) C. P. Casey, H. Guan, *J. Am. Chem. Soc.* **2009**, *131*, 2499–2507.
- [70] a) Y. Blum, D. Czarkle, Y. Rahamin, Y. Shvo, *Organometallics* **1986**, *4*, 1459–1461; b) R. T. Weberg, J. R. Norton, *J. Am. Chem. Soc.* **1990**, *112*, 1105–1108; c) B. L. Conley, M. K. Pennington-Boggio, E. Boz, T. J. Williams, *Chem. Rev.* **2010**, *110*, 2294–2312.
- [71] J. S. M. Samec, J. E. Bäckvall, P. G. Andersson, P. Brandt, *Chem. Soc. Rev.* **2006**, *35*, 237–248.
- [72] B. Schneider, I. Goldberg, D. Reshef, Z. Stein, Y. Shvo, *J. Organomet. Chem.* **1999**, *588*, 92–98.
- [73] a) R. M. Bullock, *Angew. Chem. Int. Ed.* **2007**, *46*, 7360–7363; b) G. Bauer, K. A. Kirchner, *Angew. Chem. Int. Ed.* **2011**, *50*, 5798–5800.
- [74] A. Tlili, J. Schranck, H. Neumann, M. Beller, *Chem. Eur. J.* **2012**, *18*, 15935–15939.
- [75] T. Y. Luh, *Coord. Chem. Rev.* **1984**, *60*, 255–276.
- [76] A. Berkessel, S. Reichau, A. Von Der Höh, N. Leconte, J. M. Neudörfl, *Organometallics* **2011**, *30*, 3880–3887.
- [77] A. Quintard, J. Rodriguez, *Angew. Chem. Int. Ed.* **2014**, *53*, 4044–4055.
- [78] S. Fleischer, S. Zhou, K. Junge, M. Beller, *Angew. Chem. Int. Ed.* **2013**, *52*, 5120–5124.
- [79] F. Zhu, L. Zhu-Ge, G. Yang, S. Zhou, *ChemSusChem* **2015**, *8*, 609–612.
- [80] A. Rosas-Hernández, P. G. Alsabeh, E. Barsch, H. Junge, R. Ludwig, M. Beller, *Chem. Commun.* **2016**, *52*, 8393–8396.
- [81] P. Gajewski, A. Gonzalez-de-Castro, M. Renom-Carrasco, U. Piarulli, C. Gennari, J. G. de Vries, L. Lefort, L. Pignataro, *ChemCatChem* **2016**, *8*, 3431–3435.
- [82] D. Wei, C. Netkaew, C. Darcel, *Eur. J. Inorg. Chem.* **2019**, 2471–2487; b) J. L. Renaud, S. Gaillard, *Synthesis* **2016**, *48*, 3659–3683; c) A. Corma, J. Navas, M. J. Sabater, *Chem. Rev.* **2018**, *118*, 1410–1459.
- [83] a) D. Wie, C. Netkaew, C. Darcel, *Eur. J. Inorg. Chem.* **2019**, *2019*, 2471–2487; b) A. Corma, J. Navas, M. J. Sabater, *Chem. Rev.* **2018**, *118*, 1410–1459; c) A. Quintard, J. Rodriguez, *ChemSusChem* **2016**, *9*, 28–30; d) Q. Yang, Q. Wang, Z. Yu, *Chem. Soc. Rev.* **2015**, *44*, 2305–2329; e) J. M. Ketcham, I. Shin, T. P. Montgomery, M. J. Krische, *Angew. Chem. Int. Ed.* **2014**, *53*, 9142–9150; f) C. Gunanathan, D. Milstein, *Science* **2013**, *341*, 1229712; g) S. Bähn, S. Imm, L. Neubert, M. Zhang, H. Neumann, M. Beller, *ChemCatChem* **2011**, *3*, 1853–1864; h) A. J. A. Watson, J. M. J. Williams, *Science* **2010**, *329*, 635–636; i) G. Guillena, D. J. Ramón, M. Yus, *Chem. Rev.* **2010**, *110*, 1611–1641; j) T. D. Nixon, M. K. Whittlesey, J. M. J. Williams, *Dalton Trans.* **2009**, 753–762; k) M. H. S. A. Hamid, P. A. Slatford, J. M. J. Williams, *Adv. Synth. Catal.* **2007**, *349*, 1555–1575.
- [84] S. Elangovan, J. Sortais, M. Beller, C. Darcel, *Angew. Chem. Int. Ed.* **2015**, *2*, 14483–14486.
- [85] T. Yan, B. L. Feringa, K. Barta, *Nat. Commun.* **2014**, *5*, 1–7.

- [86] H. J. Pan, T. W. Ng, Y. Zhao, *Chem. Commun.* **2015**, 51, 11907–11910.
- [87] B. Emayavaramban, M. Sen, B. Sundararaju, *Org. Lett.* **2017**, 19, 6–9.
- [98] O. El-Sepelgy, A. Brzozowska, L. M. Azofra, Y. K. Jang, L. Cavallo, M. Rueping, *Angew. Chem. Int. Ed.* **2017**, 56, 14863–14867.
- [89] a) A. Gudmundsson, K. P. J. Gustafson, B. K. Mai, V. Hobiger, F. Himo, J. E. Bäckvall, *ACS Catal.* **2019**, 9, 1733–1737; b) A. Gudmundsson, K. P. J. Gustafson, B. K. Mai, B. Yang, F. Himo, J. E. Bäckvall, *ACS Catal.* **2018**, 8, 12–16; c) O. El-Sepelgy, A. Brzozowska, J. Sklyaruk, Y. K. Jang, V. Zubar, M. Rueping, *Org. Lett.* **2018**, 20, 696–699.
- [90] L. Pignataro, C. Gennari, *Eur. J. Org. Chem.* **2020**, 3192–3205.
- [91] a) T. N. Plank, J. L. Drake, D. K. Kim, T. W. Funk, *Adv. Synth. Catal.* **2012**, 354, 597–601; b) S. Moulin, H. Dentel, A. Pagnoux-Ozherelyeva, S. Gaillard, A. Poater, L. Cavallo, J. F. Lohier, J. L. Renaud, *Chem. Eur. J.* **2013**, 19, 17881–17890.
- [92] S. Elangovan, S. Quintero-Duque, V. Dorcet, T. Roisnel, L. Norel, C. Darcel, J. B. Sortais, *Organometallics* **2015**, 34, 4521–4528.
- [93] H. J. Pan, T. W. Ng, Y. Zhao, *Org. Biomol. Chem.* **2016**, 14, 5490–5493.
- [94] a) S. Moulin, H. Dentel, A. Pagnoux-Ozherelyeva, S. Gaillard, A. Poater, L. Cavallo, J. F. Lohier, J. L. Renaud, *Chem. Eur. J.* **2013**, 19, 17881–17890; b) T. T. Thai, D. S. Mérel, A. Poater, S. Gaillard, J. L. Renaud, *Chem. Eur. J.* **2015**, 21, 7066–7070.
- [95] S. Vailati Facchini, J. M. Neudörfl, L. Pignataro, M. Cettolin, C. Gennari, A. Berkessel, U. Piarulli, *ChemCatChem* **2017**, 9, 1461–1468.
- [96] T. T. Thai, D. S. Mérel, A. Poater, S. Gaillard, J. L. Renaud, *Chem. Eur. J.* **2015**, 21, 7066–7070.
- [97] S. Coufourier, S. Gaillard, G. Clet, C. Serre, M. Daturi, J. L. Renaud, *Chem. Commun.* **2019**, 55, 4977–4980.
- [98] a) K. Polidano, B. D. W. Allen, J. M. J. Williams, L. C. Morrill, *ACS Catal.* **2018**, 8, 6440–6445; b) C. Seck, M. D. Mbaye, S. Coufourier, A. Lator, J. F. Lohier, A. Poater, T. R. Ward, S. Gaillard, J. L. Renaud, *ChemCatChem* **2017**, 9, 4410–4416; c) L. Bettoni, C. Seck, M. Di. Mbaye, S. Gaillard, J. L. Renaud, *Org. Lett.* **2019**, 21, 3057–3061; d) L. Bettoni, S. Gaillard, J. L. Renaud, *Org. Lett.* **2019**, 21, 8404–8408.
- [99] a) M. B. Dambatta, K. Polidano, A. D. Northey, J. M. J. Williams, L. C. Morrill, *ChemSusChem* **2019**, 12, 2345–2349; b) C. Seck, M. D. Mbaye, S. Gaillard, J. L. Renaud, *Adv. Synth. Catal.* **2018**, 360, 4640–4645.
- [100] A. Lator, Q. G. Gaillard, D. S. Mérel, J. F. Lohier, S. Gaillard, A. Poater, J. L. Renaud, *J. Org. Chem.* **2019**, 84, 6813–6829.
- [101] A. Lator, S. Gaillard, A. Poater, J. L. Renaud, *Chem. Eur. J.* **2018**, 24, 5770–5774.
- [102] M. Cettolin, X. Bai, D. Lübken, M. Gatti, S. V. Facchini, U. Piarulli, L. Pignataro, C. Gennari, *Eur. J. Org. Chem.* **2019**, 2019, 647–654.
- [103] L. Tadiello, T. Gandini, B. M. Stadler, S. Tin, H. Jiao, J. G. de Vries, L. Pignataro, C. Gennari, *ACS Catal.* **2022**, 12, 235–246.
- [104] U. Piarulli, S. V. Fachini, L. Pignataro, *Chimia*, **2017**, 71, 580–585.
- [105] a) T. C. Johnson, G. J. Clarkson, M. Wills, *Organometallics* **2011**, 30, 1859–1868; b) J. P. Hopewell, E. D. Martins, T. C. Johnson, J. Godfrey, M. Wills, *Org. Biomol. Chem.* **2012**, 134–145.

- [106] a) P. Gajewski, M. Renom-Carrasco, S. V. Facchini, L. Pignataro, L. Lefort, J. G. De Vries, R. Ferraccioli, U. Piarulli, C. Gennari, *Eur. J. Org. Chem.* **2015**, *2015*, 5526–5536; b) P. Gajewski, M. Renom-Carrasco, S. V. Facchini, L. Pignataro, L. Lefort, J. G. De Vries, R. Ferraccioli, A. Forni, U. Piarulli, C. Gennari, *Eur. J. Org. Chem.* **2015**, *2015*, 1887–1893.
- [107] R. Hodgkinson, A. Del Grosso, G. Clarkson, M. Wills, *Dalton Trans.* **2016**, *45*, 3992–4005.
- [108] A. Del Grosso, A. E. Chamberlain, G. J. Clarkson, M. Wills, *Dalton Trans.* **2018**, *47*, 1451–1470.
- [109] C. A. M. R. Van Slagmaat, K. C. Chou, L. Morick, D. Hadavi, B. Blom, S. M. A. De Wildeman, *Catalysts* **2019**, *9*, 790.
- [110] X. Bai, M. Cettolin, G. Mazzocanti, M. Pierini, U. Piarulli, V. Colombo, A. Dal Corso, L. Pignataro, C. Gennari, *Tetrahedron* **2019**, *75*, 1415–1424.
- [111] H.-J. Knoelker, J. Heber, C. H. Mahler, *Synlett* **1992**, 1002–1004.
- [112] C. G. Krespan, *J. Org. Chem.* **1975**, *40*, 261–262.
- [113] D. Fornals, M. A. Pericas, F. Serratosa, J. Vinaixa, M. Font-Altaba, X. Solans, *J. Chem. Soc., Perkin Trans. 1* **1987**, 2749–2752.
- [114] J. L. Boston, D. W. A. Sharp, G. Wilkinson, *J. Chem. Soc.* **1962**, 3488–3494.
- [115] a) P. L. Pauson, *Tetrahedron*, **1985**, *41*, 5855–5860; b) A. J. Pearson, R. A. Dubbertb, *J. Chem. Soc. Chem. Commun.* **1991**, 202–203; c) J. B. Urgoiti, L. Añorbe, L. P. Serrano, G. Domínguez, J. Pérez-Castells, *Chem. Soc. Rev.* **2004**, *33*, 32–42.
- [116] W. J. Kerr, M. McLaughlin, P. L. Pauson, S. M. Robertson, *J. Organomet. Chem.* **2001**, *630*, 104–117.
- [117] K. Banert, O. Plefka, *Angew. Chem. Int. Ed.* **2011**, *50*, 6171–6174.
- [118] T. Hagendorn, S. Bräse, *Eur. J. Org. Chem.* **2014**, *2014*, 1280–1286.
- [119] K. Sonogashira, Y. Tohda, N. Hagihara, *Tetrahedron Lett.* **1975**, *50*, 4467–4470.
- [120] R. D. Stephens, C. E. Castro, *J. Org. Chem.* **1963**, *28*, 3313–3315.
- [121] L. Cassar, *J. Org. Chem.* **1975**, *93*, 253–257.
- [122] H. A. Dieck, F. R. Heck, *J. Organomet. Chem.* **1975**, *93*, 259–263.
- [123] M. Karak, L. C. A. Barbosa, G. C. Hargaden, *RSC Adv.* **2014**, *4*, 53442–53466.
- [124] R. Chinchilla, C. Nájera, *Chem. Rev.* **2007**, *107*, 874–922.
- [125] R. Chinchilla, C. Nájera, *Chem. Soc. Rev.* **2011**, *40*, 5084–5121.
- [126] P. Siemens, R. C. Livingston, F. Diederich, *Angew. Chem. Int. Ed.* **2000**, *39*, 2632–2657.
- [127] M. Erdélyi, A. Gogoll, *J. Org. Chem.* **2001**, *66*, 4165–4169.
- [128] a) C. Yi, R. Hua, *J. Org. Chem.* **2006**, *71*, 2535–2537; b) V. P. W Böhm, W. A. Herrmann, *Eur. J. Org. Chem.* **2000**, 3679–3681.
- [129] R. Martin, S. L. Buchwald, *Acc. Chem. Res.* **2008**, *41*, 1461–1473.
- [130] D. Gelman, S. L. Buchwald, *Angew. Chemie* **2003**, *115*, 6175–6178.
- [131] a) J. C. Hierso, A. Fihri, R. Amardeil, P. Meunier, H. Doucet, M. Santelli, *Tetrahedron* **2005**, *61*, 9759–9766; b) C. Yang, S. P. Nolan, *Organometallics* **2002**, *21*, 1020–1022.
- [132] M. Feuerstein, F. Berthiol, H. Doucet, M. Santelli, *Org. Biomol. Chem.* **2003**, *1*, 2235–2237.
- [133] T. Brenstrum, J. Clattenburg, J. Britten, S. Zavorine, J. Dyck, A. J. Robertson, J. McNulty, A. Capretta, *Org. Lett.* **2006**, *8*, 103–105.
- [134] T. Ljungdahl, K. Pettersson, B. Albinsson, J. Mårtensson, *J. Org. Chem.* **2006**, *71*, 1677–1687.
- [135] a) M. Eckhardt, G. C. Fu, *J. Am. Chem. Soc.* **2003**, *125*, 13642–13643; b) R. A. Batey, M. Shen, A. J.

- Lough, *Org. Lett.* **2002**, *4*, 1411–1414.
- [136] Y. Liang, Y. X. Xie, J. H. Li, *J. Org. Chem.* **2006**, *71*, 379–381.
- [137] H. Yang, J. L. Petersen, K. K. Wang, *Tetrahedron* **2006**, *62*, 8133–8141.
- [138] V. H. G. Rohde, M. F. Müller, M. Oestreich, *Organometallics* **2015**, *34*, 3358–3373.
- [139] G. Wang, C. Chen, J. Peng, *Chem. Commun.* **2016**, *52*, 10277–10280.
- [140] S. Saleh, M. Picquet, P. Meunier, J. C. Hierso, *Synlett* **2011**, 2844–2848.
- [141] S. Yan, W. Xia, S. Li, Q. Song, S. H. Xiang, B. Tan, *J. Am. Chem. Soc.* **2020**, *142*, 7322–7327.
- [142] F. Yang, S. Wei, C. A. Chen, P. Xi, L. Yang, J. Lan, H. M. Gau, J. You, *Chem. Eur. J.* **2008**, *14*, 2223–2231.
- [143] F. Octa-Smolín, F. Van Der Vight, R. Yadav, J. Bhangu, K. Soloviova, C. Wölper, C. G. Daniliuc, C. A. Strassert, H. Somnitz, G. Jansen, J. Niemeyer, *J. Org. Chem.* **2018**, *83*, 14568–14587.
- [144] H. T. Chang, M. Jeganmohan, C. H. Cheng, *Org. Lett.* **2007**, *9*, 505–508.
- [145] C. C. W. Law, J. W. Y. Lam, Y. Dong, H. Tong, B. Z. Tang, *Macromolecules* **2005**, *38*, 660–662.
- [146] K. Bauer, J. Sy, F. Lipmann, *Chem. Lett.* **1973**, *21*, 1154–1157.
- [147] a) L. Lombardo, *Org. Synth.* **1987**, *65*, 81; b) K. Takai, T. Kakiuchi, Y. Kataoka, K. Utimoto, *J. Org. Chem.* **1994**, *59*, 2668–2670.
- [148] S. Okamoto, *Chem. Rec.* **2016**, *16*, 857–872.
- [149] T. Katsuki, B. Sharpless, *J. Am. Chem. Soc.* **1980**, *102*, 5974–5976.
- [150] M. Manßen, L. L. Schafer, *Chem. Soc. Rev.* **2020**, *49*, 6947–6994.
- [151] a) Y. Liu, J. Schwartz, *Tetrahedron* **1995**, *51*, 4471–4482; b) M. C. Barden, J. Schwartz, *J. Org. Chem.* **1995**, *60*, 5963–5965.
- [152] a) U. Kölle, P. Kölle, *Angew. Chem. Int. Ed.* **2003**, *42*, 4540–4542; b) E. M. Zolnhofer, G. B. Wijeratne, T. A. Jackson, S. Fortier, F. W. Heinemann, K. Meyer, J. Krzystek, A. Ozarowski, D. J. Mindiola, J. Telser, *Inorg. Chem.* **2020**, *59*, 6187–6201.
- [153] a) E. S. Gould, *Coord. Chem. Rev.* **2011**, *255*, 2882–2891; b) J. M. Birmingham, A. K. Fischer, G. Wilkinson, *Naturwissenschaften* **1955**, *42*, 96.
- [154] R. Hoff and R. T. Mathers, *Handbook of Transition Metals Polymerization Catalysts*, John Wiley & Sons, Inc, Hoboken, NJ, **2010**.
- [155] O. Vassilyev, A. Panarello, J. G. Khinast, *Molecules* **2005**, *10*, 587–619.
- [156] a) T. E. Müller, K. C. Hultsch, M. Yus, F. Foubelo, M. Tada, *Chem. Rev.* **2008**, *108*, 3795–3892; b) I. Bytschkov, S. Doye, *Eur. J. Org. Chem.* **2003**, 935–946; c) L. L. Schafer, M. Manßen, P. M. Edwards, E. K. J. Lui, S. E. Griffin, C. R. Dunbar, P. J. Pérez, *Adv. Organomet. Chem.* **2020**, *74*, 405–468.
- [157] a) J. E. Hill, G. Balaich, P. E. Fanwick, I. P. Rothwell, *Organometallics* **1993**, *12*, 2911–2924; b) Z. W. Gilbert, R. J. Hue, I. A. Tonks, *Nat. Chem.* **2016**, *8*, 63–68; c) O. V. Ozerov, F. T. Ladipo, B. O. Patrick, *J. Am. Chem. Soc.* **1999**, *121*, 7941–7942; d) J. B. Urgoiti, L. Añorbe, L. P. Serrano, G. Domínguez, J. Pérez-Castells, *Chem. Soc. Rev.* **2004**, *33*, 32–42.
- [158] O. G. Kulinkovich, *Chem. Rev.* **2003**, *103*, 2597–2632.
- [159] a) E. P. Beaumier, A. J. Pearce, X. Y. See, I. A. Tonks, *Nat. Rev. Chem.* **2019**, *3*, 15–34; b) Z. W. Davis-Gilbert, I. A. Tonks, *Dalton Trans.* **2017**, *46*, 11522–11528.
- [160] W. Kaminsky, *J. Chem. Soc., Dalton Trans.* **1998**, 1413–1418.
- [161] F. N. Tebbe, G. W. Parshall, G. S. Reddy, *J. Am. Chem. Soc.* **1978**, *100*, 3611–3613.

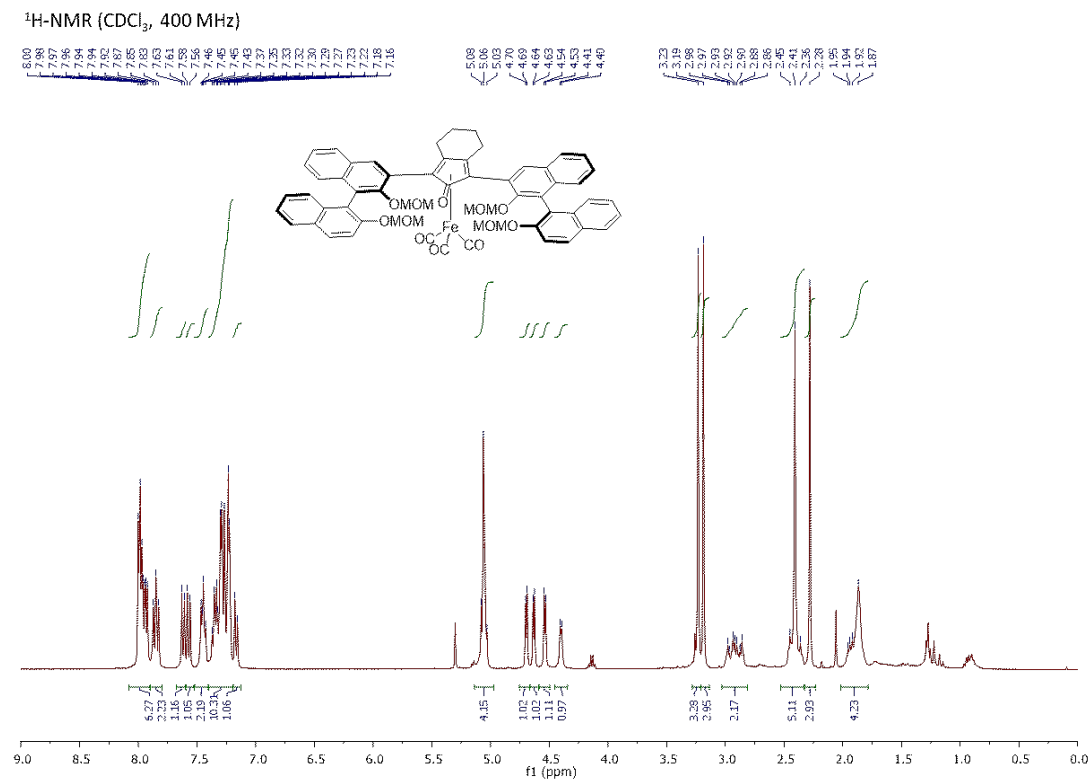
- [162] a) N. Petasis, E. Bzowej, *J. Am. Chem. Soc.* **1990**, *112*, 6392–6394; b) R. C. Hartley, J. Li, C. A. Main, G. J. McKiernan, *Tetrahedron* **2007**, *63*, 4825–4864.
- [163] a) S. B. Smith, D. W. Stephan, *Compr. Coord. Chem. II* **2003**, *4*, 31–104; b) L. N. Grant, J. R. Aguilar-Calderón, D. J. Mindiola, *Compr. Coord. Chem.* **2021**, 97–161.
- [164] a) C. T. Dalton, K. M. Ryan, V. M. Wall, C. Bousquet, D. G. Gilheany, *Top. Catal.* **1998**, *5*, 75–91; b) L. Canali, D. C. Sherrington, *Chem. Soc. Rev.* **1999**, *28*, 85–93; c) P. G. Cozzi, *Chem. Soc. Rev.* **2004**, *33*, 410–421; d) J. F. Larrow, E. N. Jacobsen, *Top. Organomet. Chem.* **2017**, *6*, 123–152.
- [165] a) T. Katsuki, *Synlett* **2003**, 281–297; b) K. Matsumoto, B. Saito, T. Katsuki, *Chem. Commun.* **2007**, 3619–3627.
- [166] T. Katsuki, *Chem. Soc. Rev.* **2004**, *33*, 437–444.
- [167] H. Sasaki, R. Irie, T. Hamada, K. Suzuki, T. Katsuki, *Tetrahedron* **1994**, *50*, 11827–11838.
- [168] T. Katsuki, *J. Mol. Catal. A Chem.* **1996**, *113*, 87–107.
- [169] a) B. Saito, T. Katsuki, *Tetrahedron Lett.* **2001**, *42*, 3873–3876; b) K. Matsumoto, Y. Sawada, B. Saito, K. Sakai, T. Katsuki, *Angew. Chem. Int. Ed.* **2005**, *44*, 4935–4939.
- [170] a) M. Tsuchimoto, *Bull. Chem. Soc. Jpn.* **2001**, *74*, 2101–2105; b) Y. N. Belokon, S. Caveda-Cepas, B. Green, N. S. Ikonnikov, V. N. Khrustalev, V. S. Larichev, M. A. Moscalenko, M. North, C. Orizu, V. I. Tararov, M. Tasinazzo, G. I. Timofeeva, L. V. Yashkina, *J. Am. Chem. Soc.* **1999**, *121*, 3968–3973.
- [171] a) K. Matsumoto, B. Saito, T. Katsuki, *Chem. Commun.* **2007**, 3619–3627; b) K. Matsumoto, Y. Sawada, T. Katsuki, *Synlett* **2006**, 3545–3547.
- [172] A. Berkessel, M. Brandenburg, E. Leitterstorf, J. Frey, J. Lex, M. Schäfer, *Adv. Synth. Catal.* **2007**, *349*, 2385–2391.
- [173] A. Berkessel, M. Brandenburg, M. Schäfer, *Adv. Synth. Catal.* **2008**, *350*, 1287–1294.
- [174] A. Berkessel, M. C. Ong, M. Nachi, J. M. Neudörfl, *ChemCatChem* **2010**, *2*, 1215–1218.
- [175] A. Berkessel, T. Günther, Q. Wang, J. M. Neudörfl, *Angew. Chem. Int. Ed.* **2013**, *52*, 8467–8471.
- [176] Q. Wang, J. M. Neudörfl, A. Berkessel, *Chem. Eur. J.* **2015**, *21*, 247–254.
- [177] M. Lansing, H. Engler, T. M. Leuther, J. M. Neudörfl, A. Berkessel, *ChemCatChem* **2016**, *8*, 3706–3709.
- [178] H. Engler, M. Lansing, C. P. Gordon, J. M. Neudörfl, M. Schäfer, N. E. Schlörer, C. Copéret, A. Berkessel, *ACS Catal.* **2021**, *11*, 3206–3217.
- [179] Y. Gao, R. M. Hanson, J. M. Klunder, S. Y. Ko, H. Masamune, K. B. Sharpless, *J. Am. Chem. Soc.* **1987**, *109*, 5765–5780.
- [180] R. M. Hanson, K. B. Sharpless, *J. Org. Chem.* **1986**, *51*, 1922–1925.
- [181] V. S. Martin, S. S. Woodard, T. Katsuki, Y. Yamada, M. Ikeda, K. B. Sharpless, *J. Am. Chem. Soc.* **1981**, *103*, 6237–6240.
- [182] G. Della Sala, L. Giordano, A. Lattanzi, A. Proto, A. Scettri, *Tetrahedron* **2000**, *56*, 3567–3573.
- [183] a) Z. Li, H. Yamamoto, *Acc. Chem. Res.* **2013**, *46*, 506–518; b) Z. Li, W. Zhang, H. Yamamoto, *Angew. Chem. Int. Ed.* **2008**, *47*, 7520–7522; c) W. Zhang, A. Basak, Y. Kosugi, Y. Hoshino, H. Yamamoto, *Angew. Chem. Int. Ed.* **2005**, *44*, 4389–4391.
- [184] a) W. Adam, R. Kumar, T. I. Reddy, M. Renz, *Angew. Chem. Int. Ed.* **1996**, *35*, 880–882; b) W. Adam, A. Corma, A. Martínez, C. M. Mitchell, T. I. Reddy, M. Renz, A. K. Smerz, *J. Moleculr Catal.* **1997**, *117*, 357–366.

- [185] W. Adam, T. Wirth, *Acc. Chem. Res.* **1999**, *32*, 703–710.
- [186] R. Doran, P. J. Guiry, *Synth.* **2014**, *46*, 761–770.
- [187] J. Mao, J. Zhong, B. Wang, J. Jin, S. Li, Z. Gao, H. Yang, Q. Bian, *Tetrahedron Asymmetry* **2016**, *27*, 330–337.
- [188] H. Lin, Y. Liu, Z. L. Wu, *Chem. Commun.* **2011**, *47*, 2610–2612.
- [189] H. Lin, Y. Tang, S. Dong, R. Lang, H. Chen, *Catal. Sci. Technol.* **2020**, *10*, 2145–2151.
- [190] a) A. Ghanem, H. Y. Aboul-Enein, *Chirality* **2005**, *17*, 1–15; b) F. A. Marques, M. A. Oliveira, G. Frensch, B. Helena L. N. Sales Maia, A. Barison, C. A. Lenz, P. G. Guerrero, *Lett. Org. Chem.* **2012**, *8*, 696–700.
- [191] E. D. Mihelich, *Tetrahedron Lett.* **1979**, *49*, 4729–4732.
- [192] a) L.-Q. Wang, W.-M. Zhao, G.-W. Qin, K-F. Cheng, R.-Z. Yang, *Nat. Prod. Lett.* **1999**, *14*, 83–90; b) S. Takahashi, R. Takahashi, Y. Hongo, H. Koshino, K. Yamaguchi, T. Miyagi, *J. Org. Chem.* **2009**, *74*, 6382–6385; c) S. Takahashi, Y. Hongo, Y. Tsukagoshi, H. Koshino, *Org. Lett.* **2008**, *10*, 4223–4226.
- [193] a) C. Wartmann, BSc thesis, Cologne University, **2017**; b) T. M. Leuther, PhD thesis, Cologne University, **2019**; c) H. Engler, PhD thesis, Cologne University, **2018**.
- [194] W. C. Still, M. Kahn, A. Mitra, *J. Org. Chem.* **1978**, *43*, 2923 – 2925.
- [195] L. M. Pitet, J. Zhang, M. A. Hillmyer, *Dalton Trans.* **2013**, *42*, 9079–9088.
- [196] S. Kobayashi, K. Fukuda, M. Kataoka, M. Tanaka, *Macromolecules* **2016**, *49*, 2493–2501.
- [197] G. Ma, J. Deng, M. P. Sibi, *Angew. Chem. Int. Ed.* **2014**, *53*, 11818–11821.
- [198] S. Zhu, C. Wang, L. Chen, R. Liang, Y. Yu, H. Jiang, *Org. Lett.* **2011**, *13*, 1146–1149.
- [199] N. Vallavoju, S. Selvakumar, S. Jockusch, M. P. Sibi, J. Sivaguru, *Angew. Chem. Int. Ed.* **2014**, *53*, 5604–5608.
- [200] N. Li, H. Feng, Q. Gong, C. Wu, H. Zhou, Z. Huang, J. Yang, X. Chen, N. Zhao, *J. Mater. Chem.* **2015**, *3*, 11458–11463.
- [201] F. Yang, S. Wei, C. A. Chen, P. Xi, L. Yang, J. Lan, H. M. Gau, J. You, *Chem. Eur. J.* **2008**, *14*, 2223–2231.
- [202] Agilent (2014). CrysAlis PRO. Agilent Technologies Ltd, Yarnton, Oxfordshire, England.
- [203] Sheldrick, G. M. (2015). *Acta Cryst.* A71, 3–8.
- [204] Sheldrick, G. M. (2015). *Acta Cryst.* C71, 3–8.
- [205] Farrugia, L. J. (2012). *J. Appl. Cryst.* 45, 849–854.
- [206] R. Patchett, I. Magpantay, L. Saudan, C. Schotes, A. Mezzetti, F. Santoro, *Angew. Chem. Int. Ed.* **2013**, *52*, 10352–10355.
- [207] C. U. Grünanger, B. Breit, *Angew. Chem. Int. Ed.* **2010**, *49*, 967–970.
- [208] A. Ramdular, K. A. Woerpel, *Org. Lett.* **2020**, *22*, 4113–4117.
- [209] M. F. El-Behairy, E. Sundby, *Tetrahedron Asymmetry* **2013**, *24*, 285–289.
- [210] D. J. Covell, M. C. White, *Angew. Chem. Int. Ed.* **2008**, *47*, 6448–6451.
- [211] J. H. Choi, Y. K. Choi, Y. H. Kim, E. S. Park, E. J. Kim, M. J. Kim, J. Park, *J. Org. Chem.* **2004**, *69*, 1972–1977.
- [212] O. V. Singh, H. Han, *Org. Lett.* **2007**, *9*, 4801–4804.
- [213] J. Louvel, J. F. S. Carvalho, Z. Yu, M. Soethoudt, E. B. Lenselink, E. Klaasse, J. Brussee, A. P. Ijzerman, *J. Med. Chem.* **2013**, *56*, 9427–9440.

- [214] Y. Kobayashi, S. Yoshida, Y. Nakayama, *Eur. J. Org. Chem.* **2001**, 1873–1881.
- [215] A. Mordini, D. Peruzzi, F. Russo, M. Valacchi, G. Reginato, A. Brandi, *Tetrahedron* **2005**, *61*, 3349–3360.

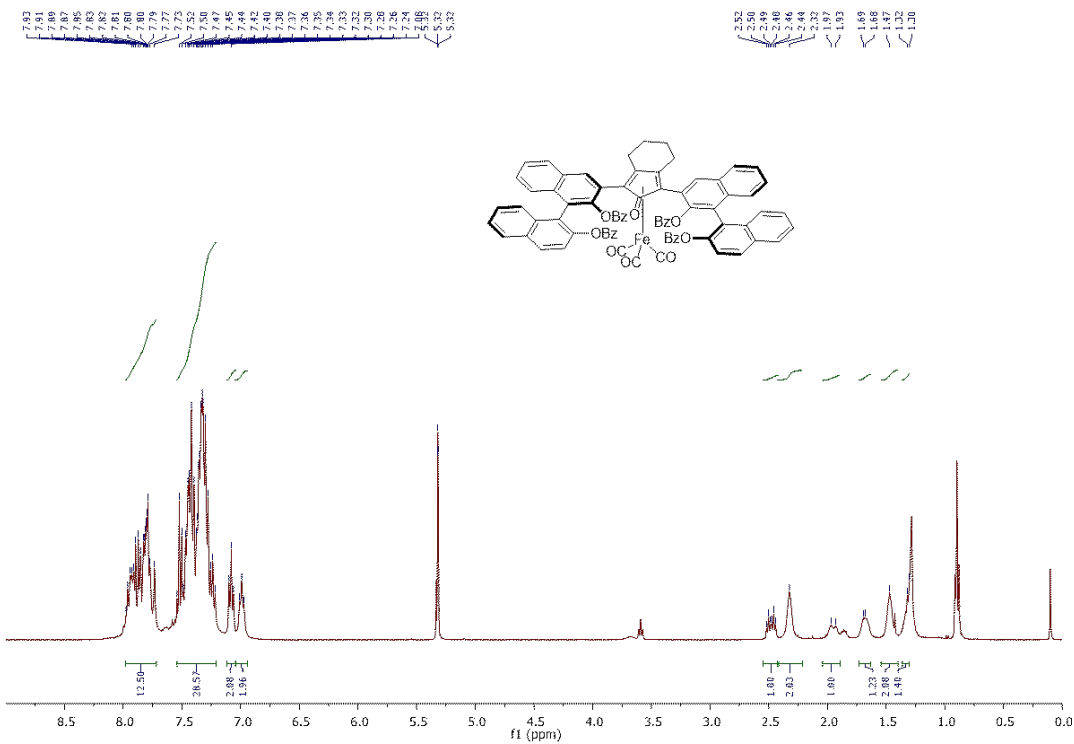
6. NMR Spectra

6.1. Complex 103

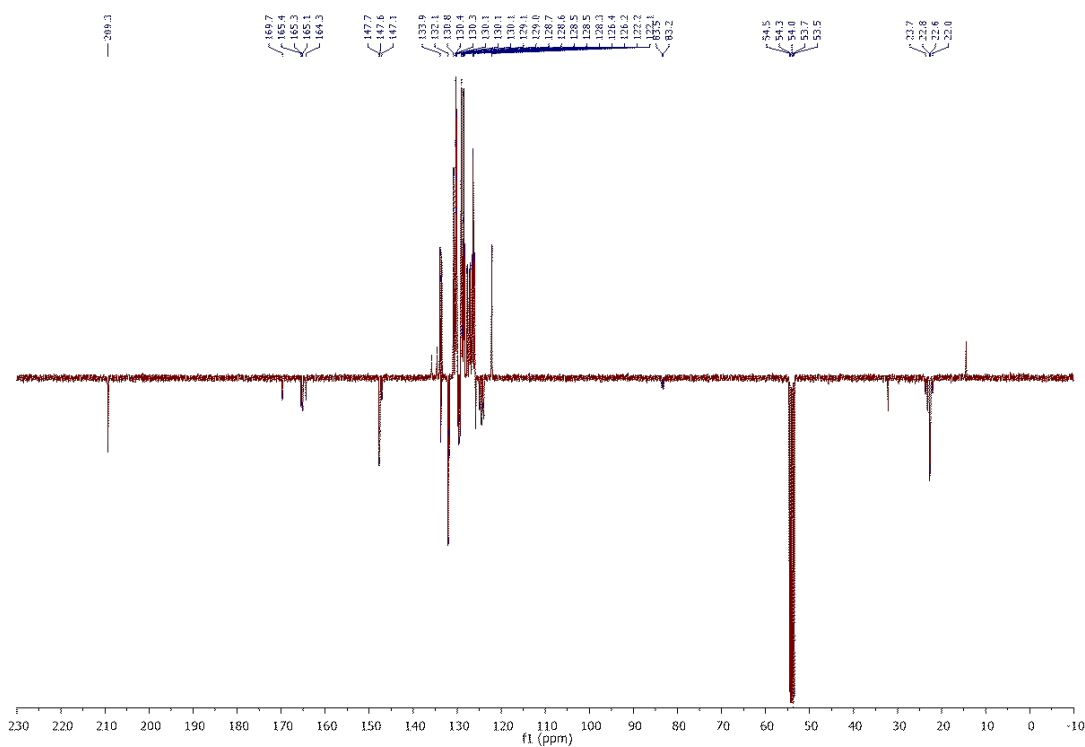


6.4. Complex 106

$^1\text{H-NMR}$ (CD_2Cl_2 , 400 MHz)

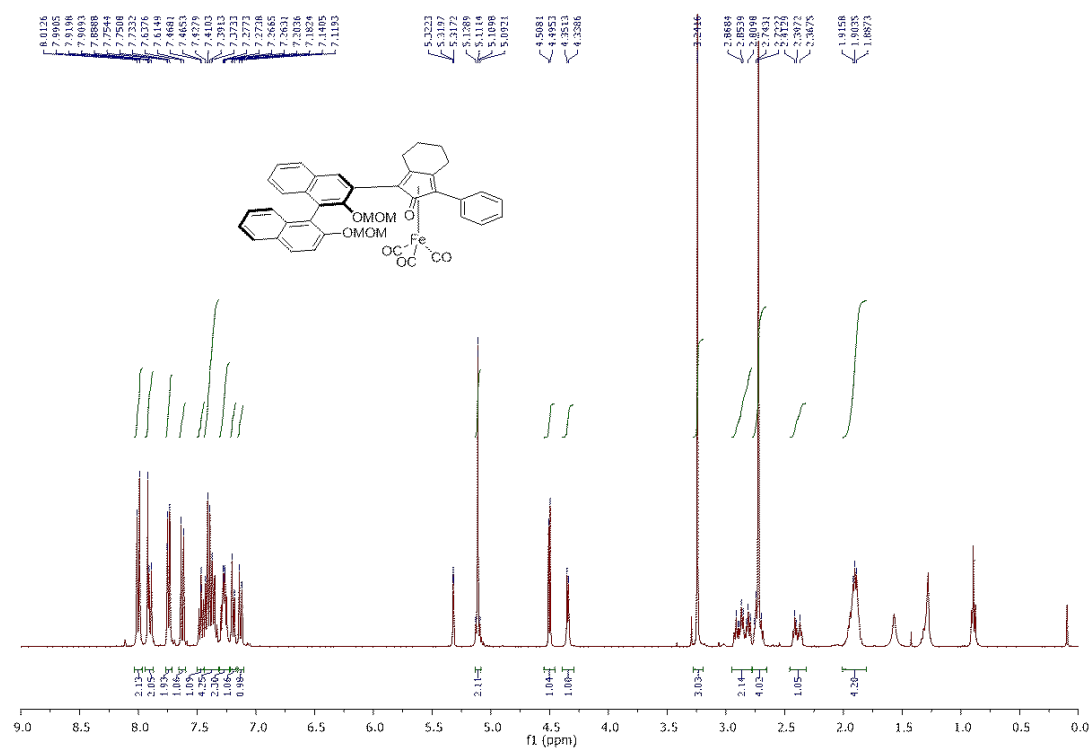


$^{13}\text{C-NMR}$ (CD_2Cl_2 , 100 MHz)

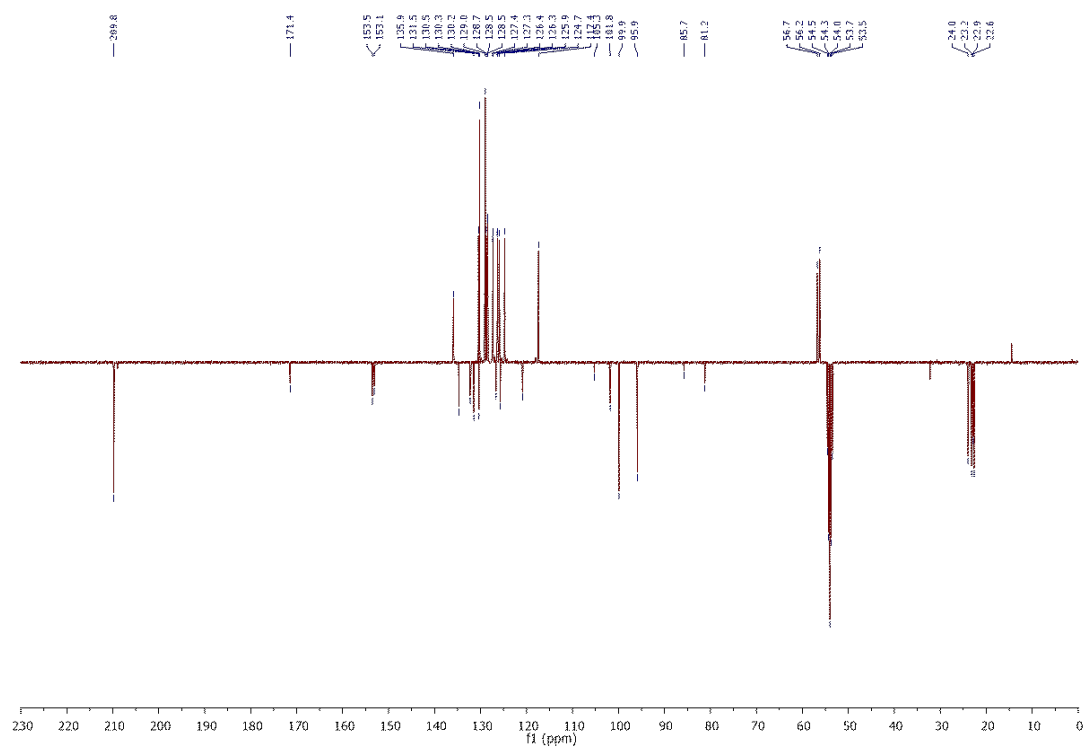


6.5. Complex 110a

$^1\text{H-NMR}$ (CD_2Cl_2 , 400 MHz)

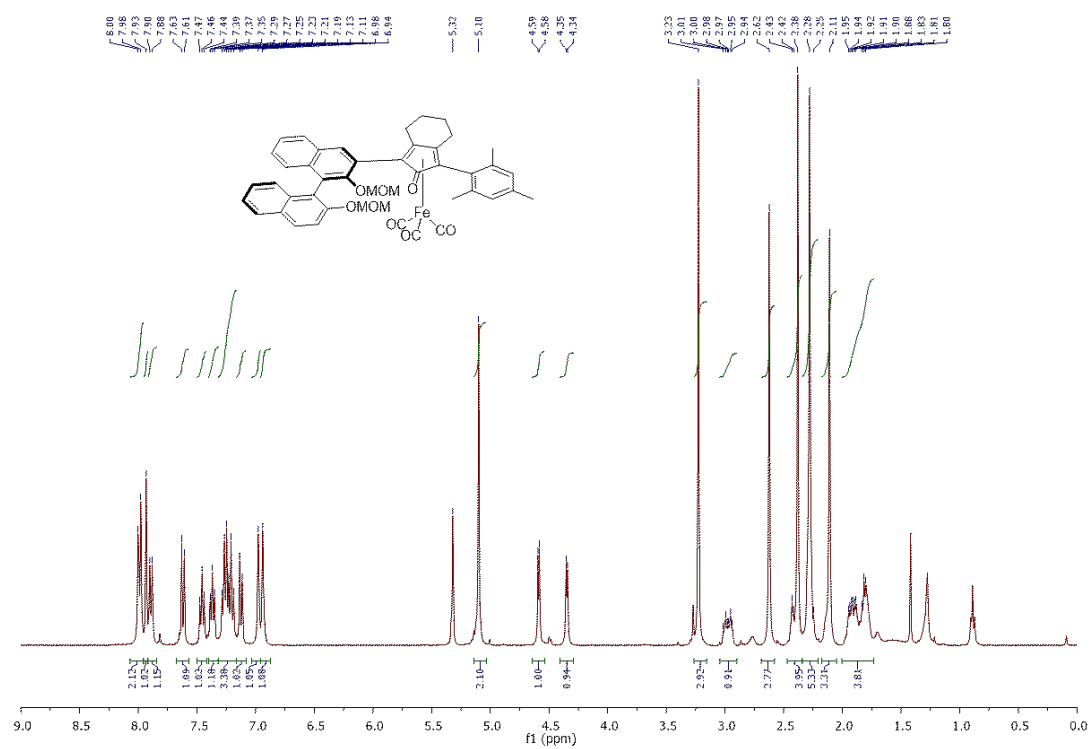


$^{13}\text{C-NMR}$ (CD_2Cl_2 , 100 MHz)

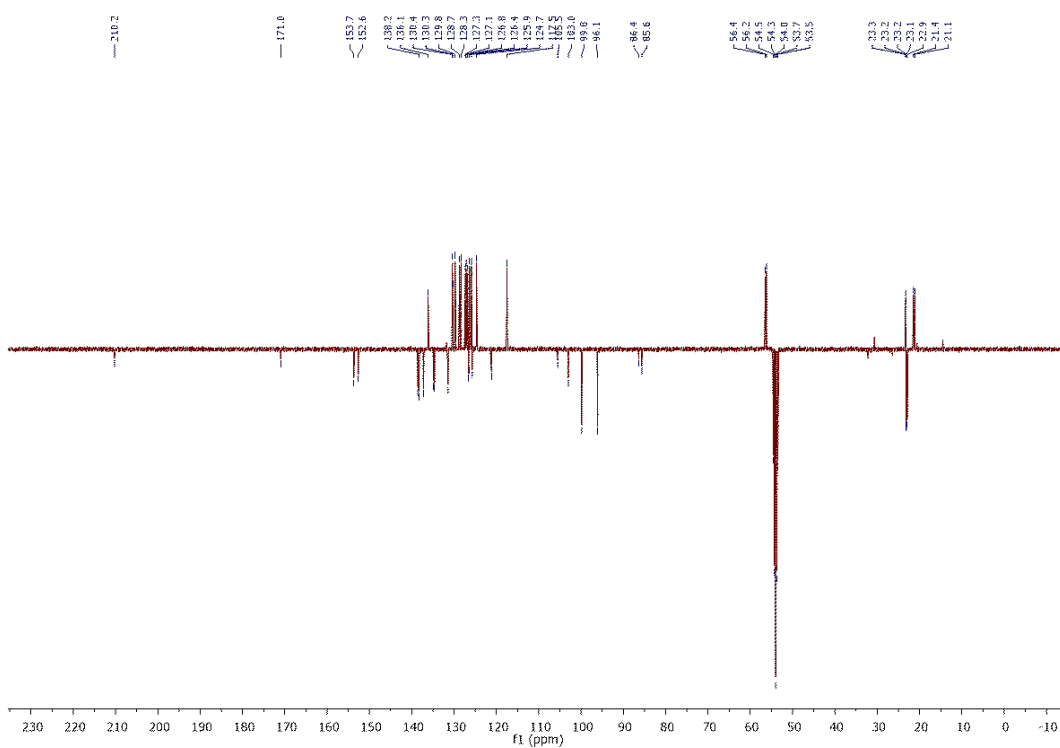


6.7. Complex 112a

$^1\text{H-NMR}$ (CD_2Cl_2 , 400 MHz)

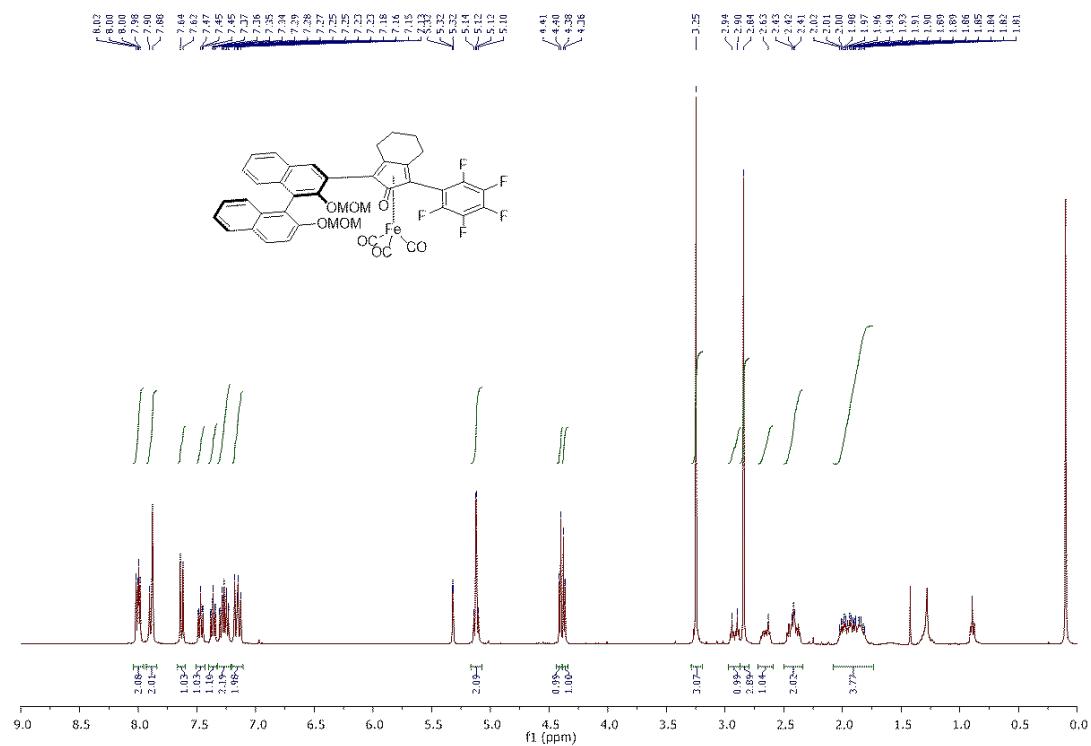


$^{13}\text{C-NMR}$ (CD_2Cl_2 , 100 MHz)

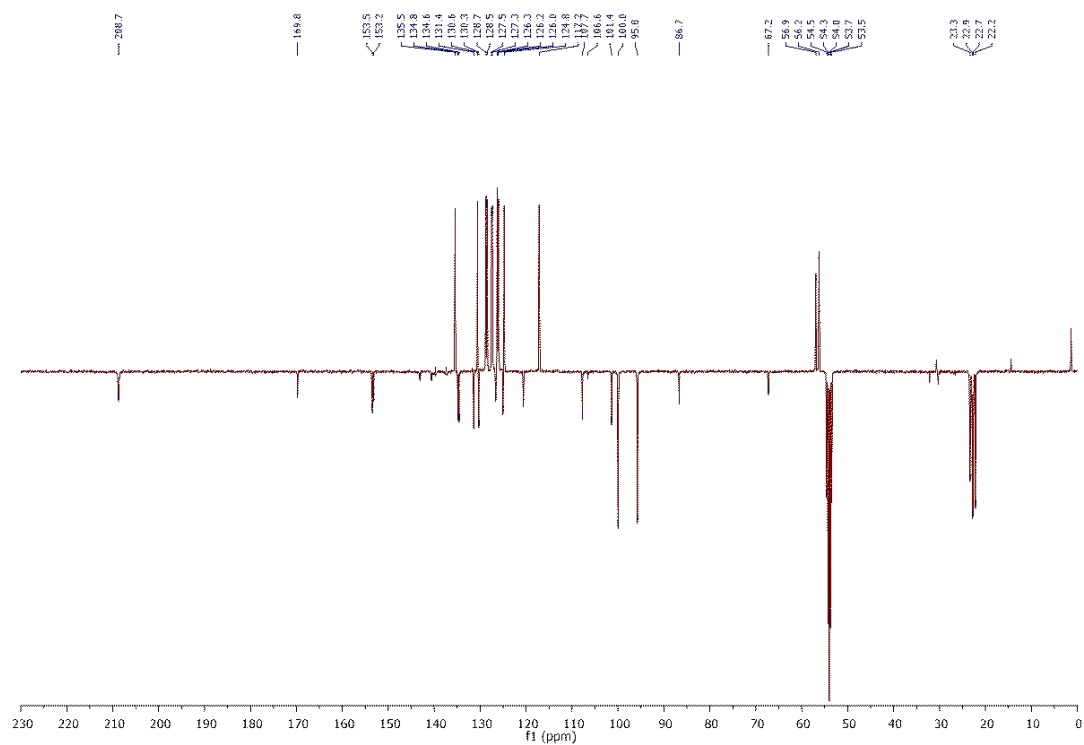


6.9. Complex 113a

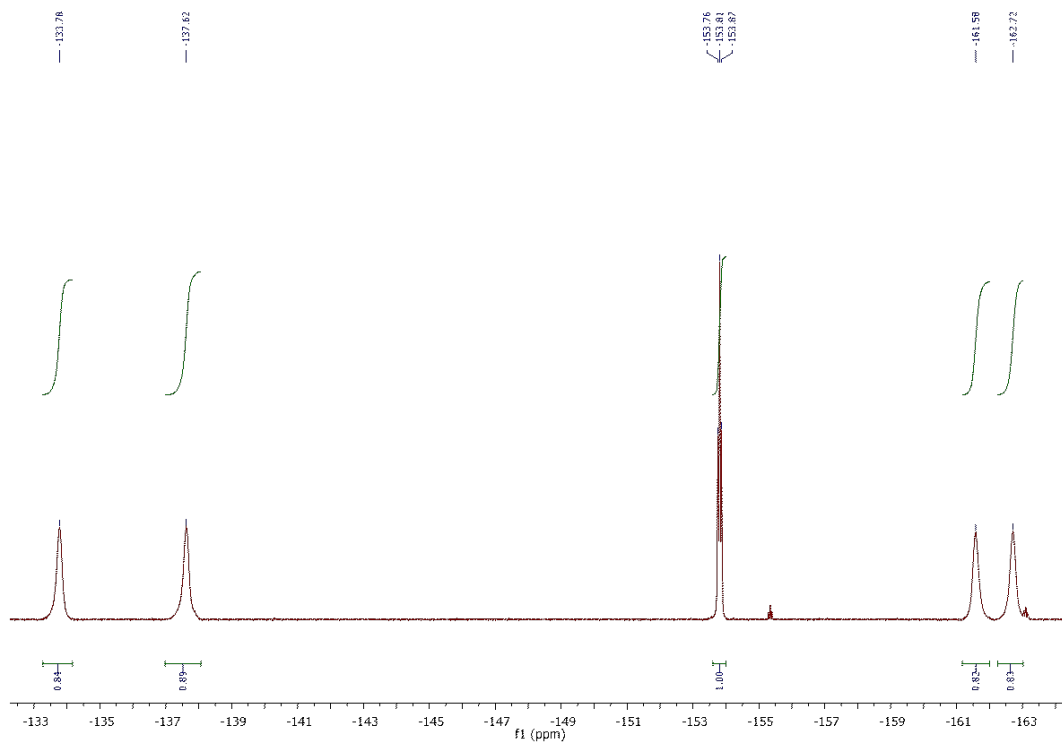
$^1\text{H-NMR}$ (CD_2Cl_2 , 400 MHz)



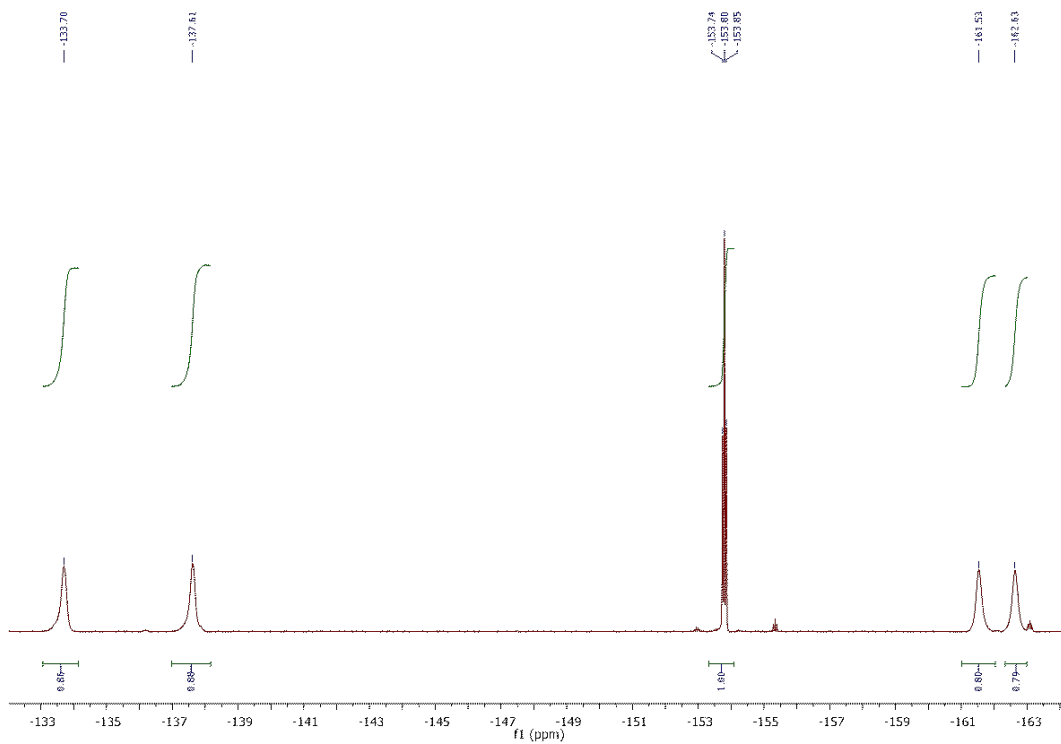
$^{13}\text{C-NMR}$ (CD_2Cl_2 , 100 MHz)



^{19}F -NMR (CD_2Cl_2 , 377 MHz)

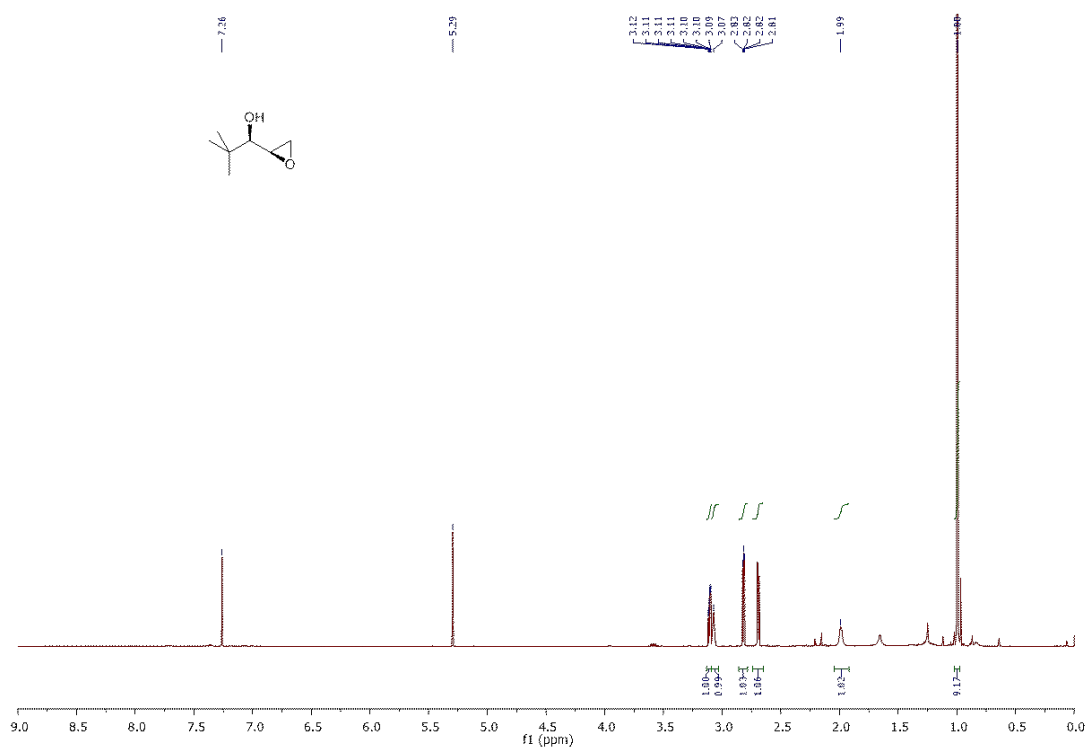


¹⁹F-NMR (CD₂Cl₂, 377 MHz)

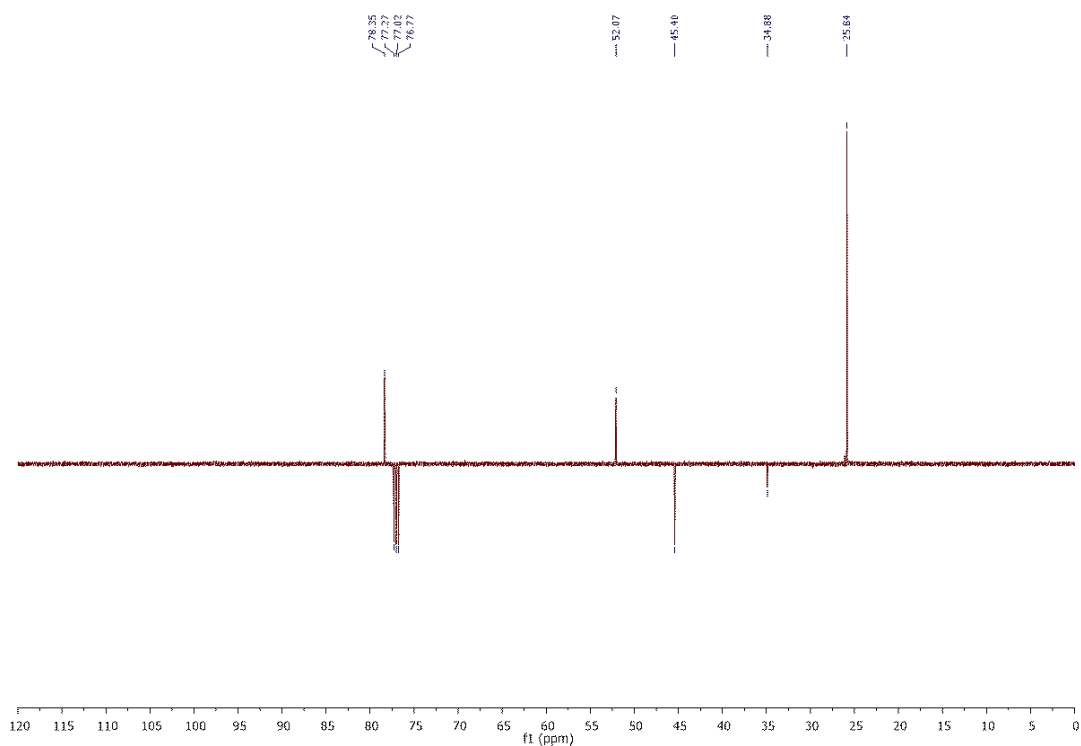


6.15. Epoxy Alcohol 159

$^1\text{H-NMR}$ (CDCl_3 , 500 MHz)

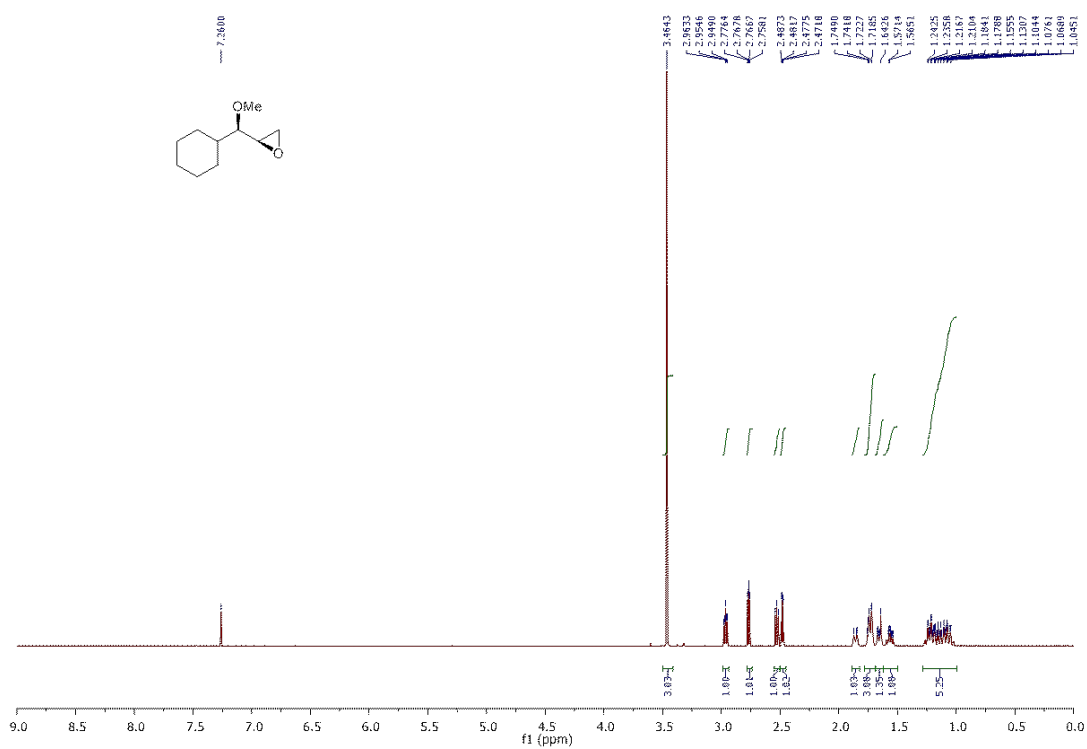


$^{13}\text{C-NMR}$ (CDCl_3 , 125 MHz)

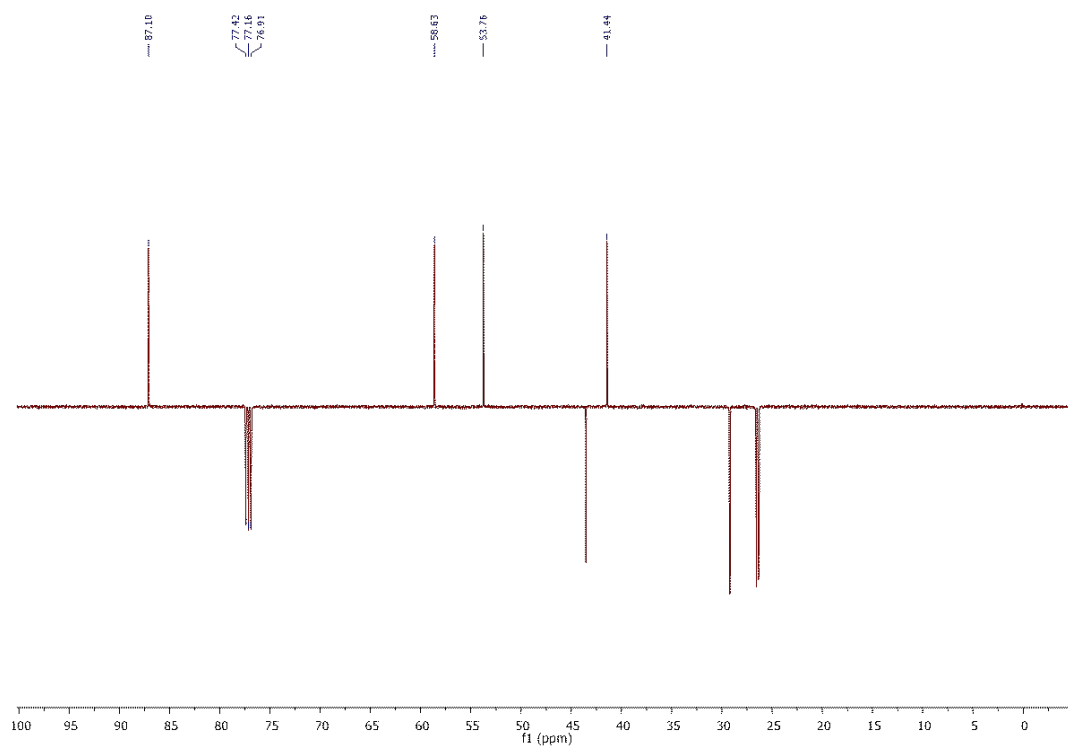


6.16. Epoxide 162

$^1\text{H-NMR}$ (CDCl_3 , 500 MHz)

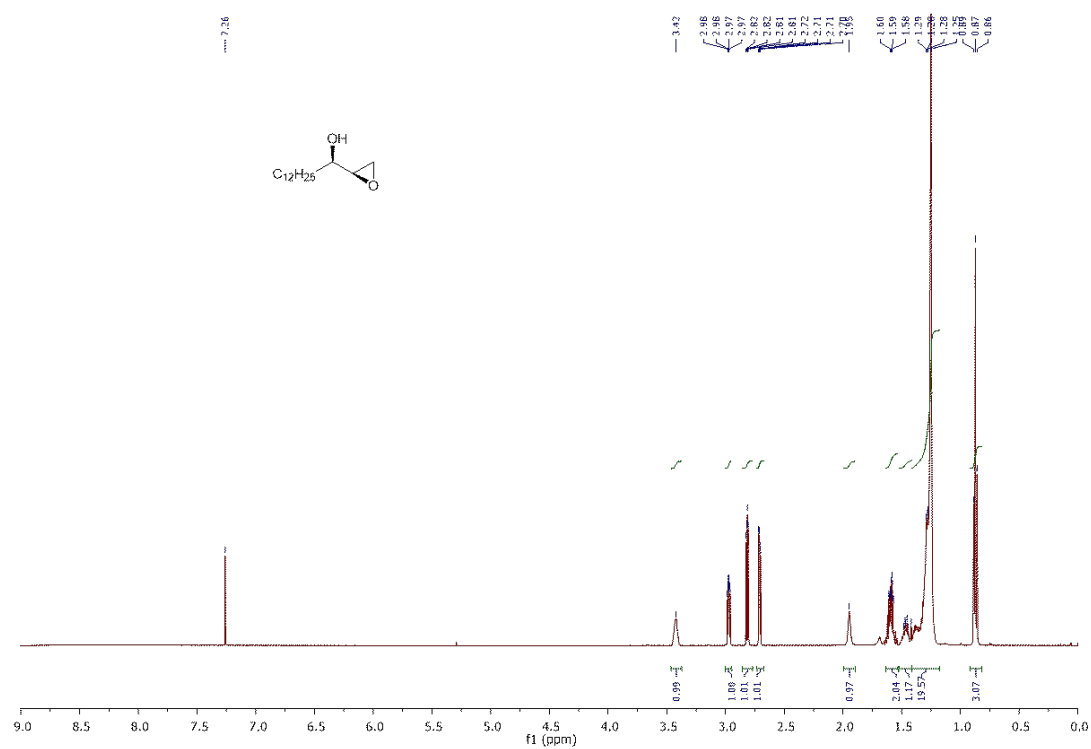


$^{13}\text{C-NMR}$ (CDCl_3 , 125 MHz)

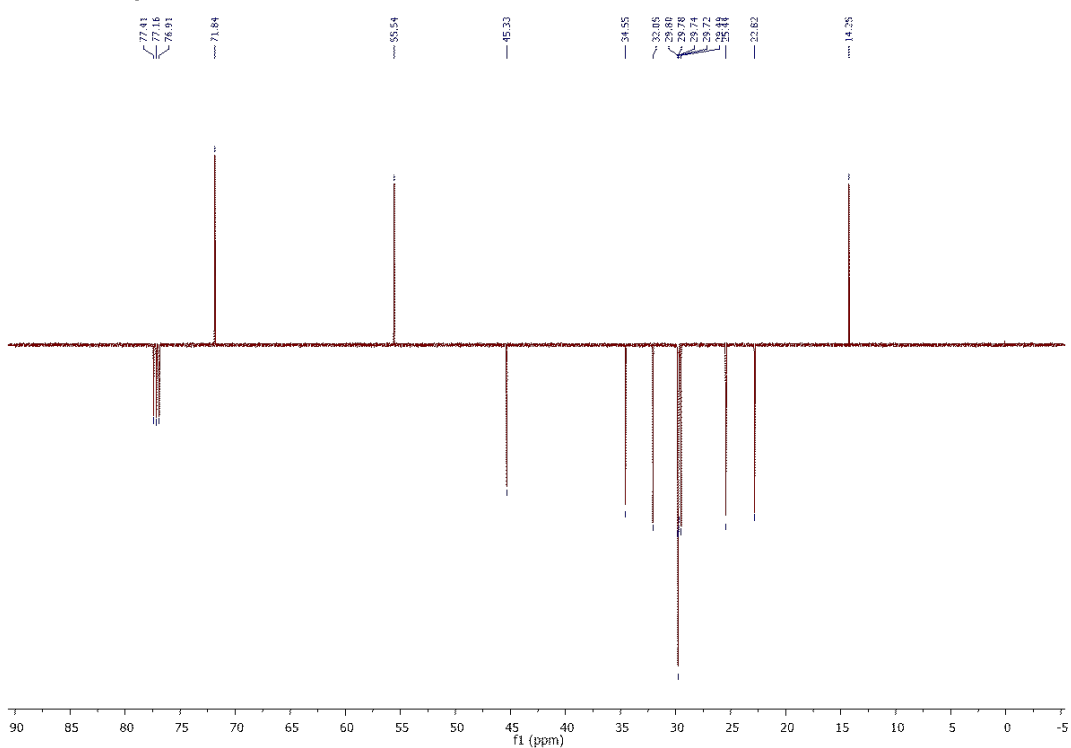


6.17 Epoxy Alcohol 145

$^1\text{H-NMR}$ (CDCl_3 , 500 MHz)

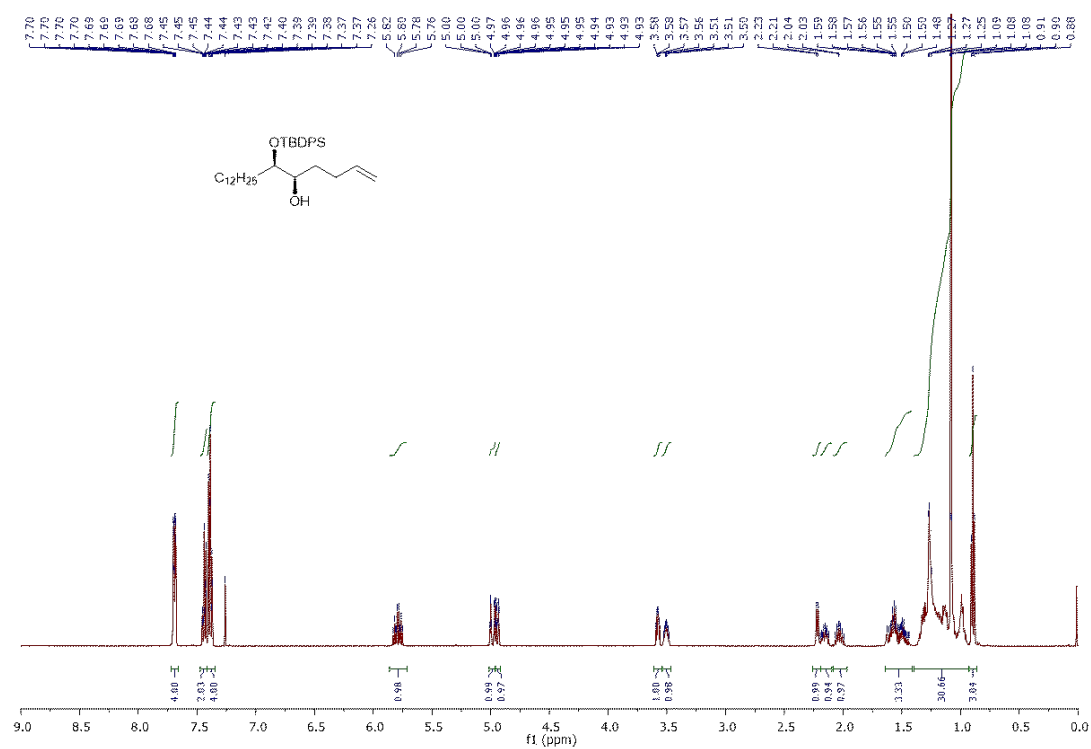


$^{13}\text{C-NMR}$ (CDCl_3 , 125 MHz)

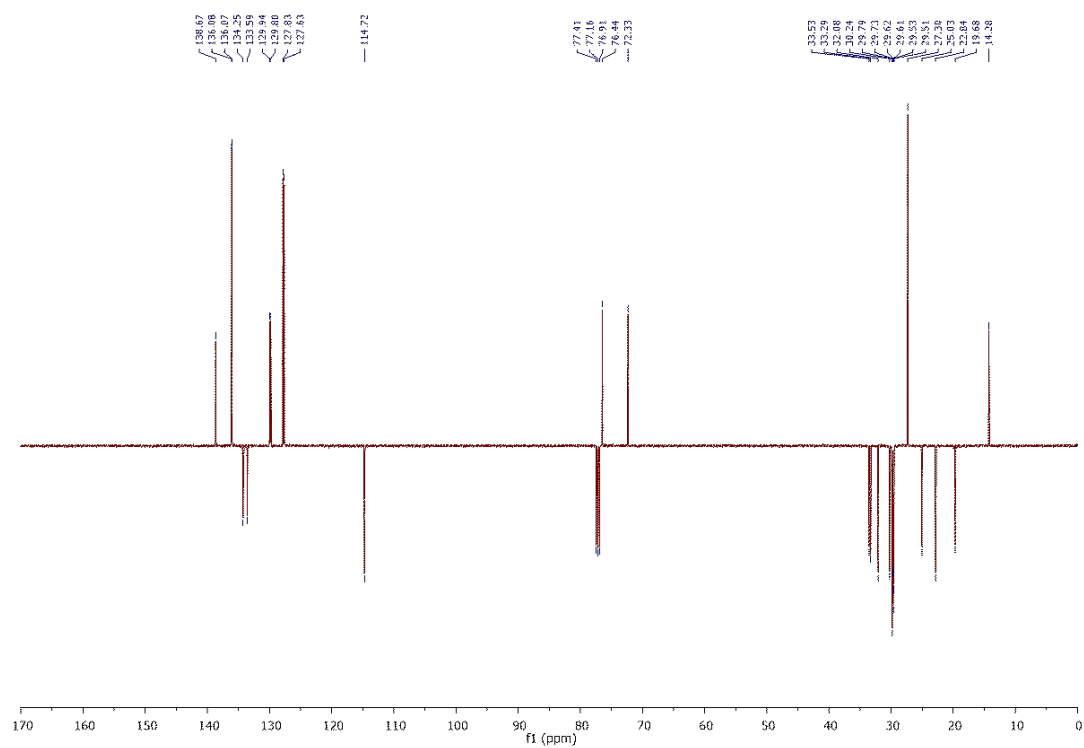


6.19. Compound 165

$^1\text{H-NMR}$ (CDCl_3 , 500 MHz)

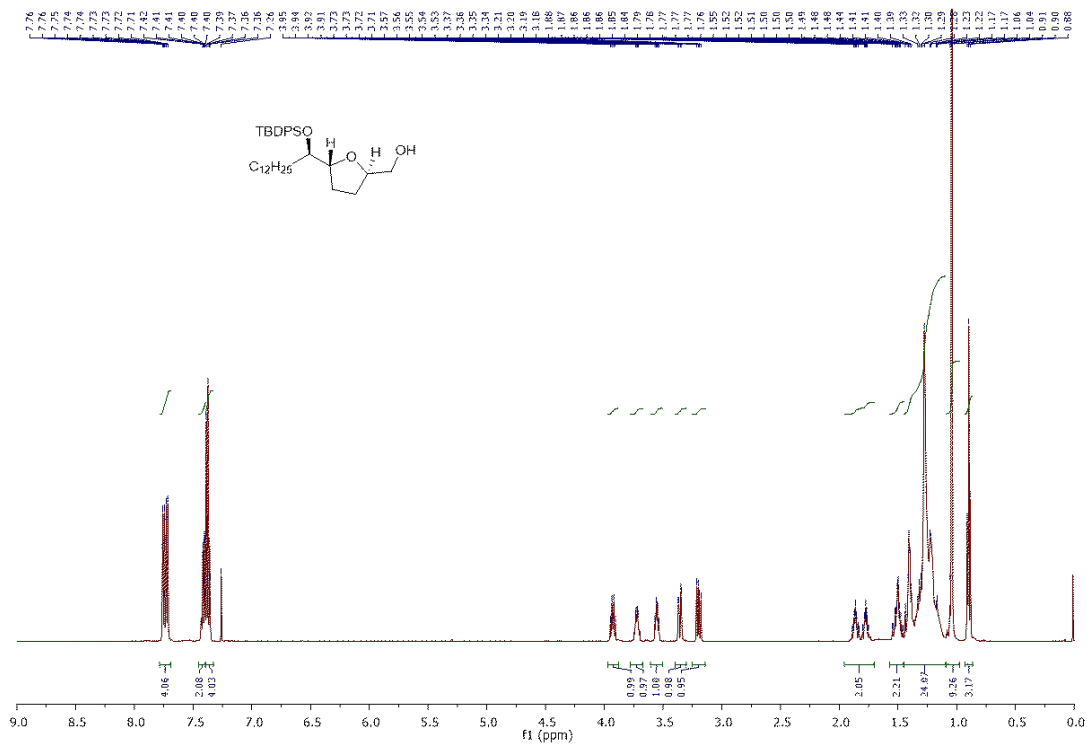


$^{13}\text{C-NMR}$ (CDCl_3 , 125 MHz)

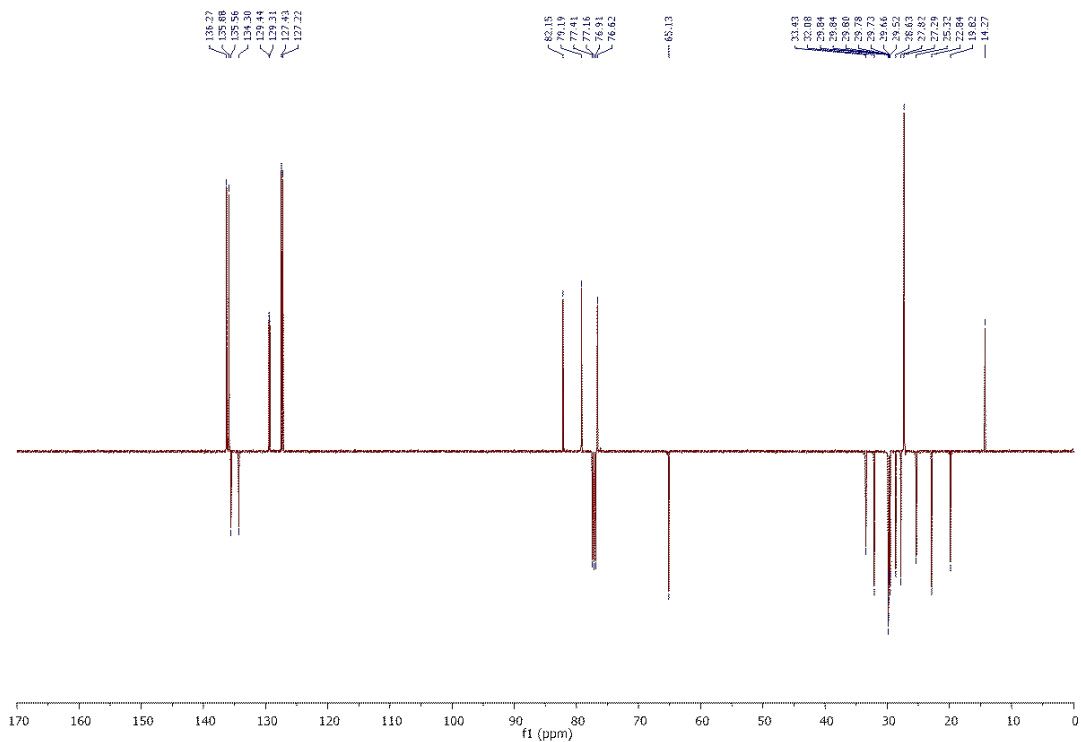


6.20. Compound 167

$^1\text{H-NMR}$ (CDCl_3 , 500 MHz)



$^{13}\text{C-NMR}$ (CDCl_3 , 125 MHz)



7. List of Abbreviations

Å	1 Angstrom (10^{-10} m)
AcOEt	Ethyl acetate
AH	Asymmetric Hydrogenation
ATH	Asymmetric Transfer Hydrogenation
BINOL	1,1'-Bi-2-naphthol
Bn	Benzyl
Bu	Butyl
Bz	Benzoyl
Cy	Cyclohexyl
DCE	1,2-Dichloroethane
DCM	Dichloromethane
DFT	Density Functional Theory
DMAP	4 Dimethylaminopyridine
DMF	<i>N,N</i> -Dimethylformamide
DIPEA	<i>N,N</i> -Diisopropylethylamine
δ	Chemical shift
eq	Equivalent
ESI	Electrospray ionization
Et	Ethyl
FTIR	Fourier transform infrared spectroscopy
GC	Gas Chromatography / Gas Chromatogram
Hex	Hexyl
HMDS	Hexamethyldisilazane
HPLC	High Performance Liquid Chromatography
HRMS	High Resolution Mass Spectrometry
Hz	Hertz
<i>i</i> Pr	isopropyl
<i>J</i>	Coupling constant
LDA	Lithium diisopropylamide
M	Molar [mol/L]
Me	Methyl
Mes	Mesityl
MS	Molecular Sieves
NHC	<i>N</i> -Heterocyclic Carbenes
NMR	Nuclear Magnetic Resonance
PG	Protecting Group
Ph	Phenyl
PMP	<i>para</i> -Methoxyphenyl

ppm	Parts per million
Py	Pyridine
R _f	Retention factor
rt	Room temperature
SAE	Sharpless Asymmetric Epoxidation
TBHP	<i>tert</i> -Butyl hydroperoxide
TBDPS	<i>tert</i> -Butyldiphenylsilyl
TES	Triethylsilyl
TFA	Trifluoroacetic acid
THF	Tetrahydrofuran
TIPS	Triisopropylsilyl
TLC	Thin Layer Chromatography
TMS	Trimethylsilyl
TOF	Turnover Frequency
TON	Turnover Number
TS	Transition State
UV	Ultraviolet
XRD	X-Ray Diffraction